The Role of DNA Damage Response Proteins in Innate Immune Signalling: A New role for BRCA1

Daniel Gaughan

Green Templeton College

University of Oxford

A Thesis submitted to the University of Oxford for the degree of

Doctor of Philosophy in Clinical Medicine

Trinity Term 2016

This thesis is the result of my own work and includes nothing that is the outcome of work done in collaboration except where specifically indicated in the text.

No part of this thesis has been, or is currently being, submitted by the author for any other degree, diploma or qualification.

This work does not exceed 50,000 words, exclusive of appendices, bibliography, diagrams and tables.

Acknowledgements

I would like to thank Prof. Alison Simmons for providing supervision throughout this work, and all members of the Human Immunology Unit for creating a friendly, motivating and most importantly stimulating environment in which to work. In particular, I would like to thank Seiji Shiraishi for helping to optimise multiple protocols which were essential in generating the data shown, and helping to run individual experiments where specifically identified. I would also like to thank James Kinchen and Lorena Preciado for assistance throughout the study.

I would like to extend great gratitude to Alice Mayer for providing superb guidance during the initial stages of this work. Her patience, understanding and exceptional knowledge provided me with the tools to complete this work to a level I am proud of. I would also like to thank Jonathan Maelfait for offering help and advice on many occasions.

My appreciation extends to the selection panel of the Weatherall Institute of Molecular Medicine for giving me the opportunity to undertake this work, and also the Medical Research Council for funding for my position.

I would lastly like to thank my family; my parents for constantly pushing me to achieve things I didn't believe I was capable of, and my family as a whole for supporting me throughout.

Abbreviations

53BP1	p53-Binding Protein 1
A20	Tumour Necrosis Factor, Alpha-Induced Protein 3
ABIN1	TNFAIP3 Interacting Protein 1
ADAR	Adenosine Deaminase, RNA-Specific
Ag	Antigen
AGS	Aicardi–Goutières Syndrome
AIDS	Acquired Immunodeficiency Syndrome
AIM2	Absent in Melanoma 2
ANOVA	Analysis Of Variance
AP1	Activator Protein 1
APC	Antigen Presenting Cell
APC	Allophycocyanin
APOBEC	Apolipoprotein B MRNA Editing Enzyme, Catalytic Polypeptide
ASC	Inflammasome Adaptor Protein Apoptosis-Associated Speck-Like Protein Containing CARD
AT	Adenosine-Thymidine
AT	Ataxia Telangiectasia
ATM	Ataxia Telangiectasia Mutated
ATP	Adenosine Triphosphate
ATR	Ataxia Telangiectasia And Rad3-Related Protein
BACH1	BTB And CNC Homology 1, Basic Leucine Zipper Transcription Factor 1
BARD1	BRCA1 Associated RING Domain 1
BASC	BRCA1-Associated Genome Surveillance Supercomplex
Bcl-10	B-cell lymphoma/leukaemia 10
BCL2	B-Cell CLL/Lymphoma 2
BER	Base Excision Repair
BRCA1	Breast Cancer 1, Early Onset
BRCA2	Breast Cancer 2, Early Onset
BRCT	BRCA1 C Terminus Domain
BRE	Brain And Reproductive Organ-Expressed (TNFRSF1A Modulator)
BSA	Bovine Serum Albumin
CARD	Caspase Recruitment Domain
CCR7	Chemokine (C-C Motif) Receptor 7
CD	Cluster of Differentiation
CDK7	Cyclin-Dependent Kinase 7
CDN	Cyclic Dinucleotides
CDS	Cytosolic DNA Sensor
cGAMP	Cyclic Guanosine Monophosphate–Adenosine Monophosphate
cGAS	Cyclic GMP-AMP Synthase
CHAPS	Dimethyl[3 propyl]. azaniumyl}propane-1-sulfonate

CHK1	Checkpoint Kinase 1
CHK2	Checkpoint Kinase 2
CMV	Cytomegalovirus
COBRA	Co-factor of BRCA1
CRISPR	Clustered Regularly Interspaced Short Palindromic Repeat
CT	Cycle Threshold
CtIP	Retinoblastoma Binding Protein 8
CTL	Cytotoxic T Lymphocytes
CYLD	Cylindromatosis (Turban Tumour Syndrome)
DAI	DNA-dependent activator of IRFs
DAMP	Damage-Associated Molecular Pattern
DAPI	4',6-diamidino-2-phenylindole
DC	Dendritic Cell
DC-SIGN	Dendritic Cell-Specific ICAM-3-Grabbing Non-Integrin 1
DD	Death Domain
DDM	Dodecyl 4-O-α-D-Glucopyranosyl-β-D-Glucopyranoside
DDM	n-Dodecyl β-D-maltoside
DDR	DNA Damage Response
DDX60	DEAD (Asp-Glu-Ala-Asp) Box Polypeptide 60
DNA-PK	DNA-Dependent Protein Kinase
DNA-PKcs	DNA-PK Catalytic Subunit
dNTP	Deoxynucleoside Triphosphate
DSB	Double Strand Breakage
dsDNA	Double-stranded DNA
dsRNA	Double Stranded RNA
DTT	Dithiothreitol
DTX4	Deltex 4, E3 Ubiquitin Ligase
DUB	Deubiquitinase
EBV	Epstein Barr Virus
ECL	Enzyme Chemiluminescence
EDTA	Ethylenediaminetetraacetic acid
EEA1	Early Endosome Antigen 1
EGFR	Epidermal Growth Factor Receptor
eIF2A	Eukaryotic Translation Initiation Factor 2A
ELISA	Enzyme Linked Immunosorbent Assay
ER	Endoplasmic Reticulum
ERK	Extracellular signal–regulated kinase
ERα	Estrogen Receptor α
ETO	Etoposide
FACS	Fluorescence Activated Cell Sorting
FANC	Fanconi Anaemia, Complementation
FCS	Fetal Calf Serum
FITC	Fluorescein Isothiocyanate

FMDV	Foot and Mouth Disease Virus
FTO	Fat Mass And Obesity Associated
GAPDH	Glyceraldehyde-3-Phosphate Dehydrogenase
GFP	Green Fluorescent Protein
GM-CSF	Granulocyte Macrophage Colony Stimulating Factor
GO	Gene Ontology
GSK3β	Glycogen Synthase Kinase 3β
GST	Glutathione S-transferase
GTP	Guanosine Triphosphate
H2AFX	H2A Histone Family Member X
H2AX	Histone 2 A-X
HA	Haemagglutinin
HCV	Hepatitis C Virus
HEK293	Human Embryonic Kidney 293
Hist3h2a	Histone Cluster 3, H2a
HIV	Human Immunodeficiency Virus
HLA-DR	Major Histocompatibility Complex, Class II, DR
HMGB1	High Mobility Group Box 1
HPV	Human Papillomavirus
HR	Homologous Recombination
HRP	Horseradish Peroxidase
HSP	Heat-Shock Protein
HSV1	Herpes Simplex Virus 1
ICAM3	Intercellular Adhesion Molecule 3
ICL	Inter-strand Crosslink Repair
IFI16	Gamma Interferon-Inducible Protein
IFIT	Interferon-Induced Protein With Tetra-tricopeptide Repeats
IFIX	Interferon-Inducible Protein X
IFN	Interferon
IFNAR	Interferon α/β Receptor
Ig	Immunoglobulin
IKKβ	Inhibitor of Nuclear Factor kappa-B Kinase subunit β
IL	Interleukin
IL1-R	Interleukin 1 Receptor
IP	Immunoprecipitation
IR	Infrared Radiation
IRAK	IL1-R-associated kinase
IRF3	Interferon Regulatory Factor 3
ISG	Interferon Stimulated Gene
ISGF3	IFN-Stimulated Gene Factor 3
ISRE	Interferon Stimulated Response Element
IVT	*In Vitro* Transcribed
JNK	Janus Kinase

KSHV	Kaposi's Sarcoma Herpes Virus
LB	Lysogeny Broth
LDS	Lithium Dodecyl Sulphate
LMA	Low Melting Point Agarose
LPS	Lipopolysaccharide
LSD1	Lysine Demethylase 1A
LVP	Lentiviral Particle
MAM	Mitochondria-Associated Membranes
MAPK	Mitogen-activated protein kinase
MAPKK	Mitogen-activated protein kinase kinase
MAVS	Mitochondrial Antiviral Signalling Protein
MDA5	Melanoma differentiation-associated 5
MDC1	Mediator Of DNA-Damage Checkpoint 1
MDP	Muramyl Dipeptide
MHC	Major Histocompatibility Complex
MHV68	Murine Gamma-Herpesvirus 68
MICA	MHC Class I Polypeptide-Related Sequence A
MICB	MHC Class I Polypeptide-Related Sequence B
MLH3	MutL Homolog 3
MoDC	Monocyte Derived Dendritic Cell
MOPS	(3-(N-morpholino)propanesulfonic acid)
MRE11	Meiotic Recombination 11
MRN	Mre11, Rad50 and Nbs1
Ms	Mouse
MS	Mass Spectrometry
MxA/MX1	MX Dynamin-Like GTPase 1
MyD88	Myeloid Differentiation Primary Response 88
NAC	N-Acetyl Cysteine
NAIP	NLR Family, Apoptosis Inhibitory Protein
NAP	NAK-Associated Protein 1
NBS1	Nijmegen Breakage Syndrome 1
NEMO	NF-kappa-B Essential Modulator
NER	Nucleotide Excision Repair
NER	Nucleotide Excision Repair
NET	Neutrophil Extracellular Trap
NFκB	Nuclear Factor κ B
NHEJ	Non-Homologous End-Joining
NK Cell	Natural Killer Cell
NKG2D	Natural-Killer Group 2, Member D
NLR	NOD-like Receptor
NLRC	NLR Family CARD Domain Containing
NLRP	NLR Family, Pyrin Domain Containing
NLS	Nuclear Localisation Signal

NOD	Nucleotide-Binding Oligomerization Domain
NP40	Nonidet P-40
Nrdp1	Ring Finger Protein 41, E3 Ubiquitin Protein Ligase
OAS	Oligoadenylate Synthetase
ORF	Open Reading Frame
OTUB1	OTU Deubiquitinase, Ubiquitin Aldehyde Binding 1
PAGE	Polyacrylamide Gel Electrophoresis
PAMP	Pathogen Associated Molecular Pattern
PARP	Poly (ADP-Ribose) Polymerase 1
PBMC	Peripheral Blood Mononuclear Cells
PBS	Phosphate Buffered Saline
PD-1	Programmed Cell Death 1
PD-L1	Programmed Cell Death Ligand 1
pDC	Plasmacytoid DC
PE	Phycoerythrin
PI3K	Phosphatidylinositol-4,5-Bisphosphate 3-Kinase
PKR	Protein Kinase RNA-Activated
pks	Polyketide synthase
PLA	Proximity Ligation Assay
PMA	Phorbol 12-myristate 13-acetate
Pold1	Polymerase (DNA) Delta 1, Catalytic Subunit
PPM1b	Protein Phosphatase, Mg2+/Mn2+ Dependent, 1B
PRR	Pattern Recognition Receptor
PTEN	Phosphatase And Tensin Homolog
PTEN	Phosphatase And Tensin Homolog
PTM	Post-Translational Modification
PVDF	Polyvinylidene Fluoride
PYHIN	Pyrin and HIN Domain
qRT-PCR	Semi-Quantitative Reverse Transcription Polymerase Chain Reaction
RB	Retinoblastoma
Rb	Rabbit
RECQL	RecQ Like Helicase
RIG-I	Retinoic Acid Inducible gene 1
RING	Really Interesting New Gene
RIP1	Receptor-Interacting Protein 1
RLR	RIG-I Like Receptor
RNF	Ring Finger Protein
ROS	Reactive Oxygen Species
RPA	Replication Protein A
RPMI	Roswell Park Memorial Institute -1640
RPS27A	Ribosomal Protein S27a
RT	Room Temperature

SAMHD1	SAM Domain And HD Domain 1
SCID	Severe Combined Immunodeficiency Disease
SDS	Sodium Dodecyl Sulphate
SEM	Standard Error of the Mean
SeV	Sendaï Virus
SHP1	Protein Tyrosine Phosphatase, Non-Receptor Type 6
shRNA	Short Hairpin RNA
SIKE	Suppressor of IKKε
siRNA	Small Interfering RNA
SLE	Systemic Lupus Erythematosus
SNP	Single Nucleotide Polymorphism
SSB	Single Strand Breakage
ssDNA	Single Stranded DNA
STAT	Signal Transducer And Activator Of Transcription
STING	Stimulator of Interferon Genes
SUMO	Small Ubiquitin-Like Modifier
TAB1	TGF-β activated kinase
TAK1	Transforming growth factor β-activated kinase 1
TANK	TRAF Family Member Associated NFKB Activator
TAX1BP1	Tax1 (Human T-Cell Leukaemia Virus Type I) Binding Protein 1
TBHP	Tert-Butyl Hydroperoxide
TBK1	TANK-Binding Kinase-1
TBST	Tris-Buffered Saline with Tween-20
TCR	T-Cell Receptor
TFIIE	General Transcription Factor IIE
TIR	Toll/IL-1R homology
TIRAP	TIR-associated protein
TLR	Toll-Like Receptor
TNF	Tumour Necrosis Factor
TOM20	Translocase Of Outer Mitochondrial Membrane 20
TRADD	Tumour Necrosis Factor Receptor Type 1-Associated DEATH Domain Protein
TRAF	TNFR-Associated factor
TRAM	TRIF-Related Adaptor Molecule
Trex1	Three Prime Repair Exonuclease 1
TRIF	TIR Domain-Containing Adaptor Protein-Inducing IFNβ
TRIM	Tripartite Motif Containing
TRIP	TRAF-Interacting Protein
Tyk2	Tyrosine Kinase 2
Ub	Ubiquitin
Ubc13	E2 Ubiquitin-Conjugating Protein 13
Uev1a	Ubiquitin-Conjugating Enzyme E2 variant 1A
ULD	Ubiquitin-Like Domain

UV	Ultraviolet Radiation
UVRAG	UV Radiation Resistance Associated
VEGF	Vascular Endothelial Growth Factor
VSV	Vesicular Stomatitis virus
WB	Western Blot
WCL	Whole Cell Lysate
XAB2	XPA Binding Protein 2
XIAP	X-Linked Inhibitor Of Apoptosis, E3 Ubiquitin Protein Ligase
ZAP	Zinc Finger Antiviral Protein

1 Table of Contents

Abstract

Pattern Recognition Receptors (PRRs), which have evolved to detect a diverse array of pathogenic features known as Pathogen Associated Molecular Patterns (PAMPs), are localised optimally for interaction with their cognate ligands. Upon Receptor activation, signal transduction pathways are induced which converge at different points to direct a specific inflammatory response. TBK1 is activated and recruited to multiple PRRs, where it in turn recruits and phosphorylates IRF3 which then translocates to the nucleus and induces the expression of type I IFN. In this study, the major breast cancer susceptibility protein BRCA1, known for its functional role in maintaining genomic stability, is found to be phosphorylated following PRR triggering. This event is demonstrated to be DNA Damage, DNA Damage Response (DDR) signalling, and oxidative stress-independent. Further to this, phosphorylated BRCA1 localises to Golgi-related microsomes in perinuclear zones where TBK1 and the adaptor STING can be found. Here, BRCA1 interacts biochemically with and facilitates full activation of TBK1. BRCA1-deficient cells show abrogated IRF3 phosphorylation, type I IFN production and ISG induction in response to a diverse array of PRR agonists as well as both HSV1 and Sendaï virus (SeV). Subsequently, BRCA1 deficiency impairs antiviral responses to pathogens such as HSV1.

1 Introduction

1.1 Innate Immunity

1.1.1 Pathogen sensing

In order to defend the body against constant invasion by micro-organisms, vertebrates have evolved an elaborate immune system comprising of innate and adaptive arms. The innate immune system provides a first line of defence against pathogens, giving a rapid response to any invader, whereas the adaptive immune system helps eliminate pathogens at later stages of infection. Simultaneously, it works to establish immunological memory to protect against future infections of the same or a similar pathogen. Recognition of invading microbes as non-self is therefore the first and most critical step in eliciting a successful response and controlling infection[1].

The molecular apparatus responsible for innate immune signalling is genetically conserved from *Drosophila* fruit flies to mammals. Mutations in the innate immune system can be significant, with defects in key proteins predisposing patients to a range of infections, such as pyogenic bacteria[2-6]. As many of these proteins are of such importance, loss of function is often lethal or age-limiting[7].

1.1.2 The inflammatory Response

Upon activation of the immune system by infection or tissue damage, inflammation is initiated to co-ordinately eliminate a pathogen and restore tissue homeostasis. This is accomplished by utilising a range of mechanisms which control the organism at different levels including regulation of immune cell composition in tissues, cell responsiveness to inflammatory stimuli, gene expression, and cellular metabolism and signalling[8].

Immediately after an inflammatory stimulus, signalling results in activation of transcription factors which often reside in the cytoplasm in an inactive state. These then translocate to the nucleus and bind target gene sequences to promote their expression. NF-κB induces expression of inflammatory cytokines including IL-1β, IL-6 and TNFα, whilst the IRFs induce interferons (IFNs). These cytokines are then secreted and bind their cognate receptors in either an autocrine or paracrine manner, themselves triggering signalling pathways which ultimately induce wide-scale alteration of gene expression. Whole gene modules are targeted which control key biological processes such as cell survival and proliferation, migration, differentiation, tissue regeneration, co-ordination of the adaptive immune system and production of antimicrobial products[9].

1.1.3 PRR discovery

Molecular understanding of pathogen sensing began after work by Jules Hoffman's lab in 1996[10] uncovered a critical role for the *Drosophila* Toll receptor in providing antimicrobial ability to adult flies; knock out of this resulted not only in defective development, but also lethal susceptibility to fungal infection. This work laid the path for uncovering the modern biochemistry of innate immune signalling. We now know that activation of the innate immune system relies upon stimulation of a range of germline-encoded receptors similar in function to Toll, known as Pattern Recognition Receptors (PRRs). A plethora of human receptors have been described, with new additions being frequently proposed[11].

1.1.4 PAMPS

Although it was originally thought that these receptors are relatively non-specific as they are not clonally distributed like receptors of the adaptive system, evidence from mouse

studies confirmed that each receptor does indeed possess specificity to distinct features of pathogens, known as Pathogen-Associated Molecular Patterns (PAMPS)[11]. These PAMPS are usually critical features of the pathogen which are therefore difficult for the microorganism to modify or mutate.

Cells are equipped with a number of different families of PRRs which can bind PAMPS such as nucleic acids, proteins, carbohydrates, or lipids. These include plasma or endosomal membrane-bound Toll-like Receptors (TLRs), cytosolic RIG-I-like receptors (RLRs), DNA sensors (CDSs) and NOD-like Receptors (NLRs), and recently proposed nuclear receptors such as IFI16[12]. Upon these receptors binding their cognate ligands, an inflammatory response is initiated to eliminate the pathogen.

It is important to note that PRR responses are also crucial for a natural homeostatic state, particularly for intestinal maintenance[13,14]. In addition to microbial ligands, many PRRs can also bind aberrant endogenous factors and molecules released during necrosis in order to protect the organism's integrity and regulate sterile inflammatory processes[15]. These moieties are known as damage associated molecular patterns (DAMPS) and include ATP, HMGB1[16] and heat-shock proteins[17] among many others. Importantly, genomic dsDNA released upon cell death can act as a DAMP which is sensed by PRRs to induce a potent inflammatory response and maturation of Dendritic Cells (DCs)[18].

1.2 Toll-like receptors

1.2.1 TLR structure and location

The best characterised group of PRRs are the TLRs which are type I integral membrane glycoproteins that share common functionality with IL1-R. At present, there are 11 known human and 13 mouse TLRs, each detecting a different PAMP (Table 1.1). Multidisciplinary approaches which integrate transcriptomics, genomic profiling, small-molecule screening and phosphoproteomic studies have significantly contributed to recent progression in understanding TLR signalling[19].

Expression of TLRs is focussed primarily on immune cells such as dendritic cells, macrophages, B-cells and occasionally T-cells, but some fibroblasts and epithelial cells may also express a select repertoire[11]. Structurally, TLRs comprise of extracellular domains which contain varying numbers of leucine-rich repeat (LRR) motifs which facilitate ligand binding[20]. In the case of TLR3, it was shown that its RNA ligand binds the outermost surface of TLR3's convex horseshoe shape. TLRs also possess a cytoplasmic Toll/IL-1R homology (TIR) domain that is responsible for intracellular signalling[21]. Many TLRs reside at the cell surface (TLRs 1, 2, 4, 5, 6, 11) where they encounter extracellular pathogens, but others reside in endosomal and endo-lysosomal compartments (TLRs 3, 7, 8, 9), into which their often-nucleic acid ligand must be internalised to induce signalling. This spatial organisation is important not only for ligand access, but also to control self-discrimination in prevention of inflammation[22].

TLR	Ligand	Localisation	Ligand origin
TLR1	Triacyl Lipopeptides	Plasma membrane	Bacteria
TLR2	Diacyl lipopeptides Lipoteichoic acid Zymosan Peptidoglycan	Plasma membrane	Bacteria Viruses Fungi Trypanosomes
TLR3	dsRNA	Endosome	Viruses
TLR4	Lipopolysaccharide	Plasma membrane/ endosome	Bacteria
TLR5	Flagellin	Plasma membrane	Bacteria
TLR6	Diacyl lipoprotein	Plasma membrane	Bacteria Fungi
TLR7	ssRNA	Endosome	Viruses
TLR8	ssRNA	Endosome	Viruses
TLR9	CpG DNA	Endosome	Bacteria Viruses Protozoa
TLR10	Unknown	Endosome	Unknown
TLR11	Profilin-like molecule	Plasma membrane	Bacteria Protozoa

Table 1.1 TLRs and examples of their ligands derived from microbial pathogens. Subcellular localisation is also displayed, along with the origin of each ligand.

1.2.2 TLR signalling – adaptor molecules

Stimulation of TLRs prompts hetero- or homodimerisation in addition to conformational changes which lead to the recruitment of cytosolic TIR-containing adaptor molecules that interact with the TLR's cytoplasmic TIR domain. Dependent upon which TLR is activated, a specific adaptor molecule is recruited. Broadly, this is divided into activation of MyD88-dependent or MyD88-independent pathways. There are four primary adaptor molecules including MyD88, TIRAP[23], TRIF, and TRAM[24]. It is the selectivity in recruitment of these adaptors after TLR stimulation which establishes distinct signalling pathways and a fine-tuned inflammatory response.

1.2.3 MyD88-dependent signalling

Signalling via MyD88 is critical for NFκB activation and pro-inflammatory cytokine production (Figure 1.1). MyD88 is recruited after activation of all TLRs except TLR3, in addition to its co-adaptor TIRAP upon TLR2 and TLR4 stimulation[25,26]. MyD88 then binds IRAK4 via homophilic Death-domain (DD) interactions. IRAK1 and IRAK2 are recruited to and phosphorylated by IRAK4 before associating with TRAF6. TRAF6 adds K63-linked polyubiquitin chains to itself, IRAK1 and NEMO using its E3 Ubiquitin ligase activity, in a process facilitated by the CARD domain-containing protein Bcl-10 and the E2 ligases Uev1A and Ubc13[27-29]. Shortly after, TAK1 and its regulatory binding proteins TAB2 and TAB3 are recruited to phosphorylate IKK-β[30]. This finally induces the activation of the NFκB complex via phosphorylation and degradation of IκB proteins, permitting translocation of the active NFκB components p65 and p50 to the nucleus where they induce the expression of genes with pro-inflammatory roles. Simultaneously, TAK1 facilitates phosphorylation of MAPK kinases (MAPKKs), which then activate their MAPK substrates such as p38, JNK, ERK1 and ERK2. These in turn activate other transcription factors such as AP-1 and also control translation events[31].

In addition, TLR7 and TLR9 function through MyD88 to produce type I IFN as well as NFκB-dependent cytokines. Experiments in plasmacytoid Dendritic cells (pDCs) demonstrated that a complex between MyD88, IRAK1, TRAF3, TRAF6, IKKα and IRF7 forms, leading to nuclear translocation of IRF7 and induction of type I IFN. In myeloid-derived dendritic cells, IRF1 and not IRF7 is activated, resulting in only IFN-β production[32].

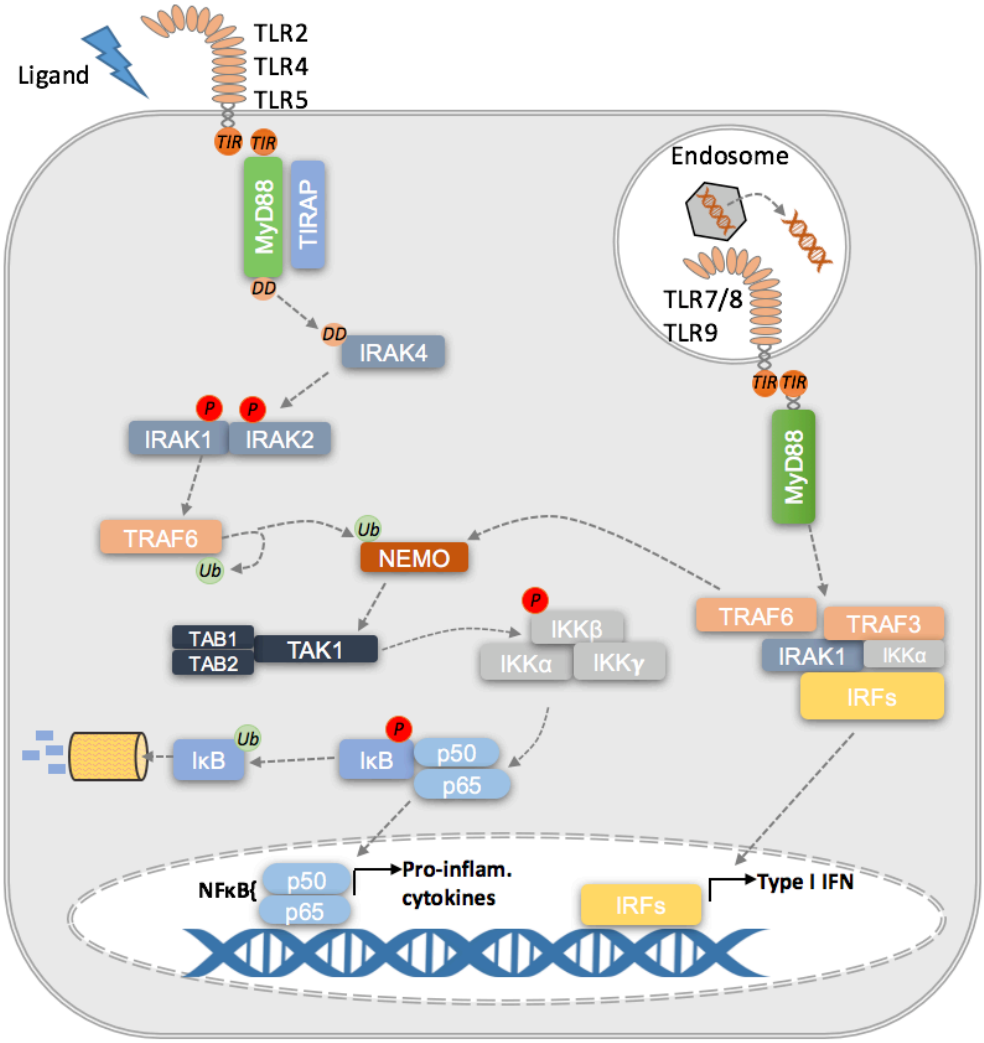

Figure 1.1 MyD88-dependent signalling. Surface TLRs such as TLR2, TLR4 and TLR5 engage their cognate extracellular ligand and induce MyD88 signalling via TIR domain interactions. MyD88 then recruits TIRAP and interacts with IRAK4 via DD homotypic interactions. IRAK1 and IRAK2 are phosphorylated, leading to activation of TRAF6, which self-ubiquitinates and also ubiquitinates NEMO. NEMO then activates TAK1, which phosphorylates IKKβ, leading to phosphorylation and proteasomal degradation of IκB. NFκB subunits p50 and p65 then translocate to the nucleus and induce expression of pro-inflammatory cytokines. Endosomal TLRs such as TLR7/8 and TLR9 bind internalized nucleic acid ligand and recruit MyD88. A complex containing TRAF6, TRAF3, IRAK1, IKKα, and certain IRFs (IRF1, 3, 5, or 7). The IRFs translocate to the nucleus and induce expression of type I IFN, whilst TRAF6 intersects back at signalling through NEMO, progressing signalling as surface TLRs do activate NFκB and induce expression of pro-inflammatory cytokines.

1.2.4 MyD88-independent (TRIF) signalling

After TLR3 or TLR4 bind their cognate ligands, the TIR-containing adaptor TRIF may be recruited to the receptor in place of MyD88 (Figure 1.2). Upon TLR4 activation, which also induces MyD88-dependent signalling as above, TRAM is additionally required when TRIF is recruited. Unlike MyD88, TRIF recruits TRAF6 directly. TRIF also recruits the adaptor RIP1 which itself binds the adaptor TRADD. TRADD then mediates K63-linked polyubiquitination of RIP1 when in concert with Pellino1[33,34]. The TRIF, TRAF6, TRADD, Pellino-1 and RIP1 complex activates TAK1, which then functions downstream as it does in MyD88 signalling to promote NFκB activation[31].

Additionally, TRIF signalling leads to IRF3 activation, making it integral for type I IFN production. The activation of IRF3 by TRIF relies heavily on TRAF3, with deficiency resulting in abrogated IFN-β production upon TLR3 activation[35]. TRAF3 then recruits IKKε and TBK1, which catalyses the phosphorylation of IRF3 to allow it to dimerise and translocate to the nucleus to induce type I IFN production. TRAF3 is also utilised for induction of IFN upon activation of TLR7, TLR9, CDSs and RLRs which do not function through TRIF, suggesting that TRAF3 is universally significant in IFN-β production[35].

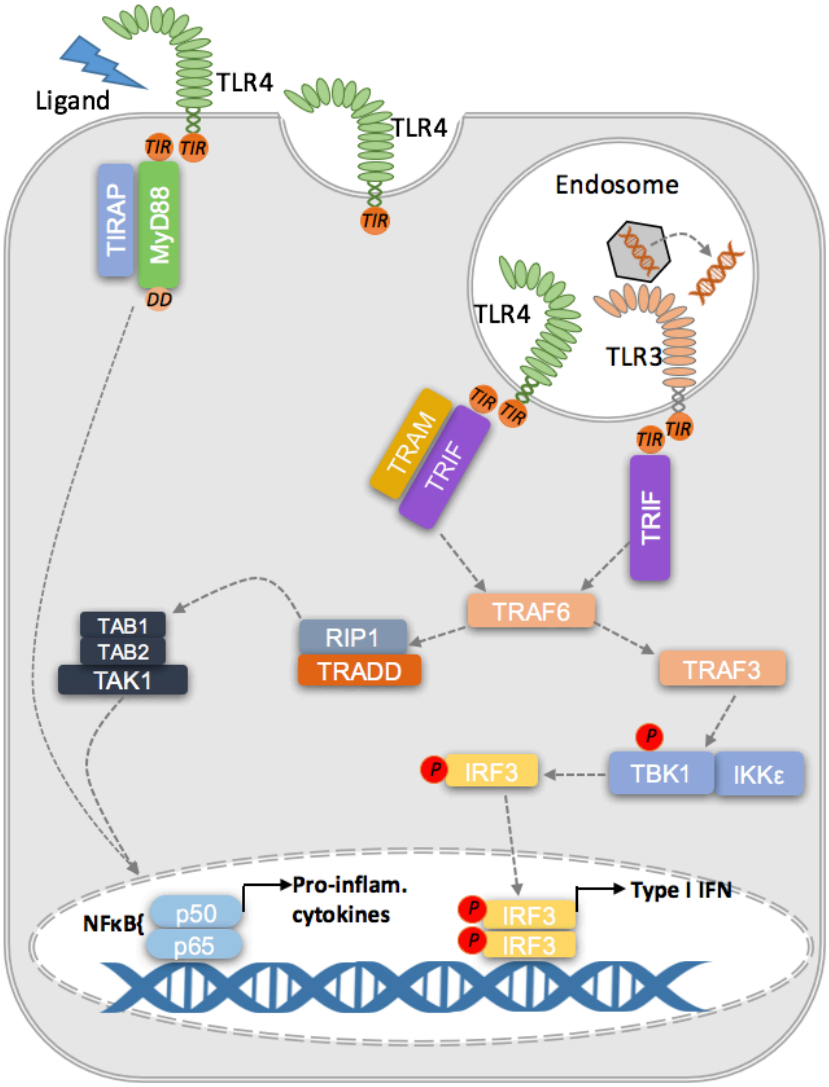

Figure 1.2 MyD88 independent signalling. TLR4 can signal via MyD88 from the cell surface. After this, TLR4 is endocytosed to endosomal compartments, where it can alternatively recruit TRIF via TIR interactions, in addition to TRAM. In these compartments, TLR3 activation also leads to the recruitment of TRIF, which recruits TRAF6. TRAF6 binds the adaptors RIP1 and TRADD, which activate TAK1 to promote NFκB activation as with MyD88-dependent signalling. TRAF6 also binds TRAF3, which recruits TBK1 and IKKε. TBK1 is phosphorylated, leading to phosphorylation and dimerisaton of IRF3, which translocates to the nucleus and induces expression of type I IFN.

1.3 Cytosolic PRRs

1.3.1 RIG-I-like Receptors

RLRs are one of many cytosolic PRRs families. It's main constituents are RIG-I itself and MDA5[36]. Structurally, they share N- terminal caspase recruitment (CARD) domains and DExD/H-box RNA helicase domains, followed by a C-terminal domain (CTD) responsible for regulatory functions. These receptors are responsible for sensing both genomic dsRNA and RNA intermediates of viral replication as non-self, potently inducing type I IFN production[37]. Each receptor has slightly different requirements in its choice of ligand; RIG-I binds relatively short stretches of RNA (<1kb) with preference for 5' triphosphorylation[38], whilst MDA5 detects longer dsRNA (>2kb) with more complicated tertiary structures[39]. As a result, each receptor recognises a distinct repertoire of RNA viruses, with some viruses requiring activity of multiple RLRs for an effective IFN response[40].

PAMP detection by RLRs induces ATPase-driven conformational changes to allow recruitment of the adaptor MAVS, analogously to MyD88 and TRIF in TLR signalling (Figure 1.3). MAVS resides at the outer mitochondrial membrane, and once activated forms prion-like aggregates[41]. TRAF3 and TRADD are then recruited and signal as they do downstream of TRIF signalling, to produce type I IFN and inflammatory cytokines.

1.3.2 Cytosolic DNA Receptors

In addition to extracellular CpG-rich unmethylated DNA being sensed by TLR9, the cell employs multiple cytosolic receptors for detection of intracellular DNA. Introduction of exogenous dsDNA into cells (which should otherwise largely be restricted to the nucleus), of synthetic, bacterial or viral origin often results in activation of the adaptor STING which

resides on ER membranes[42] (Figure 1.3). STING then translocates to the Golgi apparatus before interacting with TBK1 which phosphorylates IRF3 to permit type I IFN production. Unsurprisingly, loss of STING severely impairs type I IFN production[43] and renders cells susceptible to infection from DNA viruses such as HSV1 and Adenovirus[44].

Interest in STING was boosted when it was found to directly bind 3'-5' linked cyclic dinucleotides (CDNs) of bacterial origin, which can act as second messengers in multiple bacterial processes including their virulence and biofilm formation[45]. Upon binding CDNs, STING induces TBK1 and subsequent IRF3 activation (Figure 1.3). Quantitative Mass Spectrometry revealed a new member of the OAS-like DNA receptors, cyclic GMP-AMP synthase (cGAS)[46], which binds dsDNA directly and catalyses the formation of 2'-3' cyclic GMP-AMP (cGAMP) from ATP and GTP[47]. cGAMP then functions as an endogenous second messenger to activate STING, with far greater potency than bacterial CDNs[48]. A widespread necessity for STING activation in DNA sensing was thus uncovered. Removal of cGAS renders cells largely incompetent in type I IFN production in response to exogenous DNA transfection or DNA virus infection, whilst mice are sensitised to HSV1 lethality[49]. It was recently shown that cGAMP is packaged into viruses before they exit an infected cell, allowing rapid activation of STING in any subsequently infected cell[50,51]. Similarly, cGAMP can also be transferred to neighbour cells horizontally via gap junctions to help prepare surrounding cells before they are infected[52].

RNA Polymerase III is a proposed DNA sensor with a unique mechanism. It binds AT-rich DNA sequences in the cytosol and transcribes them into RNA for detection by RIG-I, thereby providing a link between DNA and RNA-sensing pathways to maximise the cell's sensing capabilities[53].

Another family of cytoplasmic DNA sensors is the AIM2-like receptors, including IFI16 which functions via STING as above[54]. In contrast to the heavily-studied IFN response to dsDNA, AIM2 itself interestingly bypasses STING and IFN production, instead partaking in inflammasome formation to promote IL1-β production and pyroptotic cell death[55].

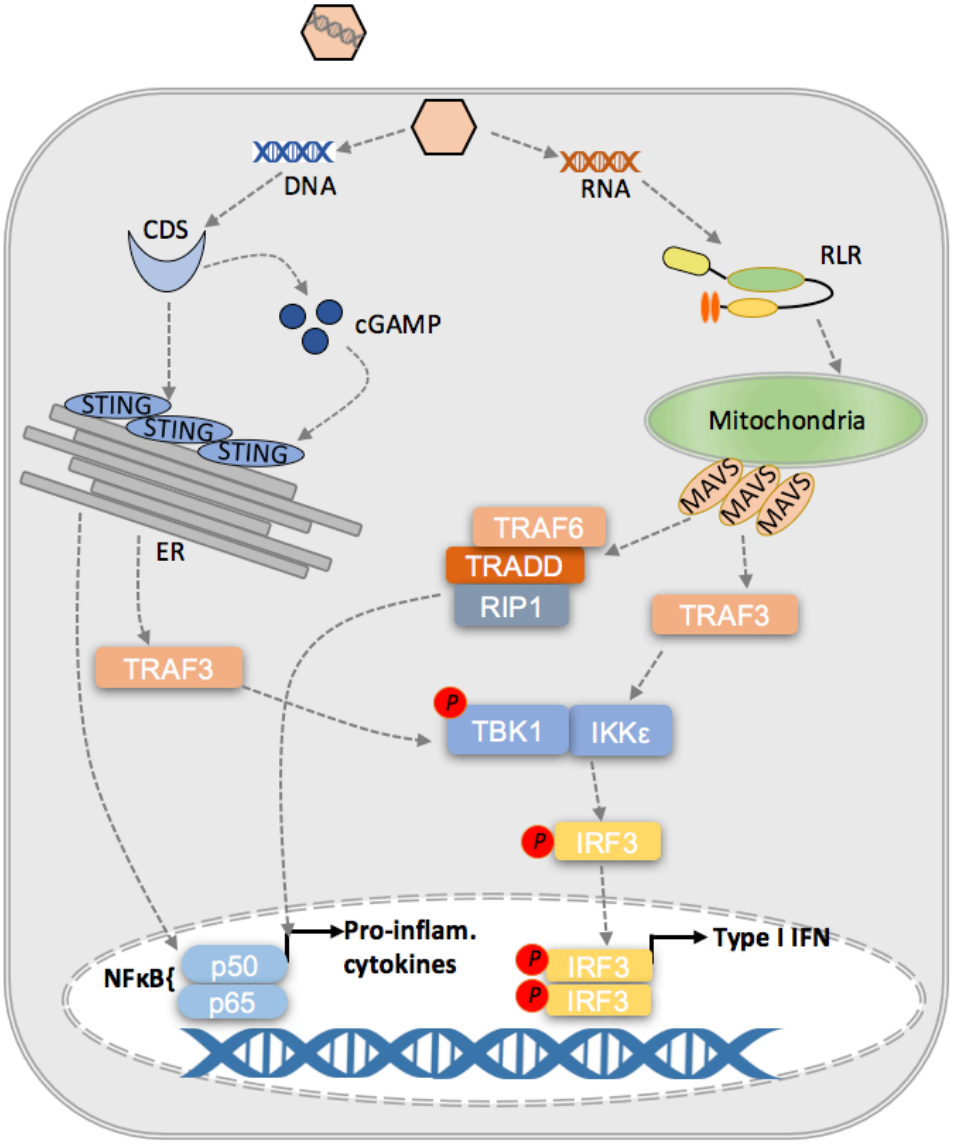

Figure 1.3 RLR and CDS signalling. Upon viral infection, sensing of the DNA or RNA genome activates CDSs or RLRs, respectively. ER-localised STING can be activated after cGAMP production by cGAS, or directly by other receptors. STING then signals via TBK1 to induce type I IFN and also NFκB-controlled pro-inflammatory cytokines. Sensing of viral RNA by RLRs induces MAVS oligomerisation at the mitochondria. This also functions via TBK1 to induce type I IFN and simultaneously promotes NFκB-mediated cytokine production

1.3.3 NOD-Like Receptors and inflammasomes

NLRs are cytoplasmic PRRs which share a central nucleotide-binding oligomerisation domain (NOD) and a C-terminal LRR domain[56]. The currently-identified 22 members of this family are divided into four subsets based on variation in their N-terminal domain. These are the NLRAs, NLRBs (NAIPs), CARD domain-containing NLRCs, and the NLRPs which contain a pyrin domain[57]. NLR complexes which can recruit caspase 1 and the adaptor ASC are known as inflammasome-inducing. These include NLRP1, NLRP3, NLRP6 and NLRC4 to name few (reviewed in[58]). Activation of inflammasome complexes results in formation of large ASC multimer 'specks'[59], prompting self-cleavage and activation of pro-caspase 1 which then cleaves pro-IL-1β and pro-IL-18 to their active form[60,61]. Other NLRs such as NOD1 and NOD2 do not induce inflammasome formation, but function via NFκB, IRFs and MAPKs[57].

Suggested ligands for NLR activation vary wildly in their nature, ranging from chemical compounds and bacterial moieties[62-64], to lysosomal and mitochondrial stress[65-68] as well as metabolic disruptions[69]. It is therefore unlikely that all of the NLRs are directly involved in specific ligand binding, and sensing cofactors are probably required in each case. Single nucleotide polymorphisms (SNPs) in NLR genes are reflected in a wide variety of human diseases, including increased susceptibility to infection or Crohn's disease[57].

1.3.4 Nuclear receptors (?)

The DNA binding protein IFI16 is a PYHIN protein found in the nucleus, and has been reported to have a role in IFN-β production in response to HSV1[54]. More importantly, this propositions IFI16 as the first viral DNA sensor to function in the nucleus[12,70]. However, controversy surrounds this, as other groups have failed to reproduce these results[71],

showing only cytosolic binding of IFI16 to viral DNA[72]. One such caveat of IFI16 acting as a true nuclear dsDNA sensor stems from the recently solved structure of its ligand-binding HIN domain in complex with dsDNA[73], which demonstrates binding of DNA is a sequence-independent event; contacts are formed only with the sugar phosphate backbone of DNA. Therefore, if IFI16's DNA binding activity is IFN-stimulatory, host genomic DNA would be activating and this could cause catastrophic auto-inflammatory responses. Nevertheless, another PYHIN family member which resides in the nucleus, IFIX, has also been reported to bind HSV1 genomic DNA in the nucleus and influence type I IFN production[74]. It is conceivable that IFI16 requires a sequence-specific co-factor which allows discrimination between self and non-self DNA in the nucleus, but such activities would have to be subject to the highest levels of regulation. The proposal itself does however aim to shift the paradigm of cytosolic sensing exclusivity, as most DNA viruses do replicate their genomes in the host nucleus.

1.4 Interferon signalling

1.4.1 Type I-IFN

Type I IFNs are made up of multiple IFNα subtypes, a single IFNβ molecule and several poorly defined gene products[75]. They are produced downstream of IRF activation, and once secreted they bind to heterodimeric IFN-associated receptors (IFNARs) (Figure 1.4), the importance of which has been heavily documented in murine studies[76].

Binding to their cognate receptors induces secondary intracellular signalling (reviewed in[77]), which begins with activation of Janus Kinase 1 (JAK) and tyrosine kinase 2 (Tyk2). Signal transducer and activator of transcription 1 (STAT1) and STAT2 are then phosphorylated and dimerise before translocating to the nucleus, where they bind IRF9 to form a complex known as IFN stimulated gene factor 3 (ISGF3). The ISGF3 complex binds to interferon stimulatory response element (ISRE) sequences in the promoter regions of interferon stimulated genes (ISGs), which are then expressed and act to restrict pathogen replication.

The actions of type I IFNs are not limited to cell intrinsic responses, as they can also direct natural killer (NK) cell activation[78], as well as B-cell[79,80], T-cell[81,82] and myeloid cell activity to enhance the immune response. They also have been shown to influence the differentiation of DC precursors[83,84], as well as their maturation[85].

1.4.2 ISGs

Several hundred genes possess ISRE sequences, whose gene products work to restrict the replication of pathogens (Table 1.2), particularly viruses. Dependent on the pathogen, the cell induces expression of distinct subgroups of ISGs to restrict specific microbes, adding

further specificity to the response initiated[86]. In response to viral infection, these ISGs induce an 'antiviral state' within the cell, co-operating to target all stages of a virus life cycle including entry and uncoating, replication, assembly and egress. They do this by targeting both the virus directly, or by targeting host mechanisms which are hijacked to facilitate viral replication such as protein translation and nucleotide synthesis (reviewed in[87]).

ISG15 is a well-studied ISG which can be catalytically added to substrate proteins to act as an activating mark, similar to the ubiquitin modification[88,89]. This addition induces general antiviral signalling, including IFN and inflammatory cytokine production[90,91]. MxA is an important ISG which is induced to limit viral release; it surveys exocytic events and mediates vesicle trafficking to segregate viral components in order to prevent final assembly and egress[92]. 2'-5' oligoadenylate synthetase (OAS) on the other hand is part of a set of ISGs which is constitutively expressed at low levels, but is increased upon IFN signal transduction[93,94]. This particular ISG can catalyse a unique 2'-5' linked phosphodiester bond formation to add ATP oligomers onto adenosine. This species then activates a resting form of RNaseL which degrades dsRNA[95], for example of viral origin. The products of this can then further activate other PRRs[96]. RNaseL-deficient mice are thus unsurprisingly susceptible to infection by viruses with RNA genomes[97,98]. Another constitutively expressed ISG that is activated by dsRNA is protein kinase R (PKR). This protein dimerises and phosphorylates the eukaryotic initiation factor 2A (eIF2A), reducing protein translation to abrogate viral replication capacity[99].

Almost all viruses expend a large proportion of their genetic economy to antagonise IFN and ISG signalling, illustrating the importance of these in protecting from viral infection[100]. In brief, they employ a few main strategies to antagonise host defence proteins. These

include inhibition of gene expression, sequestration of IFN-signalling molecules, and proteolytic cleavage or proteasomal degradation of signalling or effector molecules[100]. This agonism and antagonism of effector proteins by host and virus can be traced as far back as evolutionarily possible[101], and will most likely continue as long as we co-exist.

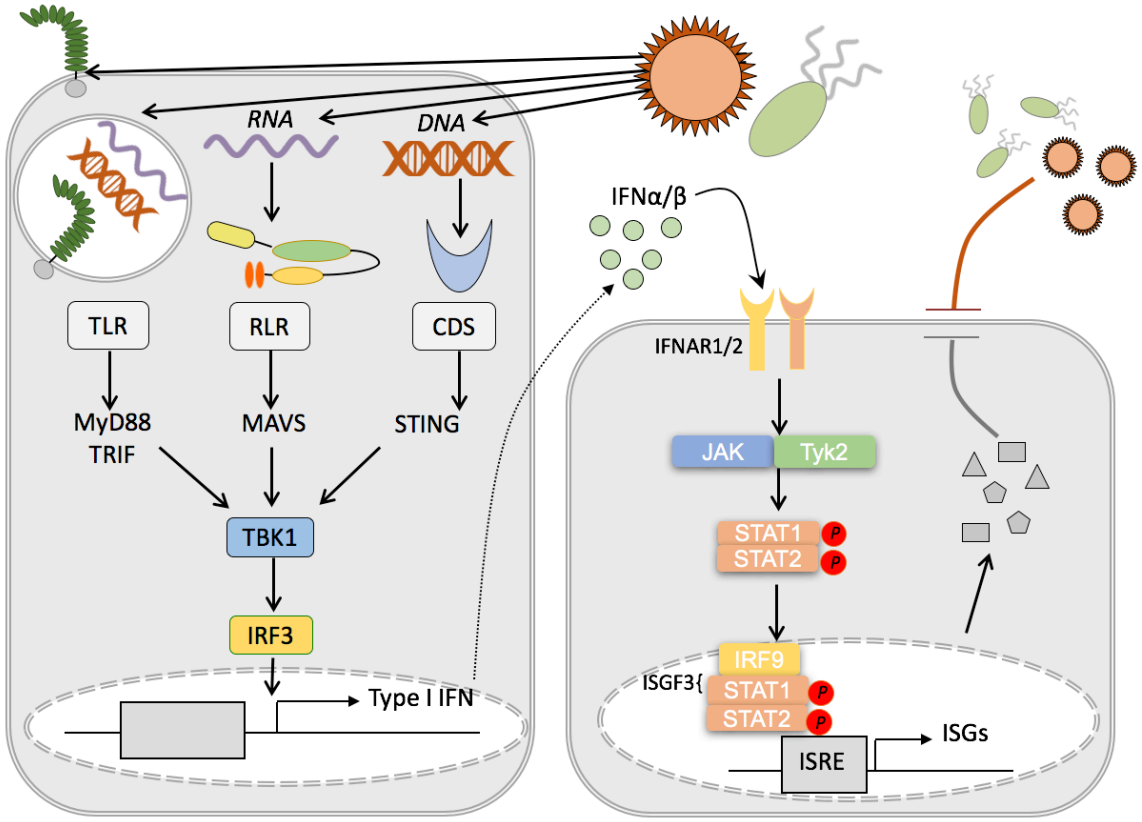

Figure 1.4 IFN production and signalling. Type I IFN produced downstream of TLR, RLR or CDS activation is secreted and binds its cognate receptors at the cell surface in an autocrine or paracrine manner. IFNAR1 and IFNAR2 form a heterodimer which induces activation of intracellular JAK and Tyk2. STAT1 and STAT2 are then phosphorylated and dimerise, before translocating to the nucleus and binding IRF9 to form the ISGF3 complex. This binds to ISRE sequences in gene promoters and induces their expression.

ISG	Antiviral Mechanism
ADAR	Converts adenosine to inosine via deamination, disrupting A:U pairing and reducing RNA stability.
PKR	Downregulates eIF2A to reduce translation of viral components
ISG15	Ubiquitin like molecule used to coat proteins to modulate their activity. Both cellular proteins and viral proteins identified as targets (ISGylation)
MX1	Part of the dynamin-like GTPase family. Forms ordered oligomers, but exact antiviral mechanism unknown
OAS1	Catalyses the formation of 2'-5' linked oligomers which activate RNase L to degrade viral genome
Viperin	Perturb lipid rafts to prevent viral egress
TRIM5	Recognises incoming viral capsid, intereferes with uncoating and promotes inflammatory signalling
TRIM25	E3 Ubiquitin ligase which ubiquitinates RIG-I to induce its signalling

Table 1.2 ISGs and their activity. List of well-studied ISGs and their mechanism of action. Adapted from[102].

1.5 Regulation of PRR signalling

1.5.1 Cellular Regulation

To mediate the balance between an elastic yet specific immune response with minimal collateral damage, the innate immune response has evolved several regulatory mechanisms. The largest scale comes at the cellular level, with specific cells possessing specific receptors and pathways. For example, almost all cells express nucleic acid sensing pathways and MHC I machinery to raise alarm after viral challenge. Conversely, most TLRs are reserved for expression in Antigen-presenting cells (APCs) and some epithelial cells[31], presumably to limit inflammatory responses against commensal bacteria. Similarly pDCs and inflammatory monocytes possess unique antiviral signalling pathways not found in other cells[103]. The location of cells is also regulated to facilitate appropriate sensing of pathogens.

1.5.2 Transcriptional regulation

In addition to regulation of gene expression by NFκB, IRFs, IFN and inflammatory cytokines as discussed above, epigenetic control exists in innate immune signalling. Histone modifications which both negatively and positively regulate expression of key immune proteins allow an added layer of security on gene segments, by restricting factors which can engage and alter gene expression[104,105].

1.5.3 Spatiotemporal Regulation

As alluded to, PRRs localise optimally for ligand accessibility. Additionally, nucleic acid-sensing TLRs such as TLR3 and TLR9 are restricted to specific compartments to prevent

self-detection. In a unique case, TLR4 signalling can progress via both the MyD88-dependent and independent pathways[106,107] (Figure 1.2). This feat is the result of an exquisite temporal and spatial regulation of TLR4 itself. It initially functions via MyD88 and TIRAP from the plasma membrane to activate NFκB and MAPK before it is endocytosed to an endosomal compartment[108], where it signals via TRIF[109] and TRAM[110] to induce type I IFN and late-phase NFκB signalling. Similarly, it is now thought that other key proteins in innate sensing pathways relocalise during signalling, including STING[43]. Concurrently, many adaptors and downstream signalling molecules need active recruitment to the receptor for full activation, thereby preventing constitutive activation and auto-inflammatory diseases.

1.5.4 Post-Translational modifications

Multiple methods are used by the cell to conditionally amplify or dampen PRR-mediated signalling. Post-translational modification of signalling molecules is arguably the most important feedback mechanism used. For example, phosphorylation events are crucial for kinase cascade progression and amplification of downstream of PAMP sensing[111], whilst phosphatases such as SHP1 and SHP2 can negatively regulate TLR activation[112,113]. Ubiquitination is another key modification which can be activatory or inhibitory (reviewed in[114]); K63-linked polyubiquitination of RIG-I by TRIM25[115] or RNF135[116] is required for its activation, whilst inhibition of this by CYLD prevents its antiviral activity[117]. Similarly, STING activation at the ER and recruitment of TBK1 requires K27-linked polyubiquitination[118], whilst K48-linkages can negatively regulate the antiviral response by inducing proteasomal degradation of modified proteins[119]. Deubiquitinases play just an equally important opposing role; for example, Deubiquitinating enzyme A (DUBA) removes K63-lined chains

from TRAF3, suppressing type I IFN production[120]. TLRs themselves are also subject to ubiquitination events; immediately after PAMP sensing, they can be targeted for degradation to terminate inflammatory signalling. In the case of TLR4, this can either be by direct lysosomal trafficking and degradation[121], or via proteasomal degradation after ubiquitination[122].

Further increasing complexity is the addition of the ubiquitin-like protein SUMO, termed SUMOylation, which can result in competitive protection from Ubiquitin-mediated degradation as is the case when added to IκBα[123]. Other modifications have also recently been identified as important regulators of immune activity; acetylation of MKP1 was shown to lead to inhibition of MAPK responses[124], whilst negative regulation of cGAS by glutamylation has very recently has opened up another new PTM field[125].

1.5.5 Crosstalk and synergy

Given that many PRR-induced pathways have relatively independent yet overlapping signalling, they must co-operate to achieve an appropriate response. This may be as part of either a synergistic or antagonistic relationship. Synergy is a common phenomenon in PRR activation which is used to give an amplified response as opposed to an additive response when multiple receptors are activated. In the case of TLR2, functionally distinct heterodimers may form with TLR1 or TLR6 depending on the ligand bound[126]. A combination of TLR2 and TLR4 stimulation with TLR7, TLR8 and TLR9 increases IFNγ/IL-12 production and polarises DCs to a T-helper 1 (T_H1) response[127]. Similarly, TLR2 and NOD2 have a historical synergism which has now been utilised for adjuvant vaccine therapy[128].

PRR co-operation is also seen between TLRs and inflammasomes. Two signals are required for functional IL-1β to be secreted; the first can be initiated by TLR activation, inducing

NFκB-mediated pro-IL1β production. The second signal then often comes from activation of NLRP inflammasomes such as NLRP3, which can recruit caspase 1 to cleave pro-IL1β to its active form for secretion[58]. TLR activation further enhances this as NFκB activity promotes NLRP3 expression, increasing any downstream effect on IL-1β production[129].

Inflammatory crosstalk and regulation can also be achieved temporally in a more direct manner. After TLR4 has been stimulated and is endocytosed to an endosomal compartment, the E3 Ubiquitin-ligase Nrdp1 targets the previously-activated MyD88 for degradation, whilst simultaneously potentiating TBK1 activation to promote an IFN response via TRIF signalling[130]. On the other hand, MyD88-dependent signalling induces K48-linked polyubiquitination of TRAF3 and its proteasomal degradation, reducing type I IFN production whilst increasing MAPK activity and production of inflammatory cytokines[131].

1.5.6 Aberrant PRR activation

As discussed, inflammatory signalling can alter gene expression of thousands of genes in an infected or bystander cell, whilst also directing the adaptive immune system. If the above regulatory systems are defective or fail, the over-activation of inflammatory signals may cause considerable auto-immune damage to the host. Excess cytokine and chemokine production may activate lymphocytes which can promote B and T-cell responses, in some cases against self-antigens. In an attempt to exploit the mechanism behind these diseases, TLR ligands are now used as vaccine adjuvants in addition to antigens to increase antibody responses[132].

Although cells attempt to strictly differentiate between self and non-self nucleic acids to avoid auto immune disease, TLR7 and TLR9 have been reported to induce autoantibody

generation, likely after sensing endocytosed DNA fragments from necrotic cells which have bound other DAMPS such as HMGB1[133] or antimicrobial peptides[134]. Similarly, endogenous RNA-protein complexes can activate DCs and autoreactive B-cells via TLR9 to produce more IFN[135], thereby amplifying the autoimmune effect.

So called interferonopathies (reviewed in[136]) most-notably include Aicardi-Goutières syndrome (AGS), which is characterised by fatal encephalopathy and an increased IFN signature in peripheral blood[137]. This can result from mutations most notbaly in RNase H2[138], SAMHD1[139], or most commonly the 3' exonuclease Trex1[140]. Mutations in these genes or others linked to this disease were shown to permit accumulation of endogenous retroviral DNA which is sensed by CDSs, inducing excess type I IFN[141]. Systemic lupus erythematosus (SLE) also presents a similar yet milder phenotype, with overlapping clinical presentation and underlying genetic risk factors[142,143]. In addition to self-pathogenesis, excess IFN can also exacerbate viral and bacterial infection as a result of specific immunosuppressive actions or tissue damage[144]. This has even been suggested to enable higher viremia during HIV infection[145] in addition to suppressed T-cell responses[146,147]. Increased susceptibility to *Listeria monocytogenes* among other pathogens has also been linked with excess IFN production[148].

Polymorphisms resulting in truncated NOD2 are a strong genetic risk factor for Crohn's disease, an inflammatory bowel disorder with various proposed models of pathogenesis[149]. One concept is that of dysregulated inflammatory responses to intestinal bacteria as a result of NOD2 malfunction, resulting in over-compensatory mechanisms against non-pathogenic bacteria to create a hyperinflamed state[150] .

1.6 TBK1

1.6.1 TBK1 structure and function

TBK1 is a crucial IKK-related protein which helps to bridge the activation of multiple PRRs to type I IFN production. It is highly evolutionarily conserved in mammals, with 99% sequence homology seen between human and mouse homologues, illustrating its biological importance. Biochemically, TBK1 is composed of an N-terminal kinase domain, a ubiquitin-like domain, a dimerisation domain and C-terminal interaction domain which contains a leucine zipper region and a helix-turn-helix motif[151,152]. Many PRRs are known to utilise TBK1 for IFN production including TLRs, RLRs and CDSs[153]. Once activated, TBK1 phosphorylates the upstream adaptor on a specific consensus motif, allowing recruitment of IRF3 via binding of its positively charged phospho-binding domain. TBK1 then phosphorylates IRF3[154] which dimerises and translocates to the nucleus where it binds ISRE sequences and induces the expression of type I IFN. TBK1 can also target IKKβ to influence NFκB signalling and inflammatory cytokine production[152]. Deficiency of TBK1 predictably results in decreased IRF3 DNA binding capacity and therefore decreased type I IFN production[155,156], leading to increased susceptibility to viral infection and secondary pathologies[157,158].

TBK1 has also been reported to have alternative antimicrobial functions; upon bacterial detection, it can regulate autophagic processes to influence the direct destruction of ubiquitin-coated bacteria in a process known as xenophagy[159,160]. This activity of TBK1 has been suggested to play a role in a range of pathologies, such as neurodegenerative diseases and cancer[161,162].

1.6.2 TBK1 signalling diversity

The ability of TBK1 to co-ordinate distinct inflammatory responses stems from its ability to form a multitude of protein complexes. It is specifically recruited to each individual adaptor molecule employed by its upstream PRR, including TRIF, MAVS, and STING[154], all of which signal to produce type I IFN.

The formation of microscopic TBK1-containing, stimulus-specific protein complexes on membranous compartments supports the notion that localisation of TBK1 can act as a regulatory platform for its signal transduction[41,43]. In the case of RLR and downstream MAVS activation, TBK1 is recruited to the mitochondrial outer membrane[154] with the help of IFIT3[163]. Activation of STING via dsDNA sensing however, recruits TBK1 to perinuclear ER/Golgi-derived microsomal organelles[43]. Therefore, spatial segregation of TBK1 from other known binding partners may influence its functional activity. For example, when TBK1-NAP[164] interactions are favoured over TBK1-IRF3, IFN production is decreased and xenophagy increased[159]. Thus, TBK1s involvement in distinct cellular processes is largely controlled by its binding proteins.

1.6.3 Regulation of TBK1 signalling

As a critical kinase involved in antiviral immunity, the activity of TBK1 must be tightly regulated. As with many other immune signalling proteins, this can be achieved by phosphorylation, ubiquitination, domain-modulation and prevention of active complex formation[153]. In steady state conditions, TBK1 associates with IKKε and SIKE, with the latter sterically inhibiting TBK1 activation and signalling. Upon PRR triggering, TBK1 trans-autophosphorylates at Serine 172[165], a process enhanced by association with glycogen synthase kinase 3β (GSK3β)[166]. SIKE then dissociates to allow signalling and production of

type I IFN[167]. Additionally, TRAF3 promotes the addition of activatory K63-linked polyubiquitin chains to TBK1 in concert with the E3 ligase Nrdp1[130]. After this signalling process has begun, NLRP4 activates the E3 ligase DTX4 which catalyses K48-polyubiquitination of TBK1, inducing its proteasomal degradation to restore inflammatory homeostasis[168,169]. TRAF-interacting protein (TRIP) also functions much the same[170]. In addition, TBK1 can be switched off by either by the SHP1 and PPM1B phosphatases[171,172], or by deubiquitinases such as CYLD which remove the activatory K63-polyubiquitin mark[173]. Likewise, RNF11 acts in concert with the A20 regulatory complex which consists of A20, TAX1BP1 and ABIN1 to antagonise TBK1's association with TRAF3, thereby blocking the addition of further activatory K63-linked polyubiquitin chains[174,175].

TBK1 catalytic activity is also tightly regulated; SHP2 directly binds to and inhibits the kinase domain of TBK1 to reduce its phosphorylation of IRF3[113]. Finally, interrupting TBK1 complex formation can also attenuate its activity. Overexpression of MIP-T3, which binds TRAF3, competitively inhibits TBK1-TRAF3 binding to attenuate downstream production of type I IFN[176]. Together, the numerous methods used by the cell to regulate TBK1 activity demonstrates the importance of this protein's activity in the cell.

Due to its key antiviral function, many viruses have developed elaborate strategies to antagonize and evade TBK1's potent IFN-inducing activity[153]. KSHV tegument protein ORF45 acts as a surrogate substrate for TBK1, reducing its phosphorylation of IRF7 and downstream IFN production[177]. Other viruses such as foot and mouth disease virus (FMDV) inhibit the activatory K63-linked polyubiquitination of TBK1[178]. Hepatitis C virus (HCV) and HSV1 encodes proteins that directly bind TBK1 to sterically prevent its association with IRF3[179,180]. TBK1-TRAF3 interactions are also targeted[181], as is TBK1 catalytic activity[182].

These examples demonstrate how viruses attempt to target TBK1 activity at all stages of its activity, signifying its importance in restricting viral replication.

1.6.4 Pharmacological inhibition of TBK1 activity

Like other immune signalling proteins, aberrant regulation or activity of TBK1 can lead to inflammatory diseases such as rheumatoid arthritis[183] and SLE[184]. In addition, neurodegenerative diseases[185] and oncogenesis[186-189] may transpire. There is therefore a requirement to develop highly-specific pharmacological inhibitors for therapeutic intervention in these pathologies. This method of TBK1 regulation could also provide a means to control interferonopathies caused by defects in upstream proteins such as Trex1[184]. A limited number of TBK1-specific small-molecule inhibitors have been developed, including BX795. This inhibitor has off-target effects on TAK1, JNK and p38 kinases[190] making it unsuitable for clinical applications. It does however, provide a valuable tool to complement RNAi-mediated study. Approaches to inhibit TBK1 have shown some promise translationally; inhibition of TBK1 using 'Compound II' reduced the IFN signature in both mice and SLE patient cells[184], whilst use of the anticancer drug SU6668 was also found to inhibit TBK1 and control its pro-angiogenic activity in cancer development[191].

1.7 Dendritic Cells

1.7.1 Dendritic cell activation

As so-called professional APCs, DCs derive from the bone marrow and reside in an immature state in local tissues, where they act as the first line of defence, scanning for pathogens using their high endocytic capacity and broad range of PRRs expressed. Once a pathogen is detected, PRR signalling cascades are initiated as outlined previously. Co-ordination of the adaptive immune system also ensues; of all the APCs, DCs are the most potent at orchestrating this[192].

Immediately after PRR stimulation, immature DCs begin the maturation process by reducing their antigen-capture activity. Peptide antigens are then created and loaded onto Major histocompatibility complex (MHC) molecules. MHC I molecules are loaded with endogenously-derived antigens, whilst peptides loaded onto MHC II are derived from exogenously internalised proteins. MHC I and II molecules themselves are also up-regulated and trafficked to the cell surface. Simultaneously, T-cell adhesion molecules (CD54, CD48) and co-stimulatory molecules (CD40, CD80, CD86) are upregulated. Together, this vast increase in cell surface residents gives rise to the morphological appearance of dendrites typically associated with DCs, hence their name.

A migratory phenotype is then developed by the DCs, characterised by secretion of soluble cytokines[193]. The DC traverses to the lymph nodes using its chemokine receptors such as CCR7, where it can engage a naïve antigen-specific T-cell with complimentary T-cell Receptor (TCR) to the MHC-peptide assembly[194]. The interaction between TCR and MHC-antigen complex occurs at the immunological synapse, a contact zone strengthened and facilitated by binding of adhesion and co-stimulatory molecule pairs such as CD86/CD28 and DC-SIGN/ICAM3, on DCs and T- cells respectively.

1.7.2 T-cell and B-cell activation by DCs

DC-mediated TCR triggering induces a signalling cascade that can polarise T-cells to form a longer term immune response against the pathogen. CD4+ T cells can differentiate into T_H1, T_H2, T_H17 or T_{FH} subsets which promote B-cell differentiation to antibody-secreting plasma cells, whilst T_{reg} cells can be induced to downregulate the function of other lymphocytes. Otherwise, naïve CD8+ T cells can be encouraged to differentiate into effector cytotoxic T-lymphocytes (CTLs). Non-activated immature DCs usually can present self-antigens to T-cells to promote immune tolerance via T-cell deletion or T_{reg} induction[195,196]. The response produced depends partly on the DC subset which has presented antigen[197], which itself can be influenced by other immune cells such as γδ-T cells, mast cells, stromal cells and their cytokine production[198]. For example, pDCs show incredible abilities in integrating all aspects of adaptive immune activation. They can produce high levels of IFNα, which accounts for rapid initiation of CD8+ T-cells in response to viral infection, whilst also inducing the maturation of other DC subsets, thereby influencing the expansion of different types of T-cell. Additionally, pDCs can co-ordinate B-cell differentiation into active plasma cells[199] via cytokine and cell-surface signalling in addition to presenting unprocessed antigens[200]. Mechanistically, the method behind this remains elusive.

1.7.3 Cross-presentation

All nucleated cells express MHC class I molecules, allowing presentation of endogenously derived peptides to activate CD8+ T-cell responses. This is crucial for inducing responses against pathogens and tumours by processing viral or mutated-self antigens. However, CD8+ T-cell differentiation to effector CTLs requires APC stimulation as above. This

presents an issue; if the APC is not itself infected or transformed, how can it present endogenous peptide to the CD8+ T-cell? DCs, and macrophages to a lesser extent, overcome this by using the unique ability of cross-presentation[201], a feature which allows loading of exogenous antigens onto MHC I molecules. The CD8+ T-cell transition to CTL can then proceed, in a secondary process known as cross-priming[202].

In cross presentation, it is thought that adaptation of normal MHC surface trafficking is used to load MHC I molecules with exogenous peptides. An early study showed that cross-presentation was sensitive to proteasomal inhibitors, suggesting that antigen reaches the cytosol[203] before being loaded in the classical MHC I pathway, relying upon TAP1/TAP2-mediated peptide trafficking into the ER. A recent report however suggests that TAP1 may be dispensable in this pathway[204], whilst another model suggests a vacuolar pathway of cross-presentation, as supported by proteasome inhibitor resistance and TAP-independence[205,206]. This idea proposes that antigen doesn't reach the cytosol and therefore is expected to be processed and loaded onto MHC in endocytic compartments. The exact mechanism of cellular sorting of antigen and MHC molecules is still largely unknown.

A clear inverse correlation exists between volume of antigen degradation and efficiency of cross presentation[207]; that is, cells more efficient at cross-presenting have decreased rates of antigen degradation. Therefore, lower proteolytic activity of DCs compared with other phagocytes provides insight as to why DCs are so effective in their cross-presenting ability. Certain subtypes may also have differing capabilities depending on their specialised function and location[208]. For example, knockout of ATF3 which confers lack of CD8+ and migratory CD103+ DCs, results in reduction in cross presentation and downstream antiviral and antitumour responses[209], demonstrating the importance of these cells in performing

this. Clinically, a lowered antigen-degradative phenotype and therefore induced cross-presentation activity, can be promoted with addition of type I IFNs[210], which encourages survival of key antitumour CD8+ DCs[211,212].

1.7.4 DCs in tumour immunology

The immune system employs multiple approaches in order to detect and eliminate neoplastic cells, together forming the immunosurveillance programme (reviewed in[213]). This has been shown to have sizeable dependence upon the ability of DCs to present tumour-derived antigens to T-cells[212]. Mouse models suggest that DCs utilise antigens released from both dead and alive cancer cells to cross-present to T-cells, promoting a tumour-specific CTL response[211,212]. In accordance with this, DCs can often be found in the tumour microenvironment, sampling for antigens released by the transformed cells. The DCs here can be activated by apoptotic and necroptotic markers such as ATP release and phosphatidylserine re-orientation[214], in addition to dsDNA released[215].

Contrastingly, tumours also possess mechanisms to interfere with DC maturation. They can secrete the anti-inflammatory cytokine IL-10[216], or hijack DC function to become tumour-promoting. Here, they trick DCs into polarising a T_H2 response with its accompanying production of IL-4 and IL-13, which worsens breast carcinoma by both inhibiting apoptosis[217] and indirectly promoting cell proliferation[218]. Other studies have also reported DC-induced pro-tumour activity[219,220].

Due to their plasticity in activating both the cellular and humoral arms of the adaptive immune system, DCs have now been employed in cancer vaccination studies. Promising results in eliciting anti-tumour B- and T-cell responses have been observed using both *in vivo* and *ex vivo* loading of DCs with tumour-derived antigen[214,221-224]. It is of paramount

importance that precise signalling of DCs is understood in order to be able to skew their response to that of strictly anti-tumour.

1.8 DNA Damage Response

1.8.1 Activation of the DNA Damage Response

In addition to cellular responses deployed to prevent cancer, an extremely complex intracellular molecular signalling network exists, collectively known as the DNA Damage Response (DDR). It protects the integrity of the cellular genome by rapidly detecting and repairing genotoxic modifications which could otherwise promote genomic instability and eventually cancer. It has been estimated that the cell can attain hundreds of thousands of DNA lesions per day, either spontaneously or as a result of environmental stresses[225]. Environmental stresses can be further divided into those of physical or chemical sources. The former includes Ionising radiation (IR) or ultraviolet (UV) radiation, whilst the latter can include smoking or even genotoxic cancer medications[226]. Spontaneous DNA damage can comprise of modification or interconversion of DNA bases, oxidisation of bases as a result of metabolic processes, or misincorporation of dNTPs during normal replication[227]. Each form of genotoxic stress can damage the DNA in a different capacity. Chemical modifications are self-explanatory, with oxidisation, deamination, alkylation and depurination accounting for most of the alterations which affect normal function and replication. Increasing in scale, Inter- or intra-strand crosslinking of DNA strands can be induced by the likes of cisplatin treatment. Larger still, etoposide can inhibit topoisomerase I or II, trapping enzyme-DNA complexes and preventing replication and maintenance processes. Subsequently, this can lead to single strand breakages (SSBs) and double-strand breakages (DSBs) which are seen as the most dangerous types of damage due to the lack of templates to repair from.

Given the range in variety of genomic insults, numerous distinct repair pathways have evolved to allow specific responses to each type of damage. DNA base modifications are

usually repaired using the base-excision repair pathway (BER)[228], whilst incorrect base pairing is fixed with the mismatch repair pathway (MMR)[229]. Intrastrand crosslinks and pyrimidine dimers are rectified by removal of a ~30bp oligonucleotide stretch as part of the nucleotide excision repair (NER) or interstrand crosslink repair (ICL) programmes[230,231]. DSBs are repaired using the non-homologous end-joining (NHEJ) programme which can allow some potential mistakes during resection[232,233], or a more precise homologous recombination (HR) system. The molecular mechanisms of each of these are reviewed in depth in[227].

1.8.2 DDR signalling

The DDR network is similar to that of innate sensing in many ways; an insult is sensed and signal transduction pathways are activated which induce an appropriate response pathway, whilst simultaneously altering cellular processes as the response ensues. The whole signalling axis is dependent on multiple different PTMs, also akin to PRR signalling. Phosphorylation, ubiquitination[234], SUMOylation[235] and methylation are all key in the response. This adds a critical layer of regulation which permits rapid activation and deactivation of signalling without the need for *de novo* protein synthesis.

Immediately after DNA damaging events, sensor proteins are actively recruited to lesion sites. A number of reported sensors may mediate this initial detection. DSBs for example have been shown to be sensed by multiple independent protein complexes[236], including PARP, Ku70/Ku80 heterodimers and the well-studied MRN complex whose constituents include MRE11, NBS1 and Rad50. These sensors are directly responsible for downstream induction of distinct effector repair pathways[237], dependent on the requirement of the DNA end-processing. In the decision making period, large discrete microscopically-visible

foci form around the damage site. The order and kinetics in which proteins are recruited is thought to ultimately influence the repair programme employed[238]. Kinase signalling cascades proceed, largely driven by the kinases ataxia telangiectasia mutated (ATM) and ATM-related kinase (ATR), which have hundreds of substrates each[239]. ATM drives a predominantly DSB response, whilst ATR controls SSB pathways in response to RPA-coated ssDNA. Phosphorylation of H2AX at Serine 139 is a general marker for ATM/ATR activation, and this so called γH2AX is seen spread for up to 2 megabases around the site of damage[240]. γH2AX is bound by MDC1, which is also phosphorylated by ATM[241], allowing active recruitment of 53BP1 and BRCA1[242]. From here, other mediators are phosphorylated, allowing amplification of the response and recruitment of effector proteins. Effectors can themselves either be directly phosphorylated by ATM and ATR, or via CHK1 and CHK2 checkpoint proteins amongst others[243], before attempting to fix the damage.

1.8.3 Cellular processes affected by the DDR

Initiation of the ATM-CHK2 axis after DSB sensing can regulate the activity of p53, which controls cell cycle progression and cell survival. Importantly, a biological timer is activated upon which the fate of the cell rests. If damage is extensive and repair is incomplete once the timer reaches its limit, the cell will enter apoptosis or senescence[244].

The DDR also alters many other cellular processes during repair, including transcription and translation, which are downregulated in order to prevent formation of misfolded proteins from mutated DNA templates[245]. A range of inflammatory processes may also be induced upon DNA Damage sensing, including activation of NK cells by increased expression of the NKG2D ligands such as MICA and MICB[246,247]. This process is lost when

ATM expression is silenced[246]. Similarly, NFκB signalling is known to be induced by the DDR[248-250], which in turn has also been shown to activate a specific pathway that results in IFNα and IFNλ production[251].

The development of the adaptive immune system also relies heavily on co-ordinated and controlled activation of the DDR. T-cell receptor and immunoglobulin (Ig) production requires the generation of specific DSBs during V(D)J recombination[252], in order to generate diversity in the receptors and increase the ability to recognise of a diverse range of antigens. Similarly, class-switching[253] and somatic hypermutation[254] requires deamination to be catalysed by the DDR enzyme AID which changes cytosine to uracil.

1.8.4 Roles of the DDR in disease

Mutations of proteins in the DDR manifests in a multitude of disease states[254]. In relation to the development of adaptive immune diversity outlined above, mutations can lead to hyper-IGM syndrome in which patients possess normal IgM levels but very little IgG, IgA or IgE[255]. At worst, severe combined immunodeficiency disease (SCID) may develop from mutations in the NHEJ system, due to defective TCR and Ig development[256]. Other profound immunodeficiencies such as lymphopenia may also develop[255,257].

As neurons are capable only of limited self-renewal, any DNA lesions in these must be carefully and precisely fixed throughout the entire lifetime of the cell. Incidentally, neuronal metabolism combines high levels of oxygen consumption and mitochondrial activity, creating an extremely oxidative environment for DNA. Defects in DDR machinery therefore allow neurons to succumb to such genotoxic environments, which often presents in neurodegenerative motor defects[258]. Similarly, mutations in ATM further increase cellular ROS levels[259] and leads to ataxia telangiectasia (AT), a disease where

patients lose motor co-ordination early on and become wheelchair-bound. Mutations in the MRN complex member NBS1 result in Nijmegen Breakage Syndrome, from which the protein found its name. Here, growth retardation and microcephaly occur, demonstrating detrimental effects as far back as embryonic development[260].

Importance of these proteins can be traced even further back to gamete production; in meiosis, DSB formation is required for efficient chromosome exchange[261], so obvious reliance is placed upon proteins of the DDR to mediate this without complication. Unsurprisingly, many patients with DDR syndromes show abnormalities in meiotic progression, leading to infertility[254,262].

On the other end of the scale, the DDR also has important roles in maintaining telomere homeostasis. Faults in ATM and ATR can result in chromosomal instability and insufficient processing of shortening telomeres[263]. This has been reported to accelerate ageing in mice[264], and is also thought to be the case in humans[265].

1.8.5 DDR and cancer

As many of the proteins in the DDR are tumour suppressors, mutations in these unsurprisingly increases risk of cancer (reviewed in[266]). For example, in Li-Fraumeni syndrome, germline p53 is commonly mutated which predisposes patients to a spectrum of malignancies such as breast cancer, leukaemia, melanomas, brain tumours, gastrointestinal cancers and sarcomas[267]. Sporadic cancers also frequently arise, resulting from mutations which confer a selective advantage in the growing tumour[236]. Mutations gained in DDR proteins also facilitate tumorigenesis by allowing bypassing of the apoptotic pathways otherwise initiated upon their activation. Predictably, p53 mutations are

present in over 50% of sporadic cancers, whilst 15% acquire mutations in ATM. Mutations in most other DDR proteins also predispose to cancers (reviewed in[254,268]).

1.9 BRCA1

1.9.1 BRCA1 mutations in cancer

BRCA1 was initially identified and cloned after genetic studies into hereditary breast and ovarian cancer uncovered it as a major susceptibility gene[269,270]. Now, there have been over 1800 clinically-relevant mutations identified within the BRCA1 gene. Along with the related BRCA2, germline mutations in BRCA1 account for up to 45% of inherited breast carcinomas. Likewise, mutations confer a lifetime risk of 45-87% and 36-66% for breast and ovarian cancer, respectively[271,272]. Risk of other cancers including pancreatic[273-275], gastric, bowel and prostate cancers are also increased by 20-60% with BRCA1 mutations(reviewed in[276]). Moreover, genetic testing for BRCA1 defects provides an invaluable diagnostic tool to determine the risk of cancer development in an individual.

In addition to development of breast cancers accredited to hereditary BRCA1 mutations, 50-70% of sporadic breast tumours have at least one defective BRCA1 allele[277]. Similarly, hypermethylation of the BRCA1 promoter region and repression of BRCA1 transcription is also frequently observed in sporadic breast cancer[278].

1.9.2 BRCA1 is a key tumour suppressor

Study into BRCA1's cellular functions has exposed it as a pleiotropic master regulator of genomic integrity, controlling an array of processes which relate to DNA repair. These include cell-cycle checkpoint control, transcriptional regulation, chromatin remodelling, mRNA splicing and cell survival[279]; the mechanistic role of BRCA1 in each of these however is still largely unknown. Together, these characteristics make BRCA1 a *bona fide* tumour suppressor protein.

Biochemically, the BRCA1 gene encodes an 1,863 amino acid protein which comprises of multiple functional domains (Figure 1.5). At its N-terminus, it harbours a highly conserved RING domain which gives it E3 ubiquitin ligase functionality, allowing it to facilitate the transfer of ubiquitin which has been pre-activated by E2 ligases on to lysine residues of bound substrate proteins. Following this are dual nuclear localisation signals (NLSs)[280], with a controversial non-canonical third proposed[281]. This central region of BRCA1 is largely disordered with no distinguishable domain structures, a common feature in scaffold proteins that is thought to permit flexibility for binding a diverse selection of interacting proteins[279]. Towards the C-terminus is a Serine/Threonine-rich (SQ) cluster, with at least 10 reported exclusive phosphorylation sites stretching from residues 1280-1524, in addition to the functionally important Serine 988 residue[282]. Multiple different upstream kinases have been demonstrated to phosphorylate BRCA1 including ATM, ATR, CHK1 and CHK2 amongst others[282]. Phosphorylation of each distinct residue occurs in certain cellular settings and encourages specific downstream functions[282]. Phosphorylation of BRCA1 itself has been shown to be required for activation of some of its upstream kinases, including ATM, ATR and CHK1, illustrating a mechanism by which BRCA1 can self-regulate its activation via feedback loops[283,284]. The extreme C-terminus of BRCA1 contains dual BRCA1 C-terminal (BRCT) domains. As the name suggests, these were originally identified in BRCA1 itself but have now been identified in a wide range of proteins, many of which belong to the DDR[285]. These domains are essential for protein-protein binding capability, in particular binding of phospho-proteins[286,287], as well as mediation of transactivation events[288]. Other parts of the full-length BRCA1 protein also contain highly conserved sequence stretches, suggesting that much about potential BRCA1 roles remains to be elucidated.

BRCA1 is heavily subject to alternative splicing. Many isoforms have been reported, each expressed in a cell-cycle and cell-type specific manner (reviewed in[289]). Certain isoforms of BRCA1 are observed disproportionately in specific cancers[290], suggesting each isoform may have distinct tumour-suppressive functions. However, understanding of the regulation and function of these isoforms is currently very poor, but will be crucial for determining the exact role in tumour suppression.

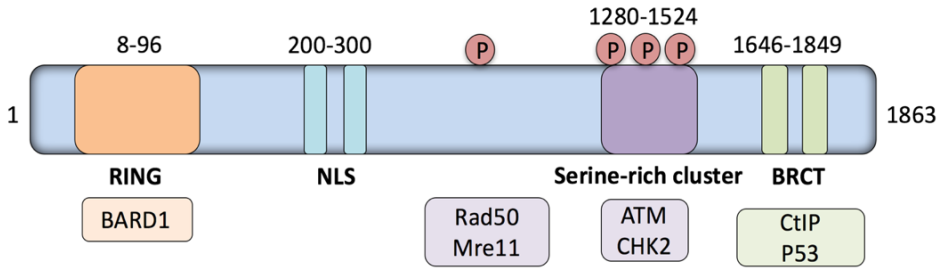

Figure 1.5 BRCA1 gene. Functional domains of BRCA1 full-length protein from N to C terminus. P denotes exclusive phosphorylation sites, of which there are 10 in the SQ domain (1280-1524) and one out of this region (S988). Select binding partners are included, positioned spatially relative to where they bind BRCA1.

1.9.3 BRCA1 E3 ligase activity

BRCA1 mediates its E3 ubiquitin ligase activity primarily when in concert with its binding partner BARD1[291], which binds via RING-RING homotypic interactions[292]. This interaction is thought to fortify both nuclear localisation and biochemical stability of BRCA1[293]. The heterodimer of BRCA1-BARD1 has been shown to bind many different E2 ligases and substrates, suggesting an expanse of cellular functions which are modulated by BRCA1-

BARD1 complexes[294]. Target proteins notably include histones, CtIP, TFIIE and BRCA1 itself to induce a positive feedback loop[295].

Early studies using tumour-derived BRCA1 RING-mutants demonstrated reduced E3 ligase ability and increased sensitivity to ionising radiation, directly linking BRCA1 E3 ligase activity to tumour suppressive functions[296]. Moreover, recent studies on mice with clinically-relevant C61G mutations which confer both defective E3 ligase and BARD1 binding activity, also have and increased predisposition to cancer through a reduced DNA repair capability[297]. In contrast, I26A mutant mice, which have defective E3 ligase activity but retain BARD1-binding potential, develop tumours at similar frequency to wild-type mice, suggesting that the E3 ligase activity of BRCA1-BARD1 is dispensable in its tumour suppressive capacity and may have as yet undefined roles[298]. It is important to note however that E3 ligase inability alone does impair DNA repair ability[299], but redundancy in the DDR may account for the observed wildtype-like phenotype.

In addition to K48 or K63-linked polyubiquitination, which induce proteasomal degradation or signalling activation of tagged proteins, respectively, BRCA1 can catalyse non-conventional K6-linked ubiquitination of proteins[300] as well as mono-ubiquitination events[301 302].

1.9.4 BRCA1 cellular localisation

BRCA1's NLSs help retain it in the nucleus where it undertakes its main roles in genome maintenance (extensively reviewed in[279]). Curiously however, BRCA1 contains a nuclear export signal at the N-terminus which facilitates nuclear-cytoplasmic shuttling[303]. One study found that BRCA1 movement to the cytoplasm was facilitated by binding of p53[304], and abrogation of this interaction to sequester BRCA1 in the nucleus resulted in impaired

DNA repair and increased cancer susceptibility. Another study also suggested that BRCA1 function must be in part undertaken in the cytoplasm[305].

Additionally, phosphorylated BRCA1 can be observed at the mitochondria where it may maintain mitochondrial DNA integrity[306]. Other studies have reported that BRCA1 localises to the ER where it acts to regulate apoptosis[307,308].

Despite these studies, much focus has been aimed at BRCA1's nuclear roles, and therefore the many functions of BRCA1 in the non-nuclear compartments remain unknown. Its requirement to be exported however, does strongly suggest that it is functionally active outside of the nucleus.

1.9.5 BRCT domains and complex formation

Through use of its BRCT domains, BRCA1 is thought to mediate many of its functions by acting as a scaffold protein to facilitate the formation of countless different protein complexes, a feature which underlies its ability to influence such a quantity of cellular processes[309]. Indeed, well over 100 distinct binding partners have been identified for BRCA1, with as many as 561 suggested using BioGRID algorithm-based prediction. Many binding partners are DDR-related proteins, and given BRCA1's multiple roles within the DDR, mutations the BRCT domains are common in BRCA1-related cancers[310,311].

Of these complexes, four have been extensively studied in their direct DNA repair roles, bearing the sequential names of BRCA1 A-D complexes. The specific activities of each is reviewed in[299]. In addition to BARD1, some of the primary components of these BRCA1 'supercomplexes' involved in DNA repair include the MRN complex, ATM, Abraxas, CtIP and BACH1 (FANCJ)[299].

In addition to its direct roles in DNA damage repair, BRCA1 also forms transcription-regulating complexes via its BRCT domains which indirectly contribute to the maintenance of genome stability. Initially, tumour-derived mutations in BRCA1's C-terminus highlighted that it can interact with the DNA-binding protein GAL4. This interaction is abolished with BRCT mutations and results in abrogated transactivation and growth suppression[312]. More recently, it has been established that BRCA1 fine-tunes p53's transcriptional regulation after ATM-mediated DSB sensing. Specifically, BRCA1 directs p53 to induce expression of DNA repair proteins whilst preventing pro-apoptotic gene expression, thereby demonstrating an exquisite level of control of its transcriptional binding partners' activities[313]. Similarly, BRCA1 has been shown to interact with the p50 subunit of NFκB, promoting expression of anti-apoptotic BCL2 and XIAP genes[314].

BRCA1 is also historically well-documented to interfere with estrogen receptor signalling at multiple points. Upon estrogen binding and activating its nuclear receptor ERα, the induction of proliferation-associated genes ensues, including the angiogenic VEGF and different cyclins[315]. BRCA1 usually suppresses ERα-induced signalling either directly or via COBRA, which binds and inhibits ERα. Additionally, BRCA1 has been shown to be able to transcriptionally regulate the expression of ERα[316], by positioning itself in close proximity the ERα promoter region and exploiting the sequence-specific DNA binding capabilities of other proteins such as Oct-1. In cases of BRCA1 mutation, dysregulated estrogen signalling in women may provide reasons as to the prevalence of breast and ovarian cancers over other types.

1.10 Functional co-operation between the DDR and Innate Immune system

1.10.1 Historical overlaps of the DDR and Innate Immunity

As discussed, activation of the DDR is crucial for progression of an adaptive immune response[253]. The Inflammatory responses[317], CTL responses and apoptosis resulting in the release of DC-activating DAMPs, are processes which display marked similarity to those of a cell infected with a pathogen such as a virus.

Contrastingly, reactive oxygen species (ROS) produced after metabolic re-programming of immune cells[318,319] is known to increase oxidative damage to both nuclear and mitochondrial DNA[67]. This can cause a positive feedback loop, inducing more DNA damage and therefore more immune activation[67], potentially promoting tumorigenesis[320].

1.10.2 Pathogenic oncogenesis

Historically, a plethora of different pathogens including bacteria, fungi and viruses have been found to antagonize members of the DDR to promote virulence and facilitate replication.

Most viruses infect non-dividing cells, but drive them to re-enter the cell cycle to promote a permissive environment for viral replication. This can lead to increased replicative stress and activation of the DDR, and eventually oncogenesis. It is estimated that 20% of all human cancers are consequential of pathogenic infection, with 80% of these being from viral infection[321]. The different families of DNA viruses which induce tumorigenesis and the mechanisms by which they do so are reviewed extensively in[322]. Briefly, cellular hyperproliferation is homeostatically restricted by tumour suppressor proteins such as Retinoblastoma (RB), BRCA1 and p53. These proteins are often antagonised by viruses,

either by promoting proteasomal degradation, relocalisation or mechanistically preventing their action. For example, E6 protein from human papilloma virus (HPV) targets p53 for degradation to avoid apoptosis of the infected cell[323], whilst the E7 protein disrupts Rb interaction with its binding partner E2F to promote entry into the S-phase[324]. These processes have been directly associated with the development of cervical cancer[325].

Members of the *herpesviridae* family are the most studied in cancer. Epstein-Barr virus (EBV), which is almost always present in Burkitt's lymphoma patients[326], results in activation of the ATM-CHK2 axis early on in B cell immortalisation[327]. EBV Late-gene expression then reduces DDR activation once the cell is transformed to permit survival of the cell and unrestrained replication. The same phenomenon is also observed during infection of the γ-herpesvirus Kaposi's sarcoma herpesvirus (KSHV), which responsible for Kaposi's sarcoma and lymphomas linked to AIDS progression[328,329].

In addition to exploiting DDR activation temporally, viruses can also directly regulate expression of DDR proteins, again leading to chromosomal instability. Adenovirus for example targets the whole MRN complex for proteasomal degradation[330], whilst encoding a protein to inhibit ATR activation[331].

Viruses may also encode surrogate their own functional proteins which regulate host proliferation and act as oncoproteins. KSHV encodes the cyclin homologue v-cyclin which promotes increased proliferation, but also induces polyploidy and other mitotic defects which promote cancer[329].

Bacteria and fungi also may have genotoxic properties which activate the DDR. *Helicobacter pylori*, a gram-negative gastric pathogen present in 50% of the global population, has been estimated to be responsible for 5.5% of the global cancer burden[332]. This bacteria induces extremely high levels of gastric inflammation which contributes to

carcinogenesis (reviewed in[333]). Certain strains of *Escherichia Coli* may also increase the risk of colon cancer by producing the genotoxin colibactin, encoded in the polyketide synthase (*pks*) pathogenicity island[334,335]. These strains are also found to be proportionally over-represented in an inflamed intestine, which would further promote a tumorigenic environment[336].

1.10.3 Pathogen hijacking of DDR machinery

Conversely, pathogens may exploit the active functions of DDR proteins for their virulence. For example, viruses can selectively activate and hijack proteins of the DDR to augment their replicative capability. Indeed, most DNA viruses were found to require activation of specific parts of the DDR for their replication[337]. Additionally, retroviruses require efficient integration of cDNA into the host genome after reverse-transcription of their RNA genome. This integrase-catalysed process introduces SSBs, which if inefficiently repaired can lead to DSB formation and apoptosis. Consequently, inhibition of ATR significantly decreases viral integration efficiency[338]. Retroviral replication intermediates also require general processing by DDR components; loss of ATM or MRN proteins which 'repair' these intermediates results in reduced retroviral replication[339]. Replication centres for many viruses whose genomes are deposited in the nucleus also seem to rely on the presence of specific DDR components. These include parvoviruses, herpesviruses, EBV, HPV and CMV amongst others[337]. Presumably, the viruses utilise proof-reading activity of the DDR to ensure their genomes are efficiently replicated before being packaged. An exemplar study showed that MHV68 encodes proteins that can directly phosphorylate H2AX, RPA, CHK2 and Rad51 in events which are required to facilitate successful viral replication[340]. The potential benefits of viral exploitation and activation of the DDR to such an extent seen in

this case are unexpected, due to the known inflammatory and immune-stimulating roles of the DDR. Nonetheless, these findings show that DDR proteins are important in viral replication.

The interplay between beneficiary or antagonistic features of DDR activation on viral replication are poorly understood. Future knowledge of viral mechanisms to navigate this complexity for their benefit, in terms of temporally controlling inflammatory responses and cell proliferation, will no doubt aid in clinical applications for treatment of both infection and cancer.

1.10.4 The DDR and innate immune signalling pathways co-operate

Clues suggesting a more integrated relationship between innate sensing and DDR systems surfaced upon discovery that DDR activation also induced IRF signalling and IFN production[251]. It was demonstrated that infection with both DNA and RNA viruses activates the DDR, and IFN production is at least partially-reliant on DDR activation. Recent evidence has mounted supporting the existence of a bi-directionally co-operative relationship between these two large signalling networks[341]. That is, proteins of the DDR are understood to have signalling roles in innate responses to pathogen sensing, whilst proteins believed to be reserved for innate immune signalling have been found to complement the DDR.

It is now understood that damaged DNA of nuclear or mitochondrial origin[342] can leak into the cytosol and activate STING-dependent IFN production pathways, which can lead to inflammatory phenotypes and even promote tumorigenesis, probably by cytokine and growth factor-induced proliferation[343,344]. However, the data strongly suggests anti-tumour and antimicrobial effects of endogenous dsDNA-induced activation of STING[345].

Mice lacking STING were shown to be more susceptible to colitis-associated carcinogenesis[346,347] but also have weaker T-cell responses to melanoma[348]. The complex balance between inflammatory activation progressing towards either detrimental or beneficial outcomes, in both cancer and infection, highlights the requirement for multiple levels of regulation and co-operation between the DDR and innate sensing systems.

In the case of Trex1 deficiency outlined earlier, the characteristic elevated cytosolic endogenous dsDNA and IFN signature was further studied in antimicrobial terms. Indeed, it was found that Trex1 is responsible for controlling not only endogenous retroviral element expression, but also that it is important in IFN responses to HIV[349]. Removal of Trex1 permits accumulation of HIV ssDNA species in the cytoplasm which are sensed to induce TBK1-IRF3 signalling via STING[350,351], inducing the expression of type I IFN. The cell unsurprisingly seems to have evolved a means to exploit this inflammatory mechanism; oxidative damage to DNA confers resistance to Trex1 exonuclease activity, allowing it to be sensed by STING to induce an IFN response[352]. The 8-hydroxyguanosine marker of oxidative damage was discovered on pathogenic DNA during lysosomal processing and on extracellular neutrophil extracellular trap (NET) DNA, suggesting this modification may be exploited to potentiate increased DNA sensing capacity[352]. However, this may also increase the risk of autoimmune disease in susceptible subjects, as it was found on the skin of UV-exposed Lupus patients along with increased type I IFN, and was able to induce lesions directly in lupus prone mice[352]. Therefore, lack of Trex1 activity and increased IFN can be beneficial or detrimental depending on circumstance.

A study which looked at samples from AT patients, who also suffer from elevated IFN levels in addition to motor defects, found that ATM deficiency and subsequent increase in DNA Damage was found to prime the innate immune response[353]. Specifically, the increased

amount of damaged DNA can leak into the cytosol as with Trex1-deficient cells, inducing STING-dependent type I IFN production. The elevated basal IFN resulted in an amplified innate response to subsequent pathogenic challenge. Meanwhile, this provides an explanation of the inflammatory phenotype seen in AT patients, along with their reduced susceptibility to systemic viral infections[353,354].

A similar protective outcome of DDR activation was previously reported in germ cells[355]. The study highlighted a resistance to heat and oxidative stress after addition of exogenous DNA, as a result of DDR activation. Here, it was found that proteasomal degradation was increased after DNA damage which enhanced proteostatic protection.

More direct roles of DDR proteins in innate immune sensing have also been uncovered. Pull-down experiments in HEK293 cells unveiled that Ku70, integral in the NHEJ pathway, could sense exogenous DNA and induce IFN-λ1 production[356]. Subsequently, DNA-PK, a DNA-dependent kinase complex that Ku70 is a member of along with Ku80 and its catalytic subunit DNA-PKcs, was shown in human and murine cell lines to detect cytosolic dsDNA and promote IFNβ production. This was demonstrated for both transfected DNA and whole pathogen in the form of Vaccinia virus[357]. The key finding of these studies is the demonstration that DDR proteins can bind to exogenous dsDNA in the cytoplasm, highlighting potential roles for DDR proteins out of the nucleus in detecting pathogenic nucleic acids as 'damaged'.

Shortly after these discoveries, a role for the DNA Damage sensor MRE11 was proposed in STING-dependent responses to dsDNA[358]. The authors showed that cells from a patient with an AT-like disorder stemming from MRE11 mutations, and cells with MRE11 knocked-down, had defects in STING activation and decreased type I IFN production in response to both exogenous and endogenous dsDNA. It was crucially demonstrated that MRE11

colocalises with the exogenous DNA in the cytoplasm. The MRN component Rad50 is also recruited to this MRE11-dsDNA complex after initial sensing.

Subsequently, Rad50 itself was suggested to be critical in pro-IL-1β production after cytosolic DNA sensing[359]. A direct interaction between Rad50 and the innate immune adaptor CARD9 was reported, whilst *in vivo* murine experiments showed that lack of Rad50 confers impaired inflammatory responses to DNA virus infection.

PTEN, a key tumour suppressor protein which regulates PI3K and Akt activity, has also been assigned a role in antiviral immune signalling[360]. It was shown to use its phosphatase activity to remove a previously-undescribed inhibitory phosphate on Ser97 of IRF3, allowing its activation. It was also shown to control subsequent import of IRF3 to the nucleus, where it induces type I IFN expression. Knockout of PTEN rendered mice susceptible to a range of viral infections. This study illustrates that DDR components can intersect with innate sensing and signalling machinery directly, without the need for it to bind a DNA species.

Even simple unicellular organisms such as bacteria possess systems which are bifunctional for genome protection and immune responsibilities. The bacterial Cas1, related to Cas9 which forms part of the CRISPR system that is now indispensable in gene editing processes, has been shown to repair the bacterial genome whilst also defending against viral infection by removing integrated phage DNA from the bacterial genome[361].

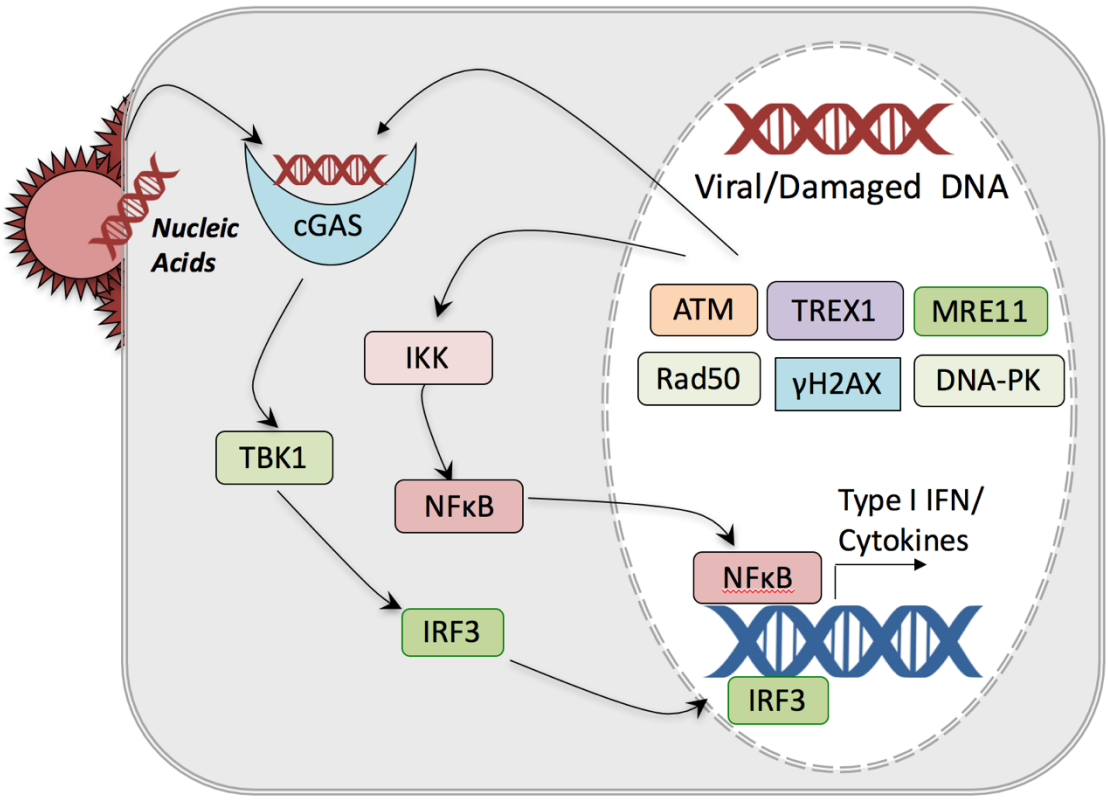

Figure 1.6. Direct functional overlaps of DDR and innate immune sensing proteins. Viral nucleic acids and damaged DNA can both be sensed by proteins of the innate immune system or of the DDR. Upon sensing, inflammatory signalling is induced, resulting in type I IFN and inflammatory cytokine production.

1.11 Conclusion and study aims

Taken together, these evidences suggest that activation of the DDR provides a pre-emptive defence mechanism which complements 'conventional' innate sensing in multiple capacities. Firstly, the proteins of the DDR which have evolved to detect aberrant endogenous DNA can detect pathogenic DNA as 'damaged' or misplaced, inducing inflammatory signalling. In addition to cell-intrinsic restriction mechanisms subsequently activated, an increased expression of NKG2D ligands and MHC I-peptide complexes upon DDR activation stimulates a cellular response. Simultaneously, activation of the DDR and downstream signalling events create a protective environment against the increased oxidative stress often seen upon APC activation[355]. Finally, loss of DDR proteins by oncogenic processes or viral targeting could activate a 'trip-switch' fail safe mechanism; the loss of such proteins would permit increased damaged DNA to leak into the cytosol, where it can be sensed by CDSs to activate the IFN and NFκB pathways outlined above, thereby reducing replication of invading pathogens as is seen in the case of ATM[353].

From a cell economic point of view, this functional relationship is logical as both pathways are designed for very similar purposes. Both encompass discrete sensing mechanisms to detect a specific type of threat and induce distinct yet partially-overlapping functional pathways. They both also utilise large kinase signalling cascades and multiple PTMs, with similar phenotypic outcomes. In either instance, the cell has a chance to repair the issue, in which time global cellular translational and metabolic events are somewhat re-organised. Moreover, adaptive immune responses are mobilised either by antigen presentation, direct inflammatory signalling, or via ligands produced if the cell undergoes apoptosis.

It remains unknown how the cell discriminates mechanistically between activation of the DDR in response DNA damage or innate immune signalling. Similarly, most recent evidence links innate sensing with DDR activation as a consequence of endogenous or exogenous DNA detection in the cytosol, but in-depth studies are lacking in regards to the possibility of non-DNA PRR ligands activating the DDR. Investigating these issues would further solidify the existence a direct relationship between both pathways and move past an 'indirect consequence' model.

The aims of this study will therefore be to try and uncover proteins of the DDR which may be employed downstream of PRR activation. We will utilise large-scale phosphoproteomics to achieve this, using both nucleic acid and non-nucleic acid ligands. Any identified proteins will be investigated for a functional role in innate immune sensing and signalling; inflammatory induction will be interrogated, and I will try to identify any mechanism of action by identifying the point of intersection with innate immune signalling cascades. Finally, effects of the presence of any identified DDR protein on pathogen replication will be assessed.

2 Materials and Methods

2.1 Cell Culture

2.1.1 Tissue culture

Cells were incubated at 37°C in humidified incubators supplemented with 5% CO_2. THP-1 cells were purchased from ATCC and cultured in R10 (RPMI-1640 supplemented with 10% FCS, 1% glutamine and 100 IU/mL Penicillin and Streptomycin (Sigma)). THP-1 cell differentiation to macrophage-like cells was achieved by incubating cells in 32nM PMA (Sigma) for 24 hours before washing. HEK293T and HeLa cells were kindly provided by Prof. Jan Rehwinkel's group, and were cultured in D10 (Dulbecco's Modified Eagle's Medium supplemented with 10% FCS, 1% glutamine and 100 IU/mL Penicillin and Streptomycin (Sigma)). HEK293-3C11 IFN reporter cells, generated and kindly provided by Dr. Jonathan Maelfait (University of Oxford, Human Immunology Unit)[50], were also cultured in D10 without antibiotic. Monocyte-derived dendritic cells (MoDCs) were isolated from leucocyte cones (NHS Blood Services, Bristol), and cultured in R10 supplemented further with 40ng/mL IL-4 and GM-CSF (Peprotech).

2.1.2 Generation of MoDCs

Whole blood from leucocyte cones (NHS, Bristol, UK) was diluted six-fold with RPMI-1640 and layered over a sodium diatroziate/polysaccharide solution (Lymphoprep, AXIS-SHIELD, Norway). Cells were separated by density-gradient centrifugation at 2000rpm for 20 minutes, and PBMCs harvested at the interface before being washed 3 times with chilled RPMI 1640 at decreasing speeds (1800 rpm, 1500 rpm, 1200 rpm). Monocytes were positively selected using CD14+ magnetic microbeads and LS columns (Miltenyi Biotec)

according to the manufacturers protocol. CD14+ monocytes were cultured as outlined above for 5-6 days to induce differentiation to dendritic cells (MoDCs). Flow cytometry was used periodically to confirm purity and maturity. CD14 was expected to drop from high to low as differentiation progressed, whilst DC markers such as CD11c would increase during differentiation. Expression of DC maturation markers such as CD86, CD83 and HLA-DR were expected to remain low in immature unstimulated cells and be increased upon stimulation.

2.1.3 Activation of MoDCs

MoDCs were harvested on day 4 or 5, depending on their morphology and downstream application, before stimulation with multiple PRR ligands at varying concentrations (Table 2.1). Activation could be assessed by flow cytometric analysis of DC maturation markers or western blot analysis of common immune signalling molecules.

2.2 Protein Biology

2.2.1 Cell lysis

Cells were harvested and washed in ice cold PBS, before being resuspended in lysis buffer (1% (v/v) Triton X-100, 250mM NaCl, 100mM Tris-HCl pH8 and 10mM EDTA supplemented with complete ULTRA protease inhibitor (Roche) and 1% phosphatase inhibitor cocktail 3 (Sigma)), and placed on a rotating mixer at 4°C for 40 minutes. Lysate was centrifuged for 20 minutes at 13,300 rpm, and supernatant transferred to a fresh pre-chilled Eppendorf. Cellular debris was discarded.

2.2.2 Protein quantification

Protein concentration of cell lysate was determined using the Bradford Assay. Briefly, 5µL of cell lysate or bovine serum albumin BSA standard (BioRad) was plated in triplicate in a 96-well flat-bottom plate and mixed with 250µL Bradford Reagent (BioRad), before absorbance was read at 595 nm subtracting the value at 450 nm. A standard curve was constructed and protein concentration calculated.

2.2.3 Phosphoprotein purification

$20x10^6$ DCs per condition were treated as required and harvested before being washed twice in cold Hanks Buffered Saline (HBS) pH7.4. Phosphorylated proteins were then purified using a Phosphoprotein purification kit (Qiagen), according to the manufacturer's instructions. Briefly, cells were lysed for 40 minutes at 4°C in 5ml CHAPS-based Phosphoprotein lysis buffer supplemented with 1 tablet of supplied protease inhibitor and 1% phosphatase inhibitor cocktail 3. Cells were vortexed every 10 minutes during lysis.

Tubes were centrifuged at 13,300 rpm and 4°C for 30 minutes, supernatant harvested and protein concentration determined. 2.5 mg of lysate (at 0.1 mg/mL) was added to resin columns supplied in the kit. A portion of the negative un-bound flow-through fraction containing unphosphorylated proteins was retained and used as a 'loading control' in downstream western blotting. The column was washed before bound phosphorylated proteins were eluted in 2ml of supplied elution buffer. This fraction was concentrated to ~250µL using 9K concentrator tubes (Pierce). Phosphoprotein concentration was determined, and lysates processed for SDS-PAGE or stored at -80°C.

2.2.4 Polyacrylamide gel electrophoresis (PAGE)

Cell lysates were mixed with NuPage 4x LDS sample buffer and 10x Reducing buffer (Invitrogen) to give 1x final concentrations. Samples were boiled at 70°C for 10 minutes, and equal mass of protein loaded into each lane of NuPage pre-cast polyacrylamide gels (Invitrogen). Either Rainbow (Invitrogen) or HiMark (Invitrogen) pre-stained protein ladder was loaded, dependent upon the gel used and target protein size. Gels were electrophoresed in Invitrogen mini tanks at 140V in MOPS or Tris-acetate running buffer (Invitrogen) when Bis-Tris or Tris-acetate gels were used, respectively.

2.2.5 Western Blotting (WB)

Electrophoresed gels were washed in 20% ethanol before proteins were electro-transferred using the iBlot dry blotting system for 7 minutes (Invitrogen), using the accompanying PVDF membrane stacks (Invitrogen). Membranes were blocked in 5% (w/v) BSA (when using phospho-specific primary antibodies) or non-fat dry milk diluted in Tris-buffered saline (20 mM Tris HCl (pH 8.0), 150 mM NaCl) with 0.1% Tween-20 (TBST), for 1

hour at room temperature (RT) with gentle agitation. Primary antibodies were then added and incubated at manufacturers recommended dilution, temperature and time. Membranes were washed in TBST three times for 5-10 minutes. Species-specific HRP-conjugated secondary antibody was added to 5% (w/v) non-fat dry milk in TBST at the manufacturers recommended dilution, and membranes incubated in this for one hour at RT with gentle mixing. Membranes were washed 4 times for 10 minutes in TBST before being covered in enhanced chemiluminescence (ECL) solution (Amersham Biosciences). Blots were developed using Hyperfilm (Amersham Biosciences) and an X-ray radiograph developing system (Xograph Healthcare).

2.2.6 Subcellular fractionation

Cells were fractionated using either a nuclear-cytoplasmic fraction kit or subcellular protein fractionation kit (Thermo Scientific), according to the manufacturer's instructions. Additionally, an extra wash with PBS was performed between each subsequent lysis step to prevent contamination of fractions with remaining lysate from previous fractions. Each fraction had its protein concentration determined and upon western blotting, equal amount of protein loaded for each fraction.

2.2.7 Native PAGE

Samples were prepared using the NativePAGE sample prep kit (Invitrogen). Briefly, cells were lysed in Native lysis buffer (1x Sample buffer, 1%(v/v) DDM, 1% Phosphatase inhibitor cocktail 3 and protease inhibitor) for 45 minutes at 4°C. Lysate was treated with 25 U/µL Benzonase (Sigma-Aldrich) supplemented with 2mM $MgCl_2$ for 30 minutes at RT, before centrifugation at 13,300 rpm and 4°C. Supernatant was transferred to fresh

Eppendorfs and protein concentration was determined using the Bradford Assay. 0.25% G-250 was added to lysate to give a net negative charge without reducing. NativeMark (Invitrogen) ladder and protein was loaded to a NativePAGE 4-16% Bis-Tris gel (15-1,000kDa). Anode buffer was added to the outer chamber, and 'dark blue' cathode buffer to the inner chamber. Gels were run at 150V for 60 mins and 250V for 30-90 mins, at 4°C. After one-third of the gel had run, dark cathode buffer was switched to 'light blue' buffer. Gels were washed 3 times in 1X NuPage transfer buffer (Invitrogen) to remove dye before transfer. Proteins were electro-transferred as with conventional western blotting, but membranes were additionally washed in 8% acetic acid for 5 minutes to fix proteins, and then washed in 100% methanol for 5 minutes with agitation to remove G-250. Immunoblotting was then carried out as above.

2.2.8 Immunoprecipitation

A minimum of $10x10^6$ cells were harvested per condition and washed twice in PBS. Cells were then lysed for 30 minutes at 4°C with rotation in IP lysis buffer (50 mM Tris-HCl, 150 mM NaCl, 1 mM EDTA, 1% NP40, protease inhibitor, 1% phosphatase inhibitor cocktail 3) at a volume of 1 mL per $20x10^6$ cells. Lysate was centrifuged at 13,300 rpm for 30 minutes at 4°C and the pellet discarded. 2% of the supernatant was taken and processed for WB as the input fraction. Manufacturers suggested dilution or pre-optimised amount of primary antibody (and equivalent isotype control), after testing a range of 1µg to 20µg per condition, was added to the remaining lysate, and rotated at 4°C for 2-3 hours. 40 µL of Protein G Dynabeads (Invitrogen) per mL of lysate were then washed in IP wash buffer (50 mM Tris-HCl, 150 mM NaCl, 1 mM EDTA, 0.1% NP40) and added to lysate, before incubating at 4°C for 1 hour, again with rotation. Tubes were placed on a DynaMag2

magnet (Invitrogen), and supernatant removed. 2% of this was taken and processed as the unbound fraction. Remaining beads were washed in 1 mL IP wash buffer four times, then resuspended in 40 µL 2x LDS Sample Buffer mixed with reducing agent, before boiling at 70°C for 10 minutes to elute and reduce bound protein. Tubes were placed on the magnet and supernatant transferred to a fresh Eppendorf. Samples were then frozen at -80°C or WB performed immediately.

2.2.9 TUBE2 Ubiquitin IP

$20x10^6$ HeLa cells in each sample were untreated or incubated with 20 µM MG132 (Sigma) and PR619 (Sigma) for 30 minutes at 37°C before being lysed in 1mL Ub-IP lysis buffer (50 mM Tris-HCl (pH 7.4), 150 mM NaCl, 1 mM EDTA, 1% NP-40, 0.5% Deoxycholate, 0.1% SDS, protease inhibitor, phosphatase inhibitor cocktail 3, 20 µM MG132, 50 µM PR614). 50 µL of control agarose resin was added to lysate and incubated for 1h at 4°C, before samples were centrifuged at 3,000 rpm for 2 minutes at 4°C, and precleared lysate transferred to fresh Eppendorfs. Either control or TUBE2 agarose beads (Labome, USA) were then added to the lysate, the latter of which contains ubiquitin binding domains bound to beads[362]. After overnight incubation at 4°C, samples were centrifuged at 3,000 rpm for 2 minutes at 4°C, and 5% of the unbound fraction removed. The pellet containing bound proteins was washed four times in wash buffer (50 mM Tris-HCl (pH 7.4), 150 mM NaCl, 1mM EDTA, 0.1% NP40), and bound proteins eluted in 40 µL 2x LDS Sample Buffer mixed with reducing agent, before boiling at 70°C for 10 minutes to elute and reduce bound protein. Samples were then frozen at -80°C or WB performed immediately, using anti-Ubiquitin primary antibody.

2.2.10 Silver staining

This procedure was carried out using a silver staining kit (Pierce). Briefly, electrophoresed gels were washed twice in ddH_2O. They were placed in fixing solution (30% ethanol, 10% acetic acid) for 15 minutes twice, before washing in 10% ethanol twice and finally once in ddH_2O. Gels were then incubated in 0.2% silver stain sensitizer diluted in ddH_2O for 1 minute, and washed in ddH_2O twice. Gels were submerged in Silver stain solution containing 2% enhancer for 30 minutes, then washed twice quickly with ddH_2O. Developer solution was then added until protein bands appeared, at which time stop solution (5% acetic acid) was added, washed off, and added again for 10 minutes.

2.2.11 ELISA

Supernatant was harvested from cells 24 hours after relevant treatment, and either processed immediately or frozen at -80°C. Sandwich ELISA kits for IL-1β, IL-6, IL-8, and TNFα were purchased from R&D Systems and performed according to manufacturer's protocol. Samples were assayed at 1x concentration or diluted as desired based on sensitivity of the particular assay, and performed in triplicate. A 7-point 2x serially diluted standard curve was constructed, and absorbances read using iMark microplate reader (BioRad).

2.2.12 Non-radioactive *In Vitro* Kinase Assay

Different amounts of recombinant kinase proteins (GST-TBK1 (Sigma), GST-IKKε (Thermo)) were mixed with 1x kinase buffer (25 mM Tris-HCl (pH 7.5), 5 mM β-glycerophosphate, 2 mM DTT, 0.1 mM Na_3VO_4, 10 mM $MgCl_2$) (Cell Signalling), and supplemented with 0.2mM ATP (Cell Signalling), before recombinant substrate proteins (GST-IRF3 (R&D Systems),

BRCA1 (Abcam)) were added and incubated at 30°C for 60 minutes. LDS sample buffer and reducing agent was then added to stop the reaction, before samples were reduced at 70°C for 10 minutes. WB was then performed, using antibodies specific for phosphorylated forms of substrate proteins.

2.2.13 Lambda Phosphatase treatment of lysate

Lambda phosphatase enzyme (NEB) was diluted in 1x buffer supplied, and supplemented with 2 mM $MnCl_2$. 20 U of enzyme was incubated with 50 µg of cell lysate for 30 minutes at 30°C. The reaction was stopped by addition of LDS and reducing buffer.

2.3 Nucleic Acid Techniques

2.3.1 DNA transformation and amplification

50µL of chemically competent E. Coli were mixed with 100ng of plasmid DNA and left on ice for 20 minutes, before being heat-shock transformed for 45 seconds at 42°C and placed back on ice for 2 minutes. STBL3 (Invitrogen) bacteria were used when amplifying plasmids encoding lentiviral shRNA, whereas DH5α (Invitrogen) were used for amplification of all other plasmids. Bacteria were recovered with 200µL SOC media (Invitrogen) for 60 minutes at 37°C with shaking at 225 rpm. 100 µL of the transformation mixture was plated

2.3.2 DNA Maxiprep

200mL of Bacterial culture was centrifuged at 3000 rpm for 15 minutes at 4°C, and the supernatant discarded. Plasmid DNA was extracted using a HiSpeed plasmid Maxi Kit (Qiagen), according to manufacturer's instructions. Purity and concentration of DNA was then assessed using spectrophotometry (NanoDrop ND 1000)

2.3.3 Alkaline Comet Assay

Superfrost Microscope slides (VWR) were coated with 0.5% Agarose IA (Sigma) dissolved in H_2O. 1.5% Low melting point Agarose VII (Sigma) (LMA) was prepared and kept in liquid phase at 37°C until cells were ready for use. Cells were harvested and washed twice in cold PBS before being resuspended to $5x10^6$/ml. 100µL ($5x10^5$) cells from each condition were diluted 10x in LMA and 100µL of this mix ($5x10^4$ cells) was spread gently on top of the Agarose-IA coated slides, and a coverslip added. Cell exposure to light was then minimized to reduce UV induced DNA damage. Slides were left at 4°C for 10 minutes on a cold tin

surface before the coverslip was gently removed, and another layer of LMA added on top. A cover slip was re-applied, and slides incubated at RT for 5 minutes, then 4°C for 10 minutes until the agarose solidified. Cover slips were removed and slides placed in ice cold alkaline lysis buffer (2.5M NaCl, 100mM EDTA, 10mM Tris, 1% Triton X-100 (added immediately before use), pH10) and left in the dark at 4°C overnight to lyse. A horizontal gel tank was filled with ice cold electrophoresis buffer (300mM NaOH, 1mM EDTA), and cells left in this for 40 minutes to allow DNA to unwind, before running at 1V/cm (distance between anode and cathode) for 45 minutes. Slides were washed for 5 minutes in neutralising buffer (0.4M Tris pH7.5), and then three times for 5 minutes in dH_2O, before being immersed in 70% ethanol for 5 minutes. They were then stained in SYBR Gold (Invitrogen) solution and viewed on an immunofluorescence microscope. Analysis was performed using Komet software, and Relative Tail Moment values taken for statistical analysis.

2.3.4 Adherent cell transfection

Cells were seeded 24 hours prior to transfection (and PMA-differentiated in the case of THP-1 cells) in the absence of antibiotic. The following morning, media was refreshed, again in the absence of antibiotic. Transfection mixes were then made per mL final media as follows; 4µL Fugene-6 (Promega), relevant amount of DNA or RNA to be transfected, and made up to 100µL (10% of final volume) with 1X OptiMem (Gibco). Transfection mixes were left for 15-30 minutes at room temperature before being added drop-wise to cells. 24 hours later, media was refreshed with the addition of antibiotic.

2.3.5 DC Electroporation

DCs were electroporated using the Neon system (Invitrogen), using 100µL neon Tips (Invitrogen) with the following settings; 2 pulses at 1475V and 20 ohms. Briefly, cells were resuspended at $50x10^6$/mL in buffer R and relevant siRNA was added at pre-optimised (after testing 1nM to 100nM) or manufacturers suggested concentration. Cells were electroporated and placed into pre-warmed antibiotic-free R10 (with the addition of Il-4 and GM-CSF if cells were harvested at day 3 or before), at a density of $1x10^6$/mL. Cells were harvested and counted 48 to 72 hours later to determine cell viability before downstream application.

2.3.6 RNA extraction

$5x10^5$ to $2x10^6$ cells per condition were harvested and washed before being homogenized using Qiashredders (Qiagen), according to manufacturer's instructions. RNA was then extracted using RNeasy kits (Qiagen), using the manufacturer's suggested protocol. An optional RNase-free DNase (Qiagen) was step included for 20 minutes at RT between RLT wash steps to remove genomic DNA and prevent downstream amplification of this during qRT-PCR reactions. RNA was finally eluted in nuclease free water (Ambion). Each step was performed using RNase-free filter tips (Axygen).

2.3.7 Reverse Transcription

RNA was reverse transcribed using a high-capacity RNA to cDNA kit (Applied Biosystems) as per manufacturer's instructions. Briefly, 500ng to 2µg of RNA was mixed with 2X Reverse Transcriptase buffer and 20x Reverse Transcriptase enzyme mix to a total volume of 20µL. This was reverse transcribed in PCR tubes for 1 hour at 37°C followed by 5 minutes

at 95°C. The cDNA was then either stored at -20°C or processed immediately.

2.3.8 Semi Quantitative Real Time – PCR (qRT-PCR)

Semi Quantitative-PCR (qPCR) was carried out using TaqMan chemistry, according to manufacturer's instructions (Applied Biosystems). Briefly, cDNA was diluted 10x in ddH_2O before a 10µL reaction mixture was made in each well of a MicroAmp Optical 96 well PCR plate (Applied Biosystems), comprising of 4.5µL cDNA, 0.5µL appropriate gene-specific TaqMan primer (Applied Biosystems) and 5µL TaqMan Universal PCR MasterMix (Applied Biosystems). Plates were then centrifuged and qPCR performed in Applied Biosystems 7500 RT-PCR machines with 40 standard cycles. CT thresholds were adjusted to be in the exponential linear phase, and relative gene expression calculated as fold-change in comparison to the GAPDH control. The difference in gene expression between treatments were calculated using the $2^{-\Delta\Delta ct}$ method. Briefly, this is derived from:

ΔCT= CT(target gene) – CT(Control gene)

ΔΔCT= ΔCT(target sample) – ΔCT(Control sample)

OR

ΔΔCT= (CT(Target gene, Pos sample) – CT(Ctrl gene, Pos sample))

– (CT(Target gene Ctrl sample) – CT(Ctrl gene, Ctrl sample))

2.4 Cellular techniques

2.4.1 Flow cytometry

Cells were washed with PBS and where stipulated, incubated with a viability dye diluted in PBS buffer for 10 minutes at 4°C away from direct light. Cells were then washed in FACS buffer (2mM EDTA, 0.2% (w/v) Bovine Serum Albumin (BSA) in PBS) before addition of an Fc-Receptor blocking reagent (BD Biosciences) for 5 minutes at RT in the dark. Cells were then incubated with fluorochrome-conjugated surface-antigen specific antibodies diluted in FACS buffer at the manufacturers recommended dilution, for 30 minutes at 4°C away from direct light. Cells were then washed twice in PBS and fixed in 2% Para-formaldehyde (Sigma) for 10 minutes at RT, before being washed twice and resuspended in FACS buffer. If no viability dye was used previously, DAPI was added at a dilution of 1:10,000 immediately prior to analysis on Cyan ADP Flow Cytometers (Dako, Cambridgeshire, UK) using Summit 4.3 software.

2.4.2 CellROX Red assay

Cells were incubated with 1µM CellROX Deep Red (Invitrogen) for 45 minutes in the dark at 37°C and 5% CO_2 before final harvesting. Cells were then prepared for FACS staining and analysis as above, as the CellROX red reagent is a cell-permeable dye which fluoresces with an absorption/emission maxima of 544/665nm upon oxidation, thereby permitting a measurement of cellular ROS production.

2.4.3 Lentivirus particle production

$1x10^6$ HEK293T cells were seeded in each well of a 6 well plate using antibiotic-free D10.

Media was refreshed with 2 mL before transfection the following day, when cells were 60-75% confluent. For each well of HEK293T cells, transfection mixes contained 8 µL Fugene-6 (Promega), 1.6 µg shRNA plasmid DNA (SHC216 scrambled, SHC203 GFP-encoding or gene-specific shRNA-encoding)(Mission, Sigma), 1 µg PAX2 packaging plasmid (a gift from Malin Parmar, Addgene 35002)[363], and 0.4 µg pMD2.G VSV-G encoding plasmid (a gift provided by Didier Trono, Addgene 12259)[364]. Mixes were made to 200 µL (10% final well volume) with OptiMem. When making LVPs for DC transduction, a second Vpx-encoding LVP was produced in addition, which targets the restriction factor SAMHD1, preventing dNTP degradation to increase transduction levels[365,366]. For this, mixes per well of HEK293T cells consisted of 8 µL Fugene-6, 0.4 µg pVSVg plasmid encoding VSV-G Env (a gift from Tannishtha Reya, Addgene 14888)[367], 2.6 µg pSIV3+ plasmid encoding Vpx (kindly provided by Dr. Jonathan Maelfait, University of Oxford, Human Immunology Unit), and again this was made up to 200 µL with OptiMem. After 15-30 minutes of incubation at RT, mixes were added to HEK293T cells drop-wise. Media was refreshed after 16 hours and transfection efficiency assessed by GFP-encoding plasmid expression, using an epifluorescence microscope (JuLi, NanoEntek) or Flow cytometry.

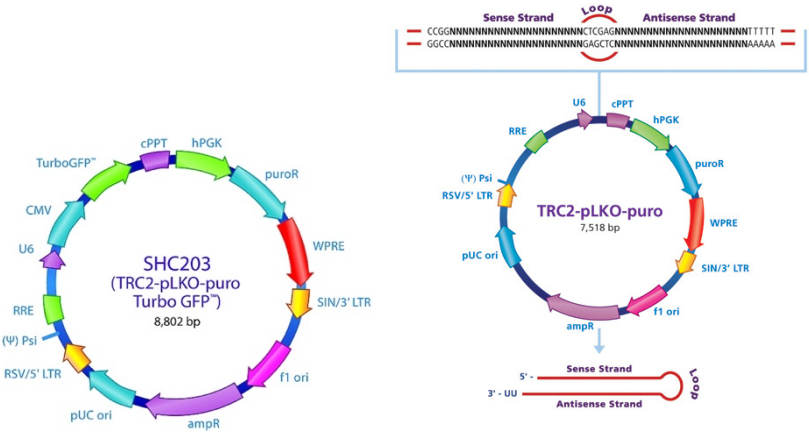

Figure 2.1 Vector maps of lentiviral shRNA plasmids. Vector Map of GFP-expressing positive control plasmid SHC203 (left), and general vector map for TRC2 backbone plasmids encoding shRNA that targets no known genes (Scrambled) or genes of interest (right).

2.4.4 Lentiviral transduction and stable cell-line selection

48 hours after transfection, LVP-containing supernatant was harvested and passed through a 0.45 µm pore (Sartorius), before being added immediately to cells of interest at a ratio of 1 mL supernatant to $2x10^6$ cells, for 3-4 hours. Following this, cells were washed and resuspended at $1x10^6$/mL in their relevant growth media, with the addition of penicillin, streptomycin and pre-optimised concentration of selection antibiotic where appropriate. When making shRNA-expressing MoDCs, transduction was performed immediately upon CD14+ cell isolation (Day 0), and IL-4 and GM-CSF added after the 3-hour transduction period. Approximate transduction efficiency was determined using flow cytometry, by assessing the proportion of cells expressing GFP from the LVPs made using SHC203.

2.4.5 Confocal microscopy

$1x10^5$ cells were seeded into each well of an 8 well chamber slide (Lab-Tek, Nunc) 24 hours prior to treatment. Chambers were pre-coated in 0.1 mg/mL Poly-L-Lysine (Sigma) for 30 minutes at RT before seeding suspension cells. After treatment, cells were washed 3x with 250 µL cold PBS, and fixed for 10 minutes at RT using 4% Paraformaldehyde (PFA). Cells were washed twice more and permeabilised using 0.2% Triton X-100 in PBS for 7 minutes at RT. 4 drops of Image-IT FX signal enhancer (Cell Signalling) was added to each well for 30 minutes at RT, before being washed 3x in PBS. Cells were incubated at RT for 90 to 120 minutes in blocking buffer (5% (v/v) FCS, 5% (v/v) human serum, 5% (v/v) Normal goat serum, 1% (w/v) BSA, 0.1% (v/v) Triton X-100, in PBS). Primary antibody was then added to blocking buffer at the manufacturer's suggested or pre-optimised dilution, and 140 µL of this mix added to relevant wells and incubated overnight at 4°C. Isotype IgG and

unstained (blocking buffer only) controls were included to determine background binding and specificity of antibodies. Cells were then washed 3x with PBS. Fluorophore-conjugated species-specific secondary antibody (Alexa, Molecular Probes) was added to blocking buffer at the manufacturer's suggested dilution before 140µL was added to chambers and incubated for 60 minutes at RT in the dark. In experiments requiring staining of multiple target proteins, secondary antibodies' host species were chosen with minimal cross reactivity to prevent false positive signal. Control samples with primary antibody or secondary antibody only were included to assess background fluorescence in each case. Secondary antibody was washed off 3x in PBS and the chamber removed and air dried in the dark for 20 minutes. Prolong Diamond Mounting medium containing DAPI (Cell Signalling) was added to each well and a cover slip applied, which was sealed using coverslip sealant (Biotium). Slides were stored at -20°C or processed immediately on a Zeiss 780 Inverted Confocal Microscope. Images were saved as .czi files and analysed using Fiji software.

2.4.6 Proximity Ligation Assay (PLA)

This procedure was carried out using DuoLink *In Situ* Red reagents (O-Link, Sigma) according to manufacturer's suggested protocol. Cells were prepared as with the confocal microscopy protocol above, up to and including incubation of primary antibodies. After washing in PBS 3x, PLA PLUS (rabbit-specific) and MINUS (mouse-specific) probes were diluted in blocking buffer. 70 µL was added to relevant chambers (covering the surface) and incubated at 37°C for 1 hour. Mixes were removed and chambers washed in 'Buffer A' twice. 70 µL Ligation mix was added to the chambers and incubated at 37°C for 30 minutes. Remaining steps were performed in low light. Ligase mix was removed and

chambers washed twice in Buffer A. 70 µL Amplification mix was added and incubated at 37°C for 100 minutes. This was removed and chambers washed in Buffer B for 10 minutes, and then once again for 1 minute. This was removed and slides air dried for 10-20 minutes in the dark. DuoLink mounting medium containing DAPI was then added and slides sealed, before being either stored out of direct light at -20°C or processed immediately.

2.4.7 Interferon Reporter Assay

HEK293-3C11 cells, stably expressing Luciferase under control of the ISRE promoter[50] were seeded into a flat-bottom 96 well plate at $2.5x10^4$ cells per well in antibiotic-free D10. Media was replaced 24 hours later with 50 µL in triplicate of either; IFNα standards ($1x10^4$ U/mL 4x-serially diluted five times), media-only blank or supernatant from treated cells. These were incubated for 24 hours before 50 µL OneGlo Luciferase reagent (Promega) was added and mixed for 3 minutes at RT in the dark. 50µL of this mix was transferred to white 96 well plates (Costar), and bioluminescence read on a luminometer (GloMax). Results were read as fold-change of luminescence against the media-only blank.

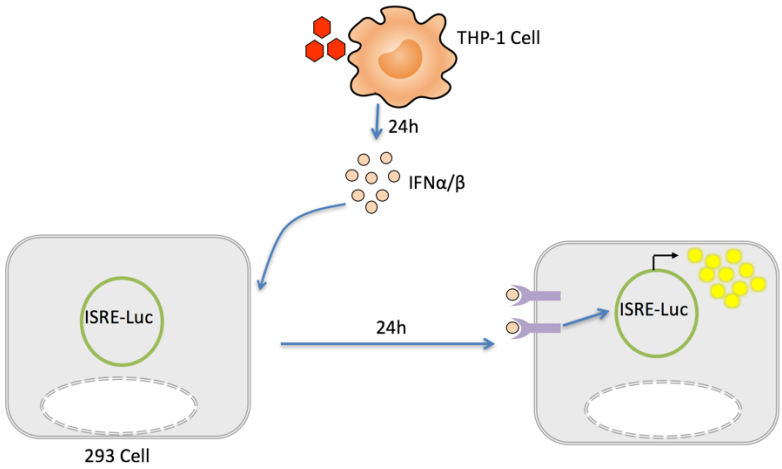

Figure 2.2 IFN Reporter Assay workflow. THP-1 cells were treated, and supernatant containing IFN taken 24 hours later. 293T cells transfected with plasmid encoding luciferase under the control of ISRE promoter were incubated in collected supernatant or IFNα of standard concentrations for 24 hours, before luciferase substrate was added and luminescence read.

2.5 Statistics

2.5.1 Statistical analysis

Numerical analysis was undertaken on Prism (GraphPad) software to determine statistical significance in the mean values of experimental subgroups. Experiments consisting of two sample groups and one comparative parameter only were analysed using the students t-test (paired, two-tailed). Groups requiring multiple comparisons on a data set larger than two samples were analysed by One-Way ANOVA, with Bonferroni post-test correction. All Bar charts are displayed with error bars representing the mean +/- standard error of the mean (SEM).

2.6 Materials Appendix

Table 2.1 Antibodies used

Target	Manufacturer	Species	Cat.	Application/ Dil.
Actin-HRP	Sigma	Ms	A2228	WB 1:200,000
ATM	Cell Signalling	Rb	2873	WB 1:1,000
ATM (pS1981)	Cell Signalling	Rb	13050	WB 1:1,000
BARD1	Santa Cruz	Rb	sc-11438	WB 1:500
BRCA1	Cell Signalling	Rb	9025	WB 1:1,000
BRCA1	Millipore	Rb	07-434	IP 1:100
BRCA1	Santa Cruz	Rb	sc-642	IF 1:100
BRCA1	Santa Cruz	Ms	sc-6954	IF 1:100
BRCA1 (p1189)	Bethyl	Rb	A300-003A	WB 1:1,000
BRCA1 (p1387)	Bethyl	Rb	A300-007A	WB 1:1,000
BRCA1 (p1457)	Bethyl	Rb	A300-009A	WB 1:1,000
BRCA1 (p1466)	Bethyl	Rb	A300-011A	WB 1:1,000
BRCA1 (pS1524)	Cell Signalling	Rb	9009	WB 1:1,000
BRCA1 (pS1524)	Santa Cruz	Rb	sc-101648	IF 1:100
Calreticulin	Cell Signalling	Rb	12238	WB 1:1,000
CD11c-PE	BioLegend	Ms	301605	FC 1:250
CD86-PE	BioLegend	Ms	305405	FC 1:250
CHK2	Cell Signalling	Rb	6334	WB 1:1,000
CHK2 (pT68)	Cell Signalling	Rb	2197	WB 1:1,000
DC-SIGN-APC	BioLegend	Ms	330107	FC 1:250
EEA1	Abcam	Ms	Ab70521	IF 1:100
Giantin	Abcam	Ms	Ab37266	IF 1:100
H2AX	Cell Signalling	Rb	7631	WB 1:1,000
H2AX (pS139)	Cell Signalling	Rb	9718	WB 1:1,000 IF 1:400
Histone H3	Cell Signalling	Rb	4499	WB 1:1,000
HSP90	Cell Signalling	Rb	4877	WB 1:1,000
LSD1	Cell Signalling	Rb	2139	WB 1:1,000
MAVS	Cell Signalling	Rb	3993	IF 1:50
p38 (pT180/Y182)	Cell Signalling	Rb	4511	WB 1:1,000
p44/42 MAPK (pT202/T204)	Cell Signalling	Rb	4370	WB 1:1,000
p44/42MAPK	Cell Signalling	Rb	4695	WB 1:1,000
pIRF3 (S396)	Cell Signalling	Rb	29047	WB 1:1,000
STING	Abcam	Rb	Ab181125	IF 1:100
TANK	Cell Signalling	Rb	2141	WB 1:1000
TBK1	Cell Signalling	Rb	3504	WB 1:1,000 IP 5 µg/mg lysate
TBK1	Santa Cruz	Ms	sc-398366	IF 1:100
TBK1 (pS172)	Cell Signalling	Rb	5483	WB 1:1,000 IF 1:100
TOM20	Santa Cruz	Ms	sc-17764	IF 1:100
Ubiquitin	Cell Signalling	Ms	3936	WB 1:1,000

Table 2.2 shRNA plasmids used

Target	Sequence	Clone
BRCA1	CCGGACTGATACTGCTGGGTATAATCTCGAGATTATACCCAGCAGTATCAGTTTTTTG	TRCN0000244987
BRCA1	CCGGTTGCAACCTGAGGTCTATAAACTCGAGTTTATAGACCTCAGGTTGCAATTTTTG	TRCN0000244986
BRCA1	CGGGAGTATGCAAACAGCTATAATCTCGAGATTATAGCTGTTTGCATACTCTTTTTG	TRCN0000244984
BRCA1	CCGGAGAATCCTAGAGATACTGAACTCGAGTTCAGTATCTCTAGGATTCTCTTTTTG	TRCN0000010305
TBK1	CCGGGCGGCAGAGTTAGGTGAAATTCTCGAGAATTTCACCTAACTCTGCCGCTTTTTG	TRCN0000314840

Table 2.3 PRR agonists used

PRR	Agonist	Supplier
cGAS	E. Coli dsDNA	Invivogen
NOD2	MDP	Invivogen
RIG-I	IVT dsRNA	In-House
STING (Adaptor)	2'3'-cGAMP	Invivogen
TLR2	Pam3CSK4	Invivogen
TLR3	Poly (I:C)	Invivogen
TLR4	LPS	Invivogen
TLR5	Flagellin	Invivogen
TLR8	R848	Invivogen
TLR9	CpG ODN 2216	Invivogen

3 BRCA1 is phosphorylated upon PRR agonism in a DNA Damage-independent manner

3.1 Introduction

Protein phosphorylation on serine, threonine and tyrosine residues is an essential regulatory PTM employed to co-ordinate signal transduction pathways in almost all cellular processes. Phosphorylation dynamics are controlled by kinases and phosphatases, which respond to intracellular and extracellular stimuli to initiate a response. The addition and removal of phosphate groups can alter a protein's activity, localisation, stability and interacting partners. Moreover, it provides a mechanism for rapid, reversible regulation of protein activity, bypassing the requirement for *de novo* protein synthesis. Signal amplification can also occur, with a single kinase or phosphatase regulating many substrate proteins, thereby facilitating a robust response to proportionally small amounts of stimuli.

It is estimated that at least 30% of all eukaryotic proteins can be phosphorylated[368], with at least 100,000 distinct phosphorylation sites in existence across the proteome. Progress in mass-spectrometry (MS) based proteomics, which has vastly accelerated due to advances in instrument performance and power of computational biology, has made it possible to dissect large sets of data and quantitatively profile protein phosphorylation on a proteome-wide scale[369].

In addition to being used to identify kinases, phosphatases and substrates, including their exclusive phosphorylation sites and cellular circumstances regulating these, this approach can be used to uncover direct or indirect relationships between whole signalling networks.

Indeed, such methods have led to the identification of valuable therapeutic targets in many diseases[370] including multiple cancers[371,372] as well as neurodegenerative, metabolic and immune disorders in which phosphorylation defects can be a causative factor[373-378].

PRR activation is one such signalling module which relies heavily on PTMs for regulation of protein activity. Phosphorylation events in these pathways can be observed generally within minutes of immune stimuli being applied, due to the triggering of kinase cascades which result in the activation of NFκB, IRFs and MAPKs. The phosphorylation of target proteins can be activatory or inhibitory, as is the case with IκB, in which phosphorylation permits disengagement and loss of inhibition of the NFκB complex[379]. Regulators of proteins can also be themselves regulated by phosphorylation in the same way, together forming a complex web of phosphorylation.

APCs express a large repertoire of PRRs in order recognise the widest range of pathogens possible. A limited number of phosphoproteomic studies have recently been performed after stimulation of different PRRs[380-382], highlighting novel regulators of the immune response. Interestingly, proteins belonging to networks outside of immune regulation were identified, indicating crosstalk between signalling pathways. LPS stimulation of TLR4 prompted phosphorylation events in the DDR kinases ATM, ATR, CHK1 and Aurora A[382], suggesting that components of the DDR are activated in response not only to consequential sensing of foreign nucleic acids as recent literature suggests, but also in a more general context. Aside from these few specific studies, phosphoproteomic data after general PRR activation is sparse. Notwithstanding this, Dr. Tessa Steevels and Dr. Alistair Leslie of the Simmons lab performed quantitative phosphoproteomic screens in MoDCs of five blood donors after agonism of TLR2 and TLR8, respectively. In these, lysate from stimulated cells was phospho-enriched using a commercial kit which relies on affinity

chromatography techniques. Peptide fragments were then generated after trypsin digestion, before being loaded onto an Orbitrap Velos high capacity ion trap mass-spectrometer. Raw data was run through the Mascot proteomics server, in collaboration with Dr. Benedikt Kessler (Core Proteomics Facility, University of Oxford) and the Computational Biology Research Group (University of Oxford). The large data-set generated, which identifies proteins as phosphorylated or dephosphorylated versus an unstimulated control, was then analysed using gene ontology databases to reconstruct signalling networks and subnetworks. This can then be used to identify novel proteins phosphorylated upon the given stimulus, and interactions between distinct signalling pathways.

3.2 Aims

Accounting for the phosphoproteomic study which reported DDR kinases as differentially phosphorylated upon TLR4 stimulation in macrophages[382], and the accumulation of recent data which suggests direct roles for DDR proteins in innate sensing of DNA[349,352,353,356-360], aims of this part of the study were to identify any DDR proteins as phosphorylated in the nucleic acid-free screens performed within our group. Additionally, the kinetics of such phosphorylation were investigated, as was the exclusivity of these events in PRR-induced signalling pathways; that is, whether phosphorylation of DDR proteins is restricted to activation of specific PRRs or whether it is a more general phenomenon. Further to this, studies were undertaken to determine whether any phosphorylation events were due to consequential induction of DNA damage after PRR agonism, or if the activation of such proteins was DNA damage-independent.

3.3 Results

Data sets from both in-house screens (TLR2 and TLR8) were analysed, and a threshold established for a protein to be deemed as 'significantly' differentially phosphorylated after stimulation; this was restricted to a 50% median increase or 33% median decrease. To identify proteins relating generally to DNA Damage and repair in the remaining data, Amigo2 gene ontology web software was employed. The ontology term 'DNA Repair' (GO:0006281), whose 'children' ontology groups and gene products relate to all aspects of the DDR, was used as a dynamic and broad search parameter. Indeed, each screen identified distinct DNA Repair proteins as significantly phosphorylated or dephosphorylated upon PRR stimulation (Table 3.1A, B).

TLR2 stimulation	
Protein	Fold Change
FTO	2.028061126
RECQL	1.799989221
Pold1	1.651478922
BRE	0.663759617
Hist3h2a	0.619377578
UVRAG	0.294081377
XAB2	0.17637686
OTUB1	0.563095052

TLR8 stimulation	
Protein	Fold Change
CDK7	1.877716469
H2AFX	0.583353507
EGFR	0.018571541
RPS27A	0.60356345
MLH3	0.579102265

Table 3.1 Proteins differentially phosphorylated upon TLR2 and TLR8 stimulation. MoDCs from 5 individual blood donors were stimulated with **A.** 1 µg/mL Pam3CSK4 or **B.** 1µg/mL R848 for 1h before phosphoprotein enrichment. Lysate was trypsinised and subjected to LC-MS/MS, and data run through MASCOT proteomics server. Data was then applied to the Amigo2 gene ontology server using the ontology term 'DNA Repair' and proteins relating to this network identified as significantly differentially phosphorylated tabulated.

3.3.1 MoDC generation and maturation capacity

CD14+ monocytes were isolated from peripheral blood and cultured for 5 days in the presence of IL-4 and GM-CSF to induce their differentiation to immature MoDCs. The purity and differentiation status was occasionally assessed immediately after isolation and after the 5-day culture period using flow cytometry. A high percentage of cells expressing CD14 at day 0 demonstrated a successful monocyte isolation. This CD14 expression was expected to decrease as cells differentiate. Contrastingly, the DC marker DC-SIGN increased from very low to very high over the 5-day culture period (Figure 3.1A)

The ability of differentiated MoDCs to mature after activation was then assessed, by their surface expression of CD83, CD86 and HLA-DR[383,384]. Different PRR ligands were titrated and added to day 4 MoDCs, before harvesting and flow cytometric analysis 24 hours later A representative experiment using CD86 as a maturation marker after Poly I:C stimulation is shown (Figure 3.1B).

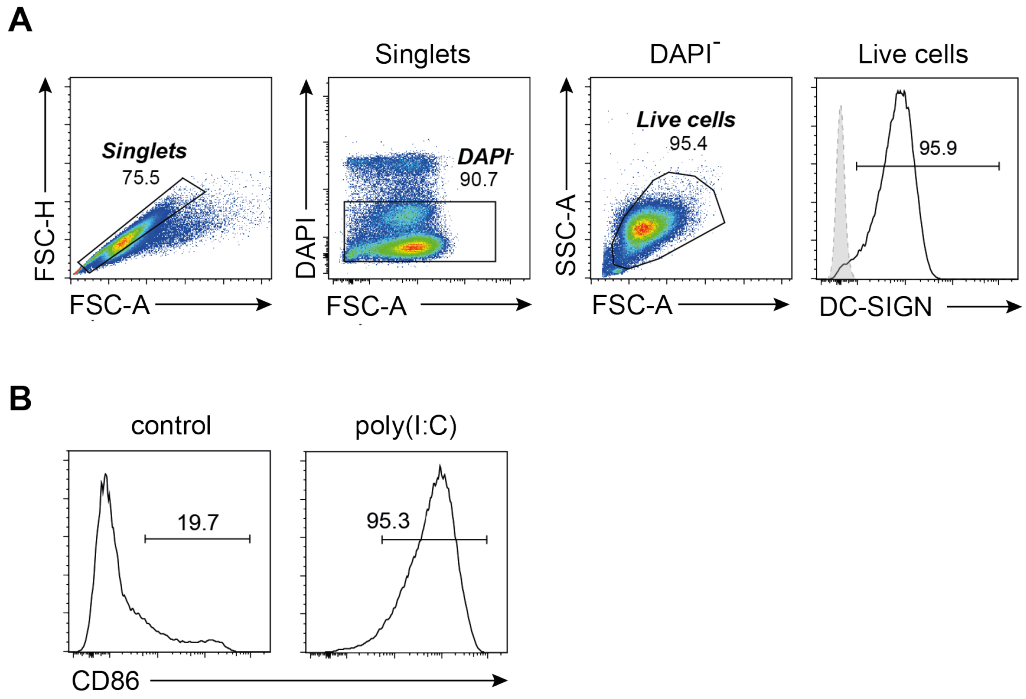

Figure 3.1 Dendritic cell isolation and maturation Representative Flow cytometry data performed with Dr. Jonathan Maelfait using cells 5 days post-CD14+ isolation and incubated in 40ng/mL IL-4 and GM-CSF**. A.** Gating strategy to isolate live single DC-SIGN positive dendritic cells using DAPI and DC-SIGN-APC conjugated primary antibody. **B.** MoDCs untreated or stimulated with 1 µg/mL Poly (I:C) for 16 hours, stained with anti CD86-Violet antibody.

3.3.2 Optimisation of stimulation and phospho-enrichment

A secondary smaller WB screen was then undertaken to validate the phosphorylation of any DDR proteins upon PRR stimulation, using screening conditions originally used by Dr. Tessa Steevels and Dr. Alastair Leslie. MoDCs were harvested after 5 days and incubated with the TLR2 and TLR8 agonists Pam3CSK4 and R848, respectively. Additionally, cells were incubated with etoposide (ETO) for one hour as a positive control, as this induces multiple forms of DNA damage[385,386]. Samples were then subjected to phosphoprotein enrichment and WB. Increased visual density of p44/42 MAPK, a protein broadly phosphorylated in innate immune signalling, in fractions phospho-enriched after PRR activation but not etoposide treatment, confirmed successful enrichment and stimulation of cells (Figure 3.2). Likewise, reduction in density of β-Actin in enriched samples also demonstrates successful enrichment whilst allowing an indirect loading control of enriched samples, as equilibrated amounts of whole cell lysate (WCL) from each sample was loaded onto enrichment columns. Secondary fluorescent antibodies (Li-COR) were used in this initial set-up experiment as they allow co-probing for two proteins of similar molecular mass with use of primary antibodies raised in different species, as lysate was limited.

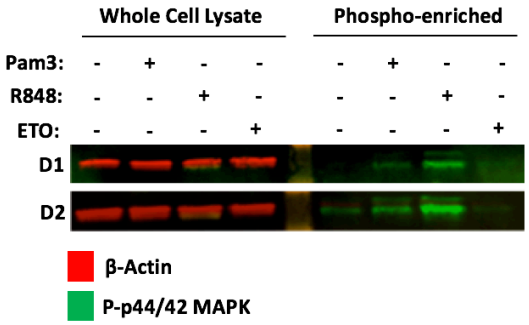

Figure 3.2 Successful phosphoprotein enrichment and cell stimulation. WB of whole cell lysate and phospho-enriched samples using anti p-p44/42 MAPK and β-actin primary antibodies, and LiCOR secondary antibodies after MoDCs were stimulated with 1µg/mL Pam3CK4, 1µg/mL R848, or 100 µM etoposide 1h and subject to phosphoprotein enrichment. D1 and D2 denote donors.

3.3.3 BRCA1 is rapidly phosphorylated at S1524 upon agonism of multiple PRRs

After successful stimulation and enrichment procedures were confirmed, the phosphorylation status of major DDR proteins was assessed in both PRR-stimulatory conditions, using the method above. One protein which was reproducibly identified as increased upon WB using phospho-enriched samples of stimulated MoDCs was the tumour suppressor protein BRCA1 (Figure 3.3). Interestingly, this protein was not phosphorylated by etoposide at this timepoint, which is unexpected as etoposide is known to induce BRCA1 phosphorylation at this residue[385]. Other general markers of DNA damage such as CHK2 and H2AX were phosphorylated with etoposide treatment. Contrastingly, CHK2 and H2AX phosphorylation were not visible in TLR2 and TLR8 stimulated conditions, where BRCA1 was. Other DDR-related proteins such as ATM, ATR, CHK1, p53, Rad23, Rad50, MRE11, NBS1 and DNA-PK were also assessed and no phosphorylation was detected (data not shown).

Detection of p44/42 MAPK again served as an innate immune specific activation marker for these. This result was reproduced using cells from 7 consecutive individual blood donors. Together, this suggested that BRCA1 may be activated in DCs in an alternative pathway to DNA Damage.

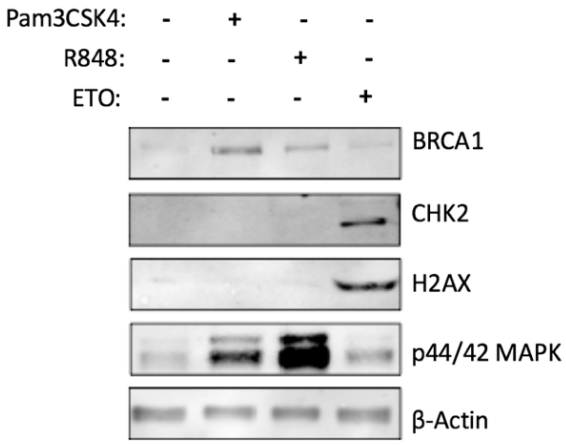

Figure 3.3 BRCA1 is phosphorylated upon PRR stimulation. WB of phospho-enriched samples after MoDCs were stimulated with 1µg/mL Pam3CK4, 1µg/mL R848, or 100 µM etoposide for 1h, using primary antibodies recognising total protein levels of BRCA1, CHK2, H2AX, p44/42 MAPK and β-actin.

A more focussed screen of BRCA1 phosphorylation was then undertaken to determine specific residues modified after PRR activation. Cells were stimulated with the TLR2 ligand Pam3CSK4 and WB performed using antibodies which recognise exclusive BRCA1 phosphorylation sites (reviewed in[282]) (Figure 3.4). Multiple different residues of BRCA1 were seen to be phosphorylated upon agonism of TLR2, including S1466 and S1189. The biological relevance of phosphorylation of these residues is currently unknown[282]. However, these events were relatively weak in comparison to phosphorylation of S1524 (Figure 3.5).

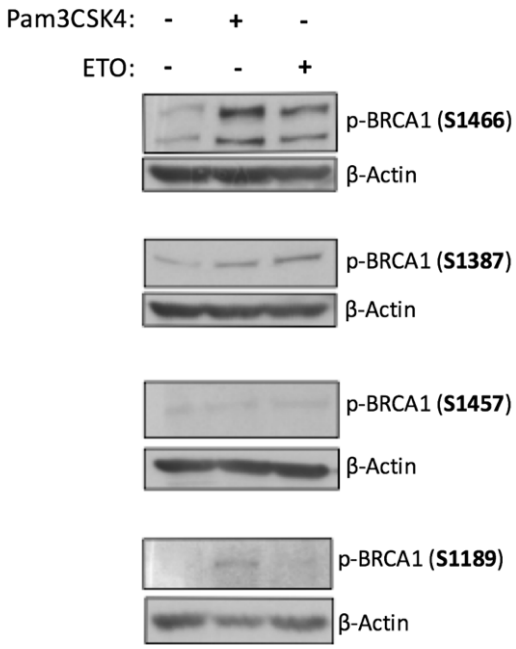

Figure 3.4 Different BRCA1 residues are phosphorylated in response to PRR activation. WB on total cellular lysate after MoDCs were stimulated with 1μg/mL Pam3CK4 or 100 μM etoposide for 1h, using primary antibodies specific to different phosphorylated residues of BRCA1 and β-actin.

The concentrations of agonists activating a range of PRR families were titrated, spanning MyD88-dependent and independent TLRs, RLRs, NLRs, and CDSs. Specifically, Pam3CSK4 is a synthetic triacylated lipopeptide agonist of the plasma membrane TLR2[387] which signals via MyD88 to potently induce NFκB activation and inflammatory cytokine production, before being internalised to endosomal compartments to promote type I IFN signalling[388-391] (Figure 3.5A). LPS on the other hand activates TLR4 signalling, initially via MyD88, before it is endocytosed and signals endosomally via TRIF to produce type I IFN[392] (Figure 3.5B). Flagellin, a bacterial flagellum protein, activates TLR5 which again signals from the plasma membrane via MyD88 to activate NFκB and induce inflammatory cytokine production[393] (Figure 3.5C). Muramyl-dipeptide (MDP) is a bacterial peptidoglycan motif which is recognised specifically by cytosolic NOD2[394] which works through RIP2 and CARD9 to induce NFκB signalling[395](Figure 3.5D). The cytosolic RLR RIG-I was stimulated by transfecting *in vitro* transcribed (IVT) RNA which has a characteristic 5'-triphosphate moiety that is detected by RIG-I[38] (Figure 3.5E). *E. Coli* dsDNA (ECD) of different lengths was transfected to activate CDSs[341] (Figure 3.5F). Additionally, exogenous second messenger 2'-3' cGAMP was transfected as a stimulus (Figure 3.5G). As this molecule is catalytically produced downstream of cGAS-mediated DNA sensing to activate the adaptor STING[46], use of this would help to determine whether the phosphorylation of BRCA1 is a direct result of PRR activation, or whether it is part of a signalling event downstream of adaptor recruitment. Finally, whole pathogen was used to stimulate cells. In this case, the murine parainfluenza Sendaï virus (SeV) was used, with varying multiplicity of infections (MOI) (Figure 3.5H). This virus has a negative sense, single strand RNA genome, and has been shown to infect human cells and activate RIG-I signalling[396]. All agonists were incubated with cells for 1 hour prior to lysis, except transfected ligands (cGAMP, IVT, ECD)

which were incubated for 90 minutes to allow for time taken to enter the cell. WB for phospho-BRCA1 (S1524) (pBRCA1) was then performed, along with total BRCA1 as a control. Antibody against phospho-p38 (T180/Y182) (p-p38) was used as a positive control in each sample, as this is another MAPK that can be used as a general marker of immune activation. Once optimal concentrations of each agonist was determined to visualise BRCA1 phosphorylation, a kinetic time-course experiment was performed with each stimulus using the pre-optimised concentration or amount of each, as determined in the left hand panels. Detection of pBRCA1 was observed relatively swiftly upon stimulation with all agonists, from as early as 15 to 30 minutes.

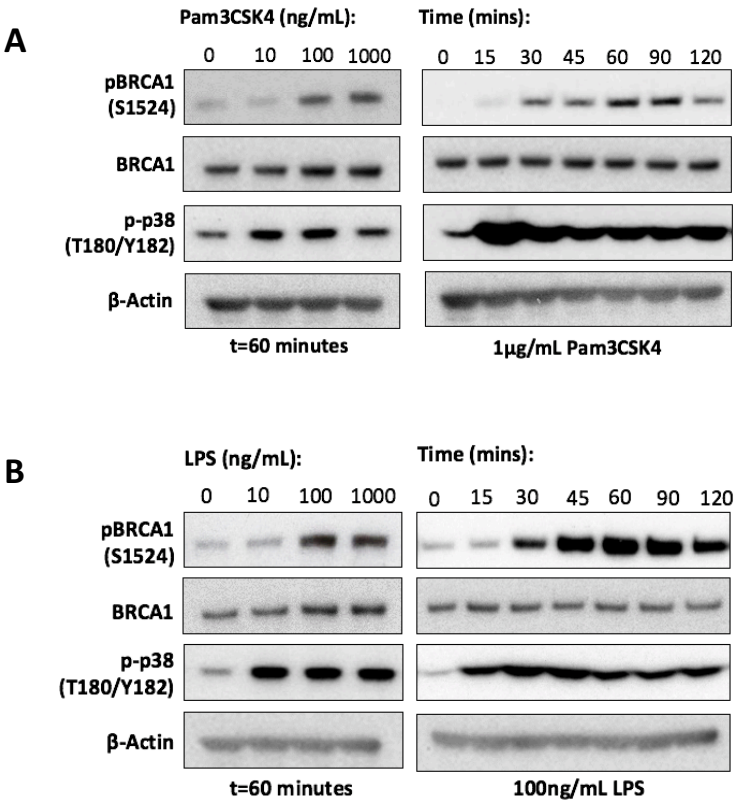

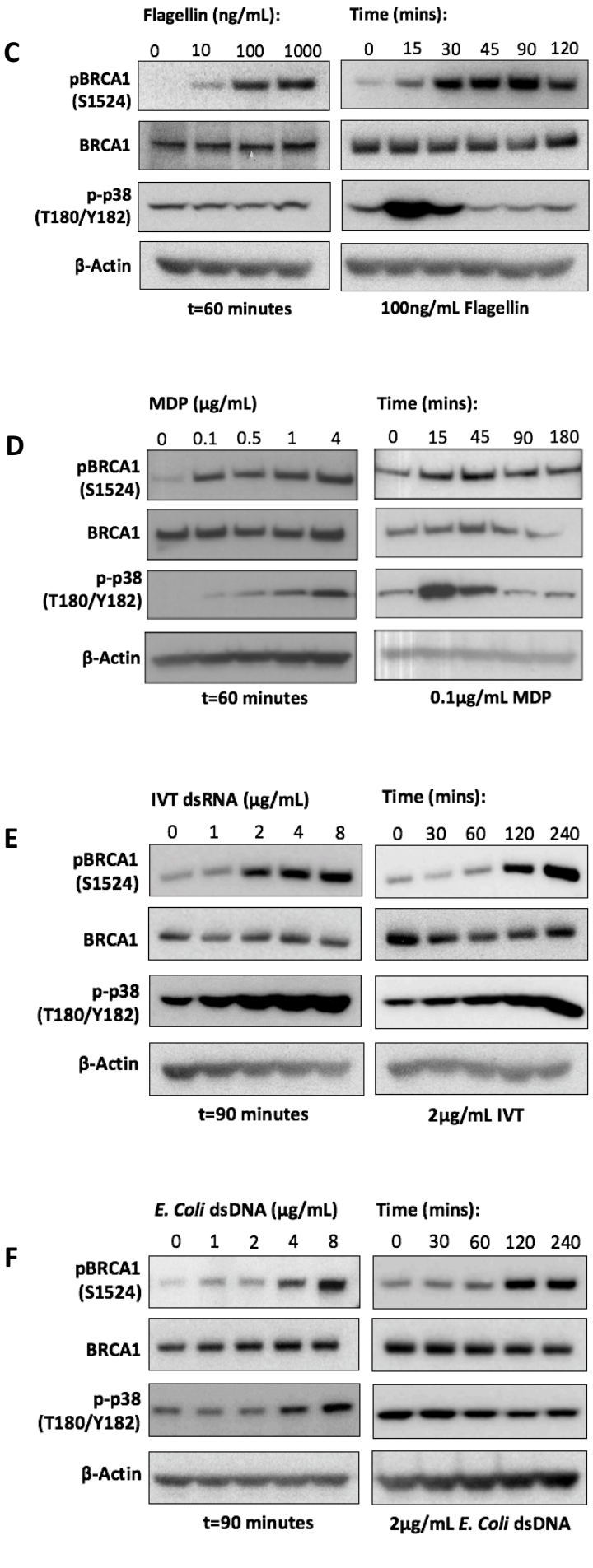
C
Flagellin (ng/mL):
0 10 100 1000
Time (mins):
0 15 30 45 90 120
pBRCA1 (S1524)
BRCA1
p-p38 (T180/Y182)
β-Actin
t=60 minutes
100ng/mL Flagellin
D
MDP (μg/mL)
0 0.1 0.5 1 4
Time (mins):
0 15 45 90 180
pBRCA1 (S1524)
BRCA1
p-p38 (T180/Y182)
β-Actin
t=60 minutes
0.1μg/mL MDP
E
IVT dsRNA (μg/mL)
0 1 2 4 8
Time (mins):
0 30 60 120 240
pBRCA1 (S1524)
BRCA1
p-p38 (T180/Y182)
β-Actin
t=90 minutes
2μg/mL IVT
F
E. Coli dsDNA (μg/mL)
0 1 2 4 8
Time (mins):
0 30 60 120 240
pBRCA1 (S1524)
BRCA1
p-p38 (T180/Y182)
β-Actin
t=90 minutes
2μg/mL E. Coli dsDNA

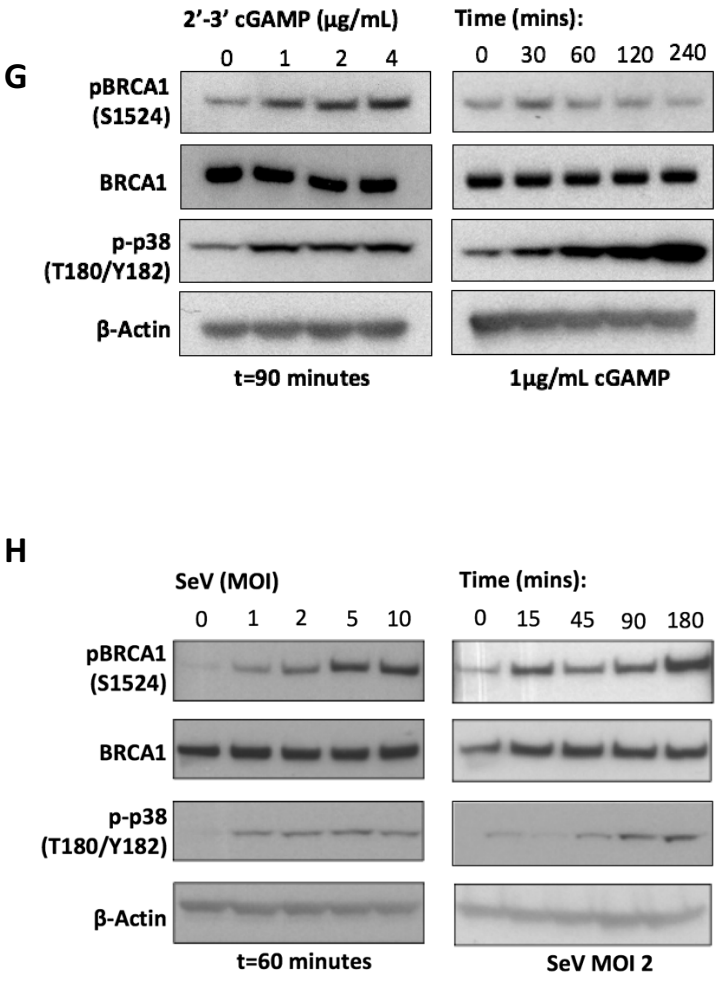

Figure 3.5 BRCA1 is phosphorylated at S1524 upon incubation with multiple immune stimulatory species. WB for pBRCA1, total BRCA1, p-p38 and β-actin using cellular lysate from MoDCs stimulated with **A.** Pam3CSK4 **B.** LPS **C.** Flagellin **D.** MDP **E.** IVT dsRNA **F.** E Coli dsDNA **G.** 2'-3' cGAMP **H.** Sendai Virus, at various concentrations (left panels) and over time (right panels).

3.3.4 The antibody used to detect pBRCA1 (S1524) is phospho-specific

MoDCs were then treated with IVT RNA or bleomycin, another DNA-damaging agent which can induce SSBs and DSBs[397]. This was carried out in the presence or absence of lambda-phosphatase, which is a Mn^{2+}-dependent broad-spectrum phosphatase that cleaves phosphates from serine, threonine and tyrosine residues. Induction of pBRCA1 can be

seen with both IVT and bleomycin (Figure 3.6), although phosphorylation is much more visible after incubation with the RIG-I agonist. Addition of lambda-phosphatase reduces the phosphorylation markedly, demonstrating that the antibody is indeed specific for phosphorylated BRCA1.

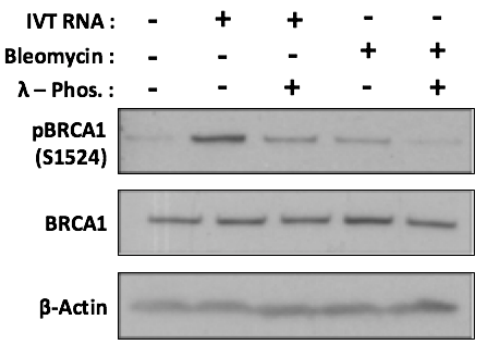

Figure 3.6 Lambda phosphatase treatment of cellular lysate. WB for pBRCA1, total BRCA1 and β-actin on lysates from MoDCs stimulated with 2µg/mL IVT RNA for 90 minutes. Lysate was incubated in the presence or absence of Lambda phosphatase (λ-phos) at a concentration of 20 U per 50 µg lysate, for 30 minutes at 30°C prior to SDS-PAGE.

3.3.5 BRCA1 phosphorylation after PRR stimulation is DDR signalling-independent

BRCA1 is usually phosphorylated in response to a range of DNA Damage stimuli, where it acts at multiple levels to direct DNA repair and regulate cell survival and proliferation[279]. In particular, the phosphorylation of S1524 is thought to be mediated by ATM in response to DSB formation and radiation, for example by treatment with etoposide or after UV or IR exposure[282,398]. It was therefore sought to establish whether the increase in pBRCA1 after PRR activation was due to induction of DNA damage, for example by the characteristic increase in ROS production after APC activation, or if the phosphorylation is a direct result of PRR signalling.

Firstly, MoDCs were treated with etoposide or bleomycin at different concentrations to establish optimal conditions to capture DDR signalling in these cells, to serve as a positive control in further experiments. Indicative of DSB formation[399,400], pATM (S1981) increases in a dose-dependent manner upon incubation with both etoposide (Figure 3.7A) and bleomycin (Figure 3.7B), whilst total ATM remains stable. Similarly, after incubation with 100 μM or 10 μM bleomycin, pCHK2 which is usually induced by autophosphorylation or by ATM kinase activity after DNA damage sensing is increased[239]. Curiously, pCHK2 can only be seen with incubation of cells in 10 μM etoposide at this 1 hour timepoint, perhaps due to high levels of damage incurred with 100 μM inducing pCHK2 at an earlier timepoint. Interestingly, pBRCA1 does not increase with any concentration of either DNA-damaging agent, whilst total BRCA1 expectedly remains stable in each sample.

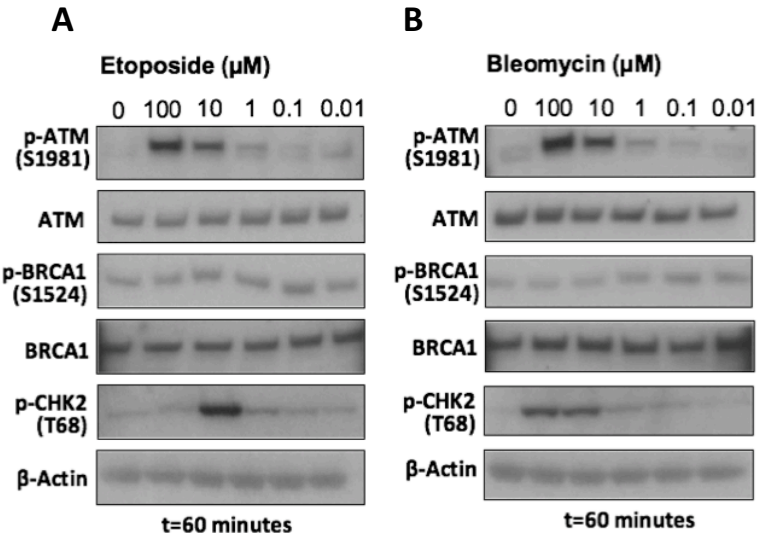

Figure 3.7 Optimisation of DNA Damaging agent concentrations. WB using p-ATM, total ATM, p-BRCA1, total BRCA1, p-CHK2, and β-actin after MoDCs were treated with differing concentrations of etoposide or bleomycin for 1h.

In order to assess the kinetics of DNA damage signalling and whether this is circumstantially variable for BRCA1 phosphorylation, this experiment was repeated using 100 µM of each DNA damaging agent, which induced the highest level of pATM previously. Additionally, a sample using cells treated with 100 ng/mL LPS for 1 hour was included as a positive control for BRCA1 phosphorylation at S1524, as pre-optimised earlier (Figure 3.5B). Here, peak levels of pATM were observed between 0 and 15 minutes of incubation with etoposide (Figure 3.8A), and between 45 and 90 minutes of bleomycin treatment (Figure 3.8B), before returning to basal levels in both. pCHK2 after etoposide treatment was detected between 0 and 15 minutes before decreasing back to basal levels, explaining why this was not visible when 100 µM was used for 1 hour in Figure 3.7. Mirroring pATM, pCHK2 appearance upon treatment with bleomycin occurs later, with peak levels observed at 45 to 90 minutes. Finally, γH2AX is detected after 3 hours or 45 minutes of etoposide or bleomycin treatment, respectively. Use of neither treatment at any timepoint induces pBRCA1, which is strongly induced in the LPS treated sample. Conversely, neither pATM nor pCHK2 appear to be increased in this sample, suggesting BRCA1 phosphorylation in PRR-activatory conditions bypasses upstream DNA damage signalling.

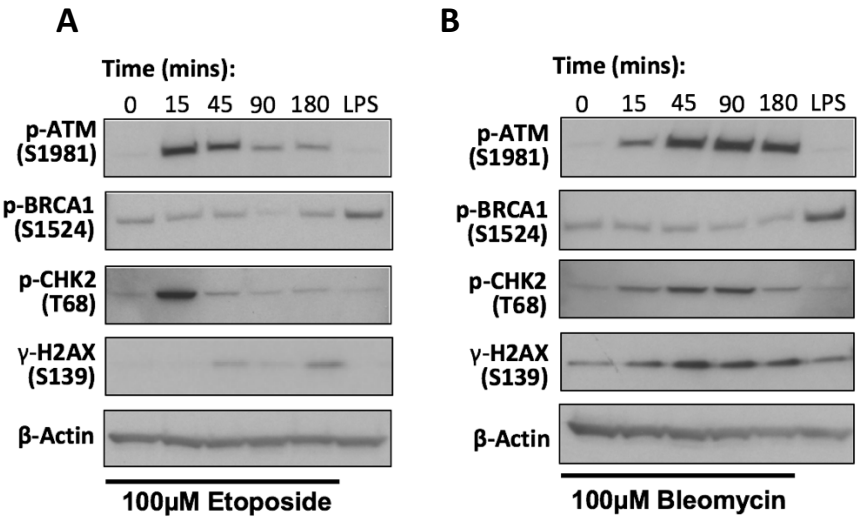

Figure 3.8 Etoposide or bleomycin-induced DNA Damage does not result in increased pBRCA1(S1524). Immunoblot for p-ATM, pBRCA1, p-CHK2, p-H2AX and β-actin on lysates from MoDCs after incubation with **A.** 100 μM etoposide or **B.** 100 μM Bleomycin for various times, or alternatively with 100 ng/mL LPS for 45 minutes.

To further investigate this phenomenon, an inverse experiment was undertaken; samples subjected to time-course incubations with different PRR ligands or etoposide were assessed by WB. This showed that no DNA damage signalling, via ATM or CHK2, is induced upon innate PRR stimulation, as is seen with etoposide (Figure 3.9). Together, this shows that BRCA1 is not phosphorylated downstream of activation of DNA damage signalling.

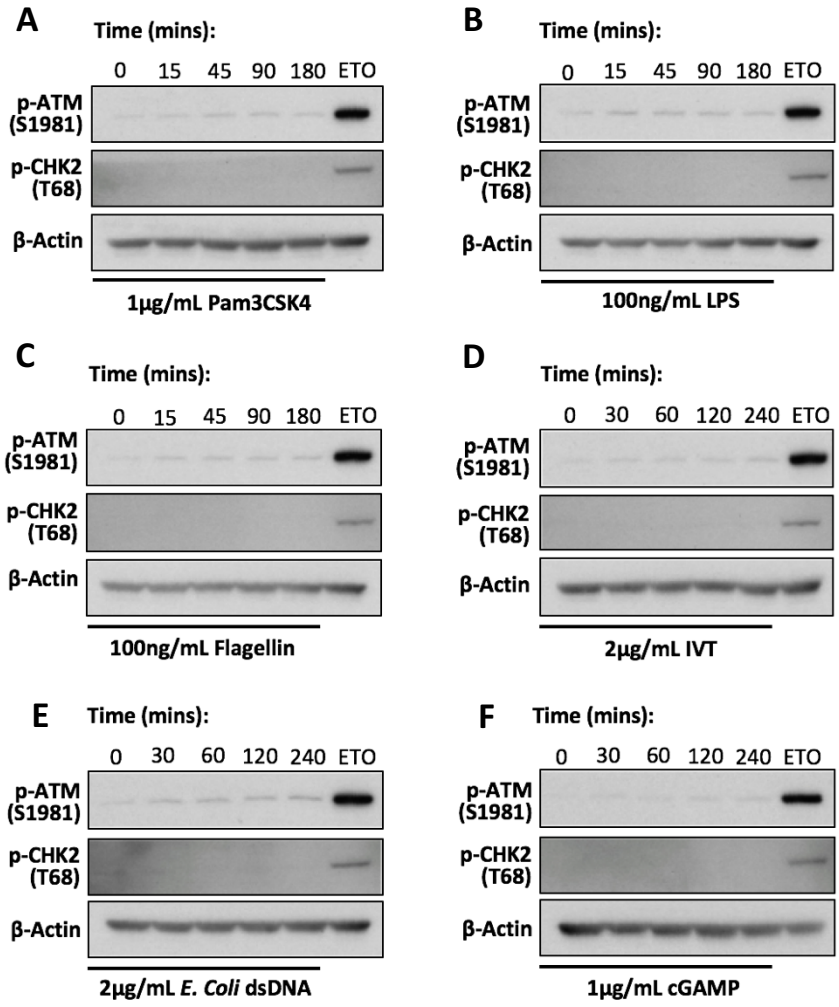

Figure 3.9 PRR agonism does not induce DNA damage signalling. MoDCs were stimulated with **A.** 1 µg/mL Pam3CSK4 **B.** 100 ng/mL LPS **C.** 100 ng/mL Flagellin **D.** 2 µg/mL IVT dsRNA **E.** 2 µg/mL E. Coli dsDNA **F.** 1 µg/mL 2'-3' cGAMP for various times, or with 100 µM etoposide for one hour. Immunoblot for p-ATM, p-CHK2 and β-actin shown.

3.3.6 BRCA1 phosphorylation is independent of genotoxic stress

The alkaline comet assay (also known as single cell gel electrophoresis) was then employed to test whether any physical DNA damage is accumulated upon PRR activation. This procedure is very sensitive and can allow rapid evaluation and quantification of DNA Damage in a cell[401]. Types of damage detected include DSBs, SSBs, alkali labile sites, oxidative base damage and DNA cross-links[402]. Cells are treated and placed in an agarose bilayer before all components are stripped with an alkaline lysis buffer, leaving only genomic DNA. This is then unwound before being horizontally electrophoresed, with broken segments of DNA migrating faster due to decreased size, leaving a distinctive 'comet' tail preceding an intact genomic DNA head (Figure 3.10A). Stained DNA is then subjected to Komet software analysis, which calculates the head to tail ratio, which is directly proportional to the amount of DNA damage. This so called Relative Tail Moment is calculated for 50 cells in each sample and used for statistical analysis.

An initial time course experiment was performed to optimise the conditions for DNA Damage detection after incubation with 100 µM of etoposide or bleomycin (Figure 3.10B). Highest levels of DNA damage were detected after 2 hours of incubation of each DNA-damaging agent, but cell viability also dropped heavily at this time in each case (Figure 3.10C), so 1 hour incubations were taken forward for further experiments.

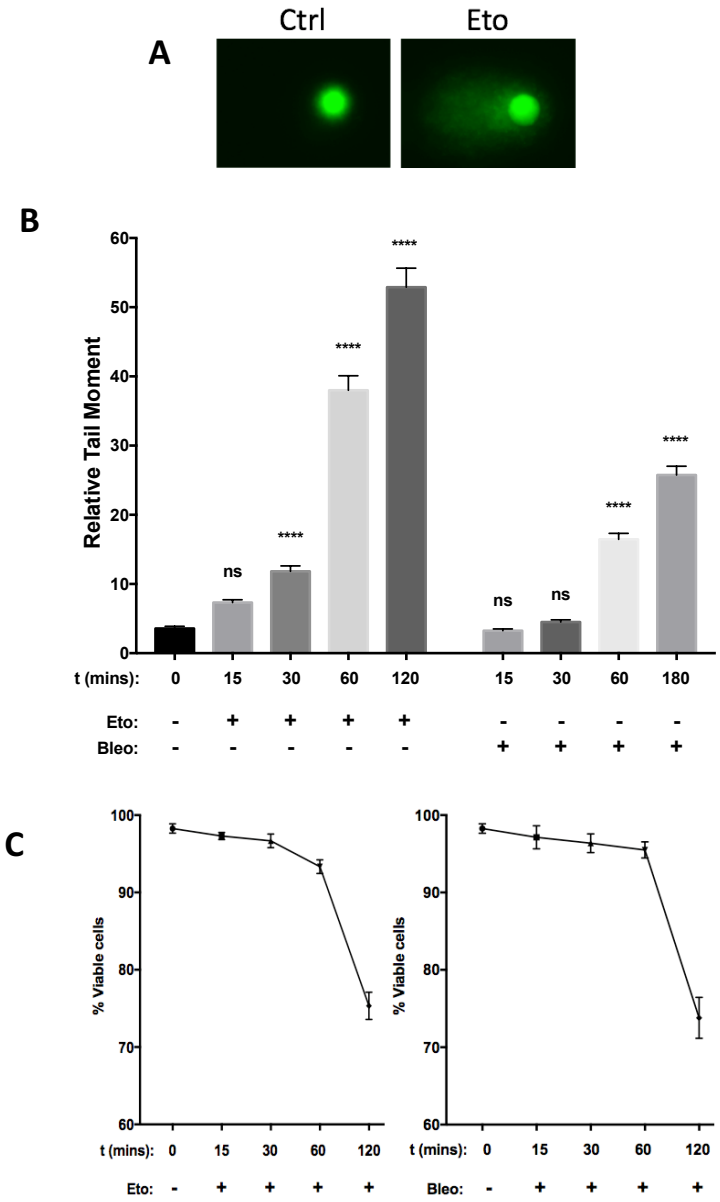

Figure 3.10 Optimisation of DNA Damage induction. MoDCs were incubated with 100 µM etoposide or bleomycin for various times, before being subject to the alkaline comet assay. **A.** representative image of an untreated or etoposide treated cell. **B.** Relative tail moment taken from 50 cells per condition after a time-course incubation with 100 µM of etoposide or bleomycin **C.** Cell viability for each sample measured by Trypan Blue staining. Results representative of experiments performed on cells combining three individual blood donors. ****p<0.0001

A time course experiment was then performed incubating cells with either Pam3CSK4 or etoposide (Figure 3.11). Alkaline comet assay was once again undertaken, and pBRCA1 tracked by WB for each sample. Additionally, p-p38 and p44/42 MAPK were probed to determine successful immune stimulation, whilst γH2AX was used as a marker for DNA damage signalling pathway activation. Representative images demonstrate a large comet tail induced with use of etoposide, but not after incubation with Pam3CSK4 at any timepoint. This translates in Relative Tail moment calculations, with etoposide inducing high levels of DNA damage, in addition to increased γH2AX detection by WB. Pam3CSK4 stimulation on the other hand does not induce any DNA Damage of γH2AX activation. Again, pBRCA1(S1524) appears exclusively after PRR agonism in MoDCs, whilst remaining stable upon induction of DNA damage by etoposide.

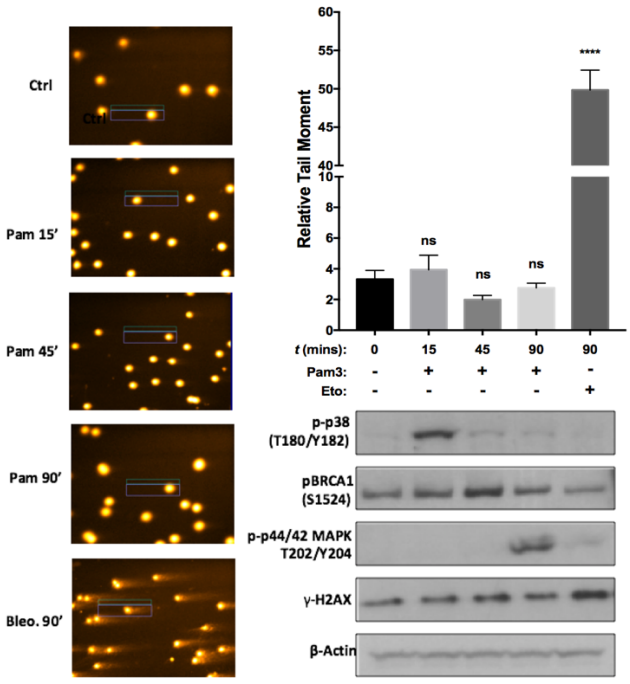

Figure 3.11 PRR stimulation does not induce DNA Damage. MoDCs were stimulated with 1 µg/mL Pam3CSK4 for various times or 100 µM etoposide for 90 minutes before alkaline comet assay was performed. Representative images shown for each sample (left) and relative tail moment calculated from 50 cells per condition (top right). WB analysis of each sample was also performed (bottom right). Results representative of experiments performed on cells combined from three individual blood donors. ****p<0.0001

To determine whether this DNA damage-independent activation of BRCA1 is a general reaction to PRR activation, the experiment was repeated using multiple PRR agonists to activate a variety of receptor families, using the concentrations of each optimised in Figure 3.5. In addition, etoposide and bleomycin were used again as positive controls to induce DNA damage. Incubation with any PRR agonist for 45 minutes (Figure 3.12A) or 90 minutes (Figure 3.12B) did not result in increased DNA damage, apart from LPS which induced very little in comparison to etoposide and bleomycin. This ligand is historically known to be genotoxic[403], providing an explanation for the small amount of damage seen at this time point.

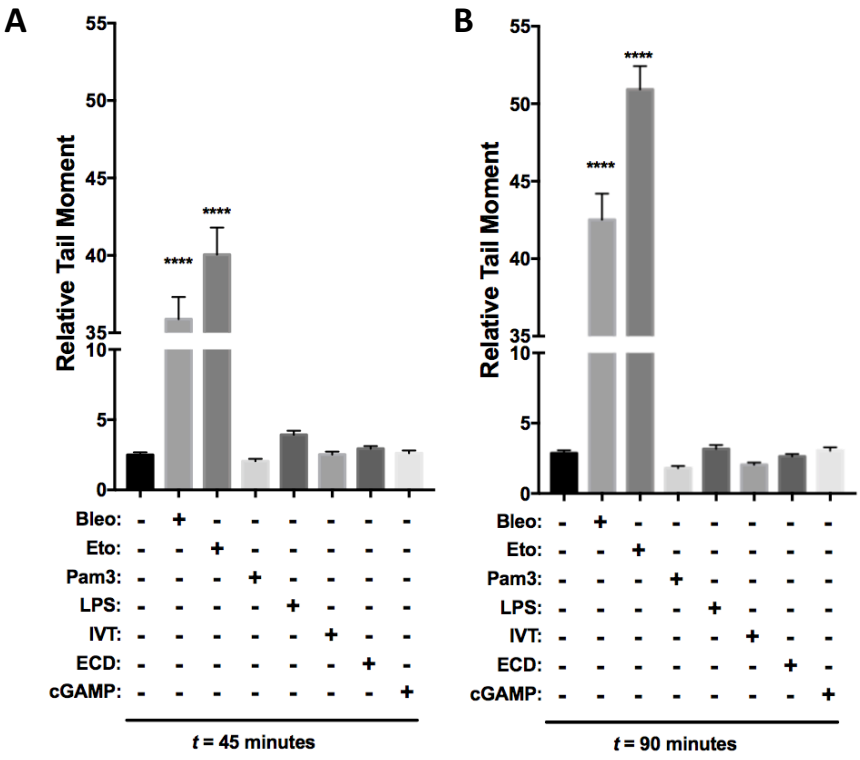

Figure 3.12 MoDC stimulation with multiple PRR agonists does not induce DNA damage. MoDCs were stimulated with 100 µM bleomycin, 100 µM etoposide, 1 µg/mL Pam3CSK4, 100 ng/mL LPS, 2 µg/mL IVT dsRNA or 2 µg/mL *E. Coli* dsDNA, for either **A.** 45 minutes or **B.** 90 minutes before alkaline comet assay was performed, and relative tail moment of 50 cells per sample taken. Results representative of experiments performed on cells combined from three individual blood donors. ****p<0.0001

3.3.7 BRCA1 phosphorylation after PRR stimulation is independent of oxidative stress

APCs such macrophages and DCs undergo large metabolic reprogramming upon activation, which often leads to vastly increased production of cellular ROS[404,405] that can have direct signalling properties in addition to providing a cell survival signal[406]. These ROS have also been reported to have direct antimicrobial properties[407,408].

Although the oxidative burst is less intense in DCs than neutrophils, its induction can nevertheless induce oxidative damage to both genomic and mitochondrial DNA[409,410]. Therefore, it was important to interrogate whether increased cellular ROS production in MoDCs can trigger the phosphorylation of BRCA1 prior to any physical damage induced.

Under DNA-damaging conditions, ATM autophosphorylates at S1981 which induces the dissociation of subunits from an inactive homodimer complex[411,412], to allow active monomers to co-ordinate DNA repair which includes phosphorylation of BRCA1 at S1524[413]. Incubation of cells with H_2O_2 has been shown to activate ATM to mediate an appropriate response against the oxidative stress incurred[414,415]. This activation can be prevented by treatment with the antioxidant N-Acetyl cysteine (NAC)[416]. Incidentally, loss of ATM in AT patients is characterised by vastly increased cellular ROS levels and increased susceptibility to ROS-inducing agents[414,417]. Interestingly, this activity of ATM was demonstrated to be prompted in a DNA damage-independent manner, whilst the configuration of active ATM in this circumstance is not as a phosphorylated monomer as in DNA damaging conditions, but as a dimer held together by covalently-linked disulphide bonds which requires an oxidative environment for its formation[418]. Native PAGE was therefore undertaken to assess whether ATM is activated in this fashion after PRR activation and the subsequent oxidative burst, as opposed to phosphorylation at S1981

which was shown to be absent upon PRR activation. This was chosen in addition to the comet assay, in case dimerisation provides a more sensitive approach to detecting oxidative stress-induced ATM activation, which could therefore activate BRCA1. MoDCs were stimulated with Pam3CSK4 for various times, or with etoposide as a positive control, before cells were lysed and Native PAGE undertaken. Using representative results from cells of two blood donors, the visual density of ATM monomer (350kDa) and ATM dimer (700kDa) levels does not change significantly over the time-course tested or with etoposide treatment, suggesting ATM is not activated by dimerisation upstream of BRCA1 phosphorylation (Figure 3.13). As the gel chemistry used (Tris-Acetate) was optimised to detect such large protein components, no direct loading control was possible, but ATM monomer levels can indirectly serve this purpose in this instance.

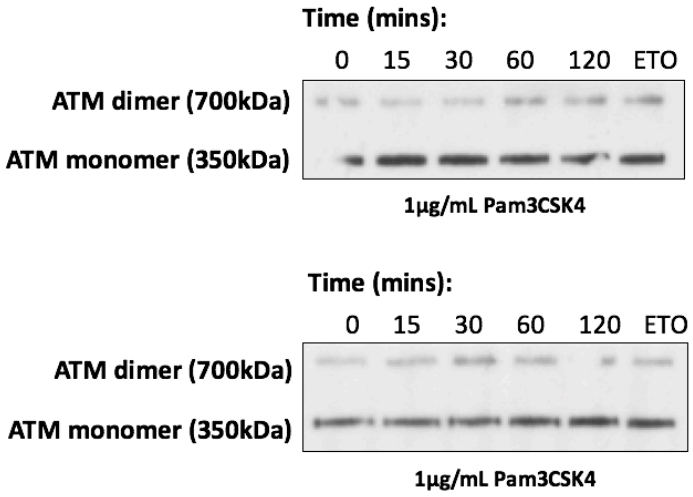

Figure 3.13 Native PAGE shows ATM dimer levels do not change upon PRR activation. MoDCs were incubated with 1 µg/mL Pam3CSK4 for various times, or 100 µM etoposide for 1h before Native Page was performed to assess levels of ATM monomer and dimer. Immunoblot with anti-ATM antibody shown.

To determine whether cellular ROS produced generally downstream of phagocyte activation could promote the direct phosphorylation of BRCA1 at S1524, in the absence of DNA damage signalling or oxidation-induced ATM activation, the CellROX red assay was employed. This procedure uses a cell permeable dye which exhibits bright fluorescence with an emission maxima of 655nm upon oxidation by ROS, thereby permitting measurement of oxidative stress in a cell by flow cytometry. As a positive control, cells were incubated with Tert-butyl-hydroperoxide (TBHP), a potent ROS inducer[419-421]. This was either in the presence or absence of N-Acetyl cysteine (NAC), an antioxidant that promotes the neutralisation of the ROS produced[422] to prevent oxidative DNA Damage[423]. Firstly, titrated concentrations of both TBHP and NAC were tested and optimal concentrations for use in MoDCs was determined (Figure 3.14A). Cells were then treated with these concentrations of either TBHP alone or in conjunction with NAC for one hour, whilst a Pam3CSK4-stimulated sample served as a positive control for BRCA1 phosphorylation. Cells were lysed and pBRCA1 levels assessed by WB (Figure 3.14B). Treatment with TBHP alone or in conjunction with NAC did not induce an increase in pBRCA1 levels, in comparison to Pam3CSK4-mediated TLR2 stimulation. This demonstrates that BRCA1 phosphorylation is not prompted by large increases in cellular ROS and its associated genotoxic stress.

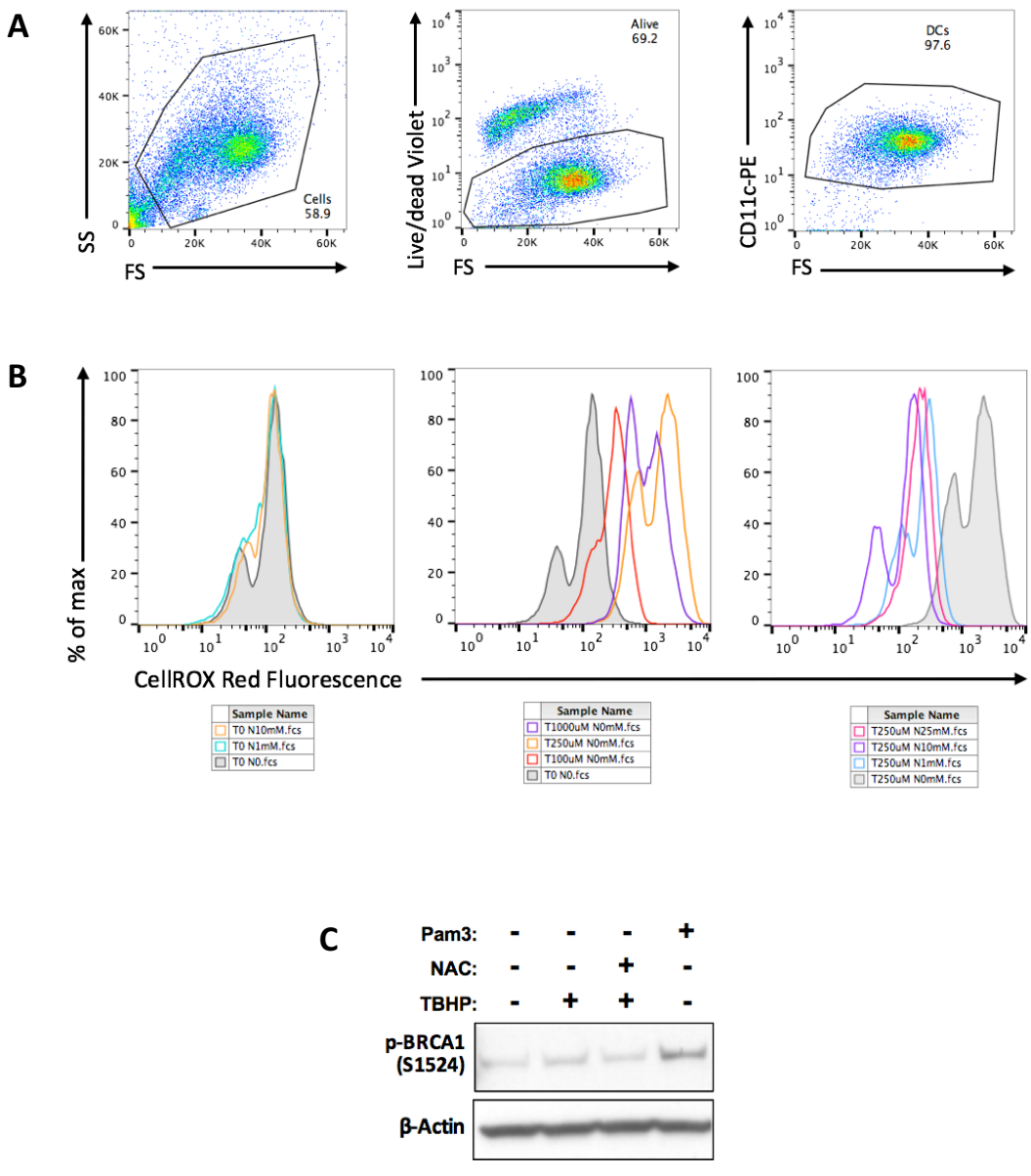

Figure 3.14 BRCA1 phosphorylation is independent of ROS production. A. Flow cytometric (FACS) gating strategy to isolate only viable MoDCs using LiveDead Violet stain and anti CD11c-PE antibody as a DC marker **B.** FACS analysis of CellROX red fluorescence, relating to cellular ROS levels after incubation of MoDCs with different concentrations of TBHP (T) or NAC (N) for 1h. **C.** WB analysis after incubation of MoDCs with 1 µg/mL Pam3CSK4, or optimal concentrations of TBHP (250 µM) and/or NAC (10mM) for 1h.

3.4 Discussion

In this part of the study, I demonstrate for the first time that the pleiotropic protein BRCA1, well-known for its multiple roles relating to DNA damage and repair, is phosphorylated upon activation of a range of PRR families in MoDCs. In particular, Serine 1524 was identified as a heavily phosphorylated residue after agonism of members of cell surface and endosomal TLRs, cytosolic DNA and RNA sensors, NLRs and also in response to whole pathogen in the form of Sendaï virus. Interestingly, very small amounts of non-transfected agonists are needed to induce this phosphorylation, showing a high sensitivity to PRR activation.

Ordinarily, ATM phosphorylates BRCA1 at S1524 predominantly after IR and UV[398,413] exposure at its consensus sequence (S/T-Q) to promote cell survival by permitting interaction with the antiapoptotic protein XIAP, which is important in radio-resistance. Unexpectedly here, although use of genotoxic agents succeeded in inducing DNA damage and signal transduction via H2AX, ATM and CHK2, BRCA1 phosphorylation at S1524 was unaffected, suggesting that this event is reserved for DDR-independent functions in these cells.

The data also shows that this phosphorylation of BRCA1 is rapid, and kinetics demonstrate that the pathway which regulates this is different to that of p38, as different PRR agonists show non-overlapping kinetics for phosphorylation of each of the two proteins. The treatment of cells with PRR agonists does not activate DDR signalling by ATM, CHK2 or H2AX, nor does it induce the accumulation of any physical DNA damage as assessed by the alkaline comet assay and ATM dimerisation. Similarly, I demonstrated that induction of high levels of cellular ROS, often seen after APC activation, does not induce pBRCA1.

It is important to recognise that BRCA1 and other upstream DDR proteins detected in this study such as ATM and CHK2 are indeed expressed in MoDCs and can be functionally activated to a high level in these cells, which is somewhat unexpected as MoDCs are terminally differentiated primary cells with no proliferative capacity[424,425]. They in theory should express low levels of DDR components[426,427] as they need not pass on their genetic material like stem cells would. Nonetheless, certain pathways are expressed in terminal cells to protect transcriptionally active sequences[428]. However, it has been noted that dendritic cells and macrophages have an increased expression of DDR proteins compared to progenitor monocytes[429,430], whilst BRCA1 is well expressed in immune cells generally (Figure 3.S1). The reasons for this are still undefined, although it is thought that this may protect against oxidative stress induced after activation. However, given the multiple publications identifying distinct immuno-regulatory roles of DDR proteins[352,353,356-360], reports of DNA damage-independent activation of proteins within the DDR[237,431], and an acceptance that there are as-yet undefined non-tumour suppressor functions of BRCA1[279,289,290], it is conceivable that BRCA1 expression is relatively high in myeloid-derived cells to confer a specific functional role in immune signalling.

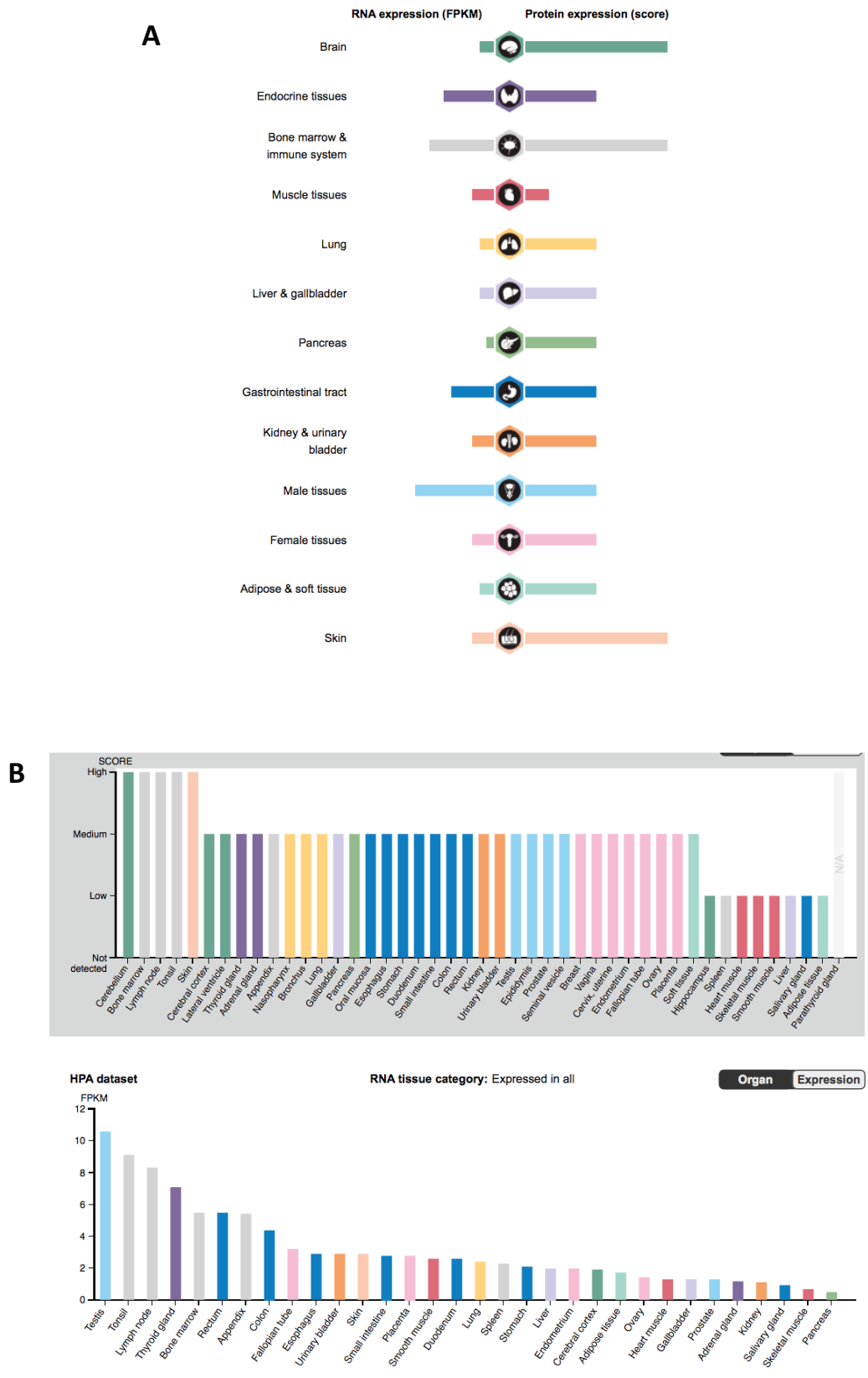

Figure 3.S1 BRCA1 RNA and expression profile in different tissues and organs. **A.** General RNA and protein expression of BRCA1 in different areas of the body. **B.** Distinct protein expression profile in organs, ranked highest to lowest. **C.** RNA expression profile in organs (taken from RNASeq data, ranked highest to lowest. All taken from proteinatlas.org

4 BRCA1 phosphorylation at S1524 occurs downstream of TBK1 activation at Giantin-containing perinuclear zones

4.1 Introduction

BRCA1 is usually phosphorylated in a cell cycle-dependent manner in response to different genotoxic stresses; each of these in turn will induce the phosphorylation of one of the 15 thus-far identified distinct phosphorylation sites within the protein, 12 of which reside between amino acids 1148 and 1542[282]. Much complexity exists in BRCA1 phosphorylation patterns, with putative upstream kinases such as ATM and ATR reported to phosphorylate BRCA1 at exclusive or overlapping residues, dependent on the specific genotoxic insult incurred[413]. ATM is the only kinase currently known to directly mediate phosphorylation of BRCA1 at S1524[398], an event which has been proposed to regulate the G2/M checkpoint[432] and cell survival in response to radiation damage, in addition to preventing binding of XIAP to caspase 8 to promote caspase 3 cleavage. However, due to the intricate nature of DDR signalling, others kinases such as ATR and CHK2 can indirectly influence phosphorylation of this residue. Once BRCA1 has been activated, most of its functions are restricted to the nucleus where it co-ordinates multiple processes relating to DNA repair and maintenance of genome integrity, with the use of its two (potentially three[281]) nuclear localisation signals[279]. Few sources have also cited a movement of BRCA1 out of the nucleus to the cytoplasm, where it seems to have a yet-undefined function[303,433]. In the previous chapter, a DNA damage and DDR signalling-independent phosphorylation of BRCA1 at S1524 in response to PRR stimulation was demonstrated. These PRR-induced signalling events rely heavily on cytoplasmic kinase cascades to transduce and amplify an

initial signal in order to elicit appropriate inflammatory responses. This is ultimately facilitated by activation of canonical and non-canonical IKK proteins, including TBK1, whose functions activate transcription factors including NFκB and IRF3 which then translocate to the nucleus and induce expression of inflammatory cytokines and IFN, respectively.

4.2 Aims

The aims of this chapter will be to determine whether BRCA1 phosphorylation after activation of innate immune signalling is downstream of its canonical kinases or innate immune kinase activity. If any innate signalling axis is identified as upstream of BRCA1 phosphorylation in this context, activation kinetics will be assessed to determine the proximity of BRCA1 phosphorylation to this signalling point. I will also investigate the cellular location of BRCA1 upon phosphorylation, to resolve whether the phosphorylated form of the protein functions inside or outside of the nucleus. Finally, I will establish whether pBRCA1 is recruited to any specific organelle, with a view to hypothesising a potential function or mechanism.

4.3 Results

4.3.1 BRCA1 is not phosphorylated by canonical kinases

Firstly, the activity of canonical kinases upstream of BRCA1 were assessed in PRR-activatory conditions. MoDCs were incubated with small molecule inhibitors to each upstream kinase, including KU-55933 which is a potent ATM inhibitor[434](ATMi), the CHK2 inhibitor NSC-109555 ditosylate[435](CHK2i), and the ATR inhibitor VE-822[436](ATRi). Although ATR has been shown to phosphorylate other residues of BRCA1 including S1148, S1280 and S1387, it was chosen as a candidate due to the circumstantial redundancy in BRCA1 kinase activity; that is, ATM and ATR can phosphorylate distinct or overlapping BRCA1 residues depending on the type of damage sensed[413], and this previously undescribed BRCA1 phosphorylation pathway may therefore have the potential to utilise any upstream kinase. In each case, efficacy of the inhibitors was first tested. Western blotting was performed on lysate of cells incubated with or without etoposide, probing for pATM and pCHK2 (Figure 4.1A); induction of both is seen when cells were treated with etoposide in the absence of any inhibitor, signifying the generation of DSBs. ATMi was shown to ablate phosphorylation of both ATM itself and downstream CHK2[437]. Antibody against pATR (S428), whose induction indicates formation of SSBs, was tested but not specific enough for reproducible usage. However, ATR has been shown to phosphorylate CHK2 at T68 after SSB formation, showing a level of redundancy when ATM levels are reduced[438,439]. This therefore permits the use of pCHK2 an indirect measurement of ATRi efficiency. Use of ATRi did indeed result in decreased pCHK2 levels, suggesting successful inhibition of ATR activity.

This was then repeated in the presence or absence of 1 μg/mL Pam3CSK4 for 60 minutes, which induces a significant increase in pBRCA1 levels (Figure 4.1B). Inhibition of any of the

canonical kinases did not affect pBRCA1 levels, suggesting these are not responsible for phosphorylation of S1524 after PRR activation.

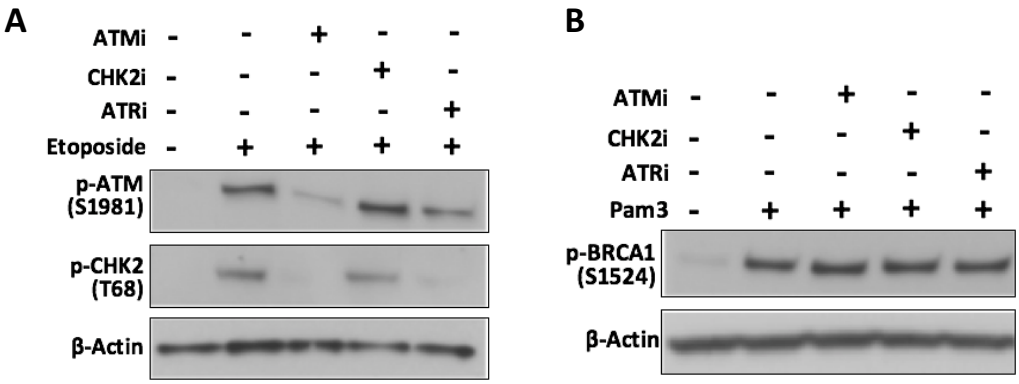

Figure 4.1 PRR stimulation-induced BRCA1 phosphorylation is independent of canonical kinases. WB analysis of MoDCs untreated or incubated with 10 µM of KU55933 (ATMi), NSC-109555 (CHK2i), or NSC-109555 ditosylate (ATRi) for 3 hours before incubation for 1 hour with **A.** 100 µM etoposide or **B.** 1 µg/ml Pam3CSK4. Cell lysates were immunoblotted using anti p-ATM, pCHK2 and β-actin antibodies.

4.3.2 BRCA1 is phosphorylated downstream of innate immune kinase activity

Next, a small WB screen was performed using small molecule inhibitors of different innate immune signalling points, to determine whether the activity of these is upstream of BRCA1 phosphorylation and therefore whether BRCA1 phosphorylation is an event which directly intersects innate immune signal transduction pathways. For this, the TLR2 ligand Pam3CSK4 was used as a general pBRCA1-inducing control. Of the inhibitors chosen, SB203580 targets the kinase activity of p38 MAPK[440], which is often seen phosphorylated upon PRR stimulation and controls cell responses to cytokines and general stress[441,442]. Bafilomycin A1 is a V-ATPase inhibitor which prevents fusion of autophagosomes and lysosomes[443], which is often used to inhibit endosomal TLR signalling. PD0325901 is a synthetic molecule which binds to and inhibits the kinase activity of the MAPK kinase MEK, which is involved in multiple stress processes including pathogenic responses and genotoxic insult[444]. This protein activates ERK as part of the Raf/MEK/ERK pathway to regulate cytokine production and cellular proliferation (reviewed in[445]). Z-VAD-FMK is a cell-permeable pan-caspase inhibitor that is frequently used in cell death studies, but has also been found to inhibit NLPR3 activity by inhibiting caspase-1, thereby ablating the processing of pro-IL1β to its active form[446,447]. The aminopyrimidine compound BX795 is a potent inhibitor of the non-canonical kinases IKKε and TBK1, which works to reduce IRF3 activation and type I IFN production[190].

MoDCs were stimulated with Pam3CSK4 for 1 hour, either alone or after incubation with the above inhibitors at the concentrations listed in Table 4.1. Samples were subjected to WB and results demonstrate that pBRCA1 is induced after incubation with Pam3CSK4 alone as expected (Figure 4.2). The addition of Bafilomycin and PD0325901 significantly affected the levels of pBRCA1 that were detected, whilst Z-VAD-FMK had a less profound

effect. BX795 however, had the greatest effect, reducing pBRCA1 levels to below even those seen in the basal state, suggesting BRCA1 phosphorylation at S1524 is indeed an event induced downstream of innate signalling pathway activation.

Inhibitor	Target	Working conc.
SB203580	p38	10 µM
Bafilomycin A1	Endosomal fusion	1 µM
Z-VAD-FMK	Pan-caspase	20 µM
PD0325901	MEK	1 µM
BX795	TBK1/IKKε	1uM

Table 4.1 Small molecule inhibitors of innate immune processes, their targets and working concentrations.

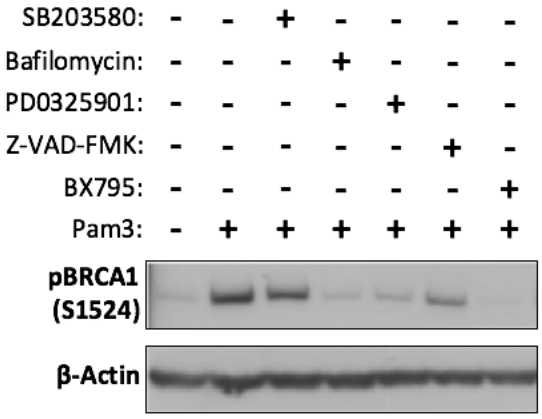

Figure 4.2 BRCA1 phosphorylation can be abrogated by innate signalling inhibition. MoDCs were either untreated or stimulated for 1h with 1 µg/mL Pam3CSK4 after incubation in the presence or absence of small molecule inhibitors to different innate immune signalling processes, and WB performed using anti pBRCA1 and β-actin antibodies.

4.3.3 A small molecule inhibitor of TBK1 inhibits BRCA1 phosphorylation

The most profound difference in levels of pBRCA1 after PRR stimulation were incurred after treatment with BX795, which inhibits TBK1 signalling to IRF3. To probe this further, MoDCs were incubated with different concentrations of BX795 to determine the optimal concentration to take forward to subsequent experiments. WB shows that total TBK1 levels remain stable, whilst pTBK levels are increased with higher BX795 concentrations, which is also reported elsewhere[190] (Figure 4.3A). Total BRCA1 levels remain stable, but basal pBRCA1 levels are reduced in a concentration dependent manner. This was then repeated, with MoDCs stimulated with 1 µg/mL Pam3CSK4 for 1 hour (Figure 4.3B) or 2 µg/mL IVT dsRNA for 2 hours (Figure 4.3C). Again, pBRCA1 is increased by PRR agonism in each case, which is reduced by BX795 in a dose-dependent manner. pTBK1 on the other hand, is also increased upon stimulation, but even further increased with BX795 concentration (Figure 4.3B,C).

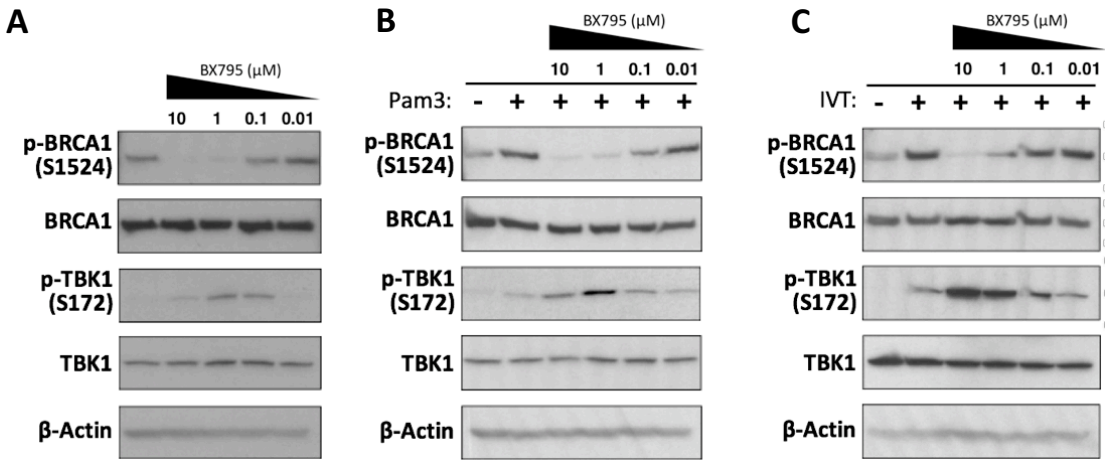

Figure 4.3 The TBK1 inhibitor BX795 reduces pBRCA1 levels in a dose-dependent manner. WB analysis of MoDCs using anti pBRCA1, total BRCA1, pTBK1, total TBK1 and β-actin antibodies after incubation with **A.** Titrated concentrations of BX795 for 3 hours prior to stimulation with **B.** 1 µg/mL Pam3CSK4 or **C.** 2 µg/mL IVT dsRNA

4.3.4 Lentiviral knockdown of TBK1 reduces phosphorylation of BRCA1

To confirm that this dependence of BRCA1 phosphorylation on TBK1 signalling was not due to off-target effects of BX795, which have been reviewed previously[448], knockdown of TBK1 at the protein level was attempted. For this, lentiviral transduction was chosen as the method of choice. This is due to the difficulty in transfecting primary MoDCs, in which both efficiency and cell viability is often well below 50% (data not presented). Lentiviral transduction additionally utilises the almost pantropic VSV glycoprotein envelope which permits entry into most cell types[449]. Additionally, the lentivirus-encoded short hairpin RNA (shRNA) can be continuously and stably expressed after integration into the genome, removing the need for repeated transfections whilst increasing the relative amount of interfering RNA in comparison to small-interfering RNA (siRNA).

A lentiviral system used by Dr. Jonathan Maelfait (University of Oxford, Human Immunology Unit) was adapted and optimised for use in primary dendritic cells. This procedure utilises a second generation lentiviral production technique that requires a three-way transfection of HEK293T producer cells. A packaging plasmid encodes essential enzymes needed for lentiviral packaging of the shRNA, including Gag, Pol, Tat and Rev. The VSV envelope is encoded on a separate plasmid, whilst the shRNA sequence is encoded on the third plasmid, along with a packaging sequence. This protocol produces replication-incompetent virus particles for safety reasons.

The HIV-1 protein Vpx can induce proteasomal degradation of SAMHD1[365], a restriction factor which usually degrades dNTPs upon viral entry in order to prevent efficient reverse transcription or retroviral genomes[450-452]. Using an LVP encoding Vpx alongside shRNA-encoding LVPs facilitates increased LVP transduction[453,454].

For this experiment, constructs encoding TBK1-targeting shRNA (Table 4.2), GFP under the CMV promoter (SHC203), or a negative control shRNA targeting no known genes (SHC216) were used. All plasmids derive from the TRC2 pLKO vector backbone. Transfection efficiency of each plasmid into producer cells was assessed using an immunofluorescence microscope at 18 hours and 48 hours (Figure 4.4A), using the expression of GFP from the SHC203 plasmid as a reference. Supernatant containing LVPs was then harvested and filtered before CD14+ monocytes were transduced using this supernatant, in presence of polybrene to help virus binding[455]. After differentiation to MoDCs with IL-4 and GM-CSF for 5 days, GFP expression was once again assessed by flow cytometry to determine transduction efficiency (Figure 4.4B). Cell viability was also routinely assessed at this stage and was always above 90% (data not shown).

TBK1 mRNA levels in cells from three blood donors were assessed by qPCR to determine the effectiveness of shRNA (Figure 4.4C), before cells were stimulated with Pam3CSK4, *E.Coli* dsDNA, or IVT dsRNA (Figure 4.4D). WB was used to demonstrate a successful protein knockdown of TBK1, as seen by vastly decreased total and pTBK1 levels in both basal and stimulated state. Levels of pBRCA1 were also decreased in both the basal state and upon PRR stimulation, again suggesting BRCA1 phosphorylation is downstream of TBK1 activity.

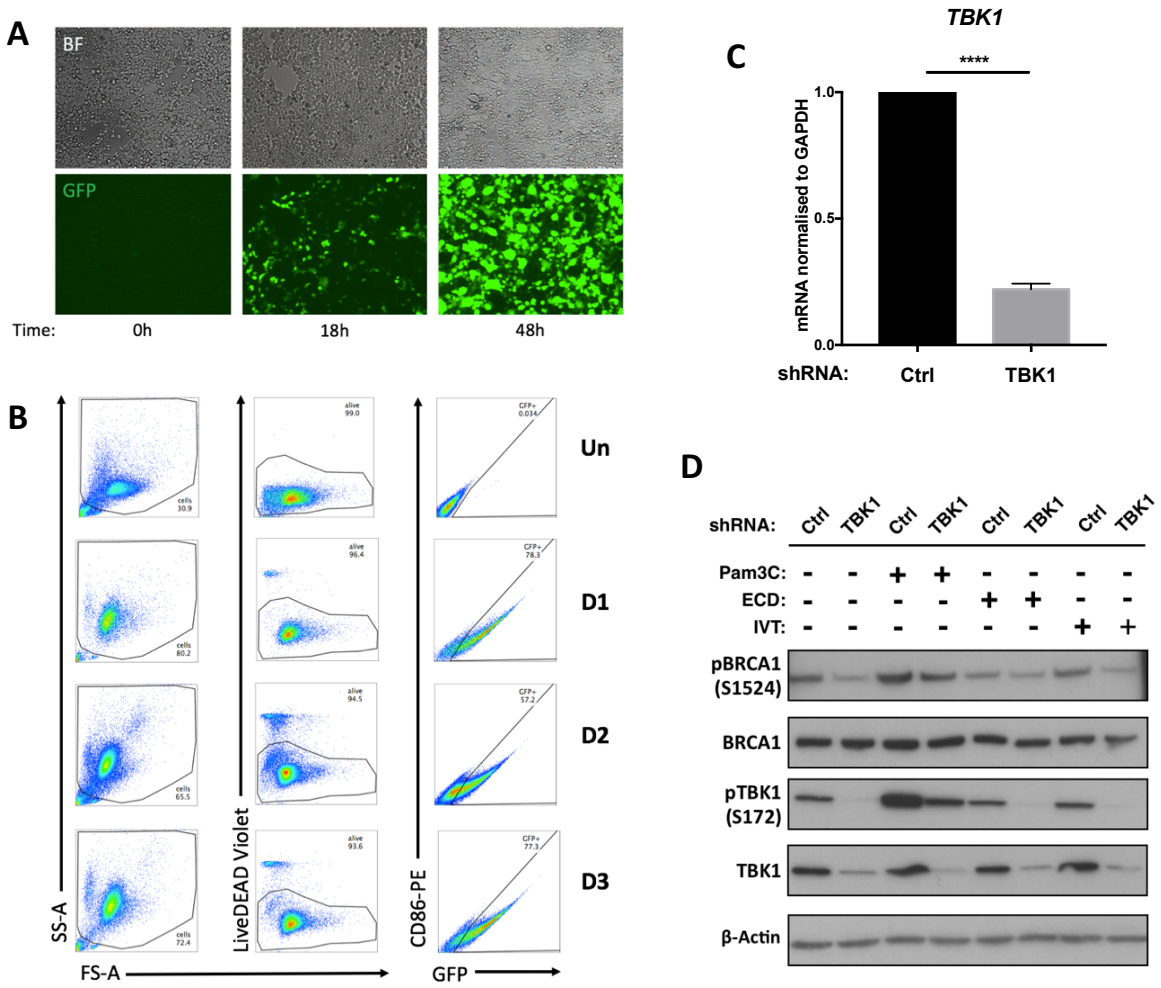

Figure 4.4 Successful production of lentivirus and transduction of MoDCs. A. HEK293T cells were co-transfected with packaging plasmid, VSV-g encoding plasmid and shRNA lentiviral plasmids and transfection efficiency determined by assessment of GFP expression from SHC203 control lentiviral plasmid at 0h, 18h and 48h post-transfection, using an immunofluorescence microscope. **B.** Transduction efficiency of MoDCs with LVPs assessed by Flow cytometry using a LiveDEAD violet viability dye and anti-CD86 PE-conjugated antibody to determine activation. GFP expression was detected in the FITC channel **C.** qRT-PCR analysis of TBK1 mRNA levels after transduction with LVPs encoding shRNA targeting no known genes (Ctrl) or TBK1. Values were normalised against GAPDH and TBK1 mRNA levels from cells transduced with control LVPs set to 1. **** $p<0.0001$ **D**. WB analysis of MoDCs untreated or stimulated with Pam3CSK4 for 1h, 2 µg/mL *E. Coli* dsDNA for 2h, 2 µg/mL IVT dsRNA 5 days post-transduction with Ctrl or TBK1 shRNA-encoding LVPs. Anti pBRCA1, pTBK1, total BRCA1, total TBK1 and β-actin antibodies were used.

4.3.5 The kinetics of pBRCA1 induction closely follow the phosphorylation of TBK1

To establish the proximity of BRCA1 phosphorylation kinetically to TBK1 activation, previously probed membranes using samples from cells stimulated with multiple PRR agonists at various concentrations and timepoints (Figure 3.5) were reprobed with antibodies recognising total TBK1 and pTBK1. Blots were aligned with pBRCA1 and β-Actin from the same experiment. Results demonstrate that upon use of each PRR agonist, BRCA1 phosphorylation closely follows induction of TBK1 phosphorylation temporally (Figure 4.5).

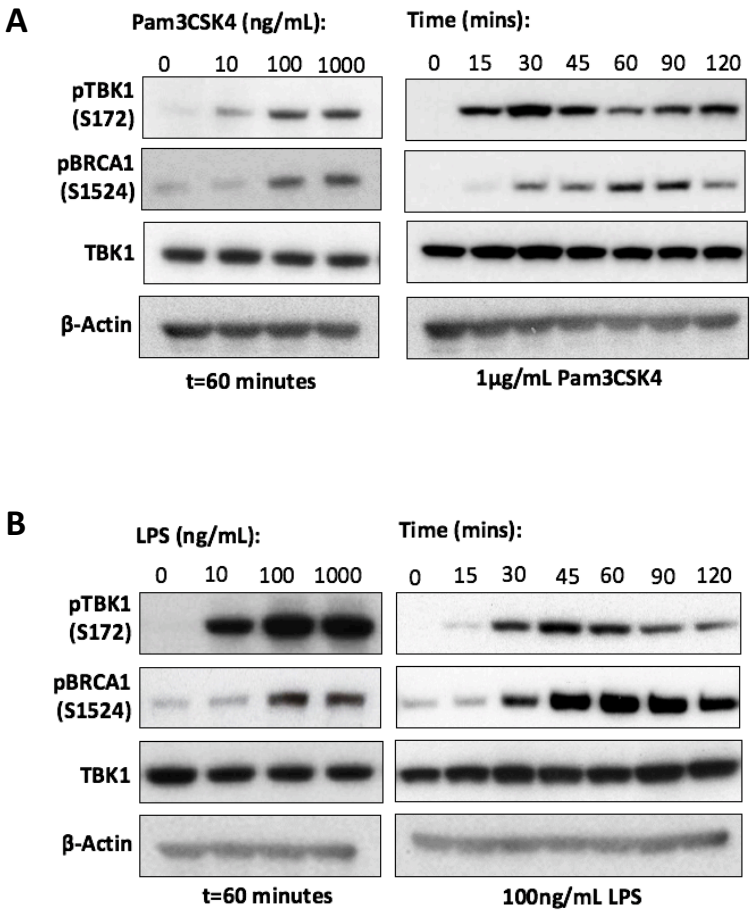

C

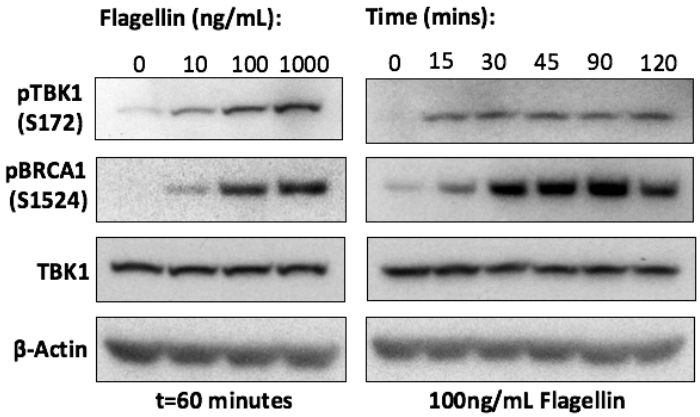
Flagellin (ng/mL):
0 10 100 1000
Time (mins):
0 15 30 45 90 120
pTBK1 (S172)
pBRCA1 (S1524)
TBK1
β-Actin
t=60 minutes
100ng/mL Flagellin

D

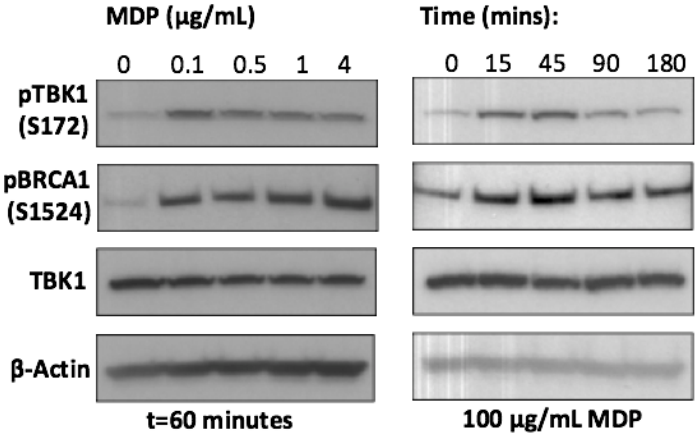
MDP (µg/mL)
0 0.1 0.5 1 4
Time (mins):
0 15 45 90 180
pTBK1 (S172)
pBRCA1 (S1524)
TBK1
β-Actin
t=60 minutes
100 µg/mL MDP

E

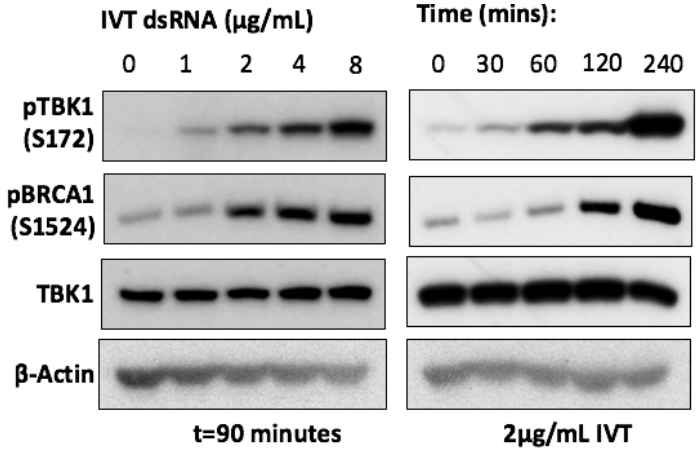
IVT dsRNA (µg/mL)
0 1 2 4 8
Time (mins):
0 30 60 120 240
pTBK1 (S172)
pBRCA1 (S1524)
TBK1
β-Actin
t=90 minutes
2µg/mL IVT

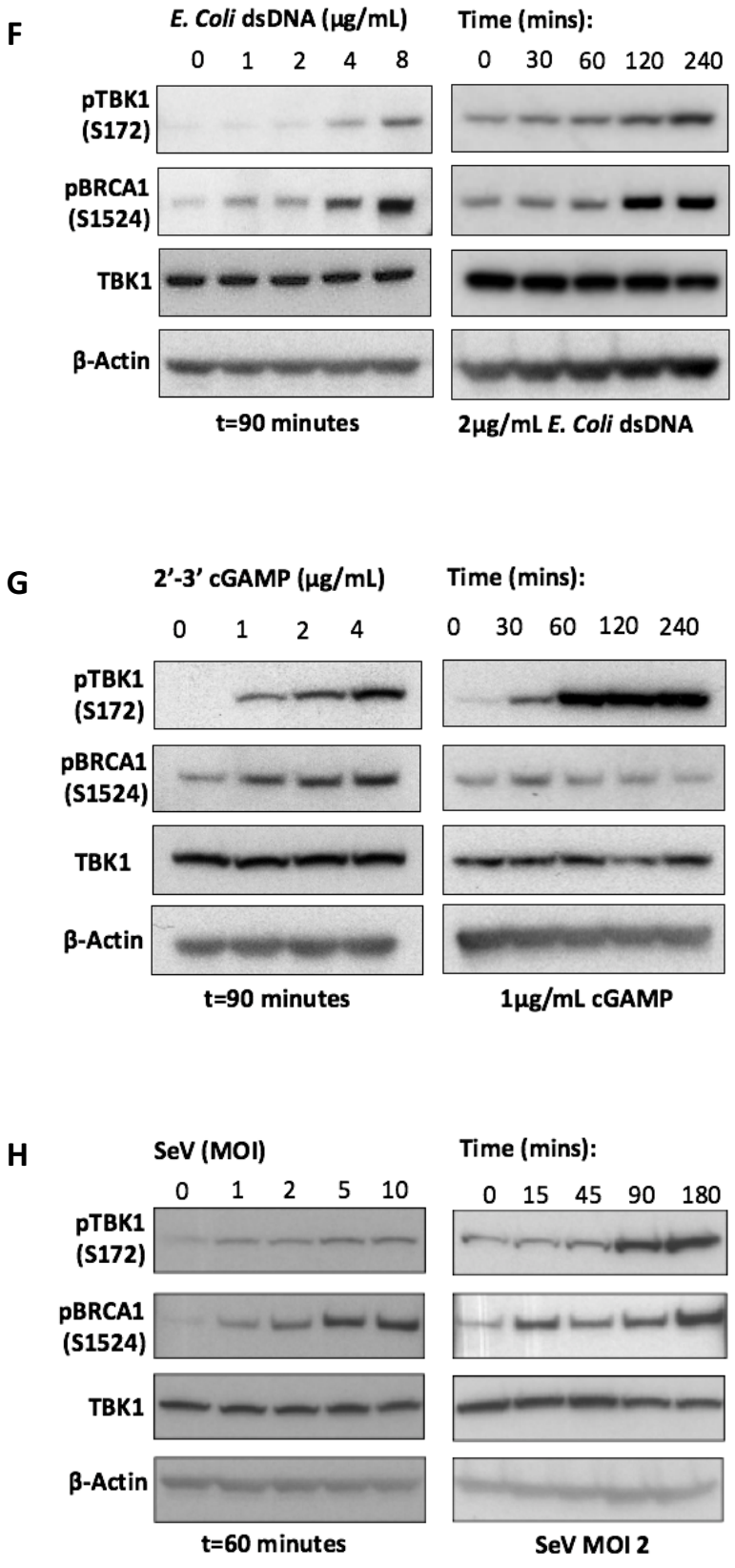

Figure 4.5 BRCA1 phosphorylation shortly follows TBK1 phosphorylation upon PRR stimulation. Samples from figure 3.5 were reprobed for pTBK1 (S172) and total TBK1 to assess kinetics in relation to BRCA1 phosphorylation.

4.3.6 pBRCA1 (S1524) increases predominantly in the cytoplasm

BRCA1 is known mainly for its roles for nuclear genomic protection, but TBK1 activity is known to be principally cytosolic, so to determine location of pBRCA1 upon PRR stimulation and to gain insight into how BRCA1 phosphorylation connects with TBK1 activity, subcellular fractionation was performed. MoDCs were stimulated with Pam3CSK4 or etoposide before lysis using a fractionation kit. Successful fractionation was confirmed by WB using antibodies against common markers of each compartment (Figure 4.7A). HSP90 was used to confirm isolation of soluble cytosolic proteins[456,457], whilst the ER luminal resident protein calreticulin was chosen as a suitable marker for membranous compartments[458]. The soluble nuclear fraction was represented by the nuclear amine oxidase LSD1[459], and Histone 3 was used to confirm isolation of the histone-bound fraction. Total BRCA1 levels were also assessed, and were intriguingly shown to be highest in the cytosol. Some BRCA1 was detected in the membranous fraction, although this could be from contamination of the cytoplasmic fraction, as reflected by small amounts of HSP90 detection in the membranous fraction. As expected, BRCA1 is also found in the nuclear soluble fraction, but is undetected in histone bound compartments. WB analysis of Pam3CSK4 treated samples demonstrated that pBRCA1 increased predominantly in the cytosol whilst nuclear pBRCA1 was unaltered, suggesting that pBRCA1 may have a function in the cytoplasm where TBK1 is known to function. Again, use of etoposide induces no changes in pBRCA1 levels in any compartment.

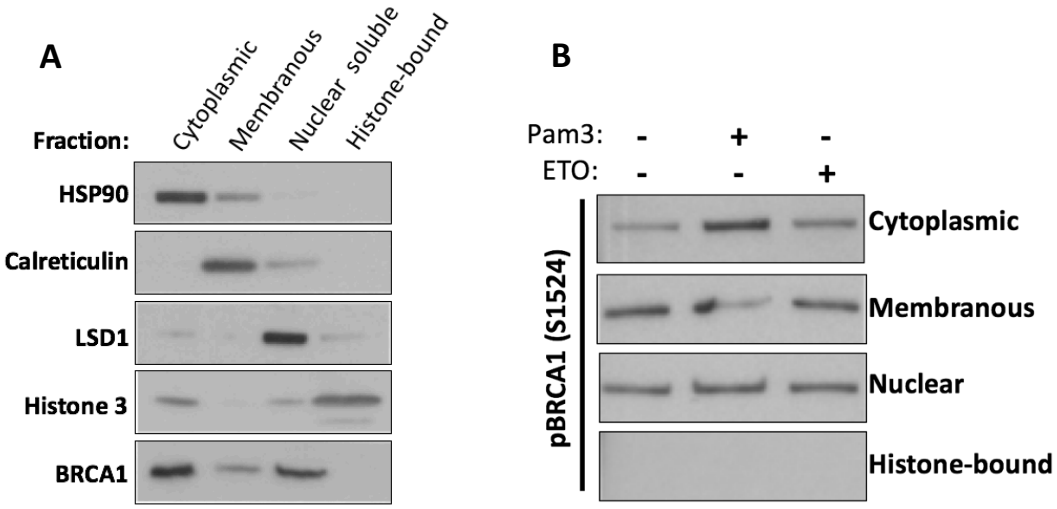

Figure 4.6 BRCA1 can be found in multiple cellular compartments whilst pBRCA1 increases predominantly in the cytoplasm. MoDCs were subjected to subcellular fractionation before WB analysis of **A.** Markers for each cellular compartment or total BRCA1 levels or **B.** pBRCA1 levels in each compartment after stimulation with 1 µg/mL Pam3CSK4 or 100 µM etoposide.

4.3.7 pBRCA1 localises to perinuclear regions after PRR stimulation

To support existing data, confocal microscopy was employed to establish the exact location of BRCA1 (and pBRCA1) within the cell upon PRR stimulation. Microscope slides with 8 separate chambers were coated with Poly-L-lysine to allow attachment of cells[460], which were seeded to each well and allowed to adhere for 24 hours before being treated. Cells were then subjected to the standard confocal microscopy protocol using antibodies that were optimised for compatibility in MoDCs. AlexaFluor-488 secondary antibody was used to detect primary antibody recognising pBRCA1 (Green), whilst primary antibodies recognising organelle marker proteins were stained with AlexaFluor 568 secondary antibody (Red). TOM20, a mitochondrial membrane protein[461], was chosen as marker for this compartment as BRCA1 has been described to relocalise here previously[306,462,463]. As TBK1 has been reported to localise with STING at the ER and Golgi, Calnexin and Giantin were chosen to visualise these organelles, respectively[464,465]. Additionally, EEA1 was chosen to observe endosomes, as TLR2 has been reported to be internalised into these after activation to promote NFκB activity and IFN production[389,391], a process involving TBK1. Results show that pBRCA1 (green) is increased upon stimulation in the cytoplasm, corresponding with subcellular fractionation results (Figure 4.8). Interestingly, pBRCA1 seems to localise in a perinuclear region in close proximity and partially overlapping with the Golgi membrane protein Giantin (Figure 4.7D), but not the other organelles tested (Figure 4.7A-C). Viewing the images at a higher magnification shows this more clearly (Figure 4.7E), with zones of overlapping red and green signal presenting as yellow. A Differential interference contrast (DIC) field of view is also included to demonstrate that both Giantin and pBRCA1 occupy the same perinuclear area, and are not diffusely localised throughout the cytoplasm.

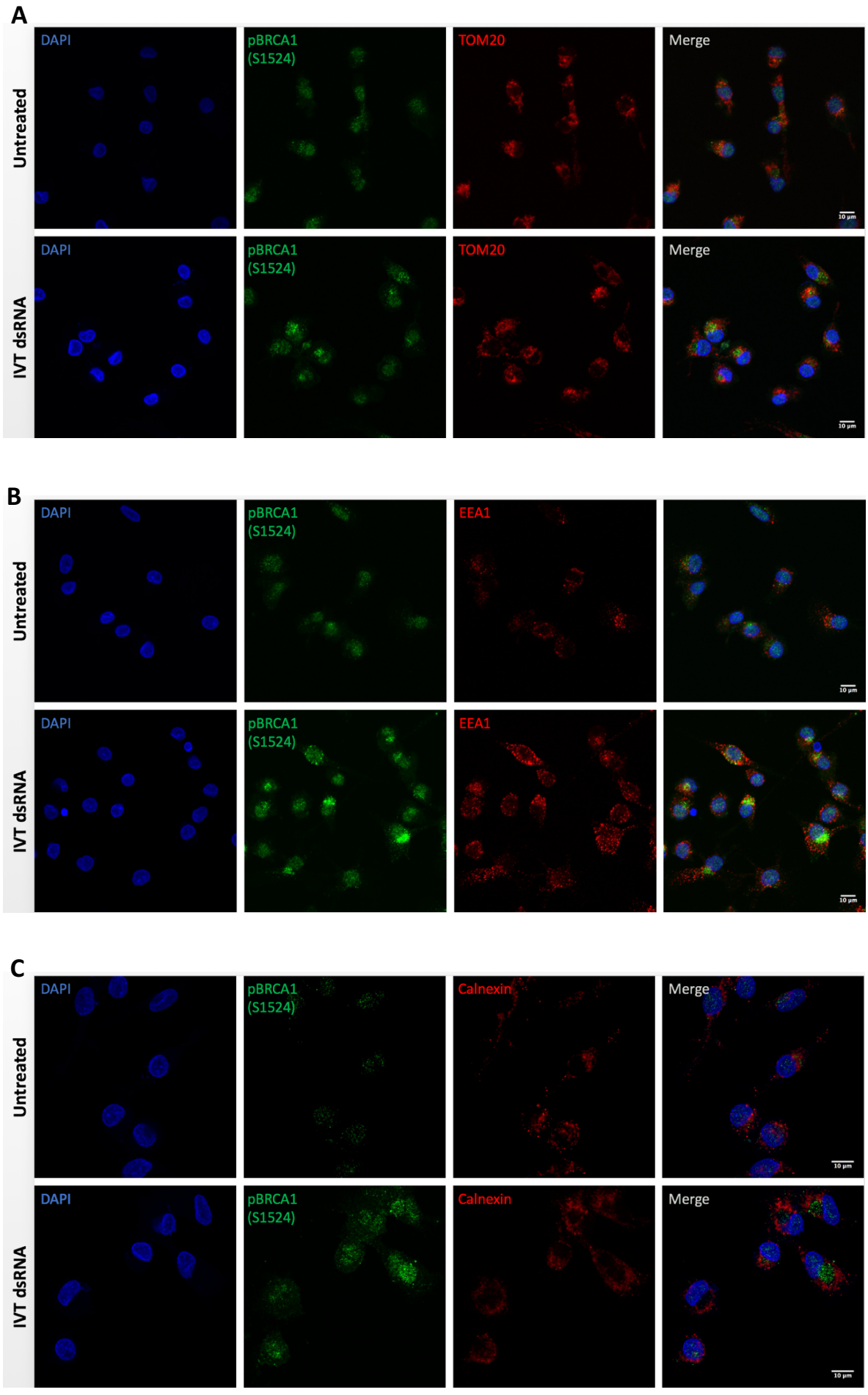
A
Untreated
IVT dsRNA
DAPI
pBRCA1 (S1524)
TOM20
Merge
B
EEA1
C
Calnexin
10 µm

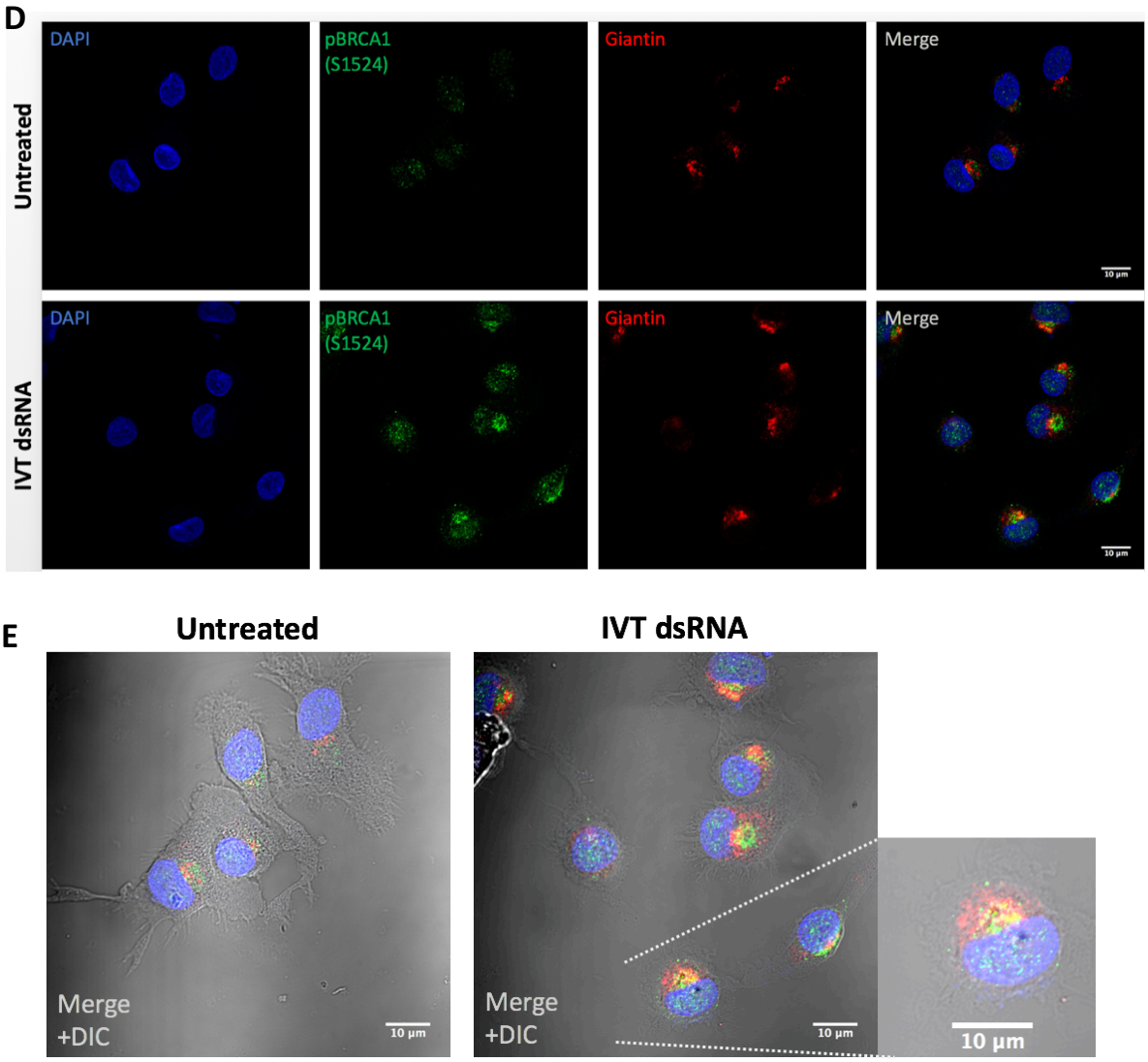

Figure 4.7 Confocal microscopy visualising pBRCA1 in relation to cellular organelles. 1x10^5 MoDCs were seeded at a volume of 200µL into each well of an 8-well chamber slide pre-coated in 0.1 mg/mL Poly-L-Lysine. Cells were untreated or stimulated with 2 µg/mL IVT dsRNA for 90 minutes before being fixed and permeabilised. Cells were stained with primary antibodies recognising pBRCA1 (S1524) (Green) and **A.** Mitochondrial marker TOM20 **B.** Endosomal marker EEA1 **C.** ER marker Calnexin or **D**. Golgi membrane marker Giantin. **E.** Cropped and enlarged image of Giantin stained cells.

4.3.8 STING and pTBK1 also colocalise with Golgi proteins after PRR stimulation

As BRCA1 phosphorylation after PRR stimulation seems to depend on TBK1 activity, confocal microscopy was repeated on MoDCs stimulated with IVT dsRNA, using antibodies against pTBK1 and Giantin to determine if this area is common to both signalling events. Results show an increase in colocalisation between these two proteins in some cells upon stimulation, mirroring pBRCA1 relocalisation (Figure 4.8A). Not all cells showed this effect, possibly due to low transfection efficiency of IVT into this cell type.

To determine whether this Golgi derived region can also harbour STING as previously reported[43], the experiment was once again repeated using MoDCs untreated or transfected *E. Coli* dsDNA to activate the cGAS/STING signalling axis. Cells were incubated with primary antibodies recognising STING and Giantin and results confirm that STING colocalisation with Giantin increases upon stimulation as seen by yellow fluorescence when both red and green emission overlaps (Figure 4.8B). Together, these results imply that pBRCA1 occupies the same space as activated STING and pTBK1.

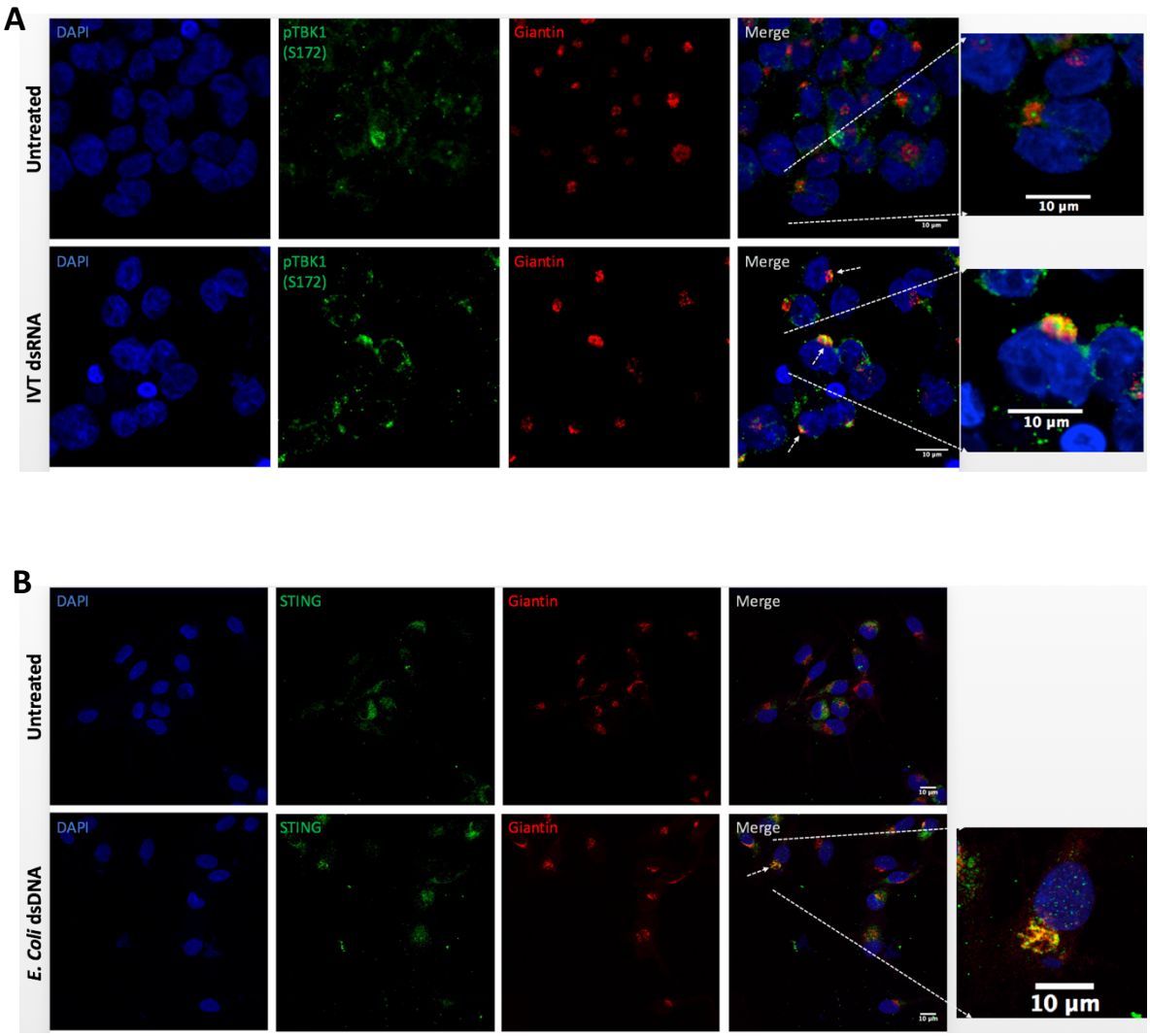

Figure 4.8 pTBK1 and STING increase colocalisation with Giantin after PRR stimulation. $1x10^5$ MoDCs were seeded at a volume of 200µL into each well of an 8-well chamber slide pre-coated in 0.1 mg/mL Poly-L-Lysine. Cells were untreated or stimulated for 2h in 2 µg/mL of **A.** IVT dsRNA and stained with primary antibody against pTBK1 (S172) (Green), or **B.** E. Coli dsDNA for 2h and stained with primary antibody against STING (Green).

4.3.9 BRCA1 colocalises with pTBK1 after PRR stimulation

To assess whether BRCA1 does localise to the same region as TBK1 upon PRR activation, MoDCs were stimulated with *E. Coli* dsDNA before confocal microscopy was undertaken using primary antibodies against pTBK1 and total BRCA1. pBRCA1 and pTBK1 could not be co-stained due to overlap of primary antibody host species and lack of alternative phospho-specific antibodies. BRCA1 can be seen to localise predominantly in the nucleus of untreated cells (Figure 4.9), but upon stimulation it relocalises to the cytoplasm where it forms distinct foci, some of which directly overlap with pTBK1 foci.

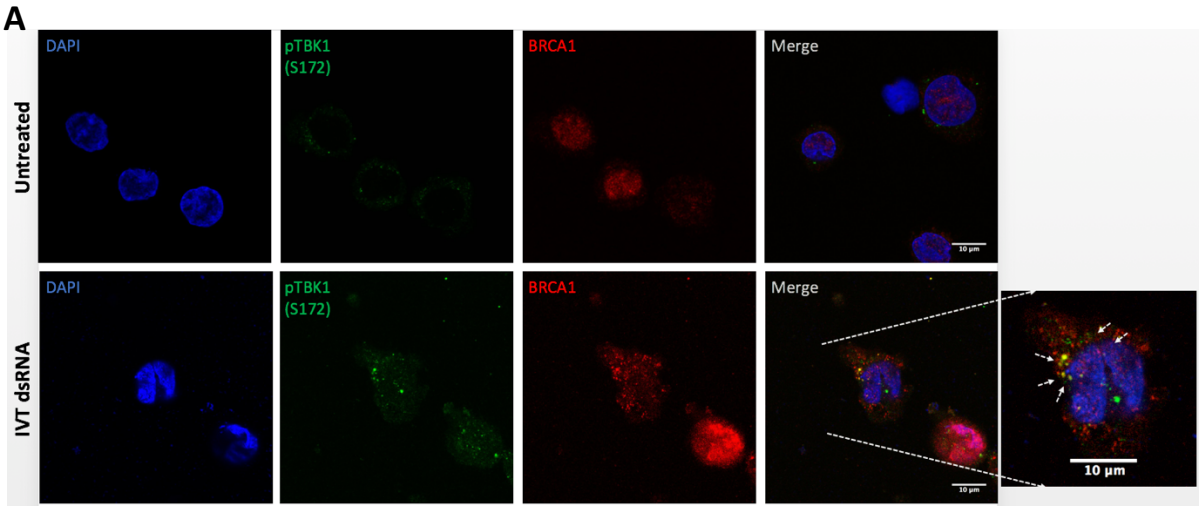

Figure 4.9 BRCA1 and pTBK1 colocalise after PRR stimulation $1x10^5$ MoDCs were seeded at a volume of 200µL into each well of an 8-well chamber slide pre-coated in 0.1 mg/mL Poly-L-Lysine. Cells were untreated or stimulated for 2h in 2 µg/mL E. Coli dsDNA before staining with primary antibody against pTBK1 (S172) (Green) and BRCA1 (Red).

4.4 Discussion

In this part of the study, it was demonstrated that BRCA1 phosphorylation at S1524 is downstream of TBK1 activation, and that levels of pBRCA1 are increased predominantly in the cytoplasm, where it localises in proximity to the Golgi-derived membranes that TBK1 and STING migrate to upon stimulation.

Specifically, BRCA1 phosphorylation at S1524 in response to PRR agonism was shown to be independent of canonical kinases ATM, CHK2, or ATR, which usually activate BRCA1 after DSBs, IR or UV damage[282]. Interestingly, the endo-lysosomal acidification inhibitor Bafilomycin A1 abrogates the phosphorylation of BRCA1 in response to a TLR2 agonist. This implies that the receptor, or some other cell surface moiety must be internalised to trigger the phosphorylation of BRCA1. As alluded to earlier, TLR2 internalisation is required for IFN stimulatory signalling via MyD88 and TRAM[390,391], which may provide a place for BRCA1 in this signalling cascade.

The MEK inhibitor PD0325901 also ablates the induction of pBRCA1, suggesting BRCA1 may be involved downstream of MEK activation in some capacity. MEK normally coordinates MAPK signalling in response to cellular stress. This includes the ERK signalling pathway, which itself controls transcription and translation events related to multiple cellular functions including cell cycle and proliferation, apoptosis and inflammation (Reviewed in[466]). This pathway is frequently deregulated in cancer[444], and BRCA1 has been shown to have a role in regulating the ERK pathway, during estrogen receptor signalling[467]. Interestingly, MAPK activation is reported to require activation by TBK1 in certain circumstances[468] but curiously not after stimulation with dsDNA[188,469], supporting the observation of MEK inhibition reducing pBRCA1 induction in response to TLR2 stimulation. Similarly, p38 is also controlled by upstream MEK signalling and provides an alternative

MAPK signalling pathway to ERK[470]. Inhibition of this pathway had no distinguishable effect on BRCA1 phosphorylation, suggesting that BRCA1 may be part of a more distinct set of signal transduction pathways which may have some relationship to ERK signalling.

The use of Z-VAD-FMK which inhibits the activity of caspases had little effect on BRCA1 phosphorylation.

The largest effect on pBRCA1 levels was brought about by TBK1 inhibition by BX795. This reduced detectable levels to below basal levels in untreated cells, signifying that this signalling pathway is key in BRCA1 phosphorylation even in the steady state. Importantly, TBK1 activity has been heavily linked to the activities blocked by Bafilomycin and Z-VAD-FMK, respectively. TBK1 is required to promote the maturation of autophagosomes into lytic bactericidal organelles via autophagy in a process which first requires TBK1's regulation of IL-1β activity[471]. Therefore, the use of these inhibitors may result in decreased downstream activation of TBK1 after TLR2 stimulation, which in turn may cause reduced levels of pBRCA1.

Further inquiry into the potential upstream requirement of TBK1 for BRCA1 phosphorylation, using differing concentrations of BX795 with untreated, Pam3CSK4 or IVT dsRNA treated cells demonstrates that indeed BRCA1 phosphorylation at S1524 after PRR stimulation is at least partially dependent on TBK1 activity. In this experiment, there was a positive correlation between inhibitor concentration and pTBK1 levels, which is observed elsewhere[190]. This may possibly be due to a continued signal which builds up as TBK1 cannot phosphorylate IRF3 as required, and negative feedback loops may remain inactive.

Production of lentivirus to target TBK1 by RNAi was shown to be successful from high GFP expression from the control plasmid in both the transfected producer cell line and the

virally transduced MoDCs. Successful mRNA and protein knockdown of TBK1, as assessed by qPCR and WB, correlated expectedly with reduced pTBK1 in response to stimulation. This also resulted in abrogation of pBRCA1 induction, confirming that the reliance of BRCA1 phosphorylation on TBK1 activity is specific and not a result of off-target effects of BX795. Similarly, kinetic assessment of pTBK1 induction after agonism of each PRR family using samples remaining from Figure 3.5 demonstrates a striking correlation with the kinetics of BRCA1 phosphorylation, which proceeds swiftly after TBK1 phosphorylation in each case.

The use of subcellular fractionation illustrates that in addition to the expected nuclear localisation of BRCA1, the protein can also be found in cytoplasmic and membranous compartments of MoDCs, which is not completely unexpected given recent reports of activity at the mitochondria[306] and ER[307]. Although BRCA1 shuttling to the cytoplasm has been reported previously[303,433], the cytoplasmic levels in comparison to nuclear levels is surprising.

Confocal microscopy data using cells transfected with IVT dsRNA showed that pBRCA1 partially overlaps at perinuclear zones with the Golgi marker Giantin, which has previously been shown to localise with STING and TBK1 upon DNA stimulation[43,472]. I could also confirm STING localisation to this area increases after stimulation with *E. Coli* dsDNA, and TBK1 after stimulation with IVT dsRNA, validating this zone as a signalling hub. As subcellular fractionation showed that pBRCA1 increases predominantly in the soluble cytoplasmic fraction, it could be assumed that pBRCA1 localises to the cytoplasmic interface of these Giantin-containing membranes, as opposed to entering the organelle.

Although TBK1 is known to translocate to these Golgi-derived microsomes upon STING activation by dsDNA sensing, relatively little is known about the spatial regulation of TBK1

activity upon RIG-I signalling, aside from its recruitment to mitochondrial MAVS. Recently however, mitochondria-associated membranes (MAMs) in close proximity to ER membranes, where STING resides, have been suggested as the major site of MAVS signalling. Additionally, genetically engineered MAVS which localises at the ER whilst maintaining dimerisation capability is constitutively active[473]. Further to this, Golgi network rearrangements are required for full antiviral signalling to take place in response to RNA agonists[474-476]. Together, this evidence suggests that both MAVS and STING may function through the same ER-Golgi membrane-derived organelles, providing a common spatial niche for TBK1 to function, and explaining the relocalisation of pTBK1 observed to this area upon IVT dsRNA stimulation.

Interestingly, in untreated cells, basal levels of pTBK1 are seen in distinct foci surrounded by Giantin, which increase in number and disperse into Giantin-containing areas upon PRR activation. The basal activated TBK1 may therefore be sequestered away from activated adaptors such as STING and MAVS to prevent improper inflammatory activation.

The requirement of TBK1 activity for BRCA1 phosphorylation, in conjunction with the spatial and temporal relationship I have demonstrated between both of these, suggests that BRCA1 phosphorylation is a PRR-activation specific event which is part of a common signalling cascade employing TBK1. Hence, functional studies using this hypothesis will be undertaken on BRCA1 in the next chapter.

5 BRCA1 interacts with TBK1 to promote type I IFN production

5.1 Introduction

BRCA1 functions to maintain genomic stability by regulating multiple cellular processes relating to cell cycle control and DNA repair[279,477]. To undertake these roles, BRCA1 functions predominantly in the nucleus of cells, being retained there with its multiple NLSs[280,281]. The exact mechanisms of BRCA1 in each process remain elusive, irrespective of the intense study into its functional domains[297,298,478]. However, broadly speaking, BRCA1's ability to direct such a diverse range of cellular activities has been suggested to depend on its ability to act as a scaffold protein and bind a multitude of partners, a feature conferred predominantly by its dual C-terminal BRCT domains which allow binding to phosphoproteins. This in turn permits it to participate in the formation of many functional complexes[299], most notably with BARD1 which increases BRCA1 stability and facilitates BRCA1's RING domain-encoded E3 ligase activity[296,479-482], which can catalyse the addition of mono- and polyubiquitin chains to substrate proteins[483]. This study has so far demonstrated a DNA Damage and DDR signalling-independent redistribution of BRCA1 exclusively upon PRR stimulation, to perinuclear areas of the cytoplasm where STING can be found and where it forms distinct foci overlapping with pTBK1. Relatively few other studies have demonstrated cytoplasmic signalling roles for BRCA1, although it has been suggested that BRCA1 must shuttle to the cytoplasm to perform some unknown function downstream of p53[304].

Like BRCA1, TBK1 is phosphorylated upon its activation[165,282] which prompts it to bind a selection of its many interacting partners[151], allowing it to regulate multiple cellular

processes including inflammatory responses, autophagy[159,160], proliferation[186] and hormonal signalling[484]. The best characterised role of TBK1 is in type I IFN production, where it is employed by and binds to multiple adaptor proteins activated by a range of PRRs[154]. Here, it phosphorylates the upstream adaptor which allows recruitment of IRF3, which itself is phosphorylated at the same consensus sequence by TBK1[154]. Phosphorylated IRF3 then translocates to the nucleus where induces the expression of type I IFN. This is then secreted and binds its cognate receptor in an autocrine or paracrine manner, inducing signalling which ultimately results in the expression of ISGs that work to establish an antiviral state, as well as to direct an adaptive immune response[485]. This is important for a range of pathologies including bacterial and viral infection, as well as antitumour responses[212,215,486-488]. In addition, TBK1 can undertake its immune roles by regulating xenophagy[471,489] and NFκB signalling[468,490].

In conjunction with data generated in previous chapters, these abilities of TBK1 to bind a diverse set of partners and direct a range of cellular process, dependent upon its localisation and complex constituents, presents an opportunity to hypothesize that BRCA1 interacts with TBK1 in a PRR-stimulatory setting and potentially influences TBK1's cytoplasmic activities.

5.2 Aims

Experiments in this chapter explore the function of BRCA1 in relation to TBK1 activity in innate immune cells. This involved manipulating BRCA1 expression levels in cells and investigating the effect of this on TBK1's downstream activity. I examine whether BRCA1 and TBK1 interact using co-immunoprecipitation and the proximity ligation assay. The activation of TBK1 in the absence of BRCA1 is assessed, as is downstream activation of

IRF3 and subsequent induction of Type I IFN and cytokine production. Additionally, the transcription of key ISGs is followed in these cells. The effect of BRCA1 on viral replication is also assessed.

5.3 Results

5.3.1 Co-immunoprecipitation of BRCA1 and TBK1 on PRR stimulation

Given the findings that pBRCA1 and pTBK1 overlap at Golgi related microsomes where STING can be found upon activation, I examined whether BRCA1 biochemically interacts with TBK1. In collaboration with Seiji Shiraishi (University of Oxford, Human Immunology Unit), MoDCs were stimulated with Pam3CSK4 (Figure 5.1A), IVT dsRNA or E Coli dsDNA (Figure 5.1B) and immunoprecipitation (IP) performed using antibody recognising TBK1 or a rabbit IgG isotype control. TBK1 Immunoprecipitation conditions and cell stimulation conditions were optimised by myself. The final Western blot was then undertaken by Seiji Shiraishi under my instructions, using samples from both input (total cellular lysate) and IP fractions. Results show that TBK1 is precipitated successfully and specifically, as seen by increased detection of TBK1 in IP samples compared to input samples, in which total TBK1 levels are equal throughout. Samples immunoprecipitated with an IgG isotype control antibody show very low binding of TBK1, further demonstrating specificity of primary antibody. Similarly, detection of β-Actin is diminished in IP samples. Visual density of BRCA1 in each input sample is equal, but BRCA1 is exclusively detected in TBK1-IP samples upon stimulation with different PRR ligands, confirming that it interacts with TBK1 upon activation. This was repeated, and an etoposide control used to assess whether this phenomenon is specific to PRR stimulation or whether it can be induced by DNA damage (Figure 5.1C). Antibody against pATM was used to show successful genotoxic effects of etoposide, whilst TANK was used as a positive control for TBK1 IP conditions, as this is a constitutive binding partner of TBK1. Indeed, only PRR activation was able to induce the binding of BRCA1 to TBK1. To attempt the reverse experiment, pulling-down BRCA1 and probing for TBK1, multiple antibodies recognising BRCA1 were tested and many steps

within the IP protocol altered. Unfortunately, no condition tried was able to achieve a successful IP of BRCA1.

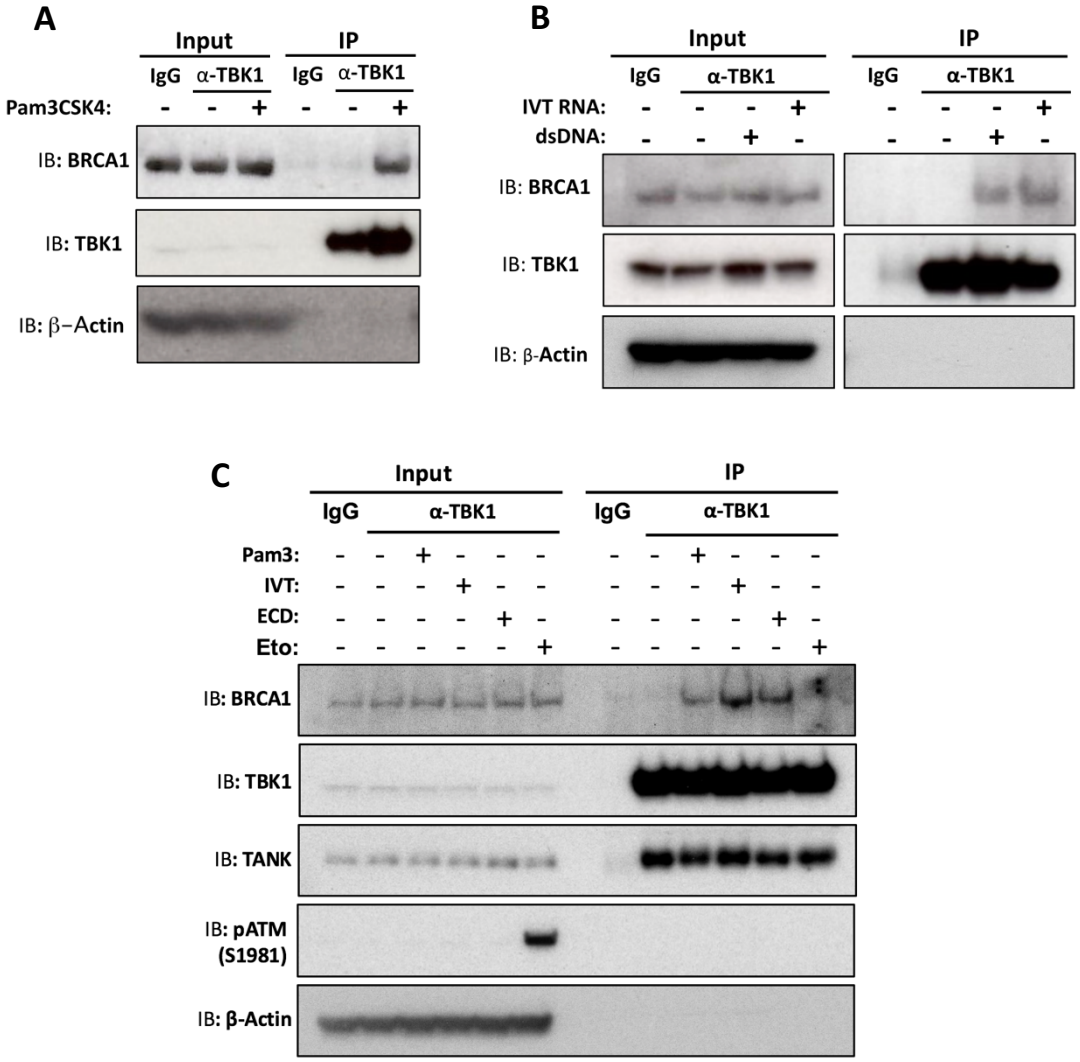

Figure 5.1 BRCA1 interacts with TBK1 upon PRR stimulation. WB analysis using antibodies recognising BRCA1, TBK1, TANK, pATM and β-actin after stimulation of MoDCs with **A.**1 μg/mL Pam3CSK4 for 1h **B.** 2 μg/mL IVT dsRNA or 2 μg/mL *E. Coli* dsDNA for 2h or **C.** 1 μg/mL Pam3CSK4 for 1h, 2 μg/mL IVT dsRNA for 2h, 2 μg/mL *E. Coli* dsDNA for 2h or 100μM etoposide for 1h, before 1mg of lysate was immunoprecipitated using 5 μg anti-TBK1 or Rabbit IgG isotype control primary antibody conjugated to Protein G-coupled Dynabeads.

5.3.2 BRCA1 interacts with TBK1 exclusively upon PRR stimulation – PLA

To show this interaction by other means, and also to determine where this takes place spatially, the Proximity Ligation Assay (PLA) was used. This procedure is similar to conventional confocal microscopy when probing for two proteins. Primary antibodies must be raised in different host species, but secondary antibody is conjugated to an oligonucleotide sequence instead of a fluorophore. When two proteins detected by primary antibody are in close proximity (<40nm), addition of ligase enzyme allows the secondary antibody-conjugated oligonucleotides to ligate and form a complete DNA circle. Polymerase enzyme is then added to amplify the sequence, and fluorescent probes are added to allow visualisation of interacting points within the cell.

Control experiments for each target protein were first performed, using known interacting partners and conditions which induce interaction, to confirm the assay works for the antibodies used. For each condition, a macro created by Dominic Waithe (CBRG WIMM, University of Oxford) was applied in Fiji imaging software for a minimum of 50 cells, which calculates the number of PLA signal points per cell. These values were then used to ascertain statistical significance. MoDCs were stimulated with IVT dsRNA and interaction between TBK1 and MAVS assessed (Figure 5.2A). Similarly, the interaction between pTBK1 and IRF3 was assessed after stimulation with *E. Coli* dsDNA (Figure 5.2B). In both instances, numbers of interactions increase in the cytoplasm which can also be seen in representative images, demonstrating that the assay is successful and sensitive enough to detect changes after both RIG-I and cGAS/STING activation. BRCA1 interaction with γH2AX, which increases upon induction of DNA Damage[491,492], was also confirmed to be significantly increased after treatment with etoposide (Figure 5.2C), importantly in the nucleus as seen in representative images. In this experiment, samples stimulated with IVT

dsRNA or E. Coli dsDNA were included as controls, and neither increased the interaction between BRCA1 and γH2AX, demonstrating specificity of this interaction to DNA damage.

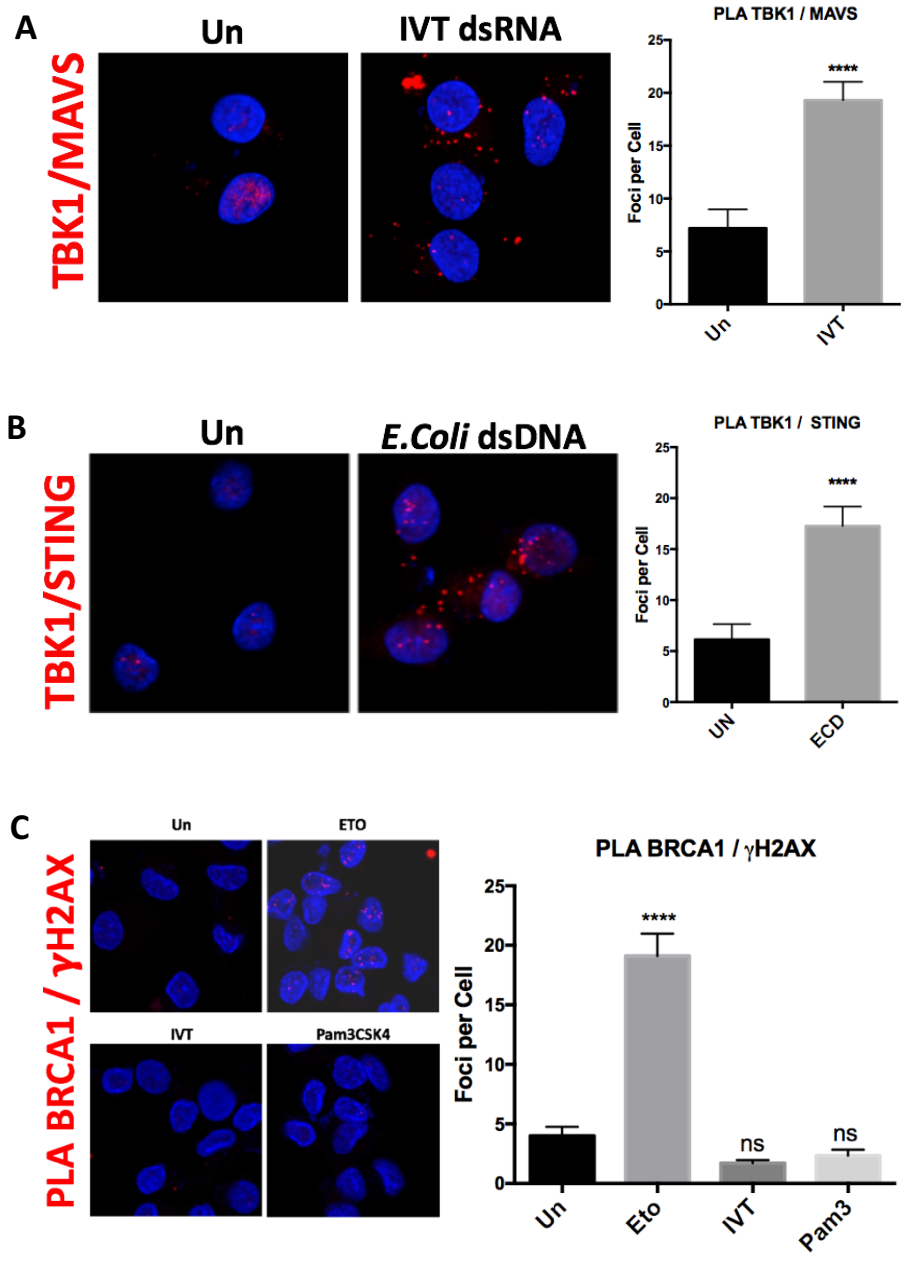

Figure 5.2 PLA controls for TBK1 and BRCA1 antibodies. MoDCs were seeded into each well of an 8-well chamber slide pre-coated in 0.1 mg/mL Poly-L-Lysine. Cells were probed with antibodies for **A.** TBK1 and MAVS after 2h incubation with 2μg/mL IVT dsRNA **B.** TBK1 and STING after 2h incubation with 2 μg/mL *E. Coli* dsDNA **C.** BRCA1 and γH2AX after incubation with 100 μM etoposide for 1h, 2μg/mL IVT dsRNA for 2h or 1 μg/mL Pam3CSK4 for 1h. Proximity ligation assay was then performed using anti-rabbit PLUS and anti-mouse MINUS probes and a Red fluorescent probe.

After suitable experimental parameters and antibodies were established, PLA was repeated to determine the level of interaction between BRCA1 and TBK1 upon stimulation of cells with multiple PRR agonists (Figure 5.3). All PRR agonists significantly increased the number of detectable interaction points, including cGAMP which again suggests that this phenomenon is induced downstream of receptor activation. Crucially, representative images indicate that these PLA signal points are predominantly in the cytoplasm of cells, particularly in perinuclear zones. Use of etoposide or bleomycin had no effect on interaction between BRCA1 and TBK1 as they did with BRCA1 and γH2AX, signifying further that this biological event is specific to innate immune stimulation. As the experiment relies on a PCR reaction to amplify ligated oligonucleotide sequences, an IVT dsRNA sample was created without the addition of polymerase enzyme as an extra control to show specificity of the process and the requirement of enzymatic steps to observe signal. A ligase-free sample was also used for equivalent purposes (data not shown).

The experiment was then repeated using cells infected with the DNA virus HSV1 or Sendaï virus with its RNA genome, and again a significant increase in points of BRCA1 and TBK1 interaction is observed in the cytoplasm of cells (Figure 5.4), demonstrating that whole pathogen can promote the interaction.

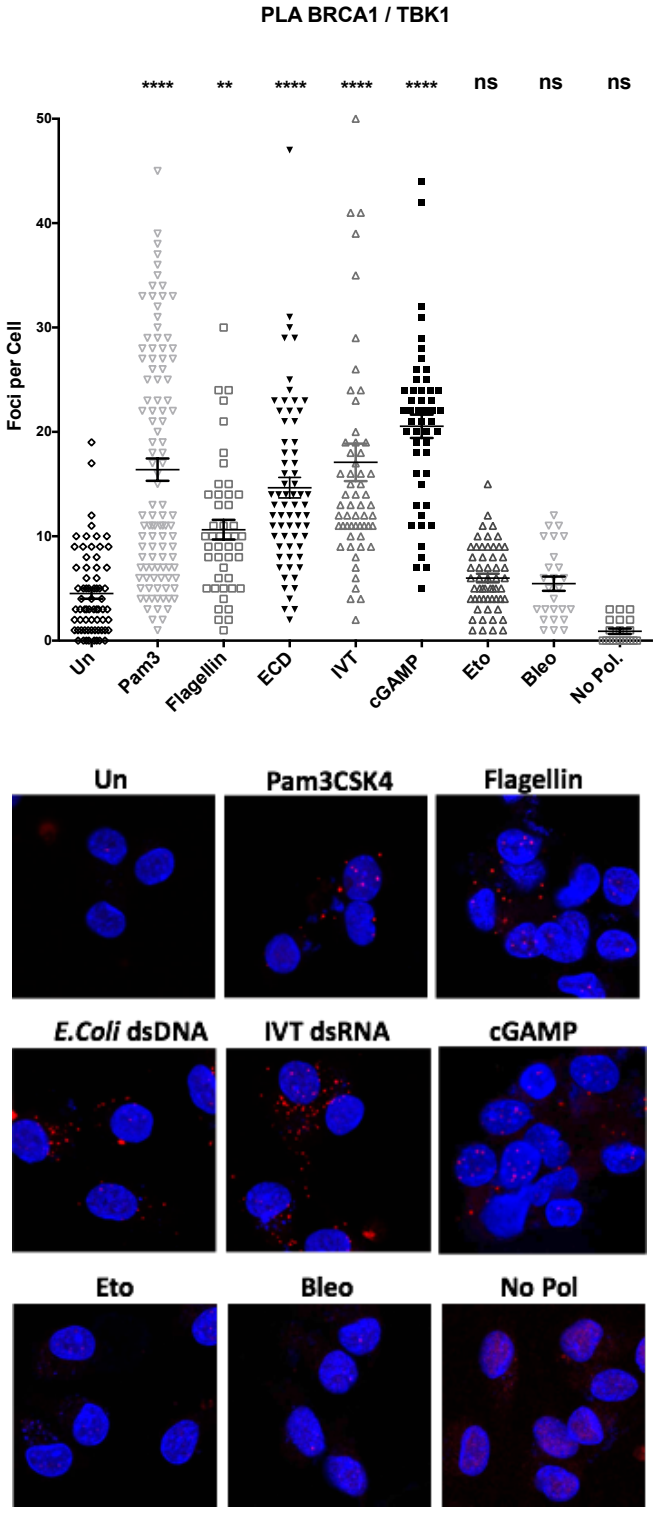

Figure 5.3 PLA confirms interaction of BRCA1 with TBK1 upon PRR stimulation. MoDCs were seeded into wells of Poly-L-Lysine coated 8-well chamber slides and probed with antibodies against BRCA1 and TBK1 after incubation with 1 µg/mL Pam3CSK4, 100ng/mL Flagellin, 100 µM etoposide or 100 µM bleomycin for 1h, or 2µg/mL E. Coli dsDNA (ECD), 2µg/mL IVT dsRNA or 1 µg/mL 2'-3'cGAMP for 2h. Proximity ligation assay was then performed using anti-rabbit PLUS and anti-mouse MINUS probes and a Red fluorescent probe, and a no polymerase control included. A macro was applied to images containing a minimum of 50 cells from three blood donors to quantify the number of interaction points per cell. **p<0.01, ****p<0.0001

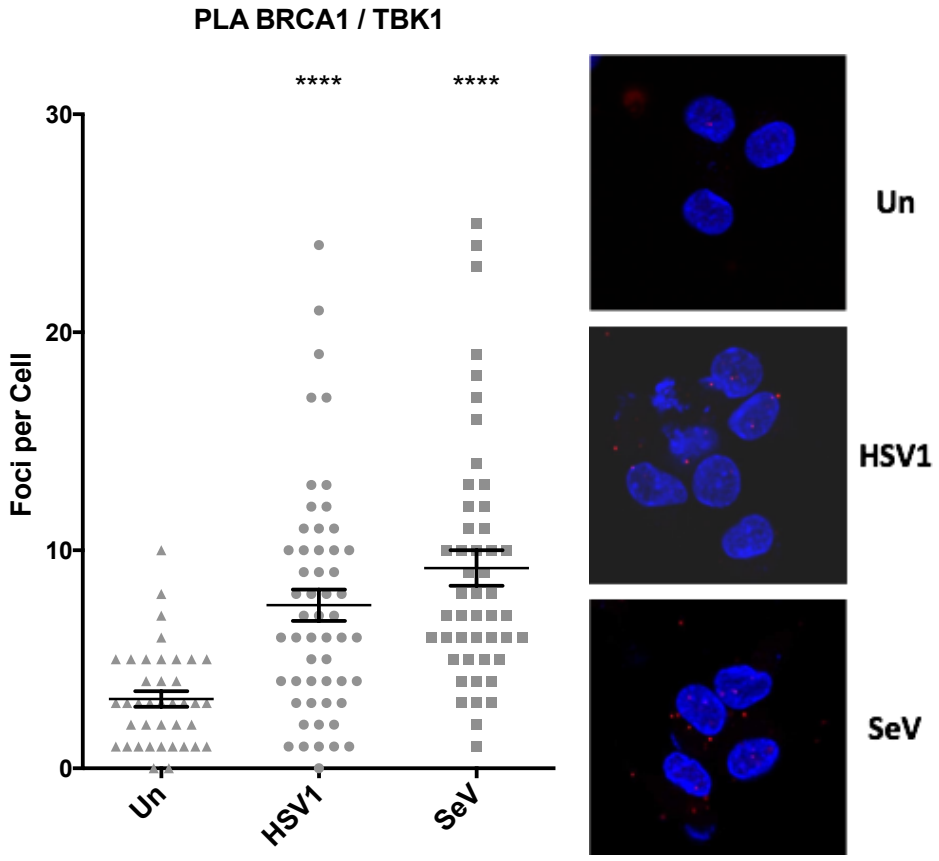

Figure 5.4 PLA analysis of BRCA1 interaction with TBK1 after viral infection. MoDCs were seeded into each well of an 8-well chamber slide pre-coated in 0.1 mg/mL Poly-L-Lysine. Cells were probed with antibodies for BRCA1 and TBK1 after infection with HSV1 at an MOI of 5 or Sendaï virus at an MOI of 1 for 1h. Proximity ligation assay was then performed using anti-rabbit PLUS and anti-mouse MINUS probes and a Red fluorescent probe. A macro was applied to images containing a minimum of 45 cells from three blood donors to quantify the number of interaction points per cell. ****P<0.0001

5.3.3 BRCA1 knockdown in primary DCs

Efforts were then made to knock-down BRCA1 in primary MoDCs to undertake functional studies. Initially, siRNA transfection was attempted using Neon electroporation apparatus, which achieves the best transfection efficiency and cell viability of all methods I tested for MoDCs (data not shown). Multiple different siRNA's targeting different parts of the BRCA1 gene were tested, either alone or in combination, but none gave a detectable knockdown at the protein level up to 72 hours post-transfection (Figure 5.5A). This was despite significant reduction in BRCA1 mRNA levels as assessed by qRT-PCR (Figure 5.5B), which decreased on average by 66%. Cells from at least 10 individual blood donors were used to try achieve a suitable knockdown using this method. A maximum reduction in protein of approximately only 20% was achieved.

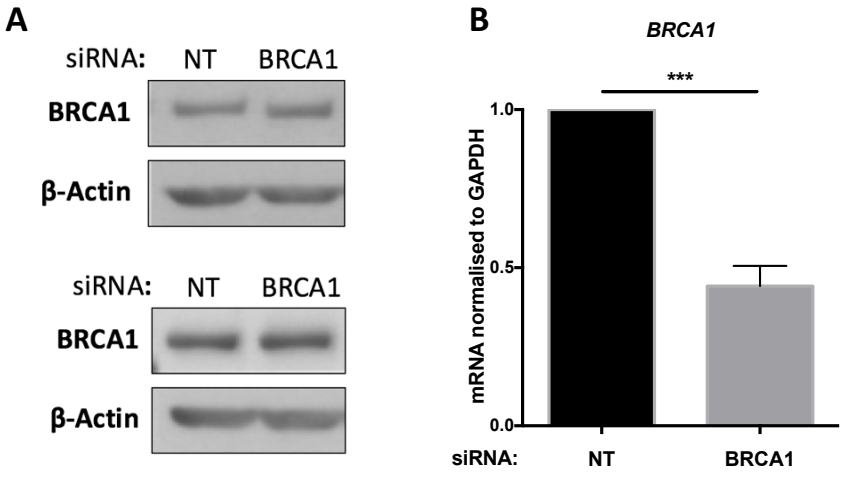

Figure 5.5 Analysis of BRCA1 levels after siRNA transfection. MoDCs were transfected with BRCA1-targeting siRNAs using Neon electroporation apparatus 3 days post CD14+ isolation. 72 hours post-transfection, cells were **A.** subject to WB using anti-BRCA1 antibody and **B.** Assessed for BRCA1 transcript level by qRT-PCR (n=4). *** $p<0.001$

To try and resolve this issue, transduction of MoDCs with BRCA1 shRNA-encoding LVPs was performed, using the same method which achieved successful TBK1 knockdown in Figure 4.4. This way, shRNA would be continually produced over the 5-day differentiation period, whilst achieving a higher transduction efficiency and cell survival rates than transfection methods. Freshly isolated CD14+ cells were transduced with LVPs encoding either a control or BRCA1-targeting shRNA sequences, or LVPs encoding GFP. Alongside, LVPs encoding Vpx were produced and used to transduce the MoDCs in order to degrade SAMHD1 and increase transduction efficiency. Again, transduction of MoDCs was routinely above 70% with low levels of maturation as determined by CD86 expression (Figure 5.6A). Knockdown of BRCA1 mRNA was also significant (Figure 5.6B). Unfortunately, protein level was still insufficiently reduced for functional studies, even with use of five different shRNA sequences which target different parts of the BRCA1 gene. This was attempted with cells from a minimum of eight different blood donors, with results much the same. The BRCA1 protein may be therefore too stable and its half-life too long to be able to knockdown by RNA-interference methods in MoDCs.

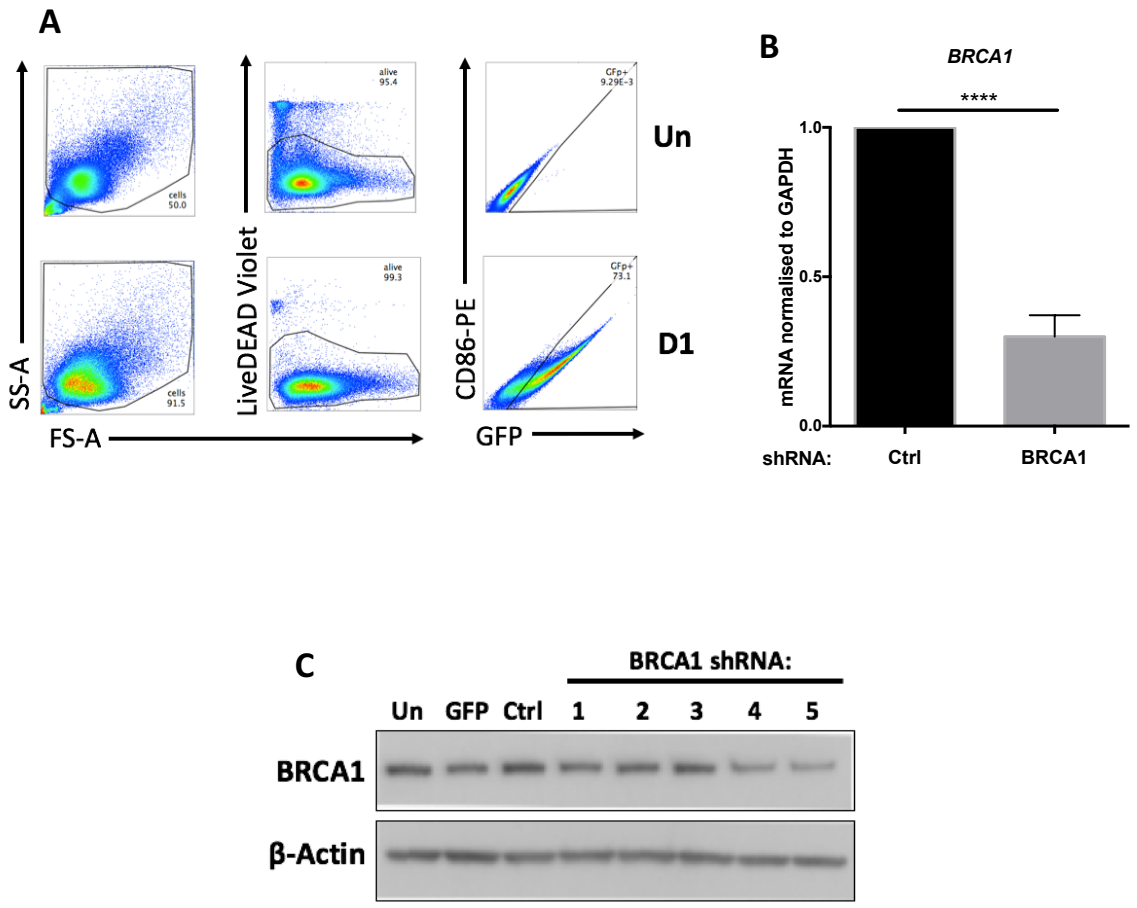

Figure 5.6 Analysis of LVP transduction efficiency and BRCA1 knockdown levels. CD14+ cells were transduced with LVPs encoding GFP, control or BRCA1-targeting shRNAs immediately after isolation. Cells were differentiated to MoDCs and 5 days post transduction and assessed for **A.** Transduction efficiency and activation status compared to untransduced cells using Flow cytometry. Cells were stained with LiveDead violet viability stain and anti-CD86 PE conjugated antibody. GFP expression was detected in the FITC channel. **B.** BRCA1 transcript level by qRT-PCR (representative result shown of cells expressing one shRNA) or **C.** BRCA1 protein level by WB

5.3.4 Generation of THP1 cells stably expressing BRCA1 shRNA using LVPs

THP-1 cells were used as a surrogate cell line to achieve knockdown of BRCA1 for use in functional studies. These extensively-used monocytic cells derived from child leukaemia[493] can be differentiated into macrophage-like cells[494,495] with the use of PMA[496]. Additionally, they proliferate relatively fast with a doubling time of approximately 48 hours in their undifferentiated state, allowing continued use with long-term expression of selectable constructs but without donor variation. THP-1 monocytes were transduced with LVPs encoding GFP, a control shRNA or shRNA sequences targeting BRCA1 as above, and puromycin added 72 hours post infection to allow selection of positively transduced cells expressing the packaged sequence. No Vpx-encoding LVPs were required here due to the ability to select successfully transduced cells. WB analysis shows significant knockdown of BRCA1 at the protein level with use of LVPs encoding four BRCA1-targeting shRNA sequences after 5 days of antibiotic selection (Figure 5.7A). From these samples, shRNA number 1 was taken forward for functional studies. Levels of pBRCA1 were also shown to be decreased from basal levels in cells expressing this shRNA (Figure 5.7B).

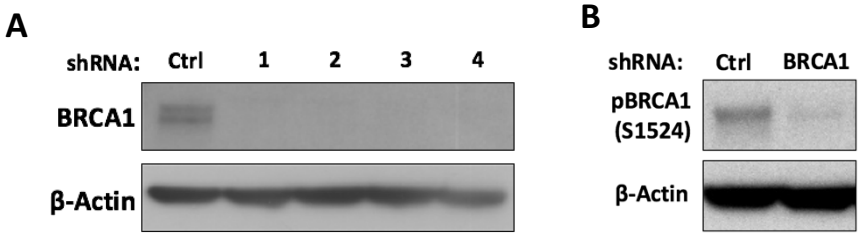

Figure 5.7 Successful BRCA1 knockdown in THP1 cells. THP1 monocytes were transduced with LVPs encoding control or BRCA1-targeting shRNAs. 1 µg/mL Puromycin was added 72 hours later, and successfully transduced cells selected. WB was performed to confirm knockdown of **A.** BRCA1, and also **B.** pBRCA1.

5.3.5 Reduction of BRCA1 results in reduced TBK1 activation and IRF3 phosphorylation

As the presence and activity of TBK1 was seen to have a profound effect on BRCA1 phosphorylation at S1524, the reverse was then examined; BRCA1 knockdown cells were interrogated for their TBK1 activation status after PRR stimulation. WB was performed on PMA-differentiated THP-1 cells which were stimulated with Pam3CSK4 (Figure 5.8A), IVT dsRNA (Figure 5.8B) or cGAMP (Figure 5.8C). BRCA1 knockdown again is confirmed in each relevant sample, whilst total TBK1 is stable throughout. TBK1 phosphorylation is observed upon addition of PRR ligand in cells expressing the control shRNA, but this is noticeably reduced in BRCA1 knockdown cells.

As TBK1 then normally mediates the phosphorylation of IRF3 at S396 (pIRF3), which then translocates to the nucleus to promote type I IFN production, BRCA1 knockdown cells were stimulated with IVT dsRNA and fractionated into nuclear and cytoplasmic compartments, before the induction of pIRF3 visualised by WB. HSP90 and LSD1 were used as cytoplasmic and nuclear markers, respectively, to confirm efficient fractionation. The level of nuclear pIRF3 observed is noticeably less in BRCA1 knockdown cells in comparison with control cells, corresponding with the observed reduction in TBK1 activation (Figure 5.8D).

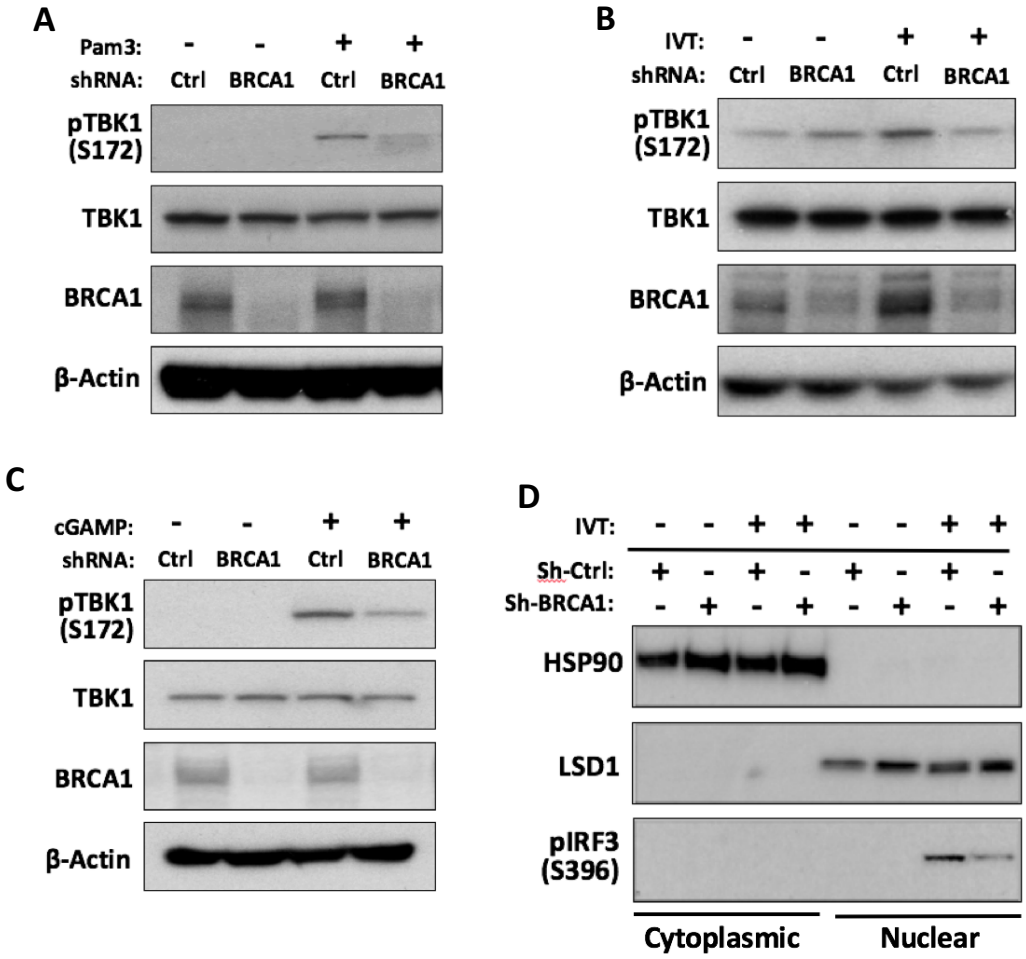

Figure 5.8 BRCA1 knockdown cells show impaired TBK1 and IRF phosphorylation. THP-1 monocytes stably expressing control or BRCA1-targeting shRNA were PMA differentiated before WB analysis after stimulation **A.** with 1 µg/mL Pam3CSK4 for 1h **B.** with 2 µg/mL IVT dsRNA for 2h **C.** with 2 µg/mL 2'-3' cGAMP for 2h **D.** with 2 µg/mL IVT dsRNA for 6h and subsequent nuclear-cytoplasmic fractionation.

5.3.6 BRCA1 Knockdown cells have impaired induction of IFNβ and ISG transcription

Given the observation that BRCA1 deficient cells have reduced TBK1 and IRF3 phosphorylation levels, these cells were assessed for their type I IFN production capability, which would normally be produced downstream of activation of these proteins. THP-1 monocytes were differentiated to macrophage-like cells with PMA and stimulated with multiple different nucleic acids, which are the classical type I IFN-inducing ligands. These included a 60 base pair oligonucleotide with HSV viral motifs known as HSV-60[54], and a 45 base-pair CpG-free oligomer from *Listeria monocytogenes* known as Interferon-stimulatory dsDNA (ISD), both of which activate the STING-TBK1-IRF3 axis[43,497]. Poly(dA:dT) is a synthetic dsDNA sequence which was used and is recognised by multiple sensors including DAI, LRRFIP1, AIM2 and also indirectly by RIG-I[53]. A mix of sheared dsDNA fragments derived from *E. Coli* dsDNA strain K12 which activate TLR9 in addition to the STING-TBK1-IRF3 signalling axis[498] were also utilised. As the TLR2 ligand Pam3CSK4 has also been shown to induce IFN production, this was included as a non-nucleic acid control[388,390,391]. Samples were subjected to qRT-PCR after 6 hours of stimulation to assess transcript levels of IFNβ1, encoded by the *ifnb1* gene. Cells with reduced BRCA1 produce slightly less IFNβ mRNA in the basal state (UT; untreated), but they produce significantly less IFNβ mRNA upon stimulation of all PRR families (Figure 5.9A-E).

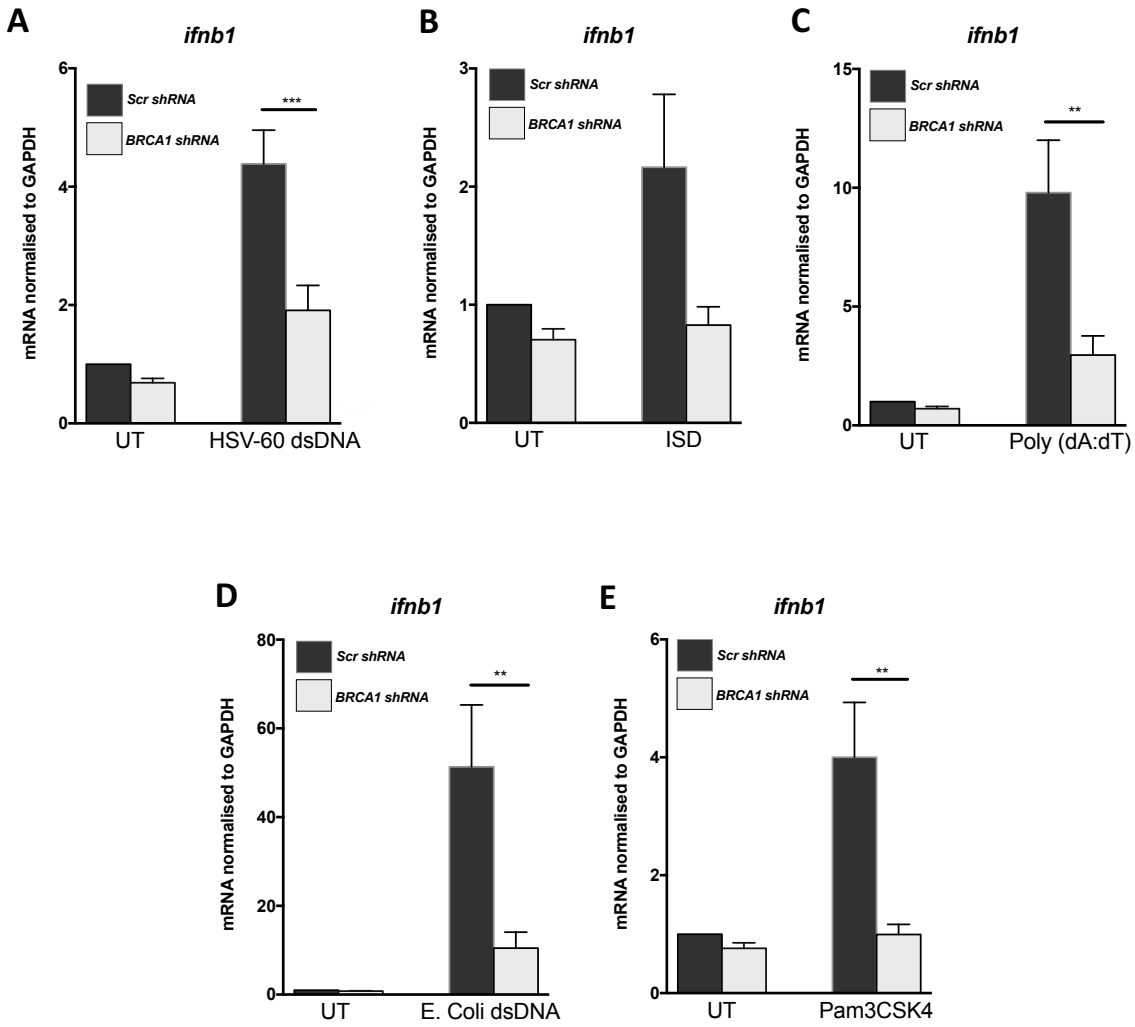

Figure 5.9 BRCA1 knockdown cells have an impaired induction of IFNβ transcription. THP-1 monocytes stably expressing control or BRCA1-targeting shRNA were differentiated to macrophage-like cells and assessed for *ifnb1* transcript level after stimulation for 6h with **A.** 1 µg/mL HSV-60 dsDNA **B.** 1 µg/mL ISD **C.** 1 µg/mL Poly(dA:dT) **D.** 2 µg/mL *E. Coli* dsDNA **E.** 1 µg/mL Pam3CSK4. Results representative of at least three separate experiments. ** p<0.01, ***p<0.001

The transcript levels of key ISGs which are usually induced upon IFN signalling was also evaluated. These included the general antiviral protein IFIT1 which can inhibit both translation and replication of viruses whilst promoting further IFN production[499], the enzyme 2'-5' OAS which degrades viral RNA in combination with RNaseL[98], and the GTPase Mx1 (also known as MxA) which forms oligomers around viral components to inhibit their activity[500]. Control or BRCA1 knockdown cells were stimulated with IFN-inducing ligands HSV-60 dsDNA, IVT dsRNA, or cGAMP, or with whole pathogen in the form of HSV1 or SeV for 6 hours before samples were prepared for and assessed by qRT-PCR. The induction of the IFIT1, OAS1 and MX1 transcript expression was ablated upon stimulation of BRCA1 knockdown cells with all stimuli in comparison to control cells (Figure 5.10). This demonstrates that BRCA1 activity is important for IFN production after sensing of both DNA and RNA genomes, whilst the use of cGAMP again illustrates BRCA1 participation in this signalling axis is downstream of initial receptor activation.

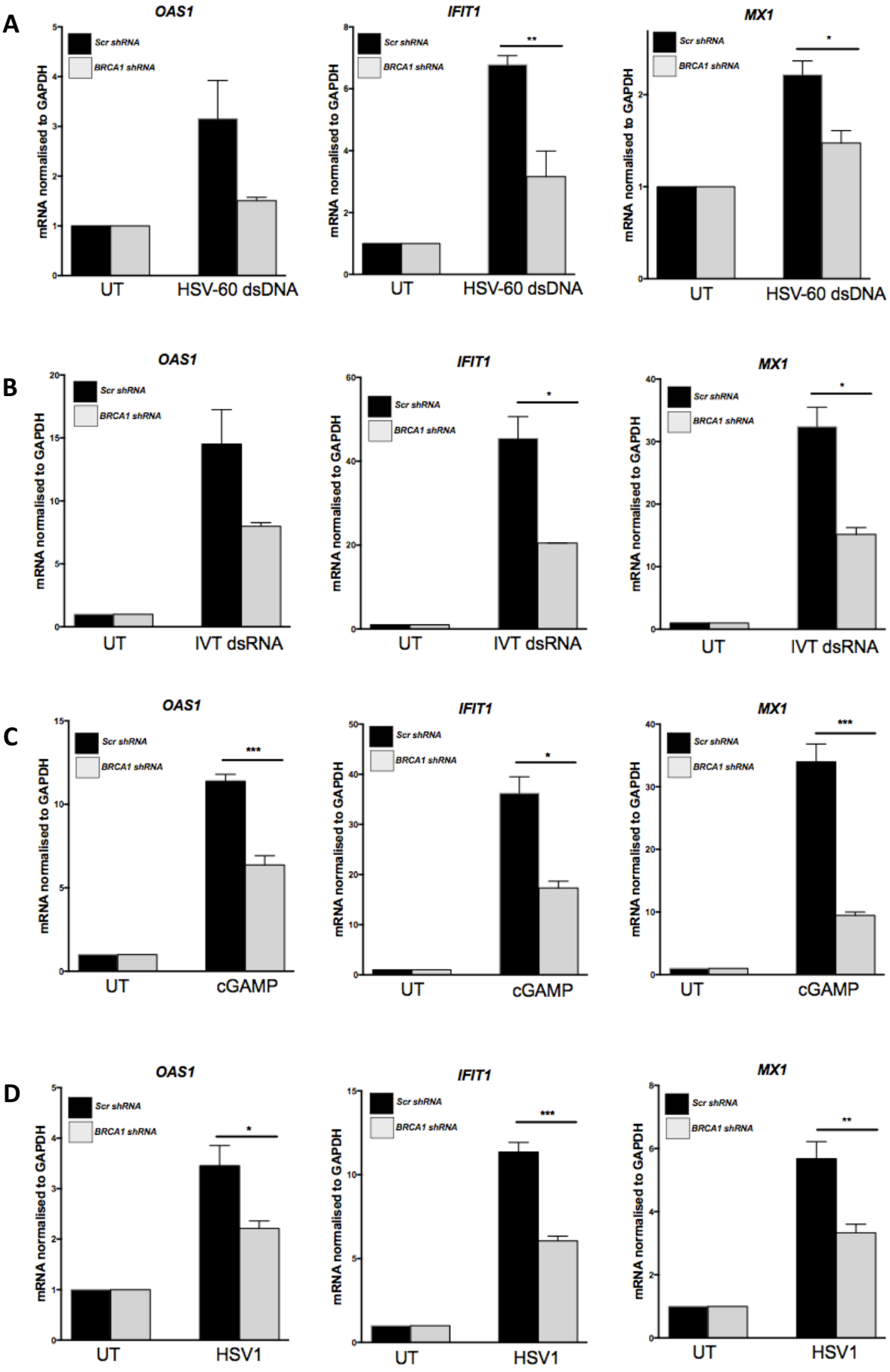
A
OAS1
IFIT1
MX1
Scr shRNA
BRCA1 shRNA
mRNA normalised to GAPDH
UT
HSV-60 dsDNA
B
IVT dsRNA
C
cGAMP
D
HSV1

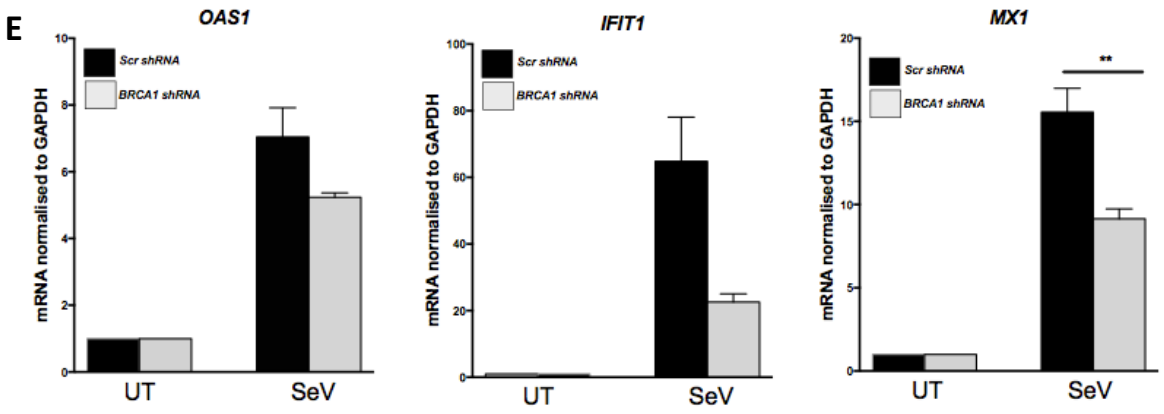

Figure 5.10 BRCA1 knockdown cells have an impaired induction of ISGs. THP-1 monocytes stably expressing control or BRCA1-targeting shRNA were differentiated to macrophage-like cells and assessed for *IFIT1, OAS1* and *MX1* transcript level after stimulation for 6h with **A.** 1 µg/mL HSV-60 dsDNA **B.** 2 µg/mL IVT dsRNA **C.** 2 µg/mL 2'-3' cGAMP **D.** HSV1 at an MOI of 5 **E.** SeV at an MOI of 1. Results representative of at least three separate experiments. *p<0.05, **p<0.01, ***p<0.001

5.3.7 BRCA1 knockdown cells secrete lower levels of type I IFN and IL-1β

As the above experiments assess only the transcript level of IFNβ and ISGs, a cellular bioassay was performed to investigate the induction of type I IFN at the protein level. Cells derived from the HEK293 line which stably express luciferase under the control of an ISRE promoter sequence, termed 3C11 cells, were produced by Dr. Jonathan Maelfait (University of Oxford, Human Immunology Unit). Supernatant from control or BRCA1 knockdown THP-1 macrophages was collected 24 hours after stimulation with HSV-60 dsDNA, ISD, Poly (dA:dT), E. Coli dsDNA, Pam3CSK4 or cGAMP. 3C11 cells were then incubated for a further 24 hours in either the collected supernatant, or titrated concentrations of recombinant IFNα in order to demonstrate reproducible cellular sensitivity in each experimental repeat. Cells were then lysed and luciferase substrate added before luminescence read and the fold induction of the ISRE-driven luciferase product calculated against a media only control. In each case, BRCA1 knockdown cells were significantly hindered in their ability to produce IFN in comparison to control cells (Figure 5.11A-F).

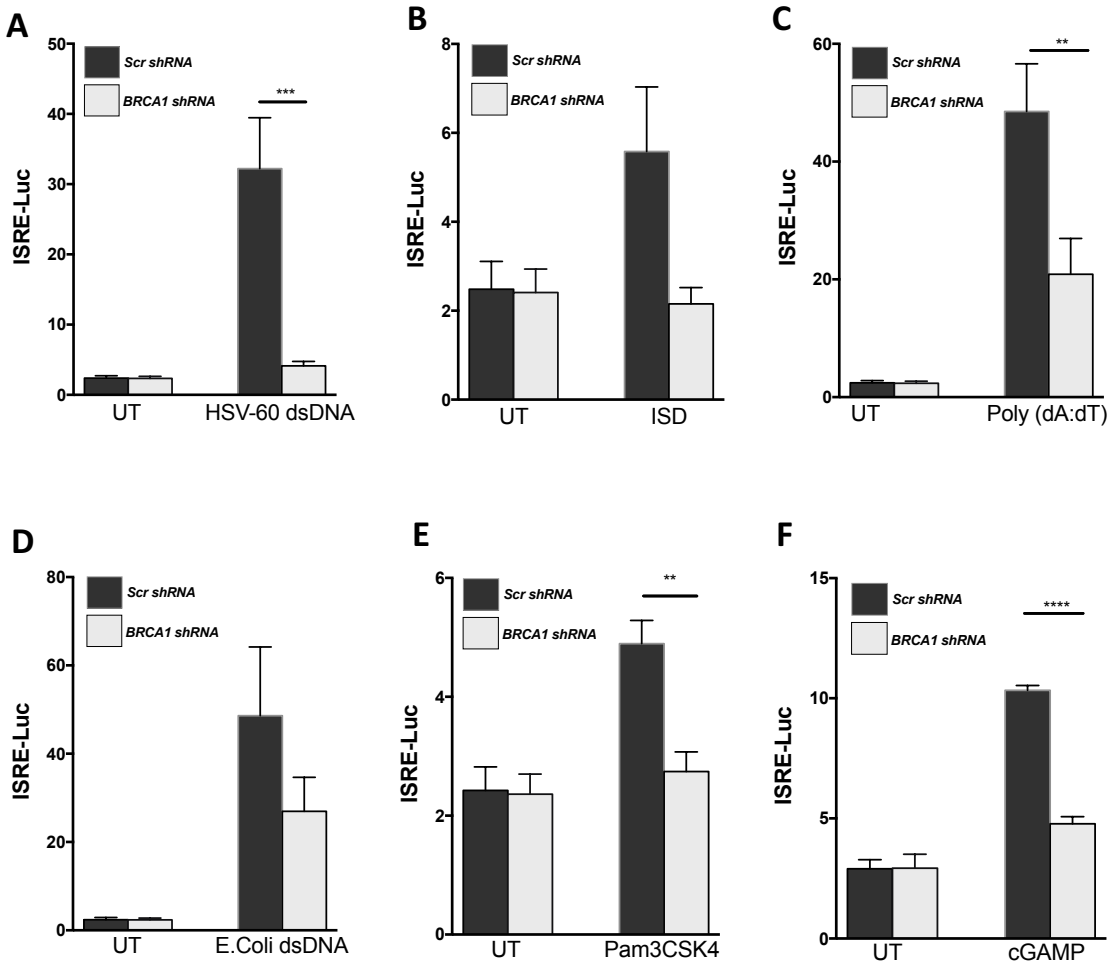

Figure 5.11 BRCA1 knockdown cells have impaired secretion of type I IFN. THP-1 monocytes stably expressing control or BRCA1-targeting shRNA were differentiated to macrophage-like cells and stimulated for 24 with **A.** 1 µg/mL HSV-60 dsDNA **B.** 1 µg/mL ISD **C.** 1 µg/mL Poly(dA:dT) **D.** 2 µg/mL *E. Coli* dsDNA **E.** 1 µg/mL Pam3CSK4 **F.** 1 µg/mL cGAMP, and supernatant collected. 3C11 IFN bioassay was then performed and IFN fold induction calculated. Results representative of at least three separate experiments. ** p<0.01, ***p<0.001, ****p<0.0001

This experiment was repeated with HSV1 to determine whether this phenomenon is relevant in infection settings. Cells expressing two separate BRCA1-targeting shRNAs were used, with successful protein knockdown confirmed by WB (Figure 5.12A). Supernatant from both sets of knockdown cells induce lower luciferase activity, suggesting decreased type I IFN secretion in response to viral challenge (Figure 5.12B). Moreover, IL-1β production was investigated in these samples by use of ELISA on collected supernatant, as TBK1 activity has been previously shown to influence this via regulation of both inflammasome and NFκB activity[468,469,471]. In response to HSV1, IL-1β secretion was also severely impaired in BRCA1 knockdown cells (Figure 5.12C).

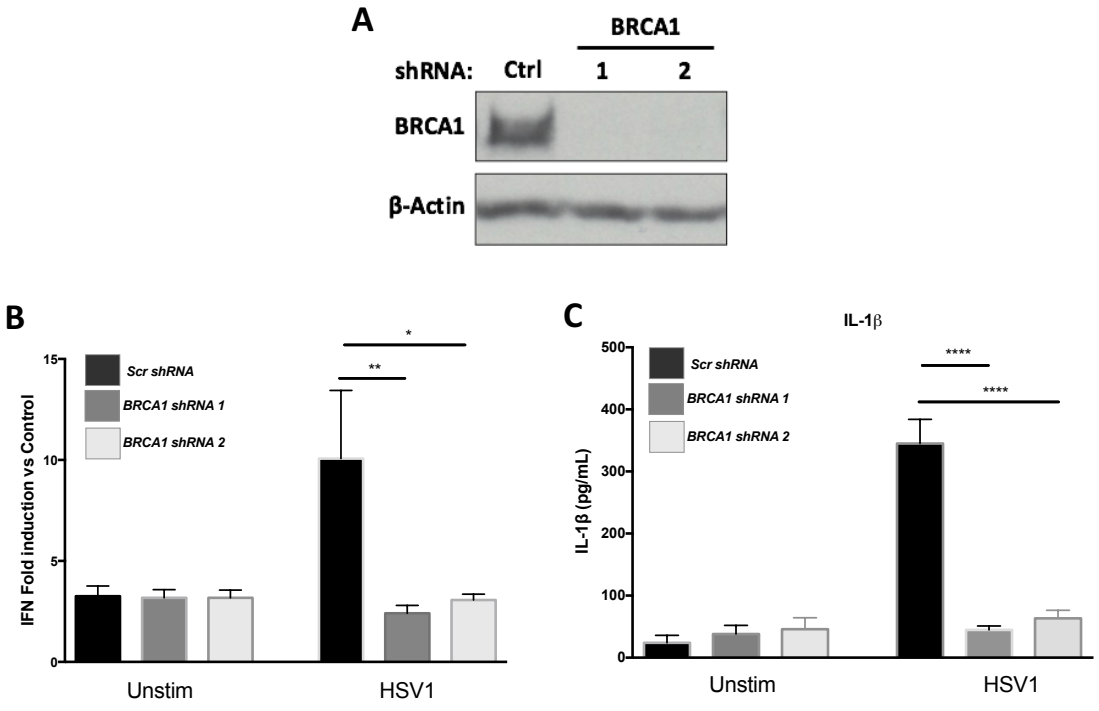

Figure 5.12 BRCA1 knockdown cells have impaired induction of type I IFN and IL-1β in response to HSV1 infection. THP-1 monocytes stably expressing control or BRCA1-targeting shRNAs were differentiated to macrophage-like cells and **A.** assessed for BRCA1 knockdown by WB, or stimulated for 24h with HSV1 at an MOI of 5 and supernatant collected before performing **B.** 3C11 IFN bioassay to calculate IFN fold induction or **C.** IL-1β ELISA and concentration calculated. Results representative of at least three separate experiments. *p<0.05, ** p<0.01, ****p<0.0001

5.3.8 Knockdown of BRCA1 renders cells more susceptible to HSV1 infection

The replication of HSV1 was then assessed in BRCA1 knockdown THP-1 cells, which were infected with a GFP-tagged version of HSV1 at an MOI of 0.1 for up to 20 hours. GFP levels were determined by FACS to follow the progress of infection, giving an indirect measurement of viral replication capacity. GFP detection was more than three times higher in BRCA1 knockdown cells (Figure 5.13), suggesting that these cells are more susceptible to infection, perhaps due to the decreased type I IFN produced when BRCA1 levels are reduced.

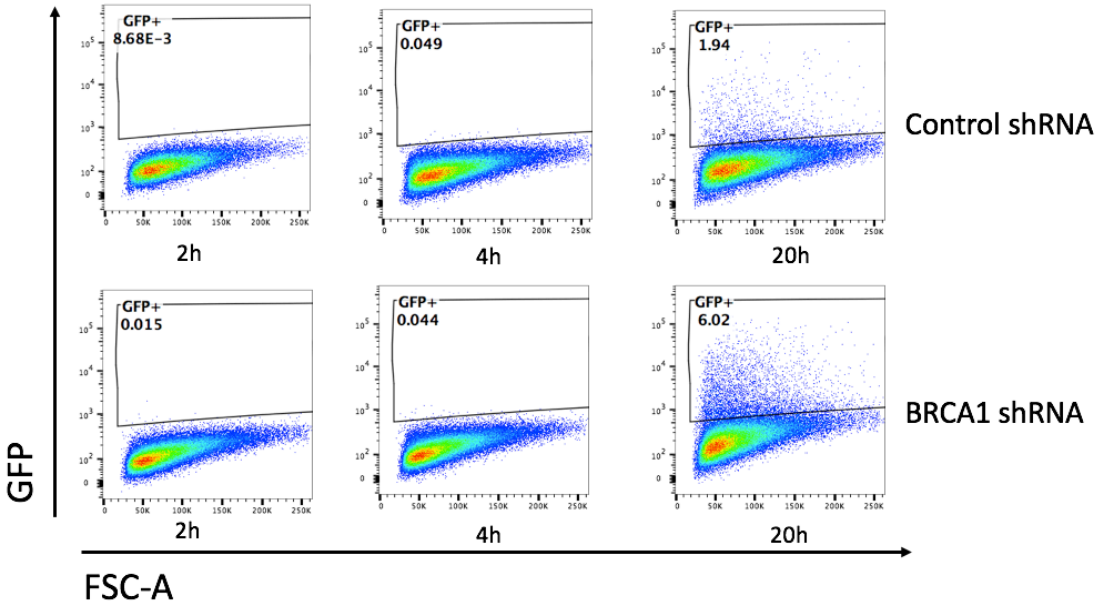

Figure 5.13 BRCA1 knockdown cells are more permissive to HSV1 replication. THP-1 monocytes stably expressing control or BRCA1-targeting shRNAs were differentiated to macrophage-like cells and stimulated for 2h, 4h and 20h with GFP-tagged HSV1 at an MOI of 0.1 before FACS analysis of GFP expression was performed.

5.4 Discussion

In this part of the study, I demonstrated that BRCA1 can be detected after IP of TBK1 exclusively in PRR-stimulatory conditions. The use of etoposide did not increase the interaction of these proteins, even though DDR signalling was shown to be successfully activated by the increase of pATM. Binding of TBK1 to its constitutive binding partner TANK remained unaffected in all samples. It was not possible to IP endogenous BRCA1 using the conditions tested; many primary antibodies recognising BRCA1 were tested, and multiple parameters within the protocol changed including lysis buffer, wash buffers, antibody to bead ratio, bead type, and incubation periods. It is possible that the antibodies tried either do not bind to the beads used, or that the BRCA1 binding epitope is masked by bead conjugation.

Instead, the proximity ligation was used as an alternative technique to confirm the interaction between TBK1 and BRCA1. This method has the added benefit of detecting primary antibodies within a 40nm proximity, allowing protein interactions that are weak or mediated by a bridging protein to be detected, thereby increasing sensitivity when compared to conventional IP. In addition, it gives a spatial output, showing where the interaction takes place within the cell. Finally, it requires small cell numbers, permitting multiple conditions to be assayed and control experiments to be performed for each antibody used[501,502]. After control samples confirmed increased cytoplasmic interaction of TBK1 with MAVS and STING after stimulation of RIG-I and cGAS with IVT dsRNA and *E. Coli* dsDNA, respectively, induction of DNA damage with etoposide demonstrated elevated points of interaction in the nucleus between BRCA1 and γH2AX. However, the stimulation of cells with IVT dsRNA or Pam3CSK4 did not increase the levels of this interaction, validating that is specifically induced in genotoxic conditions. The subsequent increase in

BRCA1 and TBK1 interaction demonstrated after treatment of cells with a range of PRR ligands was visible in the cytoplasm of cells, and discernibly in perinuclear zones in some samples. This supplements data obtained using confocal microscopy which demonstrates BRCA1 and TBK1 localising to this cellular area after stimulation. Remarkably, the inability of etoposide or bleomycin to induce the interaction between BRCA1 and TBK1 suggests that this event is immune-specific, in contrast with BRCA1- γH2AX interactions which are DNA Damage-specific. Infection with HSV1 and SeV also significantly increase the number of visible interactions between the two proteins, although the number of interactions detected in each case is generally lower than with use of PRR ligand. This may be due to unphysiologically high amounts of agonists used, or the virus having mechanisms to reduce this interaction if it does indeed have antiviral downstream functions.

I also show that BRCA1 is difficult to knock down at the protein level by RNAi methods in primary MoDCs, even when transcript levels are significantly depleted. The BRCA1 protein may have a long half-life in these cells, and thus the incubation time permitted may not be sufficient to allow for degradation of existing protein. CRISPR- based knockout was not used in the primary cells as the same problem of low transfection efficiency and stable existing protein would remain. Nonetheless, the transduction of LVPs encoding BRCA1-targeting shRNA into THP1 cells allowed a longer expression and incubation period to permit degradation of existing protein, whilst also enabling antibiotic selection. Experiments performed using these occasionally included wild-type THP1 cells, to demonstrate that the control shRNA did not have abnormal inflammatory responses, which would give a false disparity between these and BRCA1 knockdown cells.

This method proved to be extremely successful, and allowed functional studies to uncover defects in TBK1 phosphorylation and subsequent levels of nuclear pIRF3 in BRCA1

knockdown cells, in response to multiple PRR ligands. Low levels of pTBK1 were still detected in PRR-stimulated BRCA1 knockdown cells, which may be due to the initial autophosphorylation[165] which does not fully activate the protein. Complete functional activation of TBK1 is induced either by high local concentration[41] or by other kinases being recruited to specific signalling platforms[503]. BRCA1 may facilitate this by binding to TBK1 and recruiting other protein mediators which promote its phosphorylation to allow full enzymatic activity. BRCA1 may do this by utilising its ability to interact with a plethora of various binding partners and act as a scaffold protein to promote the progression of multiple signalling pathways[299,309].

Reduced nuclear pIRF3 levels in BRCA1 knockdown cells expectedly translate to reduced transcription and secretion of type I IFN upon stimulation of a range of PRRs including TLRs, RLRs and CDSs in addition to pathogens with a DNA or RNA genome. The use of cGAMP demonstrates that BRCA1 intersects with innate signalling pathways downstream of initial receptor activation, whilst the finding that BRCA1 is involved in cellular responses to IFN-stimulatory dsRNA and an RNA virus is novel; most studies are restricted to its interaction with DNA in relation to repair and transcriptional control. In the case of all stimuli, type I IFN was not completely blocked however, possibly due to redundancy in the pathways leading to its production; as many viruses target IFN production to facilitate efficient replication, alternative pathways can intervene to ensure a successful immune response. Secreted IFN would usually bind its cognate IFNAR and induce signalling via the Jak/STAT pathway to promote the expression of antiviral ISGs, a pathway which is hindered as a result of reduced IFN production in BRCA1 knockdown cells. Additionally, cells expressing two separate shRNA sequences targeting different parts of the BRCA1 genome secrete almost no IFN in response to HSV1 infection. The use of these differing

shRNA sequences greatly reduces the probability that this phenomenon is caused by an off target effect of the specific shRNA sequence used. The substantially reduced IL-1β produced in these samples further suggests that BRCA1 is important in general inflammatory responses downstream of TBK1 activation, which has known roles in regulating NFκB signalling[162,468,469] and IL-1β production[471] in addition to its IFN-stimulating function. Finally, viral replication in the form of GFP-tagged HSV1 is increased in BRCA1 deficient cells compared to cells expressing the full complement of functional BRCA1, probably due to the decreased IFN produced upon sensing of the pathogen.

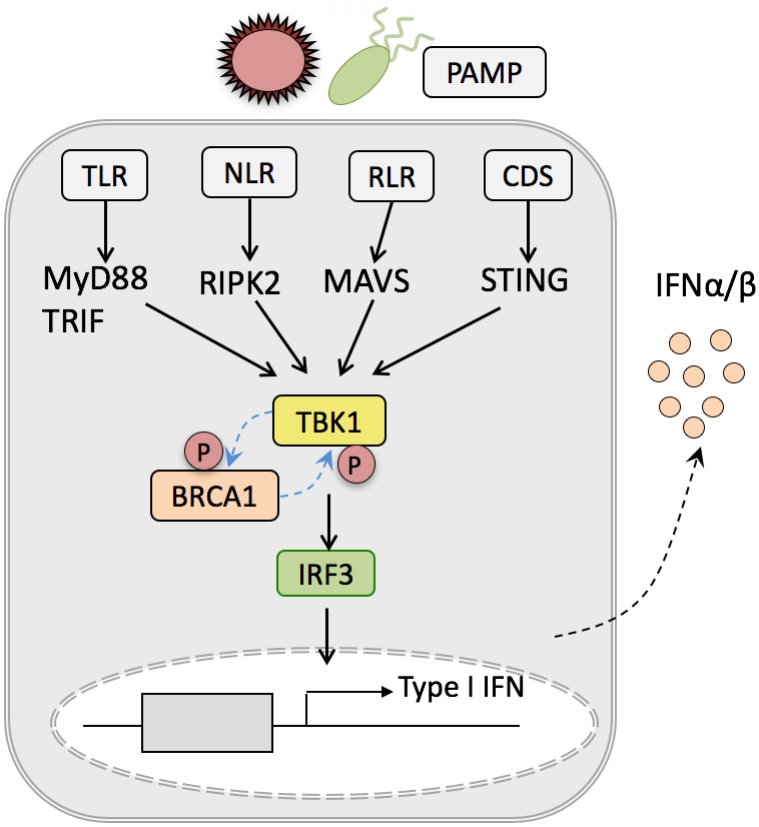

Figure 5.14 Proposed model of BRCA1 action in innate immune signalling. Upon PRR sensing of PAMPS, signalling can converge upon TBK1 activation, initiating some transautophosphorylation of TBK1 at S172. BRCA1 phosphorylation at S1524 is then promoted by TBK1 activity, which then prompts binding of BRCA1 to TBK1, facilitating full phosphorylation of TBK1 and downstream activation of IRF3 leading to type I IFN production.

6 Concluding Discussion

6.1 Introduction

In this study, BRCA1 has been identified as phosphorylated at S1524 upon activation of a range or PRRs spanning the TLR, RLR, CDS and NLR families which are located in different parts of the cell. It was demonstrated that PRR stimulation does not induce any observable DNA damage or DDR signalling, and that BRCA1 phosphorylation in this specific context is independent of genotoxicity or oxidative stress. Additionally, BRCA1 phosphorylation is not mediated by its canonical kinases, but rather intersects with innate immune signalling downstream of adaptor recruitment and specifically downstream of TBK1 activation. It was also demonstrated that BRCA1 biochemically interacts with TBK1 at organelles derived from Golgi-related proteins, where activated TBK1 and STING reside after PRR stimulation. The presence of BRCA1 is required for full activation of TBK1, as assessed by its phosphorylation. Consequently, it was shown that this requirement for BRCA1 also has effects on downstream activity of TBK1, in nuclear levels of phosphorylated IRF3 and subsequent expression of type I IFN and ISGs. Finally, reduced BRCA1 confers an increased susceptibility to HSV1 replication.

6.2 DNA Damage-independent BRCA1 phosphorylation

In this section of study, phosphoproteomic results identified proteins belonging to the DDR as significantly differentially phosphorylated upon PRR stimulation. Interestingly, the proteins identified in this manner were exclusive to each receptor stimulated. The phosphorylation status of many of these proteins could not be validated, but upon further specific study, BRCA1 was identified as phosphorylated in a general manner upon activation of a range of PRRs spanning most families and cellular localisations. However, BRCA1 was not identified in the proteomic data as differentially phosphorylated upon PRR agonism.

Together, this highlights the strengths and caveats of large-scale phosphoproteomics. Firstly, such techniques can allow the identification of novel crossovers between protein networks and pathways which may be employed in specific cellular circumstances. However, specificity and variability is an issue which may be alleviated by complementary techniques of validation such as Western Blotting, where reagents permit. Sample number may also hinder specific protein identification; as phosphorylation is a transient modification, restricted sample numbers as a result of high computational and resource burden may prevent capture of the specific time frame in which certain proteins are differentially phosphorylated.

Nonetheless, the availability of phospho-specific antibodies to proteins identified by such phosphoproteomics techniques has permitted the identification of BRCA1 S1524 as a residue significantly phosphorylated under PRR-activatory conditions. Previously, this residue was known to be phosphorylated predominantly by ATM, and to a much lesser extent ATR, under genotoxic conditions[282,413]. Specifically, phosphorylation of S1524 is important in radio-resistance, with cells mutated at this residue displaying hypersensitivity

to UV and IR exposure[398]. Under these circumstances, S1524 phosphorylation occurs most frequently in the S-Phase of the cell cycle[398,413], of which MoDCs that were used in this study do not enter. Instead, they reside in G_0[504,505].

This compounds to the curiosity of the observations made in this section of study which uncovered a rapid induction of pBRCA1 in MoDCs in response agonists of TLRs, NLRs, RLRs and CDSs. This level of phosphorylation of BRCA1 remains unchanged in MoDCs treated with genotoxic agents which are shown to successfully induce DNA damage and activate DDR signalling via γH2AX, ATM and CHK2. Similarly, excessively high induction of ROS, often produced after APC activation[404,405], also fails to induce BRCA1 phosphorylation at this residue. Perhaps to expand upon this finding, other types of DNA Damage should be pursued, given that each distinctly activates certain signal transduction pathways; UV and IR may be of more relevance to this residue, although UV irradiation was briefly attempted and yielded no results.

In order to determine whether this phenomenon is restricted to MoDCs, many other cell types were used to attempt to recapitulate findings; only monocytes from which the MoDCs derive show clear induction of BRCA1 phosphorylation at S1524. Other cell lines tested failed to induce discriminable levels pBRCA1 (Figure S1), perhaps due to a constitutively active or deregulated DDR which could be inherent in their transformed nature as a result of multiple persistent mutations. However, Seiji Shiraishi has now demonstrated that PRR stimulation in HeLa cells can induce visible changes in BRCA1 phosphorylation (Figure S2). These cells also induce BRCA1 phosphorylation at this residue upon etoposide treatment as would be expected. These are dividing cells, so in theory require higher levels of genome protection and also progress through the cell cycle, which

again primary non-proliferative MoDCs do not. This will therefore be a useful tool for further study, as these cells are highly transfectable where THP-1 cells and MoDCs are not. In supplement, I demonstrated that BRCA1 phosphorylation upon PRR activation was not catalysed by BRCA1's canonical kinases ATM or ATR, or their downstream kinases CHK1 and CHK2. To probe this further, lentiviral knockdown of all known kinases which phosphorylate BRCA1 will be attempted, including Aurora A and Akt in addition to those outlined above. Notwithstanding this, BRCA1 phosphorylation upon PRR agonism was shown to be downstream of immune signalling, with inhibition of either TBK1 directly, or processes which utilise TBK1, completely ablating this. Lentiviral knockdown of TBK1 confirmed specificity of this occurrence. However, to determine if TBK1 is the upstream kinase of BRCA1 in PRR-activated contexts, non-radioactive and cell-free *in vitro* kinase assays are being optimised (Figure S4). In these, TBK1 phosphorylation of IRF3 serves as a positive control, and the presence of TBK1 alone or TBK1 in conjunction with its binding partner IKKε[506] will be considered. The recently identified TBK1 consensus sequence encoded in IRF3, TRIF, MAVS and STING[154], consisting of pLxIS (p, hydrophilic residue; x, any residue; S, phosphorylation site), has been searched for in the BRCA1 gene sequence but could not be found, suggesting that TBK1 may not be the direct upstream kinase for BRCA1 in this instance.

6.3 BRCA1 binds TBK1 and facilitates its type I IFN promoting activity

Both pBRCA1 and pTBK1 were shown to increase at perinuclear areas occupied by Golgi-derived organelles previously termed 'microsomes'[43,118,507], where I confirmed the relocalisation of STING upon stimulation with dsDNA as proposed in other studies. BRCA1 was further demonstrated to colocalise with the activated phosphorylated form of TBK1 here. This was undertaken using an antibody recognising total BRCA1, and a distinct redistribution of the protein is visible after PRR stimulation, with BRCA1 moving out of the nucleus to form distinct Foci overlapping with pTBK1. Multiple sources have cited BRCA1 shuttling between cytoplasm and nucleus, but no reports identify a functional role for BRCA1 in the cytoplasm[303,305,433].

Here, I demonstrated that BRCA1 biochemically interacts with TBK1 in the cytoplasm exclusively upon PRR stimulation; the induction of DNA Damage does not promote this interaction. BRCA1 interacts with H2AX exclusively upon induction of genotoxic stress by etoposide as expected[492], further demonstrating the DNA Damage-independent specificity of BRCA1-TBK1 interactions. The presence of BRCA1 was also important for the full activation of TBK1 after initial trans-autophosphorylation, with BRCA1 reduction conferring impairment of IRF3 phosphorylation, downstream type I IFN production and ISG expression. This occurred with use of classical IFN-inducing ligands which activate RLRs and CDSs, as well as non-classical IFN inducers such as Pam3CSK4 which activates TLR2. The role of TBK1 in mediating type I IFN induction downstream of TLR2 agonism has been highlighted in recent years however[103,113,388,390,391]. IFN production in response to infection with viruses with both RNA and DNA genomes was also perturbed. The collective evidence gathered supports the notion that BRCA1 cooperates with TBK1 to promote its type I IFN

production activity in a broad manner, and has an effect to restrict viral replication as seen with increased GFP-HSV1 replication in BRCA1 deficient cells.

Induction of IL-1β was also abrogated in BRCA1 knockdown cells. Both TBK1 and BRCA1[490,508] have been suggested to have a functional role in NFκB activation and inflammatory cytokine production, in particular downstream of autophagic activity involving IL-1β[471,509]. Findings here therefore may bridge other studies and potentially identify a wide biological significance for this complex between BRCA1 and TBK1. More study would be needed on this to determine the exact functional nature and capabilities in different cellular circumstances.

The idea that BRCA1 may influence IFN production and signalling is not entirely novel; some studies in the past have suggested that BRCA1 can regulate the signalling of the type III IFN, IFNγ, through a mechanism utilising the transcriptional regulation activity of BRCA1 which targets IRF7 and type I IFN[510,511]. Additionally, this function of BRCA1 has been reported to be responsible for directly regulating the expression of key ISGs including MxA and OAS1, in the presence of IFNγ[512].

In fact, during the very late stages of this study, literature was published which directly cites BRCA1 as forming a functional complex with IFI16 in response to infection by HSV1 (or other Herpesviruses). Similarly to this study, the BRCA1-containing complex is shown to form in a DNA Damage-independent manner. The authors demonstrate that BRCA1 partakes in the formation of an ASC-containing inflammasomes in the cytoplasm which induce the production of IFNβ and IL-1β[513]. However, the authors stipulate that BRCA1 binds IFI16 in the nucleus of cells specifically alongside the Herpesvirus DNA genome, and that signal transduction begins here. An interaction between BRCA1 and IFI16 has been reported previously, with IFI16 being discovered to be a member of the large BRCA1-

associated genome surveillance supercomplex (BASC)[514], which plays multiple roles in DNA damage sensing and repair. BRCA1 binding of IFI16 upon ligand sensing in the nucleus wouldn't account for the multiple PRR ligands demonstrated in my study, including dsRNA and non-nucleic acid ligands in addition to Sendaï virus with its RNA genome, which are sensed out of the nucleus and promote BRCA1 phosphorylation and binding to TBK1. Additionally, I show that the second messenger cGAMP which activates STING at ER membranes can induce such activity of BRCA1. I propose that the study by Dutta *et. al* is not incorrect, but rather is a part of a larger concept. That is, IFI16 may detect Herpesviral DNA in the nucleus as reported previously[12,54,70], but this may be part of the scheme whereby BRCA1 is activated generally downstream of innate adaptor activation, and is recruited to TBK1 in the cytoplasm to modulate its activity in circumstances requiring IFN production. Formation of BRCA1-TBK1 complexes would facilitate IRF3 phosphorylation and downstream type I IFN production, as well as TBK1's emerging role in the formation of autophagosomes which can be linked to inflammasome activity[471]; a process which BRCA1 has also very recently been connected to[509]. Whether autophagy and mitophagy positively or negatively regulate inflammasome activation is currently hotly debated[58], due to the complexity of signal transduction networks activated, itself dependent upon the receptor stimulated. To study the extent, if any, of BRCA1 and TBK1's role in inflammasome activity, and to determine whether IFI16 employs BRCA1 specifically, one could assess pro-caspase 1 and pro-IL-1β cleavage in addition to IL-18 secretion and ASC speck formation. This would need to be performed using agonists to a range of inflammasome-activating receptors, collectively possessing diverse chemical nature, in order to show that BRCA1's recruitment to innate signalling cascades is not dependent on IFI16 and is not a result of direct ligand binding, as is suggested by Dutta et. al.

6.4 Mechanism of BRCA1 influence of TBK1 activity

To understand the mechanism by which BRCA1 may influence the activity of TBK1, it is necessary to look at the biochemical nature of the BRCA1 protein. In this study, S1524 was identified as phosphorylated in response to PRR agonism. However, I did not investigate the significance of this residue for induction of interferon responses. To assess this, expression plasmids which encode either wild type BRCA1, or S1524- to Alanine or Glutamine mutants, conferring a phosphomimetically 'off' or 'on' signal could be utilised. These could be overexpressed in a BRCA1-deficient cell type, such as HCC1937 which have mutant non-functional BRCA1[515], or a common cell line such as HeLa cells where BRCA1 is removed by CRISPR technology. Cells would then be stimulated with IFN-inducing ligand such as dsDNA or dsRNA, and IFN production assessed in each case.

Similarly, to determine the biochemical function of BRCA1 when complexed with TBK1, experiments could be performed in BRCA1 knockout cells which overexpress combinations of BRCA1 domains. This would help determine both the binding site which is required for interaction with TBK1, but also any function BRCA1 plays. It is likely the BRCT domains are important for mediating this interaction, as they are for most other interacting partners[279,299,309]. In particular, these domains facilitate binding to other phospho-proteins, of which TBK1 is one. BRCA1 may bind TBK1 and one of its regulating proteins to create a scaffold, thereby permitting regulation of TBK1. To assess this, wild-type or BRCA1 knockdown cells could be stimulated and TBK1 immunoprecipitated. Samples could then be analysed by mass spectrometry to determine which TBK1-interacting proteins rely on BRCA1.

6.5 BRCA1-mediated Ubiquitination of TBK1?

When BARD1 is bound to BRCA1 at its N-terminal RING domain, this complex acts as a RING E3 ubiquitin ligase[296] which catalyses the addition of both polyubiquitin and monoubiquitin chains onto substrate proteins. Indeed, BARD1 binding is necessary to stabilise the proper conformation of BRCA1's RING domain for E3 activity[294]. The multiple types of ubiquitin modification that BRCA1 can catalyse induce different signalling events. These include linkages via K48 which induce a proteasomal degradation, K63-linkages[516] which can be an activating mark that bypasses the 26S proteasome[517], and additionally non-conventional K6 linkages[300,518] of substrates including itself. Many substrates have been identified for BRCA1/BARD1 mediated ubiquitination, including Histone proteins, CtIP, ERα and TFIIE[295] and the binding site for most substrates is within the N-terminus of BRCA1[295]. In the case of CtIP, BRCA1's BRCT domains play the role of a recruitment adaptor, before BRCA1 polyubiquitinates CtIP in a phosphorylation-dependent manner[519]. TBK1 is also a node protein which contains a Ubiquitin-like domain (ULD) which interacts with its kinase domain[520] and is critical for full IFN promoting activity[521]. It is reported that activation of TBK1 requires the K63-linked polyubiquitination of its K30 and K401 residues, which is necessary for its full phosphorylation status at S172[520] and downstream IFN-stimulating activity. Another report suggests K69, K154, and K372 as potential polyubiquitination sites which are important for TBK1 activation in response to RNA viruses[522]. The K63-linked polyubiquitination of TBK1 has been proposed to provide a platform for recruitment of a kinase which phosphorylates TBK1 in concert with initial autophosphorylation[520], which is unsurprising given the critical role of K63-linked polyubiquitination in pathways mediated by TBK1[115,130,170,178,523-526]. In addition to activating polyubiquitin additions to TBK1 mediated by MIB1, MIB2, and nlrdp1[130,527],

deubiquitination of TBK1 an equally important role in regulating its activity; defects in the deubiquitinase CYLD, incidentally a tumour suppressor protein, results in constitutive activation of TBK1 and hyper-responsiveness to VSV infection[117,173]. Likewise, inhibition of the K63 polyubiquitination of TBK1 by A20 or RNF11 serves as an inhibitory mechanism for TBK1 activity. Additionally, E3 ligases such as DTX4, TRIP, Siglec1 and SOCS3 can catalyse K48-linked polyubiquitination of TBK1 to induce its proteasomal degradation[168,175,528,529]. Given that TBK1 contains a ULD and can interact with many E3 ligases, some containing RING finger domains, in addition to the discovery that TBK1 binds to BRCA1 after stimulation of PRRs spanning different families, it is feasible to hypothesize that BRCA1 uses its E3 ligase ability to bind to the ULD of TBK1 to regulate its activity. Dependent on the upstream PRR and adaptor activated, BRCA1 may firstly stabilise the interaction of TBK1 with other proteins in each specific complex, but BRCA1's E3 Ubiquitin ligase activity may be employed to regulate either a regulator of TBK1, or TBK1 itself, permitting full activation of TBK1 and an appropriate IFN response.

Further supporting a potential link between TBK1 and BRCA1, and the E3 ligase activity it possesses, recent studies have demonstrated that TBK1 and its binding partner IKKε can contribute directly to cell transformation[530]. IKKε is already an established breast cancer oncogene which is amplified in 30% of breast cancers, which require IKKε mediated phosphorylation of the tumour suppressor CYLD[531], whilst TBK1 is emerging as a risk factor in such cancers. It has been shown to enhance tamoxifen resistance by phosphorylating ERα[532], another target of BRCA1, whilst promoting cell survival in transformation and cancers[189,533], including those that are KRAS-driven[534]. Consequently, targeting the TBK1/IKKε axis has proven therapeutically successful in treatment of breast cancers[535-537].

Accounting for these observations, interaction with BRCA1 may not only be important for antiviral signalling, but also in cancer, which will be discussed more.

To determine whether the E3 ligase activity of BRCA1 plays any functional role in its binding to TBK1 and downstream IFN production, BRCA1 association with BARD1 could be assessed, given the necessity for this in maintaining E3 ligase activity. Immunoprecipitation of BARD1 and WB of BRCA1 is currently being optimised in both DNA damaging and PRR-stimulatory conditions, whilst PLA could be performed under these conditions to quantify and identify the localisation of this interaction. Additionally, HeLa cells stably expressing HA-Ubiquitin have been created (Figure S3), with the vision of additionally modifying these with LVPs encoding control or BRCA1-targeting shRNAs. The ubiquitin proteome will then be investigated in untreated cells or those stimulated with dsDNA or dsRNA. This would give a broad view of the E3 ligase activity of BRCA1 in PRR-stimulatory circumstances, and would help to pinpoint the nature of any E3 ligase involvement in TBK1 activity; if BRCA1 doesn't promote the ubiquitination of TBK1 itself, we may discover that BRCA1 alters the ubiquitination pattern of TBK1-regulating or interacting proteins. Similarly, I could immunoprecipitate TBK1 in BRCA1 wild-type or knockdown cells, and determine its Ubiquitination status in unstimulated and PRR-stimulated conditions, utilising mass spectrometric techniques. To determine whether BRCA1 binds the ULD of TBK1, cells could be made to overexpress wild-type or ULD-deleted TBK1 (TBK1-Δ-ULD), and the complex formation between BRCA1 and TBK1 in PRR-stimulatory conditions assessed.

6.6 Wider Implications – Pathogen Replication

The discovery of a role for BRCA1 in antiviral and antibacterial immune responses begs the question of whether people with BRCA1 mutations are more prone to infection and whether BRCA1 plays a role in regulating infection on the organism scale. Data on this subject is sparse at best, given the heavy focus on researching BRCA1 in cancer. However, BRCA1 has been shown to be hijacked by HIV-1 for its transcriptional regulation, in order to promote Tat-dependent transcription and enhance viral replication[538]. The restriction of BRCA1 to the nucleus in this process may also reduce IFN production by limiting its cytoplasmic interaction with TBK1. Historically, HIV-1 is known to largely bypass host sensing and IFN production (reviewed in[539]), and this may provide one of probably a multitude of reasons as to why this happens. Similarly, HPV proteins E6 and E7 have been found to directly interact with and modulate multiple activities of BRCA1[540], whilst another study demonstrated disparate modification of BRCA1 localisation dependent on the virus used to infect cells[541]; Herpesviral infection re-dispersed BRCA1 from its resting nuclear zones, whilst Adenovirus recruited BRCA1 to replication centres. Finally, the study outlining a role for BRCA1 in IFI16-mediated Herpesvirus sensing outlined earlier, demonstrated increased HSV1 replication in BRCA1 knockdown cells[513]. Although BRCA1 knockdown was shown to permit increased HSV1 replication in THP1 cells, the ideal system to study this would be with a BRCA1 knockout mouse. However, complete loss of both alleles results in embryonic lethality[542]. Therefore, a mouse expressing inducible Cd11c-Cre crossed with a floxed-BRCA1 mouse would provide an invaluable tool to study the effect of a loss of BRCA1 on DCs.

6.7 Wider Implications – Adaptive Immune Responses

The production of type I IFN by DCs can act in a variety of ways to co-ordinate the activation, migration, differentiation and survival of multiple immune cell subsets. They can act in a paracrine manner to influence maturation and migration of DCs, inducing the expression of co-stimulatory molecules such as CD40, CD80 and MHC II[85]. The production of type I IFN has also been shown to be key for inducing effective cross presentation by DCs[543,544], particularly by CD8+ DCs which are the most potent in this role[545,546]. The type I IFN-mediated augmentation of CD8+ DC cross presentation activity also promotes antigen retention and survival, which in turn enhances the induction of CD8+ T-cell responses[210]. This is in addition to direct CD8+ T-Cell stimulation by IFNα[547,548], which also provides protection from NK Cell-mediated cytotoxicity[549]. Moreover, type I IFN production is necessary for inducing clonal expansion of CD4+ cells during viral infection[550]. These features make type I IFN indispensable for T-cell responses to infection[85], but it is also emerging as imperative in DC-centric innate immune responses to cancer[210-212,486,488]. The current model suggests that type I IFN produced by CD11c+ DCs downstream of sensing tumour antigens, including nucleic acid or metabolites released from dying cells[551,552], is responsible for spontaneous tumour antigen-specific T-cell priming. This endogenous type I IFN production is required for accumulation of CD8+ DCs in the tumour microenvironment. *Batf3*$^{-/-}$ knockout mice which lack the CD8+ DC subset have confirmed that these cells are absolutely required for T-cell priming[209] and tumour rejection[211,212]. Therefore, I propose that mutations in BRCA1 which confer reduced type I IFN production from APCs will also be detrimental to T-Cell responses to both tumour cells and pathogen. To test this, experiments will be performed in which the ability of BRCA1-deficient cells are able to cross present to and polarise T-cells, in response to stimulation with both viral

and tumour-derived antigens. It would be expected that the cells in which BRCA1 is knocked down will polarise T-cells to a lesser extent to their wild-type counterparts, either as a result of decreased cross-presentation or antigen presentation. This would be as a consequence of decreased type I IFN and the maturation it can induce.

Additionally, the expression of PD-L1 on DCs, which induces inhibitory signalling pathways when it binds its mutual receptor PD-1 expressed on T-cells [553], will also be assessed in BRCA1 knockdown cells. We were lucky enough to establish a collaboration with a laboratory at University College London (UCL), who can procure blood from patients with familial deleterious BRCA1 mutations for their own studies, and who have agreed to provide samples for use in our studies. However, any effect observed on IFN responses or DC maturation on these patients' cells is likely to be partial as they would only be heterozygous for the defective gene. Given the increasing support for type I IFN treatment in cancer[486,488], this inhibitory axis may also provide a target for IFN therapy to BRCA1 patients, in which treatment with IFN may reduce the levels of PD-L1 and 'release' the inhibited T-cell response. However, some studies have reported an inverse relationship, where IFN treatment increases PD-L1 expression[554], which could be detrimental to prognosis. Regardless, this avenue would be useful to study.

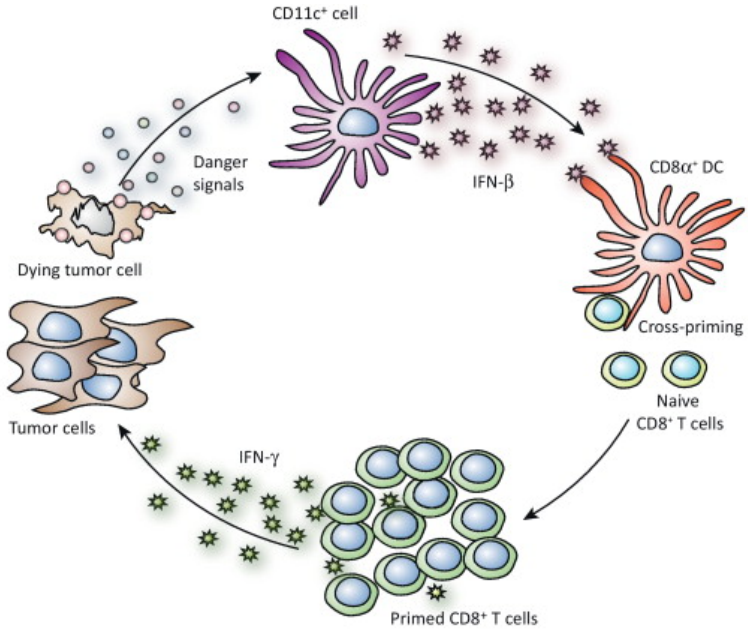

Figure 6.1 Proposed model of DC-mediated antitumour immune responses. This model proposes that DCs sense antigens from dead or dying tumour cells, which induces their maturation, including production of type I IFN. This promotes the activity of CD8+ DCs which then prime CD8+ T cells to induce an anti-tumour response. Adapted from[488]

6.8 Final remarks

This work provides evidence for a new role of BRCA1 in innate sensing, and in induction of pro-inflammatory responses following PRR activation. New work and models highlighting the critical role of type I IFN in antitumour immunity[487,488,555] suggest that lack of BRCA1 could present a 'multifaceted predisposition' to cancer. It is possible mutant BRCA1 might influence cancer aggressiveness via immune effects as well as in effects on DNA repair, in contexts where functional redundancy in innate responses is impaired. The relevance of the effect of BRCA1 on innate signalling in either specific infections or cancer will be the subject of future studies.

7 Supplementary Figures

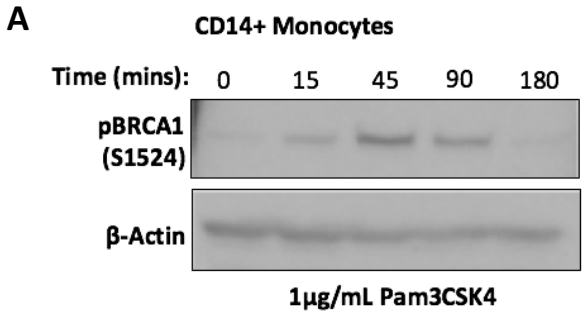

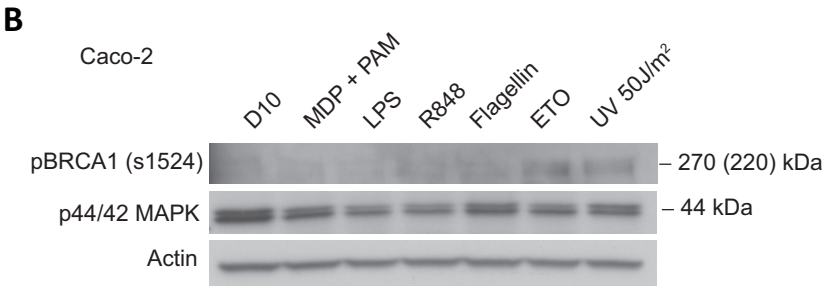

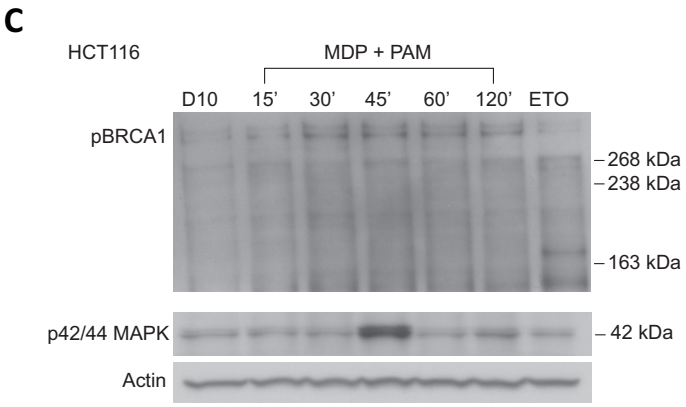

D

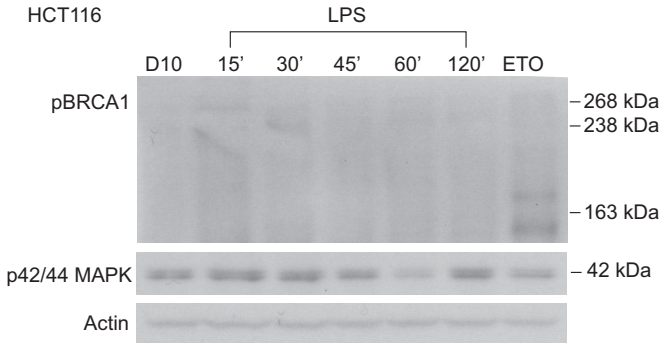
HCT116
LPS
D10
15'
30'
45'
60'
120'
ETO
pBRCA1
268 kDa
238 kDa
163 kDa
p42/44 MAPK
42 kDa
Actin

E

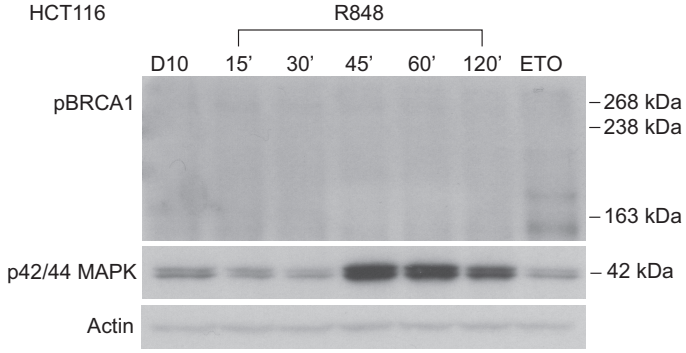
HCT116
R848
D10
15'
30'
45'
60'
120'
ETO
pBRCA1
268 kDa
238 kDa
163 kDa
p42/44 MAPK
42 kDa
Actin

F

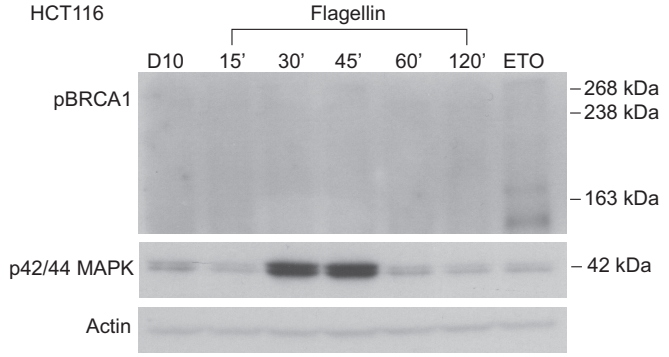
HCT116
Flagellin
D10
15'
30'
45'
60'
120'
ETO
pBRCA1
268 kDa
238 kDa
163 kDa
p42/44 MAPK
42 kDa
Actin

G

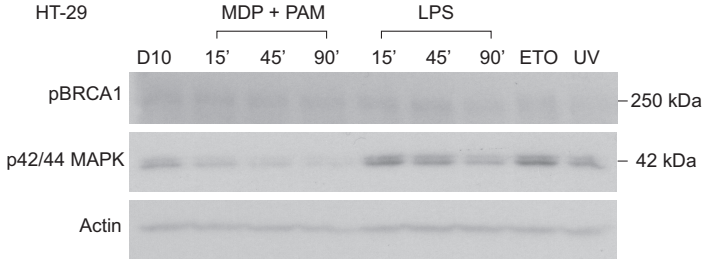
HT-29
MDP + PAM
LPS
D10
15'
45'
90'
15'
45'
90'
ETO
UV
pBRCA1
250 kDa
p42/44 MAPK
42 kDa
Actin

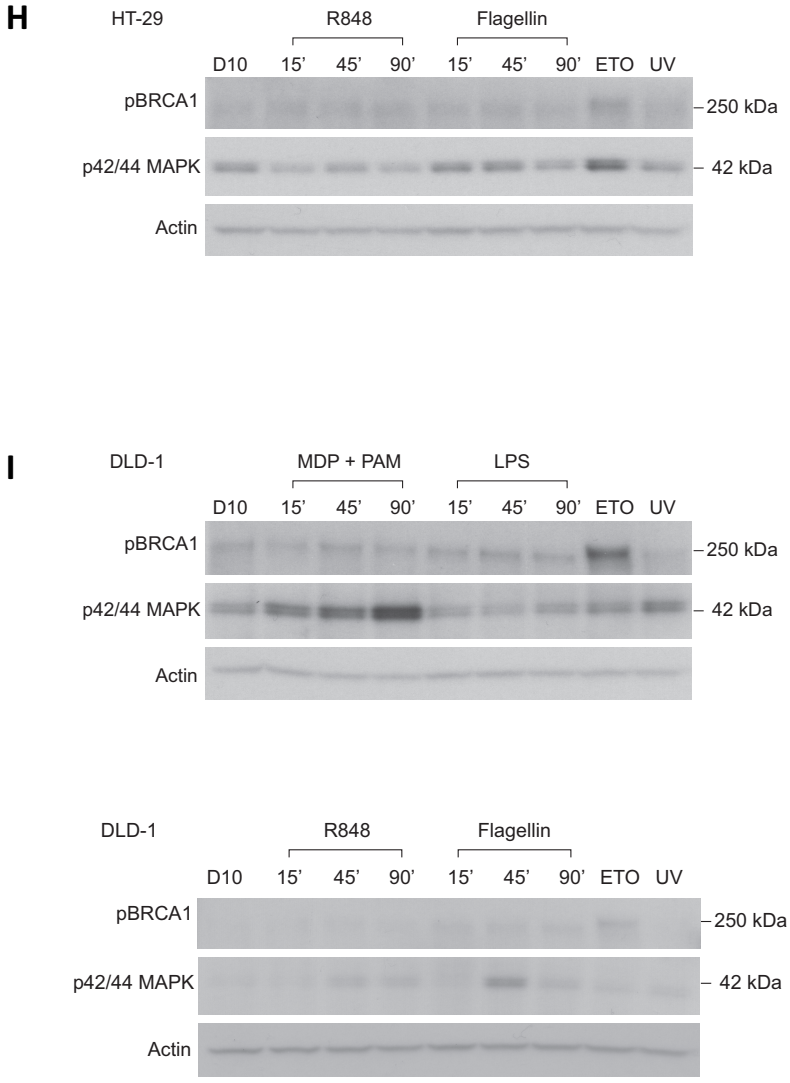

Figure S1. Assessment of pBRCA1 levels upon PRR stimulation in multiple cell lines. 1 µg/mL Pam3CSK4, 1µg/mL MDP, 100ng/mL LPS, 1 µg/mL R848, 1 µg/mL Flagellin, 100 µM etoposide, or 50J/m_2 UV radiation was used to stimulate **A.** Primary human CD14+ monocytes **B.** Caco-2 cells, **C-F.** HCT-116 colonic epithelial cells **G-H** HT29 cells **I-J** DLD1 cells, for indicated times before WB analysis using antibodies against pBRCA1, p-p44/42 MAPK and β-actin. B-J samples and western blot performed by James Kinchen under my supervision and instruction.

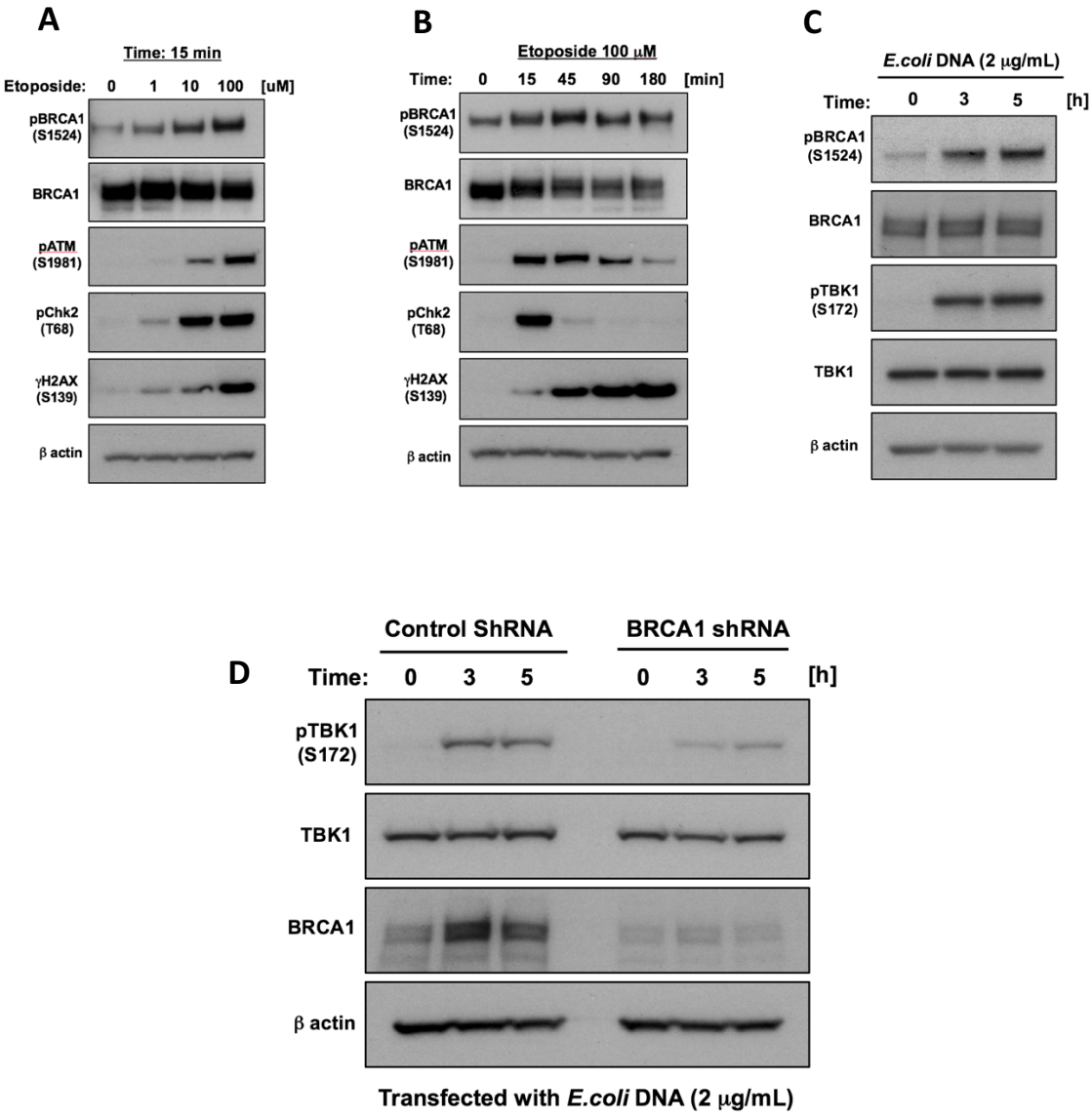

Figure S2. Optimisation of HeLa cells for BRCA1 study. WB analysis of HeLa cells **A.** stimulated with different concentrations of etoposide for 15 minutes **B.** Stimulated with 100 μM etoposide for various times **C.** Stimulated with 2 μg/mL *E. Coli* dsDNA for various times or **D.** Transduced with LVPs encoding control or BRCA-targeting shRNAs, and stimulate with 2 μg/mL E. Coli dsDNA for various times. Antibodies against pTBK1, total TBK1, total BRCA1 and β-actin were used. A-C peformed by Seiji Shiraishi under my instruction. LVP production and transduction of cells for D was performed by myself, western blot and transfection was performed by Seiji Shiraishi under my instruction.

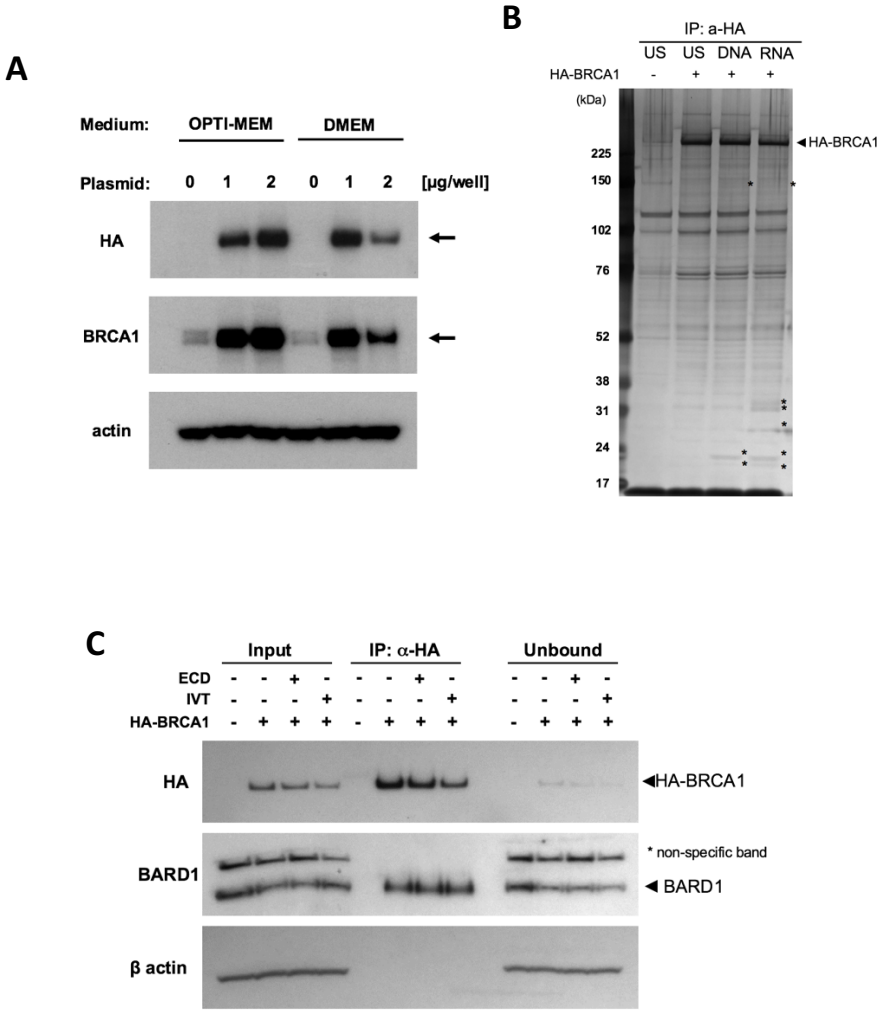

Figure S3. Optimisation of HA-BRCA1 expression. HeLa cells were transfected with HA-BRCA1 encoding plasmids and subjected to **A.** WB using anti HA and BRCA1 antibodies 72 hours later to determine expression level **B.** Immunoprecipitation using anti-HA antibody, and subsequent Silver staining after 2h stimulation with 2 µg/mL of *E. Coli* dsDNA or IVT dsRNA, or **C.** Immunoprecipitation using anti-HA antibody and WB, using BARD1 as a control.

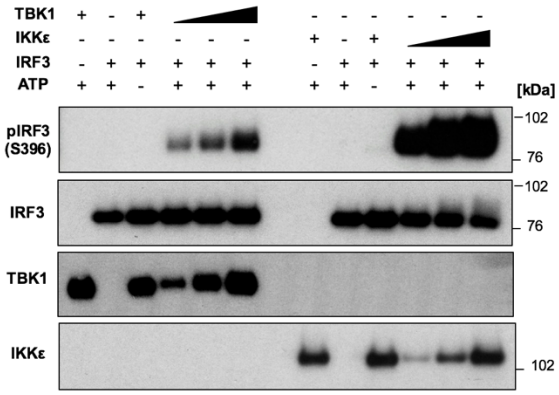

Figure S4. Optimisation of *In Vitro* kinase Assay. Different amounts of recombinant TBK1 (50ng, 100ng, 200ng) or IKKε (5ng, 10ng, 20ng) kinases were mixed with 100ng of recombinant IRF3 substrate and incubated at 30°C for 1h before WB analysis for pIRF3, total IRF3, TBK1 and IKKε.

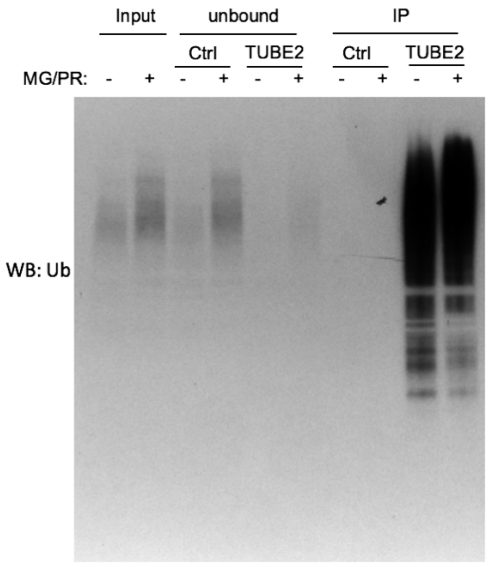

Figure S5. Optimisation of Ubiquitin precipitation. Hela Cells were untreated or incubated with 20 µM MG132 and 50 µM PR614 for 30 min before ubiquitinated proteins were precipitated with TUBE 2 ubiquitin-binding or control agarose beads. Input, unbound and precipitated samples were then subjected to WB using anti-ubiquitin antibody. Performed by Seiji Shiraishi under my instruction.

8 Bibliography

1. Janeway, C. A. & Medzhitov, R. Innate immune recognition. *Annu. Rev. Immunol.* **20,** 197–216 (2002).
2. Courtois, G. *et al.* A hypermorphic IkappaBalpha mutation is associated with autosomal dominant anhidrotic ectodermal dysplasia and T cell immunodeficiency. *J. Clin. Invest.* **112,** 1108–1115 (2003).
3. Casrouge, A. *et al.* Herpes Simplex Virus Encephalitis in Human UNC-93B Deficiency. *Science* **314,** 308–312 (2006).
4. Bernuth, von, H. *et al.* Pyogenic bacterial infections in humans with MyD88 deficiency. *Science* **321,** 691–696 (2008).
5. Picard, C. *et al.* Pyogenic Bacterial Infections in Humans with IRAK-4 Deficiency. *Science* **299,** 2076–2079 (2003).
6. Picard, C., Casanova, J.-L. & Puel, A. Infectious diseases in patients with IRAK-4, MyD88, NEMO, or IκBα deficiency. *Clin. Microbiol. Rev.* **24,** 490–497 (2011).
7. Courtois, G. & Gilmore, T. D. Mutations in the NF-kappaB signaling pathway: implications for human disease. *Oncogene* **25,** 6831–6843 (2006).
8. Medzhitov, R. & Horng, T. Transcriptional control of the inflammatory response. *Nature Reviews Immunology* **9,** 692–703 (2009).
9. Medzhitov, R. Origin and physiological roles of inflammation. *Nature* **454,** 428–435 (2008).
10. Lemaitre, B., Nicolas, E., Michaut, L., Reichhart, J. M. & Hoffmann, J. A. The dorsoventral regulatory gene cassette spätzle/Toll/cactus controls the potent antifungal response in Drosophila adults. *Cell* **86,** 973–983 (1996).
11. Akira, S., Uematsu, S. & Takeuchi, O. Pathogen Recognition and Innate Immunity. *Cell* **124,** 783–801 (2006).
12. Kerur, N. *et al.* IFI16 acts as a nuclear pathogen sensor to induce the inflammasome in response to Kaposi Sarcoma-associated herpesvirus infection. *Cell Host & Microbe* **9,** 363–375 (2011).
13. Mu, C., Yang, Y. & Zhu, W. Crosstalk Between The Immune Receptors and Gut Microbiota. *Curr. Protein Pept. Sci.* **16,** 622–631 (2015).
14. Abreu, M. T. Toll-like receptor signalling in the intestinal epithelium: how bacterial recognition shapes intestinal function. *Nature Reviews Immunology* **10,** 131–144 (2010).
15. Yu, L., Wang, L. & Chen, S. Endogenous toll-like receptor ligands and their biological significance. *Journal of Cellular and Molecular Medicine* **14,** 2592–2603 (2010).
16. Klune, J. R., Dhupar, R., Cardinal, J., Billiar, T. R. & Tsung, A. HMGB1: endogenous danger signaling. *Mol. Med.* **14,** 476–484 (2008).
17. Tsan, M.-F. & Gao, B. Heat shock proteins and immune system. *J. Leukoc. Biol.* **85,** 905–910 (2009).
18. Ishii, K. J. *et al.* Genomic DNA released by dying cells induces the maturation of APCs. *The Journal of Immunology* **167,** 2602–2607 (2001).
19. Chevrier, N. *et al.* Systematic discovery of TLR signaling components delineates viral-sensing circuits. *Cell* **147,** 853–867 (2011).
20. Botos, I., Segal, D. M. & Davies, D. R. The structural biology of Toll-like

receptors. *Structure* **19,** 447–459 (2011).
21. Bowie, A. & O'Neill, L. A. The interleukin-1 receptor/Toll-like receptor superfamily: signal generators for pro-inflammatory interleukins and microbial products. *J. Leukoc. Biol.* **67,** 508–514 (2000).
22. Barton, G. M. & Kagan, J. C. A cell biological view of Toll-like receptor function: regulation through compartmentalization. *Nature Publishing Group* **9,** 535–542 (2009).
23. Yamamoto, M. *et al.* Essential role for TIRAP in activation of the signalling cascade shared by TLR2 and TLR4. *Nature* **420,** 324–329 (2002).
24. Oshiumi, H., Matsumoto, M., Funami, K., Akazawa, T. & Seya, T. TICAM-1, an adaptor molecule that participates in Toll-like receptor 3-mediated interferon-beta induction. *Nat Immunol* **4,** 161–167 (2003).
25. Fitzgerald, K. A. *et al.* Mal (MyD88-adapter-like) is required for Toll-like receptor-4 signal transduction. *Nature* **413,** 78–83 (2001).
26. Horng, T., Barton, G. M., Flavell, R. A. & Medzhitov, R. The adaptor molecule TIRAP provides signalling specificity for Toll-like receptors. *Nature* **420,** 329–333 (2002).
27. Deng, L. *et al.* Activation of the IkappaB kinase complex by TRAF6 requires a dimeric ubiquitin-conjugating enzyme complex and a unique polyubiquitin chain. *Cell* **103,** 351–361 (2000).
28. Sun, L., Deng, L., Ea, C.-K., Xia, Z.-P. & Chen, Z. J. The TRAF6 ubiquitin ligase and TAK1 kinase mediate IKK activation by BCL10 and MALT1 in T lymphocytes. *Molecular Cell* **14,** 289–301 (2004).
29. Zhou, H. *et al.* Bcl10 activates the NF-kappaB pathway through ubiquitination of NEMO. *Nature* **427,** 167–171 (2004).
30. Wang, C. *et al.* TAK1 is a ubiquitin-dependent kinase of MKK and IKK. *Nature* **412,** 346–351 (2001).
31. Kawai, T. & Akira, S. The role of pattern-recognition receptors in innate immunity: update on Toll-like receptors. *Nat Immunol* **11,** 373–384 (2010).
32. Schmitz, F. *et al.* Interferon-regulatory-factor 1 controls Toll-like receptor 9-mediated IFN-beta production in myeloid dendritic cells. *Eur. J. Immunol.* **37,** 315–327 (2007).
33. Ermolaeva, M. A. *et al.* Function of TRADD in tumor necrosis factor receptor 1 signaling and in TRIF-dependent inflammatory responses. *Nat Immunol* **9,** 1037–1046 (2008).
34. Chang, M., Jin, W. & Sun, S.-C. Peli1 facilitates TRIF-dependent Toll-like receptor signaling and proinflammatory cytokine production. *Nat Immunol* **10,** 1089–1095 (2009).
35. Oganesyan, G. *et al.* Critical role of TRAF3 in the Toll-like receptor-dependent and -independent antiviral response. *Nature* **439,** 208–211 (2006).
36. Yoneyama, M. *et al.* Shared and unique functions of the DExD/H-box helicases RIG-I, MDA5, and LGP2 in antiviral innate immunity. *The Journal of Immunology* **175,** 2851–2858 (2005).
37. Kato, H. *et al.* Length-dependent recognition of double-stranded ribonucleic acids by retinoic acid-inducible gene-I and melanoma differentiation-associated gene 5. *J. Exp. Med.* **205,** 1601–1610 (2008).
38. Hornung, V. *et al.* 5'-Triphosphate RNA is the ligand for RIG-I. *Science* **314,** 994–

997 (2006).
39. Pichlmair, A. *et al.* Activation of MDA5 requires higher-order RNA structures generated during virus infection. *J. Virol.* **83,** 10761–10769 (2009).
40. Loo, Y.-M. *et al.* Distinct RIG-I and MDA5 signaling by RNA viruses in innate immunity. *J. Virol.* **82,** 335–345 (2008).
41. Hou, F. *et al.* MAVS Forms Functional Prion-like Aggregates to Activate and Propagate Antiviral Innate Immune Response. *Cell* **146,** 448–461 (2011).
42. Ishikawa, H. & Barber, G. N. STING is an endoplasmic reticulum adaptor that facilitates innate immune signalling. *Nature* **456,** 274–274 (2008).
43. Ishikawa, H., Ma, Z. & Barber, G. N. STING regulates intracellular DNA-mediated, type I interferon-dependent innate immunity. *Nature* **461,** 788–792 (2009).
44. Lam, E., Stein, S. & Falck-Pedersen, E. Adenovirus Detection by the cGAS/STING/TBK1 DNA Sensing Cascade. *J. Virol.* **88,** 974–981 (2014).
45. Tamayo, R., Pratt, J. T. & Camilli, A. Roles of Cyclic Diguanylate in the Regulation of Bacterial Pathogenesis. *Annual review of microbiology* **61,** 131–148 (2007).
46. Sun, L., Wu, J., Du, F., Chen, X. & Chen, Z. J. Cyclic GMP-AMP synthase is a cytosolic DNA sensor that activates the type I interferon pathway. *Science* **339,** 786–791 (2013).
47. Wu, J. *et al.* Cyclic GMP-AMP is an endogenous second messenger in innate immune signaling by cytosolic DNA. *Science* **339,** 826–830 (2013).
48. Zhang, X. *et al.* Cyclic GMP-AMP Containing Mixed Phosphodiester Linkages Is An Endogenous High-Affinity Ligand for STING. *Molecular Cell* **51,** 226–235 (2013).
49. Li, X.-D. *et al.* Pivotal Roles of cGAS-cGAMP Signaling in Antiviral Defense and Immune Adjuvant Effects. *Science* **341,** 1390–1394 (2013).
50. Bridgeman, A. *et al.* Viruses transfer the antiviral second messenger cGAMP between cells. *Science* **349,** 1228–1232 (2015).
51. Gentili, M. *et al.* Transmission of innate immune signaling by packaging of cGAMP in viral particles. *Science* **349,** 1232–1236 (2015).
52. Ablasser, A. *et al.* Cell intrinsic immunity spreads to bystander cells via the intercellular transfer of cGAMP. *Nature* **503,** 530–534 (2013).
53. Ablasser, A. *et al.* RIG-I-dependent sensing of poly(dA:dT) through the induction of an RNA polymerase III-transcribed RNA intermediate. *Nat Immunol* **10,** 1065–1072 (2009).
54. Unterholzner, L. *et al.* IFI16 is an innate immune sensor for intracellular DNA. *Nat Immunol* **11,** 997–1004 (2010).
55. Fernandes-Alnemri, T., Yu, J.-W., Datta, P., Wu, J. & Alnemri, E. S. AIM2 activates the inflammasome and cell death in response to cytoplasmic DNA. *Nature* **458,** 509–513 (2009).
56. Inohara, Chamaillard, McDonald, C. & Núñez, G. NOD-LRR proteins: role in host-microbial interactions and inflammatory disease. *Annu. Rev. Biochem.* **74,** 355–383 (2005).
57. Zhong, Y., Kinio, A. & Saleh, M. Functions of NOD-Like Receptors in Human Diseases. *Front Immunol* **4,** 333 (2013).
58. Latz, E., Xiao, T. S. & Stutz, A. Activation and regulation of the inflammasomes.

Nature Publishing Group **13,** 397–411 (2013).
59. Fernandes-Alnemri, T. *et al.* The pyroptosome: a supramolecular assembly of ASC dimers mediating inflammatory cell death via caspase-1 activation. *Cell Death Differ.* **14,** 1590–1604 (2007).
60. Thornberry, N. A. *et al.* A novel heterodimeric cysteine protease is required for interleukin-1|[beta]|processing in monocytes. *, Published online: 30 April 1992; | doi:10.1038/356768a0* **356,** 768–774 (1992).
61. Martinon, F., Burns, K. & Tschopp, J. The inflammasome: a molecular platform triggering activation of inflammatory caspases and processing of proIL-beta. *Molecular Cell* **10,** 417–426 (2002).
62. Khare, S. *et al.* An NLRP7-Containing Inflammasome Mediates Recognition of Microbial Lipopeptides in Human Macrophages. *Immunity* **36,** 464–476 (2012).
63. Abdelaziz, D. H., Amr, K. & Amer, A. O. Nlrc4/Ipaf/CLAN/CARD12: more than a flagellin sensor. *The International Journal of Biochemistry & Cell Biology* **42,** 789–791 (2010).
64. Boyden, E. D. & Dietrich, W. F. Nalp1b controls mouse macrophage susceptibility to anthrax lethal toxin. *Nature Genetics* **38,** 240–244 (2006).
65. Hornung, V. *et al.* Silica crystals and aluminum salts activate the NALP3 inflammasome through phagosomal destabilization. *Nat Immunol* **9,** 847–856 (2008).
66. Martinon, F. Dangerous liaisons: mitochondrial DNA meets the NLRP3 inflammasome. *Immunity* **36,** 313–315 (2012).
67. Shimada, K. *et al.* Oxidized Mitochondrial DNA Activates the NLRP3 Inflammasome during Apoptosis. *Immunity* **36,** 401–414 (2012).
68. Misawa, T. *et al.* Microtubule-driven spatial arrangement of mitochondria promotes activation of the NLRP3 inflammasome. *Nat Immunol* **14,** 454–460 (2013).
69. Petrilli, V. *et al.* Activation of the NALP3 inflammasome is triggered by low intracellular potassium concentration. *Cell Death Differ.* **14,** 1583–1589 (2007).
70. Orzalli, M. H., DeLuca, N. A. & Knipe, D. M. Nuclear IFI16 induction of IRF-3 signaling during herpesviral infection and degradation of IFI16 by the viral ICP0 protein. *Proc. Natl. Acad. Sci. U.S.A.* **109,** E3008–17 (2012).
71. Abe, T. *et al.* STING Recognition of Cytoplasmic DNA Instigates Cellular Defense. *Molecular Cell* **50,** 5–15 (2013).
72. Horan, K. A. *et al.* Proteasomal degradation of herpes simplex virus capsids in macrophages releases DNA to the cytosol for recognition by DNA sensors. *J. Immunol.* **190,** 2311–2319 (2013).
73. Jin, T. *et al.* Structures of the HIN domain:DNA complexes reveal ligand binding and activation mechanisms of the AIM2 inflammasome and IFI16 receptor. *Immunity* **36,** 561–571 (2012).
74. Diner, B. A. *et al.* The functional interactome of PYHIN immune regulators reveals IFIX is a sensor of viral DNA. *Mol. Syst. Biol.* **11,** 787–787 (2015).
75. Pestka, S., Krause, C. D. & Walter, M. R. Interferons, interferon-like cytokines, and their receptors. *Immunol. Rev.* **202,** 8–32 (2004).
76. Müller, U. *et al.* Functional role of type I and type II interferons in antiviral defense. *Science* **264,** 1918–1921 (1994).
77. McNab, F., Mayer-Barber, K., Sher, A., Wack, A. & O'Garra, A. Type I interferons

in infectious disease. *Nature Reviews Immunology* **15,** 87–103 (2015).
78. Martinez, J., Huang, X. & Yang, Y. Direct action of type I IFN on NK cells is required for their activation in response to vaccinia viral infection in vivo. *The Journal of Immunology* **180,** 1592–1597 (2008).
79. Coro, E. S., Chang, W. L. W. & Baumgarth, N. Type I IFN receptor signals directly stimulate local B cells early following influenza virus infection. *The Journal of Immunology* **176,** 4343–4351 (2006).
80. Chang, W. L. W. *et al.* Influenza virus infection causes global respiratory tract B cell response modulation via innate immune signals. *The Journal of Immunology* **178,** 1457–1467 (2007).
81. Marrack, P., Kappler, J. & Mitchell, T. Type I interferons keep activated T cells alive. *Journal of Experimental Medicine* **189,** 521–530 (1999).
82. Kolumam, G. A., Thomas, S., Thompson, L. J., Sprent, J. & Murali-Krishna, K. Type I interferons act directly on CD8 T cells to allow clonal expansion and memory formation in response to viral infection. *Journal of Experimental Medicine* **202,** 637–650 (2005).
83. Dauer, M. *et al.* Interferon-alpha disables dendritic cell precursors: dendritic cells derived from interferon-alpha-treated monocytes are defective in maturation and T-cell stimulation. *Immunology* **110,** 38–47 (2003).
84. Santini, S. M. *et al.* Type I interferon as a powerful adjuvant for monocyte-derived dendritic cell development and activity in vitro and in Hu-PBL-SCID mice. *Journal of Experimental Medicine* **191,** 1777–1788 (2000).
85. Montoya, M. *et al.* Type I interferons produced by dendritic cells promote their phenotypic and functional activation. *Blood* **99,** 3263–3271 (2002).
86. Diamond, M. S. & Schoggins, J. W. Host restriction factor screening: let the virus do the work. *Cell Host & Microbe* **14,** 229–231 (2013).
87. Schneider, W. M., Chevillotte, M. D. & Rice, C. M. Interferon-stimulated genes: a complex web of host defenses. *Annu. Rev. Immunol.* **32,** 513–545 (2014).
88. Narasimhan, J., Potter, J. L. & Haas, A. L. Conjugation of the 15-kDa interferon-induced ubiquitin homolog is distinct from that of ubiquitin. *Journal of Biological Chemistry* **271,** 324–330 (1996).
89. Takeuchi, T., Iwahara, S., Saeki, Y., Sasajima, H. & Yokosawa, H. Link between the ubiquitin conjugation system and the ISG15 conjugation system: ISG15 conjugation to the UbcH6 ubiquitin E2 enzyme. *J. Biochem.* **138,** 711–719 (2005).
90. Lu, G. *et al.* ISG15 enhances the innate antiviral response by inhibition of IRF-3 degradation. *Cell. Mol. Biol. (Noisy-le-grand)* **52,** 29–41 (2006).
91. Okumura, F., Zou, W. & Zhang, D.-E. ISG15 modification of the eIF4E cognate 4EHP enhances cap structure-binding activity of 4EHP. *Genes Dev.* **21,** 255–260 (2007).
92. Accola, M. A., Huang, B. & Masri, Al, A. The antiviral dynamin family member, MxA, tubulates lipids and localizes to the smooth endoplasmic reticulum. *Journal of Biological …* (2002).
93. Hoenen, A., Liu, W., Kochs, G., Khromykh, A. A. & Mackenzie, J. M. West Nile virus-induced cytoplasmic membrane structures provide partial protection against the interferon-induced antiviral MxA protein. *Journal of General Virology* **88,** 3013–3017 (2007).

94. Anthony J Sadler, B. R. G. W. Interferon-inducible antiviral effectors. *Nature Reviews Immunology* **8,** 559–568 (2008).
95. Clemens, M. J. & Williams, B. R. G. Inhibition of cell-free protein synthesis by pppA2′ p5′ A2′ p5′ A: a novel oligonucleotide synthesized by interferon-treated L cell extracts. *Cell* **13,** 565–572 (1978).
96. Malathi, K., Dong, B., Gale, M. & Silverman, R. H. Small self-RNA generated by RNase L amplifies antiviral innate immunity. *Nature* **448,** 816–819 (2007).
97. Zhou, A. *et al.* Interferon action and apoptosis are defective in mice devoid of 2′,5′-oligoadenylate-dependent RNase L. *The EMBO Journal* **16,** 6355–6363 (1997).
98. Silverman, R. H. Viral encounters with 2‘,5’-oligoadenylate synthetase and RNase L during the interferon antiviral response. *J. Virol.* **81,** 12720–12729 (2007).
99. Garcia, M. A., Meurs, E. F. & Esteban, M. The dsRNA protein kinase PKR: Virus and cell control. *Biochimie* **89,** 799–811 (2007).
100. Versteeg, G. A. & García-Sastre, A. Viral tricks to grid-lock the type I interferon system. *Curr. Opin. Microbiol.* **13,** 508–516 (2010).
101. Elde, N. C., Child, S. J., Geballe, A. P. & Malik, H. S. Protein kinase R reveals an evolutionary model for defeating viral mimicry. *Nature* **457,** 485–489 (2009).
102. Schoggins, J. W. & Rice, C. M. Interferon-stimulated genes and their antiviral effector functions. *Current Opinion in Virology* **1,** 519–525 (2011).
103. Barbalat, R., Lau, L., Locksley, R. M. & Barton, G. M. Toll-like receptor 2 on inflammatory monocytes induces type I interferon in response to viral but not bacterial ligands. *Nat Immunol* **10,** 1200–1207 (2009).
104. Álvarez-Errico, D., Vento-Tormo, R., Sieweke, M. & Ballestar, E. Epigenetic control of myeloid cell differentiation, identity and function. *Nature Publishing Group* **15,** 7–17 (2015).
105. Fang, T. C. *et al.* Histone H3 lysine 9 di-methylation as an epigenetic signature of the interferon response. *J. Exp. Med.* **209,** 661–669 (2012).
106. Kawai, T., Adachi, O., Ogawa, T., Takeda, K. & Akira, S. Unresponsiveness of MyD88-Deficient Mice to Endotoxin. *Immunity* **11,** 115–122 (1999).
107. Kawai, T. *et al.* Lipopolysaccharide stimulates the MyD88-independent pathway and results in activation of IFN-regulatory factor 3 and the expression of a subset of lipopolysaccharide-inducible genes. *The Journal of Immunology* **167,** 5887–5894 (2001).
108. Kagan, J. C. & Medzhitov, R. Phosphoinositide-mediated adaptor recruitment controls Toll-like receptor signaling. *Cell* **125,** 943–955 (2006).
109. Rowe, D. C. *et al.* The myristoylation of TRIF-related adaptor molecule is essential for Toll-like receptor 4 signal transduction. *Proceedings of the National Academy of Sciences* **103,** 6299–6304 (2006).
110. Kagan, J. C. *et al.* TRAM couples endocytosis of Toll-like receptor 4 to the induction of interferon-|[beta]|. *Nat Immunol* **9,** 361–368 (2008).
111. Cao, X. Self-regulation and cross-regulation of pattern-recognition receptor signalling in health and disease. *Nature Reviews Immunology* **16,** 35–50 (2015).
112. Hardin, A. O., Meals, E. A., Yi, T., Knapp, K. M. & English, B. K. SHP-1 inhibits LPS-mediated TNF and iNOS production in murine macrophages. *Biochem. Biophys. Res. Commun.* **342,** 547–555 (2006).

113. An, H. *et al.* SHP-2 phosphatase negatively regulates the TRIF adaptor protein-dependent type I interferon and proinflammatory cytokine production. *Immunity* **25,** 919–928 (2006).
114. Liu, X., Wang, Q., Chen, W. & Wang, C. Dynamic regulation of innate immunity by ubiquitin and ubiquitin-like proteins. *Cytokine & Growth Factor Reviews* **24,** 559–570 (2013).
115. Gack, M. U. *et al.* TRIM25 RING-finger E3 ubiquitin ligase is essential for RIG-I-mediated antiviral activity. *Nature* **446,** 916–920 (2007).
116. Oshiumi, H., Matsumoto, M., Hatakeyama, S. & Seya, T. Riplet/RNF135, a RING finger protein, ubiquitinates RIG-I to promote interferon-beta induction during the early phase of viral infection. *Journal of Biological Chemistry* **284,** 807–817 (2009).
117. Friedman, C. S. *et al.* The tumour suppressor CYLD is a negative regulator of RIG-I-mediated antiviral response. *EMBO reports* **9,** 930–936 (2008).
118. Wang, Q. *et al.* The E3 Ubiquitin Ligase AMFR and INSIG1 Bridge the Activation of TBK1 Kinase by Modifying the Adaptor STING. *Immunity* **41,** 919–933 (2014).
119. Shu, H.-B. & Wang, Y.-Y. Adding to the STING. *Immunity* **41,** 871–873 (2014).
120. Kayagaki, N. *et al.* A Deubiquitinase That Regulates Type I Interferon Production. *Science* **318,** 1628–1632 (2007).
121. Wang, Y. *et al.* Lysosome-associated small Rab GTPase Rab7b negatively regulates TLR4 signaling in macrophages by promoting lysosomal degradation of TLR4. *Blood* **110,** 962–971 (2007).
122. Chuang, T.-H. & Ulevitch, R. J. Triad3A, an E3 ubiquitin-protein ligase regulating Toll-like receptors. *Nat Immunol* **5,** 495–502 (2004).
123. Desterro, J. M., Rodriguez, M. S. & Hay, R. T. *SUMO-1 modification of IkappaBalpha inhibits NF-kappaB activation (1998) Mol. Cell*
124. Chi, H. & Flavell, R. A. Acetylation of MKP-1 and the control of inflammation. *Science signaling* **1,** pe44–pe44 (2008).
125. Xia, P. *et al.* Glutamylation of the DNA sensor cGAS regulates its binding and synthase activity in antiviral immunity. *Nat Immunol* **17,** 369–378 (2016).
126. Ozinsky, A. *et al.* The repertoire for pattern recognition of pathogens by the innate immune system is defined by cooperation between toll-like receptors. *Proceedings of the National Academy of Sciences* **97,** 13766–13771 (2000).
127. Sato, S. *et al.* Synergy and cross-tolerance between toll-like receptor (TLR) 2-and TLR4-mediated signaling pathways. *The Journal of Immunology* **165,** 7096–7101 (2000).
128. Pavot, V. *et al.* Cutting edge: New chimeric NOD2/TLR2 adjuvant drastically increases vaccine immunogenicity. *J. Immunol.* **193,** 5781–5785 (2014).
129. Bauernfeind, F. G. *et al.* Cutting edge: NF-kappaB activating pattern recognition and cytokine receptors license NLRP3 inflammasome activation by regulating NLRP3 expression. *J. Immunol.* **183,** 787–791 (2009).
130. Wang, C. *et al.* The E3 ubiquitin ligase Nrdp1 'preferentially' promotes TLR-mediated production of type I interferon. *Nat Immunol* **10,** 744–752 (2009).
131. Tseng, P.-H. *et al.* Different modes of ubiquitination of the adaptor TRAF3 selectively activate the expression of type I interferons and proinflammatory cytokines. *Nat Immunol* **11,** 70–75 (2010).

132. O'Neill, L., Bryant, C. E. & Doyle, S. L. Therapeutic targeting of Toll-like receptors for infectious and inflammatory diseases and cancer. *Pharmacological reviews* (2009).
133. Tian, J. *et al.* Toll-like receptor 9|[ndash]|dependent activation by DNA-containing immune complexes is mediated by HMGB1 and RAGE. *Nat Immunol* **8,** 487–496 (2007).
134. Takeuchi, O. & Akira, S. Pattern Recognition Receptors and Inflammation. *Cell* **140,** 805–820 (2010).
135. Means, T. K. *et al.* Human lupus autoantibody–DNA complexes activate DCs through cooperation of CD32 and TLR9. *Journal of Clinical Investigation* **115,** 407–417 (2005).
136. Crow, Y. J. & Manel, N. Aicardi–Goutières syndrome and the type I interferonopathies. *Nature Reviews Immunology* **15,** 429–440 (2015).
137. Rice, G. I. *et al.* Assessment of interferon-related biomarkers in Aicardi-Goutières syndrome associated with mutations in TREX1, RNASEH2A, RNASEH2B, RNASEH2C, SAMHD1, and ADAR: a case-control study. *The Lancet Neurology* **12,** 1159–1169 (2013).
138. Crow, Y. J. *et al.* Mutations in genes encoding ribonuclease H2 subunits cause Aicardi-Goutières syndrome and mimic congenital viral brain infection. *Nature Genetics* **38,** 910–916 (2006).
139. Rice, G. I. *et al.* Mutations involved in Aicardi-Goutières syndrome implicate SAMHD1 as regulator of the innate immune response. *Nature Genetics* **41,** 829–832 (2009).
140. Crow, Y. J. *et al.* Mutations in the gene encoding the 3|[prime]|-5|[prime]| DNA exonuclease TREX1 cause Aicardi-Gouti|[egrave]|res syndrome at the AGS1 locus. *Nature Genetics* **38,** 917–920 (2006).
141. Stetson, D. B. *et al.* Trex1 prevents cell-intrinsic initiation of autoimmunity. *Cell* **134,** 587–598 (2008).
142. Ravenscroft, J. C., Suri, M., Rice, G. I., Szynkiewicz, M. & Crow, Y. J. Autosomal dominant inheritance of a heterozygous mutation in SAMHD1 causing familial chilblain lupus. *American Journal of Medical Genetics Part A* **155,** 235–237 (2011).
143. Lee-Kirsch, M. A. *et al.* Mutations in the gene encoding the 3'-5' DNA exonuclease TREX1 are associated with systemic lupus erythematosus. *Nature Genetics* **39,** 1065–1067 (2007).
144. Davidson, S., Crotta, S., McCabe, T. M. & Wack, A. Pathogenic potential of interferon αβ in acute influenza infection. *Nature Communications* **5,** (2014).
145. Rotger, M. *et al.* Comparative transcriptomics of extreme phenotypes of human HIV-1 infection and SIV infection in sooty mangabey and rhesus macaque. *J. Clin. Invest.* **121,** 2391–2400 (2011).
146. Marshall, H. D., Urban, S. L. & Welsh, R. M. Virus-induced transient immune suppression and the inhibition of T cell proliferation by type I interferon. *J. Virol.* **85,** 5929–5939 (2011).
147. McNally, J. M. *et al.* Attrition of bystander CD8 T cells during virus-induced T-cell and interferon responses. *J. Virol.* **75,** 5965–5976 (2001).
148. O'Connell, R. M. *et al.* Type I interferon production enhances susceptibility to Listeria monocytogenes infection. *Journal of Experimental Medicine* **200,** 437–

445 (2004).
149. Cho, J. H. The genetics and immunopathogenesis of inflammatory bowel disease. *Nature Publishing Group* **8,** 458–466 (2008).
150. Philpott, D. J., Sorbara, M. T., Robertson, S. J., Croitoru, K. & Girardin, S. E. NOD proteins: regulators of inflammation in health and disease. *Nature Reviews Immunology* **14,** 9–23 (2013).
151. Helgason, E., Phung, Q. T. & Dueber, E. C. Recent insights into the complexity of Tank-binding kinase 1 signaling networks: The emerging role of cellular localization in the activation and substrate specificity of TBK1. *FEBS Letters* **587,** 1230–1237 (2013).
152. Yu, T., Yi, Y. S., Yang, Y., Oh, J. & Jeong, D. The pivotal role of TBK1 in inflammatory responses mediated by macrophages. *Mediators of inflammation* (2012).
153. Zhao, W. Negative regulation of TBK1-mediated antiviral immunity. *FEBS Letters* **587,** 542–548 (2013).
154. Liu, S. *et al.* Phosphorylation of innate immune adaptor proteins MAVS, STING, and TRIF induces IRF3 activation. *Science* **347,** aaa2630–aaa2630 (2015).
155. McWhirter, S. M. *et al.* IFN-regulatory factor 3-dependent gene expression is defective in Tbk1-deficient mouse embryonic fibroblasts. *Proceedings of the National Academy of Sciences* **101,** 233–238 (2004).
156. Perry, A. K., Chow, E. K., Goodnough, J. B., Yeh, W.-C. & Cheng, G. Differential requirement for TANK-binding kinase-1 in type I interferon responses to toll-like receptor activation and viral infection. *Journal of Experimental Medicine* **199,** 1651–1658 (2004).
157. Herman, M. *et al.* Heterozygous TBK1 mutations impair TLR3 immunity and underlie herpes simplex encephalitis of childhood. *Journal of Experimental Medicine* **209,** 1567–1582 (2012).
158. Mork, N. *et al.* Mutations in the TLR3 signaling pathway and beyond in adult patients with herpes simplex encephalitis. *Genes and Immunity* **16,** 552–566 (2015).
159. Thurston, T. L. M., Ryzhakov, G., Bloor, S., Muhlinen, von, N. & Randow, F. The TBK1 adaptor and autophagy receptor NDP52 restricts the proliferation of ubiquitin-coated bacteria. *Nat Immunol* **10,** 1215–1221 (2009).
160. Wild, P. *et al.* Phosphorylation of the autophagy receptor optineurin restricts Salmonella growth. *Science* **333,** 228–233 (2011).
161. Korac, J. *et al.* Ubiquitin-independent function of optineurin in autophagic clearance of protein aggregates. *J. Cell. Sci.* **126,** 580–592 (2013).
162. Newman, A. C. *et al.* TBK1 kinase addiction in lung cancer cells is mediated via autophagy of Tax1bp1/Ndp52 and non-canonical NF-κB signalling. *PLoS ONE* **7,** e50672 (2012).
163. Liu, X.-Y., Chen, W., Wei, B., Shan, Y.-F. & Wang, C. IFN-induced TPR protein IFIT3 potentiates antiviral signaling by bridging MAVS and TBK1. *J. Immunol.* **187,** 2559–2568 (2011).
164. Goncalves, A. *et al.* Functional dissection of the TBK1 molecular network. *PLoS ONE* **6,** e23971 (2011).
165. Ma, X. *et al.* Molecular basis of Tank-binding kinase 1 activation by transautophosphorylation. *Proc. Natl. Acad. Sci. U.S.A.* **109,** 9378–9383 (2012).

166. Lei, C.-Q. *et al.* Glycogen synthase kinase 3β regulates IRF3 transcription factor-mediated antiviral response via activation of the kinase TBK1. *Immunity* **33,** 878–889 (2010).
167. Huang, J. *et al.* SIKE is an IKK epsilon/TBK1-associated suppressor of TLR3-and virus-triggered IRF-3 activation pathways. *The EMBO Journal* **24,** 4018–4028 (2005).
168. Cui, J. *et al.* NLRP4 negatively regulates type I interferon signaling by targeting the kinase TBK1 for degradation via the ubiquitin ligase DTX4. *Nat Immunol* **13,** 387–395 (2012).
169. Charoenthongtrakul, S., Gao, L. & Harhaj, E. W. The NLRP4-DTX4 axis: a key suppressor of TBK1 and innate antiviral signaling. *Cellular and Molecular Immunology* **9,** 431–433 (2012).
170. Zhang, M. *et al.* TRAF-interacting protein (TRIP) negatively regulates IFN-β production and antiviral response by promoting proteasomal degradation of TANK-binding kinase 1. *J. Exp. Med.* **209,** 1703–1711 (2012).
171. Gabhann, J. N. *et al.* Absence of SHIP-1 Results in Constitutive Phosphorylation of Tank-Binding Kinase 1 and Enhanced TLR3-Dependent IFN-beta Production. *The Journal of Immunology* **184,** 2314–2320 (2010).
172. Zhao, Y. *et al.* PPM1B negatively regulates antiviral response via dephosphorylating TBK1. *Cell. Signal.* **24,** 2197–2204 (2012).
173. Zhang, M. *et al.* Regulation of IkappaB kinase-related kinases and antiviral responses by tumor suppressor CYLD. *Journal of Biological Chemistry* **283,** 18621–18626 (2008).
174. Gao, L. *et al.* ABIN1 Protein Cooperates with TAX1BP1 and A20 Proteins to Inhibit Antiviral Signaling. *Journal of Biological Chemistry* **286,** 36592–36602 (2011).
175. Charoenthongtrakul, S., Gao, L., Parvatiyar, K., Lee, D. & Harhaj, E. W. RING finger protein 11 targets TBK1/IKKi kinases to inhibit antiviral signaling. *PLoS ONE* **8,** e53717 (2013).
176. Ng, M.-H. J. *et al.* MIP-T3 Is a Negative Regulator of Innate Type I IFN Response. *The Journal of Immunology* **187,** 6473–6482 (2011).
177. Liang, Q. *et al.* ORF45 of Kaposi's sarcoma-associated herpesvirus inhibits phosphorylation of interferon regulatory factor 7 by IKKε and TBK1 as an alternative substrate. *J. Virol.* **86,** 10162–10172 (2012).
178. Wang, D. *et al.* The Leader Proteinase of Foot-and-Mouth Disease Virus Negatively Regulates the Type I Interferon Pathway by Acting as a Viral Deubiquitinase. *J. Virol.* **85,** 3758–3766 (2011).
179. Otsuka, M. *et al.* Interaction between the HCVNS3 protein and the host TBK1 protein leads to inhibition of cellular antiviral responses. *Hepatology* **41,** 1004–1012 (2005).
180. Ma, Y. *et al.* Inhibition of TANK Binding Kinase 1 by Herpes Simplex Virus 1 Facilitates Productive Infection. *J. Virol.* **86,** 2188–2196 (2012).
181. Alff, P. J., Sen, N., Gorbunova, E., Gavrilovskaya, I. N. & Mackow, E. R. The NY-1 hantavirus Gn cytoplasmic tail coprecipitates TRAF3 and inhibits cellular interferon responses by disrupting TBK1-TRAF3 complex formation. *J. Virol.* **82,** 9115–9122 (2008).
182. Unterstab, G. *et al.* Viral targeting of the interferon-beta-inducing Traf family

member-associated NF-kappa B activator (TANK)-binding kinase-1. *Proceedings of the National Academy of Sciences* **102,** 13640–13645 (2005).
183. Hammaker, D., Boyle, D. L. & Firestein, G. S. Synoviocyte innate immune responses: TANK-binding kinase-1 as a potential therapeutic target in rheumatoid arthritis. *Rheumatology (Oxford)* **51,** 610–618 (2012).
184. Hasan, M. *et al.* Cutting Edge: Inhibiting TBK1 by Compound II Ameliorates Autoimmune Disease in Mice. *The Journal of Immunology* **195,** 4573–4577 (2015).
185. Freischmidt, A. *et al.* Haploinsufficiency of TBK1 causes familial ALS and fronto-temporal dementia. *Nat. Neurosci.* **18,** 631–636 (2015).
186. Clément, J.-F., Meloche, S. & Servant, M. J. The IKK-related kinases: from innate immunity to oncogenesis. *Cell Res.* **18,** 889–899 (2008).
187. Chien, Y. *et al.* RalB GTPase-mediated activation of the IkappaB family kinase TBK1 couples innate immune signaling to tumor cell survival. *Cell* **127,** 157–170 (2006).
188. Delhase, M. *et al.* TANK-binding kinase 1 (TBK1) controls cell survival through PAI-2/serpinB2 and transglutaminase 2. *Proceedings of the National Academy of Sciences* **109,** E177–E186 (2012).
189. Ou, Y.-H. *et al.* TBK1 Directly Engages Akt/PKB Survival Signaling to Support Oncogenic Transformation. *Molecular Cell* **41,** 458–470 (2011).
190. Clark, K., Plater, L., Peggie, M. & Cohen, P. Use of the pharmacological inhibitor BX795 to study the regulation and physiological roles of TBK1 and IkappaB kinase epsilon: a distinct upstream kinase mediates Ser-172 phosphorylation and activation. *Journal of Biological Chemistry* **284,** 14136–14146 (2009).
191. Lee, D.-F. & Hung, M.-C. Advances in targeting IKK and IKK-related kinases for cancer therapy. *Clin Cancer Res* **14,** 5656–5662 (2008).
192. Mellman, I. & Steinman, R. M. Dendritic cells: specialized and regulated antigen processing machines. *Cell* **106,** 255–258 (2001).
193. Guermonprez, P., Valladeau, J., Zitvogel, L., Théry, C. & Amigorena, S. Antigen presentation and T cell stimulation by dendritic cells. *Annu. Rev. Immunol.* **20,** 621–667 (2002).
194. Trombetta, E. S. & Mellman, I. CELL BIOLOGY OF ANTIGEN PROCESSING IN VITRO AND IN VIVO. *http://dx.doi.org/10.1146/annurev.immunol.22.012703.104538* **23,** 975–1028 (2004).
195. Albert, M. L. & Bhardwaj, N. *Resurrecting the dead: DCs cross-present antigen derived from apoptotic cells on MHC I*. (Immunologist, 1998).
196. Heath, W. R. & Carbone, F. R. CROSS-PRESENTATION, DENDRITIC CELLS, TOLERANCE AND IMMUNITY. *http://dx.doi.org/10.1146/annurev.immunol.19.1.47* **19,** 47–64 (2003).
197. Banchereau, J. & Steinman, R. M. Dendritic cells and the control of immunity. *Nature* **392,** 245–252 (1998).
198. Ueno, H. *et al.* Harnessing human dendritic cell subsets for medicine. *Immunol. Rev.* **234,** 199–212 (2010).
199. Jego, G., Pascual, V., Palucka, A. K. & Banchereau, J. Dendritic Cells Control B Cell Growth and Differentiation. *B Cell Trophic Factors and B Cell Antagonism in Autoimmune Disease* **8,** 124–139 (2004).

200. Batista, F. D. & Harwood, N. E. The who, how and where of antigen presentation to B cells. *Nature Reviews Immunology* **9,** 15–27 (2009).
201. Jung, S. *et al.* In Vivo Depletion of CD11c+ Dendritic Cells Abrogates Priming of CD8+ T Cells by Exogenous Cell-Associated Antigens. *Immunity* **17,** 211–220 (2002).
202. Kurts, C., Robinson, B. W. S. & Knolle, P. A. Cross-priming in health and disease. *Nature Reviews Immunology* **10,** 403–414 (2010).
203. Kovacsovics-Bankowski, M. & Rock, K. L. A phagosome-to-cytosol pathway for exogenous antigens presented on MHC class I molecules. *Science* **267,** 243–246 (1995).
204. Merzougui, N., Kratzer, R., Saveanu, L. & van Endert, P. A proteasome-dependent, TAP-independent pathway for cross-presentation of phagocytosed antigen. *EMBO reports* **12,** 1257–1264 (2011).
205. Shen, L., Sigal, L. J., Boes, M. & Rock, K. L. Important role of cathepsin S in generating peptides for TAP-independent MHC class I crosspresentation in vivo. *Immunity* **21,** 155–165 (2004).
206. Bertholet, S. *et al.* Leishmania antigens are presented to CD8+ T cells by a transporter associated with antigen processing-independent pathway in vitro and in vivo. *The Journal of Immunology* **177,** 3525–3533 (2006).
207. Delamarre, L., Pack, M., Chang, H., Mellman, I. & Trombetta, E. S. Differential Lysosomal Proteolysis in Antigen-Presenting Cells Determines Antigen Fate. *Science* **307,** 1630–1634 (2005).
208. Joffre, O. P., Segura, E., Savina, A. & Amigorena, S. Cross-presentation by dendritic cells. *Nature Reviews Immunology* **12,** 557–569 (2012).
209. Hildner, K. *et al.* Batf3 Deficiency Reveals a Critical Role for CD8α+ Dendritic Cells in Cytotoxic T Cell Immunity. *Science* **322,** 1097–1100 (2008).
210. Lorenzi, S. *et al.* Type I IFNs control antigen retention and survival of CD8α(+) dendritic cells after uptake of tumor apoptotic cells leading to cross-priming. *J. Immunol.* **186,** 5142–5150 (2011).
211. Diamond, M. S. *et al.* Type I interferon is selectively required by dendritic cells for immune rejection of tumors. *J. Exp. Med.* **208,** 1989–2003 (2011).
212. Fuertes, M. B. *et al.* Host type I IFN signals are required for antitumor CD8+ T cell responses through CD8{alpha}+ dendritic cells. *J. Exp. Med.* **208,** 2005–2016 (2011).
213. Dunn, G. P., Old, L. J. & Schreiber, R. D. The Immunobiology of Cancer Immunosurveillance and Immunoediting. *Immunity* **21,** 137–148 (2004).
214. Palucka, K. & Banchereau, J. Cancer immunotherapy via dendritic cells. *Nat Rev Cancer* **12,** 265–277 (2012).
215. Corrales, L. *et al.* Direct Activation of STING in the Tumor Microenvironment Leads to Potent and Systemic Tumor Regression and Immunity. *Cell Reports* **11,** 1018–1030 (2015).
216. Steinbrink, K., Wölfl, M., Jonuleit, H., Knop, J. & Enk, A. H. Induction of tolerance by IL-10-treated dendritic cells. *The Journal of Immunology* **159,** 4772–4780 (1997).
217. Aspord, C. *et al.* Breast cancer instructs dendritic cells to prime interleukin 13-secreting CD4+ T cells that facilitate tumor development. *Journal of Experimental Medicine* **204,** 1037–1047 (2007).

218. DeNardo, D. G. *et al.* CD4(+) T cells regulate pulmonary metastasis of mammary carcinomas by enhancing protumor properties of macrophages. *Cancer Cell* **16,** 91–102 (2009).
219. Treilleux, I. *et al.* Dendritic cell infiltration and prognosis of early stage breast cancer. *Clin Cancer Res* **10,** 7466–7474 (2004).
220. Coukos, G., Benencia, F., Buckanovich, R. J. & Conejo-Garcia, J. R. The role of dendritic cell precursors in tumour vasculogenesis. *Br. J. Cancer* **92,** 1182–1187 (2005).
221. Palucka, K. & Banchereau, J. Dendritic-Cell-Based Therapeutic Cancer Vaccines. *Immunity* **39,** 38–48 (2013).
222. Dudziak, D. *et al.* Differential Antigen Processing by Dendritic Cell Subsets in Vivo. *Science* **315,** 107–111 (2007).
223. Bonifaz, L. *et al.* Efficient targeting of protein antigen to the dendritic cell receptor DEC-205 in the steady state leads to antigen presentation on major histocompatibility complex class I products and peripheral CD8+ T cell tolerance. *Journal of Experimental Medicine* **196,** 1627–1638 (2002).
224. Bonifaz, L. C. *et al.* In vivo targeting of antigens to maturing dendritic cells via the DEC-205 receptor improves T cell vaccination. *Journal of Experimental Medicine* **199,** 815–824 (2004).
225. Hoeijmakers, J. H. J. DNA Damage, Aging, and Cancer. *http://dx.doi.org/10.1056/NEJMra0804615* **361,** 1475–1485 (2009).
226. Bartek, J., Bartkova, J. & Lukas, J. DNA damage signalling guards against activated oncogenes and tumour progression. *Oncogene* **26,** 7773–7779 (2007).
227. Lindahl, T. & Barnes, D. E. Repair of endogenous DNA damage. *Cold Spring Harb. Symp. Quant. Biol.* **65,** 127–133 (2000).
228. Krokan, H. E. & Bjørås, M. Base Excision Repair. *Cold Spring Harb Perspect Biol* **5,** a012583–a012583 (2013).
229. Jiricny, J. The multifaceted mismatch-repair system. *Nat. Rev. Mol. Cell Biol.* **7,** 335–346 (2006).
230. Kim, H. & D'Andrea, A. D. Regulation of DNA cross-link repair by the Fanconi anemia/BRCA pathway. *Genes Dev.* **26,** 1393–1408 (2012).
231. Kamileri, I., Karakasilioti, I. & Garinis, G. A. Nucleotide excision repair: new tricks with old bricks. *Trends Genet.* **28,** 566–573 (2012).
232. Chiruvella, K. K., Liang, Z. & Wilson, T. E. Repair of Double-Strand Breaks by End Joining. *Cold Spring Harb Perspect Biol* **5,** a012757–a012757 (2013).
233. Price, B. D. & D'Andrea, A. D. Chromatin Remodeling at DNA Double-Strand Breaks. *Cell* **152,** 1344–1354 (2013).
234. Harper, J. W. & Elledge, S. J. The DNA damage response: ten years after. *Molecular Cell* **28,** 739–745 (2007).
235. Bergink, S. & Jentsch, S. Principles of ubiquitin and SUMO modifications in DNA repair. *Nature* **458,** 461–467 (2009).
236. Ciccia, A. & Elledge, S. J. The DNA damage response: making it safe to play with knives. *Molecular Cell* **40,** 179–204 (2010).
237. Soutoglou, E. & Misteli, T. Activation of the cellular DNA damage response in the absence of DNA lesions. *Science* **320,** 1507–1510 (2008).
238. Bekker-Jensen, S. *et al.* Spatial organization of the mammalian genome

surveillance machinery in response to DNA strand breaks. *J Cell Biol* **173,** 195–206 (2006).
239. Matsuoka, S. *et al.* ATM and ATR Substrate Analysis Reveals Extensive Protein Networks Responsive to DNA Damage. *Science* **316,** 1160–1166 (2007).
240. Rogakou, E. P., Pilch, D. R., Orr, A. H., Ivanova, V. S. & Bonner, W. M. DNA double-stranded breaks induce histone H2AX phosphorylation on serine 139. *Journal of Biological Chemistry* **273,** 5858–5868 (1998).
241. Stucki, M. *et al.* MDC1 Directly Binds Phosphorylated Histone H2AX to Regulate Cellular Responses to DNA Double-Strand Breaks. *Cell* **123,** 1213–1226 (2005).
242. Stewart, G. S., Bin Wang, Bignell, C. R., Taylor, A. M. R. & Elledge, S. J. MDC1 is a mediator of the mammalian DNA damage checkpoint. *Nature* **421,** 961–966 (2003).
243. Zhou, B. B. & Elledge, S. J. The DNA damage response: putting checkpoints in perspective. *Nature* **408,** 433–439 (2000).
244. Batchelor, E., Loewer, A. & Lahav, G. The ups and downs of p53: understanding protein dynamics in single cells. *Nat Rev Cancer* **9,** 371–377 (2009).
245. Loveless, T. B. *et al.* DNA Damage Regulates Translation through β-TRCP Targeting of CReP. *PLoS Genet.* **11,** e1005292 (2015).
246. Gasser, S., Orsulic, S., Brown, E. J. & Raulet, D. H. The DNA damage pathway regulates innate immune system ligands of the NKG2D receptor. *Nature* **436,** 1186–1190 (2005).
247. Cerboni, C. *et al.* The DNA Damage Response: A Common Pathway in the Regulation of NKG2D and DNAM-1 Ligand Expression in Normal, Infected, and Cancer Cells. *Front Immunol* **4,** (2014).
248. Li, N. *et al.* ATM is required for IkappaB kinase (IKKk) activation in response to DNA double strand breaks. *Journal of Biological Chemistry* **276,** 8898–8903 (2001).
249. Huang, T. T., Wuerzberger-Davis, S. M., Wu, Z.-H. & Miyamoto, S. Sequential modification of NEMO/IKKgamma by SUMO-1 and ubiquitin mediates NF-kappaB activation by genotoxic stress. *Cell* **115,** 565–576 (2003).
250. McCool, K. W. & Miyamoto, S. DNA damage-dependent NF-κB activation: NEMO turns nuclear signaling inside out. *Immunol. Rev.* **246,** 311–326 (2012).
251. Brzostek-Racine, S., Gordon, C., Van Scoy, S. & Reich, N. C. The DNA damage response induces IFN. *J. Immunol.* **187,** 5336–5345 (2011).
252. Gennery, A. R. Primary immunodeficiency syndromes associated with defective DNA double-strand break repair. *Br. Med. Bull.* **77-78,** 71–85 (2006).
253. Manis, J. P. *et al.* 53BP1 links DNA damage-response pathways to immunoglobulin heavy chain class-switch recombination. *Nat Immunol* **5,** 481–487 (2004).
254. Jackson, S. P. & Bartek, J. The DNA-damage response in human biology and disease. *Nature* **461,** 1071–1078 (2009).
255. Stavnezer, J., Guikema, J. E. J. & Schrader, C. E. Mechanism and regulation of class switch recombination. *Annu. Rev. Immunol.* **26,** 261–292 (2008).
256. Bassing, C. H. & Alt, F. W. The cellular response to general and programmed DNA double strand breaks. *DNA Repair* **3,** 781–796 (2004).
257. Sobacchi, C., Marrella, V., Rucci, F., Vezzoni, P. & Villa, A. RAG-dependent primary immunodeficiencies. *Human Mutation* **27,** 1174–1184 (2006).

258. Katyal, S. & McKinnon, P. J. DNA strand breaks, neurodegeneration and aging in the brain. *Mech. Ageing Dev.* **129,** 483–491 (2008).
259. Biton, S., Barzilai, A. & Shiloh, Y. The neurological phenotype of ataxia-telangiectasia: solving a persistent puzzle. *DNA Repair* **7,** 1028–1038 (2008).
260. Varon, R. *et al.* Nibrin, a novel DNA double-strand break repair protein, is mutated in Nijmegen breakage syndrome. *Cell* **93,** 467–476 (1998).
261. Richardson, C., Horikoshi, N. & Pandita, T. K. The role of the DNA double-strand break response network in meiosis. *DNA Repair* **3,** 1149–1164 (2004).
262. Agarwal, A. & Said, T. M. Role of sperm chromatin abnormalities and DNA damage in male infertility. *Hum. Reprod. Update* **9,** 331–345 (2003).
263. De Lange, T. Shelterin: the protein complex that shapes and safeguards human telomeres. *Genes Dev.* (2005).
264. Sedelnikova, O. A. *et al.* Senescing human cells and ageing mice accumulate DNA lesions with unrepairable double-strand breaks. *Nature Cell Biology* **6,** 168–170 (2004).
265. Schumacher, B., Garinis, G. A. & Hoeijmakers, J. H. J. Age to survive: DNA damage and aging. *Trends in Genetics* **24,** 77–85 (2008).
266. Negrini, S., Gorgoulis, V. G. & Halazonetis, T. D. Genomic instability |[mdash]| an evolving hallmark of cancer. *Nat. Rev. Mol. Cell Biol.* **11,** 220–228 (2010).
267. D'Orazio, J. A. Inherited cancer syndromes in children and young adults. *Journal of Pediatric Hematology/Oncology* **32,** 195–228 (2010).
268. Jeggo, P. A., Pearl, L. H. & Carr, A. M. DNA repair, genome stability and cancer: a historical perspective. *Nat Rev Cancer* **16,** 35–42 (2016).
269. Hall, J. M. *et al.* Linkage of early-onset familial breast cancer to chromosome 17q21. *Science* **250,** 1684–1689 (1990).
270. Miki, Y. *et al.* A strong candidate for the breast and ovarian cancer susceptibility gene BRCA1. *Science* **266,** 66–71 (1994).
271. Ford, D., Easton, D. F., Bishop, D. T., Narod, S. A. & Goldgar, D. E. Risks of cancer in BRCA1-mutation carriers. *The Lancet* **343,** 692–695 (1994).
272. Antoniou, A. C., Gayther, S. A., Stratton, J. F., Ponder, B. A. J. & Easton, D. F. Risk models for familial ovarian and breast cancer. *Genetic Epidemiology* **18,** 173–190 (2000).
273. Iqbal, J. *et al.* The incidence of pancreatic cancer in BRCA1 and BRCA2 mutation carriers. *Br. J. Cancer* **107,** 2005–2009 (2012).
274. Lynch, H. T. *et al.* BRCA1 and pancreatic cancer: pedigree findings and their causal relationships. *Cancer Genet. Cytogenet.* **158,** 119–125 (2005).
275. Thompson, D., Easton, D. F.Breast Cancer Linkage Consortium. Cancer Incidence in BRCA1 mutation carriers. *JNCI J Natl Cancer Inst* **94,** 1358–1365 (2002).
276. Friedenson, B. BRCA1 and BRCA2 pathways and the risk of cancers other than breast or ovarian. *MedGenMed* **7,** 60–60 (2005).
277. Welcsh, P. L. & King, M. C. BRCA1 and BRCA2 and the genetics of breast and ovarian cancer. *Hum. Mol. Genet.* **10,** 705–713 (2001).
278. Esteller, M. *et al.* Promoter hypermethylation and BRCA1 inactivation in sporadic breast and ovarian tumors. *JNCI J Natl Cancer Inst* **92,** 564–569 (2000).
279. Huen, M. S. Y., Sy, S. M. H. & Chen, J. BRCA1 and its toolbox for the maintenance of genome integrity. *Nat. Rev. Mol. Cell Biol.* **11,** 138–148 (2010).

280. Thakur, S. *et al.* Localization of BRCA1 and a splice variant identifies the nuclear localization signal. *Molecular and Cellular Biology* **17,** 444–452 (1997).
281. Korlimarla, A. *et al.* Identification of a non-canonical nuclear localization signal (NLS) in BRCA1 that could mediate nuclear localization of splice variants lacking the classical NLS. *Cell. Mol. Biol. Lett.* **18,** 284–296 (2013).
282. Ouchi, T. BRCA1 phosphorylation: Biological consequences. *Cancer biology & therapy* **5,** 470–475 (2006).
283. Yarden, R. I., Pardo-Reoyo, S., Sgagias, M., Cowan, K. H. & Brody, L. C. BRCA1 regulates the G2/M checkpoint by activating Chk1 kinase upon DNA damage. *Nature Genetics* **30,** 285–289 (2002).
284. Foray, N. *et al.* A subset of ATM- and ATR-dependent phosphorylation events requires the BRCA1 protein. *The EMBO Journal* **22,** 2860–2871 (2003).
285. Gerloff, D. L., Woods, N. T., Farago, A. A. & Monteiro, A. N. A. BRCT domains: A little more than kin, and less than kind. *FEBS Letters* **586,** 2711–2716 (2012).
286. Yu, X. C., Chini, C., He, M., Mer, G. & Chen, J. J. The BRCT domain is a phospho-protein binding domain. *Science* **302,** 639–642 (2003).
287. Manke, I. A., Lowery, D. M., Nguyen, A. & Yaffe, M. B. BRCT repeats as phosphopeptide-binding modules involved in protein targeting. *Science* **302,** 636–639 (2003).
288. Chapman, M. S. & Verma, I. M. Transcriptional activation by BRCA1. *Nature* **382,** 678–679 (1996).
289. Orban, T. I. & Olah, E. Emerging roles of BRCA1 alternative splicing. *Molecular Pathology* (2003).
290. Orban, T. I. & Olah, E. Expression profiles of BRCA1 splice variants in asynchronous and in G1/S synchronized tumor cell lines. *Biochem. Biophys. Res. Commun.* **280,** 32–38 (2001).
291. Xia, Y., Pao, G. M., Chen, H.-W., Verma, I. M. & Hunter, T. Enhancement of BRCA1 E3 ubiquitin ligase activity through direct interaction with the BARD1 protein. *Journal of Biological Chemistry* **278,** 5255–5263 (2003).
292. Brzovic, P. S., Rajagopal, P., Hoyt, D. W., King, M. C. & Klevit, R. E. Structure of a BRCA1-BARD1 heterodimeric RING-RING complex. *Nat. Struct. Biol.* **8,** 833–837 (2001).
293. Fabbro, M., Rodriguez, J. A., Baer, R. & Henderson, B. R. BARD1 induces BRCA1 intranuclear foci formation by increasing RING-dependent BRCA1 nuclear import and inhibiting BRCA1 nuclear export. *Journal of Biological Chemistry* **277,** 21315–21324 (2002).
294. Brzovic, P. S. *et al.* Binding and recognition in the assembly of an active BRCA1/BARD1 ubiquitin-ligase complex. *Proceedings of the National Academy of Sciences* **100,** 5646–5651 (2003).
295. Wu, W., Koike, A., Takeshita, T. & Ohta, T. The ubiquitin E3 ligase activity of BRCA1 and its biological functions. *Cell Div* **3,** 1–10 (2008).
296. Hashizume, R. *et al.* The RING heterodimer BRCA1-BARD1 is a ubiquitin ligase inactivated by a breast cancer-derived mutation. *Journal of Biological Chemistry* **276,** 14537–14540 (2001).
297. Drost, R. *et al.* BRCA1 RING Function Is Essential for Tumor Suppression but Dispensable for Therapy Resistance. *Cancer Cell* **20,** 797–809 (2011).
298. Shakya, R. *et al.* BRCA1 tumor suppression depends on BRCT phosphoprotein

binding, but not its E3 ligase activity. *Science* **334,** 525–528 (2011).
299. Savage, K. I. & Harkin, D. P. BRCA1, a 'complex' protein involved in the maintenance of genomic stability. *FEBS Journal* **282,** 630–646 (2015).
300. Nishikawa, H. *et al.* Mass spectrometric and mutational analyses reveal Lys-6-linked polyubiquitin chains catalyzed by BRCA1-BARD1 ubiquitin ligase. *Journal of Biological Chemistry* **279,** 3916–3924 (2004).
301. Tian, F. *et al.* BRCA1 promotes the ubiquitination of PCNA and recruitment of translesion polymerases in response to replication blockade. *Proc. Natl. Acad. Sci. U.S.A.* **110,** 13558–13563 (2013).
302. Eakin, C. M., Maccoss, M. J., Finney, G. L. & Klevit, R. E. Estrogen receptor alpha is a putative substrate for the BRCA1 ubiquitin ligase. *Proceedings of the National Academy of Sciences* **104,** 5794–5799 (2007).
303. Rodriguez, J. A. & Henderson, B. R. Identification of a functional nuclear export sequence in BRCA1. *Journal of Biological Chemistry* **275,** 38589–38596 (2000).
304. Jiang, J. *et al.* p53-Dependent BRCA1 Nuclear Export Controls Cellular Susceptibility to DNA Damage. *Cancer Res* **71,** 5546–5557 (2011).
305. Wang, H., Yang, E. S., Jiang, J., Nowsheen, S. & Xia, F. DNA damage-induced cytotoxicity is dissociated from BRCA1's DNA repair function but is dependent on its cytosolic accumulation. *Cancer Res* **70,** 6258–6267 (2010).
306. Coene, E. D. *et al.* Phosphorylated BRCA1 is predominantly located in the nucleus and mitochondria. *Mol. Biol. Cell* **16,** 997–1010 (2005).
307. Laulier, C. *et al.* Bcl-2 inhibits nuclear homologous recombination by localizing BRCA1 to the endomembranes. *Cancer Res* **71,** 3590–3602 (2011).
308. Hedgepeth, S. C. *et al.* The BRCA1 tumor suppressor binds to inositol 1,4,5-trisphosphate receptors to stimulate apoptotic calcium release. *J. Biol. Chem.* **290,** 7304–7313 (2015).
309. Christou, C. & Kyriacou, K. BRCA1 and Its Network of Interacting Partners. *Biology* **2,** 40–63 (2013).
310. Vallon-Christersson, J. *et al.* Functional analysis of BRCA1 C-terminal missense mutations identified in breast and ovarian cancer families. *Hum. Mol. Genet.* **10,** 353–360 (2001).
311. Glover, J. N. M. Insights into the Molecular Basis of Human Hereditary Breast Cancer from Studies of the BRCA1 BRCT Domain. *Familial Cancer* **5,** 89–93 (2006).
312. Monteiro, A. N., August, A. & Hanafusa, H. Evidence for a transcriptional activation function of BRCA1 C-terminal region. *Proceedings of the National Academy of Sciences* **93,** 13595–13599 (1996).
313. MacLachlan, T. K., Takimoto, R. & El-Deiry, W. S. BRCA1 directs a selective p53-dependent transcriptional response towards growth arrest and DNA repair targets. *Molecular and Cellular Biology* **22,** 4280–4292 (2002).
314. Harte, M. T. *et al.* NF-κB is a critical mediator of BRCA1-induced chemoresistance. *Oncogene* **33,** 713–723 (2014).
315. Heldring, N. *et al.* Estrogen receptors: how do they signal and what are their targets. *Physiological Reviews* **87,** 905–931 (2007).
316. Hosey, A. M. *et al.* Molecular basis for estrogen receptor alpha deficiency in BRCA1-linked breast cancer. *JNCI J Natl Cancer Inst* **99,** 1683–1694 (2007).
317. Volcic, M. *et al.* NF-κB regulates DNA double-strand break repair in conjunction

with BRCA1-CtIP complexes. *Nucleic Acids Res.* **40,** 181–195 (2012).
318. Cooke, M. S., Evans, M. D., Dizdaroglu, M. & Lunec, J. Oxidative DNA damage: mechanisms, mutation, and disease. *FASEB J* (2003).
319. Licandro, G. *et al.* The NLRP3 inflammasome affects DNA damage responses after oxidative and genotoxic stress in dendritic cells. *Eur. J. Immunol.* **43,** 2126–2137 (2013).
320. Weitzman, S. A. & Gordon, L. I. Inflammation and cancer: role of phagocyte-generated oxidants in carcinogenesis. *Blood* **76,** 655–663 (1990).
321. Bouvard, V., Baan, R., Straif, K., Grosse, Y. & Secretan, B. *A review of human carcinogens—Part B: biological agents*. (The lancet oncology, 2009).
322. Turnell, A. S. & Grand, R. J. DNA viruses and the cellular DNA-damage response. *J. Gen. Virol.* **93,** 2076–2097 (2012).
323. Narisawa-Saito, M. & Kiyono, T. Basic mechanisms of high-risk human papillomavirus-induced carcinogenesis: roles of E6 and E7 proteins. *Cancer Sci.* **98,** 1505–1511 (2007).
324. Dyson, N., Howley, P. M., Münger, K. & Harlow, E. The human papilloma virus-16 E7 oncoprotein is able to bind to the retinoblastoma gene product. *Science* **243,** 934–937 (1989).
325. Bester, A. C. *et al.* Nucleotide deficiency promotes genomic instability in early stages of cancer development. *Cell* **145,** 435–446 (2011).
326. Thorley-Lawson, D. A. & Gross, A. Persistence of the Epstein-Barr virus and the origins of associated lymphomas. *N Engl J Med* **350,** 1328–1337 (2004).
327. Nikitin, P. A. *et al.* An ATM/Chk2-Mediated DNA Damage-Responsive Signaling Pathway Suppresses Epstein-Barr Virus Transformation of Primary Human B Cells. *Cell Host & Microbe* **8,** 510–522 (2010).
328. Mesri, E. A., Cesarman, E. & Boshoff, C. Kaposi's sarcoma and its associated herpesvirus. *Nat Rev Cancer* **10,** 707–719 (2010).
329. Koopal, S. *et al.* Viral oncogene-induced DNA damage response is activated in Kaposi sarcoma tumorigenesis. *PLoS Pathog* **3,** 1348–1360 (2007).
330. Stracker, T. H., Carson, C. T. & Weitzman, M. D. Adenovirus oncoproteins inactivate the Mre11-Rad50-NBS1 DNA repair complex. *Nature* **418,** 348–352 (2002).
331. Blackford, A. N., Patel, R. N. & Forrester, N. A. *Adenovirus 12 E4orf6 inhibits ATR activation by promoting TOPBP1 degradation*. (Proceedings of the …, 2010).
332. Parkin, D. M., Bray, F., Ferlay, J. & Pisani, P. Global cancer statistics, 2002. *Ca-a Cancer Journal for Clinicians* **55,** 74–108 (2005).
333. Wroblewski, L. E., Peek, R. M. J. & Wilson, K. T. Helicobacter pylori and Gastric Cancer: Factors That Modulate Disease Risk. *Clin. Microbiol. Rev.* **23,** 713–739 (2010).
334. Raisch, J. *et al.* Colon cancer-associated B2 Escherichia coli colonize gut mucosa and promote cell proliferation. *World J. Gastroenterol.* **20,** 6560–6572 (2014).
335. Cuevas-Ramos, G. *et al.* Escherichia coli induces DNA damage in vivo and triggers genomic instability in mammalian cells. *Proc. Natl. Acad. Sci. U.S.A.* **107,** 11537–11542 (2010).
336. Arthur, J. C. *et al.* Intestinal Inflammation Targets Cancer-Inducing Activity of the Microbiota. *Science* **338,** 120–123 (2012).

337. Luftig, M. A. Viruses and the DNA Damage Response: Activation and Antagonism. *http://dx.doi.org/10.1146/annurev-virology-031413-085548* **1,** 605–625 (2014).
338. Daniel, R. *et al.* Evidence that the retroviral DNA integration process triggers an ATR-dependent DNA damage response. *Proceedings of the National Academy of Sciences* **100,** 4778–4783 (2003).
339. Smith, J. A. & Daniel, R. Following the Path of the Virus: The Exploitation of Host DNA Repair Mechanisms by Retroviruses. *ACS Chem. Biol.* **1,** 217–226 (2006).
340. Tarakanova, V. L. *et al.* Gamma-herpesvirus kinase actively initiates a DNA damage response by inducing phosphorylation of H2AX to foster viral replication. *Cell Host & Microbe* **1,** 275–286 (2007).
341. Paludan, S. R. & Bowie, A. G. Immune Sensing of DNA. *Immunity* **38,** 870–880 (2013).
342. White, M. J. *et al.* Apoptotic Caspases Suppress mtDNA-Induced STING-Mediated Type I IFN Production. *Cell* **159,** 1549–1562 (2014).
343. Barber, G. N. STING: infection, inflammation and cancer. *Nature Reviews Immunology* **15,** 760–770 (2015).
344. Ahn, J. *et al.* Inflammation-driven carcinogenesis is mediated through STING. *Nature Communications* **5,** 5166 (2014).
345. Woo, S.-R., Corrales, L. & Gajewski, T. F. The STING pathway and the T cell-inflamed tumor microenvironment. *Trends in Immunology* **36,** 250–256 (2015).
346. Zhu, Q. *et al.* Cutting edge: STING mediates protection against colorectal tumorigenesis by governing the magnitude of intestinal inflammation. *J. Immunol.* **193,** 4779–4782 (2014).
347. Ahn, J., Konno, H. & Barber, G. N. Diverse roles of STING-dependent signaling on the development of cancer. *Oncogene* **34,** 5302–5308 (2015).
348. Woo, S.-R. *et al.* STING-Dependent Cytosolic DNA Sensing Mediates Innate Immune Recognition of Immunogenic Tumors. *Immunity* **41,** 830–842 (2014).
349. Yan, N., Regalado-Magdos, A. D., Stiggelbout, B., Lee-Kirsch, M. A. & Lieberman, J. The cytosolic exonuclease TREX1 inhibits the innate immune response to human immunodeficiency virus type 1. *Nat Immunol* **11,** 1005–1013 (2010).
350. Gall, A. *et al.* Autoimmunity initiates in nonhematopoietic cells and progresses via lymphocytes in an interferon-dependent autoimmune disease. *Immunity* **36,** 120–131 (2012).
351. Ahn, J., Ruiz, P. & Barber, G. N. Intrinsic self-DNA triggers inflammatory disease dependent on STING. *J. Immunol.* **193,** 4634–4642 (2014).
352. Gehrke, N. *et al.* Oxidative Damage of DNA Confers Resistance to Cytosolic Nuclease TREX1 Degradation and Potentiates STING-Dependent Immune Sensing. *Immunity* **39,** 482–495 (2013).
353. Härtlova, A. *et al.* DNA Damage Primes the Type I Interferon System via the Cytosolic DNA Sensor STING to Promote Anti-Microbial Innate Immunity. *Immunity* **42,** 332–343 (2015).
354. Nowak-Wegrzyn, A., Crawford, T. O., Winkelstein, J. A., Carson, K. A. & Lederman, H. M. Immunodeficiency and infections in ataxia-telangiectasia. *The Journal of Pediatrics* **144,** 505–511 (2004).

355. Ermolaeva, M. A. *et al.* DNA damage in germ cells induces an innate immune response that triggers systemic stress resistance. *Nature* **501,** 416–420 (2013).
356. Zhang, X. *et al.* Cutting Edge: Ku70 Is a Novel Cytosolic DNA Sensor That Induces Type III Rather Than Type I IFN. *The Journal of Immunology* **186,** 4541–4545 (2011).
357. Ferguson, B. J. *et al.* DNA-PK is a DNA sensor for IRF-3-dependent innate immunity. *eLife Sciences* **1,** e00047 (2012).
358. Kondo, T. *et al.* DNA damage sensor MRE11 recognizes cytosolic double-stranded DNA and induces type I interferon by regulating STING trafficking. *Proc. Natl. Acad. Sci. U.S.A.* **110,** 2969–2974 (2013).
359. Roth, S. *et al.* Rad50-CARD9 interactions link cytosolic DNA sensing to IL-1β production. *Nat Immunol* **15,** 538–545 (2014).
360. Li, S. *et al.* The tumor suppressor PTEN has a critical role in antiviral innate immunity. *Nat Immunol* **17,** 241–249 (2016).
361. Babu, M. *et al.* A dual function of the CRISPR-Cas system in bacterial antivirus immunity and DNA repair. *Molecular Microbiology* **79,** 484–502 (2010).
362. Hjerpe, R. *et al.* Efficient protection and isolation of ubiquitylated proteins using tandem ubiquitin-binding entities. *EMBO reports* **10,** 1250–1258 (2009).
363. Pfisterer, U. *et al.* Direct conversion of human fibroblasts to dopaminergic neurons. *Proc. Natl. Acad. Sci. U.S.A.* **108,** 10343–10348 (2011).
364. Naldini, L. *et al.* In Vivo Gene Delivery and Stable Transduction of Nondividing Cells by a Lentiviral Vector. *Science* **272,** 263–267 (1996).
365. Hrecka, K. *et al.* Vpx relieves inhibition of HIV-1 infection of macrophages mediated by the SAMHD1 protein. *Nature* **474,** 658–661 (2011).
366. Hofmann, H. *et al.* The Vpx lentiviral accessory protein targets SAMHD1 for degradation in the nucleus. *J. Virol.* **86,** 12552–12560 (2012).
367. Reya, T. *et al.* A role for Wnt signalling in self-renewal of haematopoietic stem cells. *Nature* **423,** 409–414 (2003).
368. Dephoure, N., Gould, K. L., Gygi, S. P. & Kellogg, D. R. Mapping and analysis of phosphorylation sites: a quick guide for cell biologists. *Mol. Biol. Cell* **24,** 535–542 (2013).
369. Cox, J. & Mann, M. Is proteomics the new genomics? *Cell* **130,** 395–398 (2007).
370. Grant, S. K. Therapeutic protein kinase inhibitors. *Cell. Mol. Life Sci.* **66,** 1163–1177 (2009).
371. Arora, A. & Scholar, E. M. Role of tyrosine kinase inhibitors in cancer therapy. *Journal of Pharmacology and Experimental Therapeutics* **315,** 971–979 (2005).
372. Zhang, J., Yang, P. L. & Gray, N. S. Targeting cancer with small molecule kinase inhibitors. *Nat Rev Cancer* **9,** 28–39 (2009).
373. Hardie, D. G. Role of AMP-activated protein kinase in the metabolic syndrome and in heart disease. *FEBS Letters* **582,** 81–89 (2008).
374. Radivojac, P. *et al.* Gain and loss of phosphorylation sites in human cancer. *Bioinformatics* **24,** i241–7 (2008).
375. Reimand, J., Wagih, O. & Bader, G. D. The mutational landscape of phosphorylation signaling in cancer. *Sci Rep* **3,** 2651 (2013).
376. Tenreiro, S., Eckermann, K. & Outeiro, T. F. Protein phosphorylation in neurodegeneration: friend or foe? *Front Mol Neurosci* **7,** 42 (2014).
377. Cohen, P. Immune diseases caused by mutations in kinases and components of

the ubiquitin system. *Nat Immunol* **15,** 521–529 (2014).
378. 3rd, E. M. & Vallano, M. L. Role of protein kinases in neurodegenerative disease: cyclin-dependent kinases in Alzheimer's disease. *Front Biosci* **10,** 143–159 (2005).
379. Traenckner, E. B. *et al.* Phosphorylation of human I kappa B-alpha on serines 32 and 36 controls I kappa B-alpha proteolysis and NF-kappa B activation in response to diverse stimuli. *The EMBO Journal* **14,** 2876–2883 (1995).
380. Sjoelund, V., Smelkinson, M. & Nita-Lazar, A. Phosphoproteome profiling of the macrophage response to different toll-like receptor ligands identifies differences in global phosphorylation dynamics. *J. Proteome Res.* **13,** 5185–5197 (2014).
381. Öhman, T. *et al.* Phosphoproteomics combined with quantitative 14-3-3-affinity capture identifies SIRT1 and RAI as novel regulators of cytosolic double-stranded RNA recognition pathway. *Mol. Cell Proteomics* **13,** 2604–2617 (2014).
382. Weintz, G. *et al.* The phosphoproteome of toll-like receptor-activated macrophages. *Mol. Syst. Biol.* **6,** 371 (2010).
383. Dalod, M., Chelbi, R., Malissen, B. & Lawrence, T. Dendritic cell maturation: functional specialization through signaling specificity and transcriptional programming. *The EMBO Journal* **33,** 1104–1116 (2014).
384. Li, D.-Y., Gu, C., Min, J., Chu, Z.-H. & Ou, Q.-J. Maturation induction of human peripheral blood mononuclear cell-derived dendritic cells. *Exp Ther Med* **4,** 131–134 (2012).
385. Valentine, J. M., Kumar, S. & Moumen, A. A p53-independent role for the MDM2 antagonist Nutlin-3 in DNA damage response initiation. *BMC Cancer 2011 11:1* **11,** 1 (2011).
386. Baldwin, E. L. & Osheroff, N. Etoposide, topoisomerase II and cancer. *Current Medicinal Chemistry-Anti- …* (2005).
387. Jin, M. S. *et al.* Crystal Structure of the TLR1-TLR2 Heterodimer Induced by Binding of a Tri-Acylated Lipopeptide. *Cell* **130,** 1071–1082 (2007).
388. Bauernfeind, F. & Hornung, V. TLR2 joins the interferon gang. *Nat Immunol* **10,** 1139–1141 (2009).
389. Brandt, K. J., Fickentscher, C., Kruithof, E. K. O. & de Moerloose, P. TLR2 ligands induce NF-κB activation from endosomal compartments of human monocytes. *PLoS ONE* **8,** e80743–11 (2013).
390. Stack, J. *et al.* TRAM is required for TLR2 endosomal signaling to type I IFN induction. *J. Immunol.* **193,** 6090–6102 (2014).
391. Dietrich, N., Lienenklaus, S., Weiss, S. & Gekara, N. O. Murine Toll-Like Receptor 2 Activation Induces Type I Interferon Responses from Endolysosomal Compartments. *PLoS ONE* **5,** e10250 (2010).
392. Lu, Y.-C., Yeh, W.-C. & Ohashi, P. S. LPS/TLR4 signal transduction pathway. *Cytokine* **42,** 145–151 (2008).
393. Hayashi, F. *et al.* The innate immune response to bacterial flagellin is mediated by Toll-like receptor 5. *Nature* **410,** 1099–1103 (2001).
394. Girardin, S. E. *et al.* Nod2 is a general sensor of peptidoglycan through muramyl dipeptide (MDP) detection. *Journal of Biological Chemistry* **278,** 8869–8872 (2003).

395. Boyle, J. P., Parkhouse, R. & Monie, T. P. Insights into the molecular basis of the NOD2 signalling pathway. *Open Biology* **4,** 140178–140178 (2014).
396. Kato, H. *et al.* Differential roles of MDA5 and RIG-I helicases in the recognition of RNA viruses. *Nature* **441,** 101–105 (2006).
397. Chen, J., Ghorai, M. K., Kenney, G. & Stubbe, J. Mechanistic studies on bleomycin-mediated DNA damage: multiple binding modes can result in double-stranded DNA cleavage. *Nucleic Acids Res.* **36,** 3781–3790 (2008).
398. Cortez, D., Wang, Y., Qin, J. & Elledge, S. J. Requirement of ATM-dependent phosphorylation of brca1 in the DNA damage response to double-strand breaks. *Science* **286,** 1162–1166 (1999).
399. So, S., Davis, A. J. & Chen, D. J. Autophosphorylation at serine 1981 stabilizes ATM at DNA damage sites. *J Cell Biol* **187,** 977–990 (2009).
400. You, Z., Bailis, J. M., Johnson, S. A., Dilworth, S. M. & Hunter, T. Rapid activation of ATM on DNA flanking double-strand breaks. *Nature Cell Biology* **9,** 1311–1318 (2007).
401. Singh, N. P., McCoy, M. T., Tice, R. R. & Schneider, E. L. A simple technique for quantitation of low levels of DNA damage in individual cells. *Experimental Cell Research* **175,** 184–191 (1988).
402. Collins, A. R. The comet assay for DNA damage and repair. *Mol Biotechnol* **26,** 249–261 (2004).
403. Glukhov, I. L., Sirota, N. P. & Kuznetsova, E. A. DNA damage in human mononuclear cells induced by bacterial endotoxin. *Bull. Exp. Biol. Med.* **146,** 301–303 (2008).
404. Matsue, H. *et al.* Generation and function of reactive oxygen species in dendritic cells during antigen presentation. *The Journal of Immunology* **171,** 3010–3018 (2003).
405. Kotsias, F., Hoffmann, E., Amigorena, S. & Savina, A. Reactive Oxygen Species Production in the Phagosome: Impact on Antigen Presentation in Dendritic Cells. *Antioxid. Redox Signal.* **18,** 714–729 (2013).
406. Everts, B. *et al.* Commitment to glycolysis sustains survival of NO-producing inflammatory dendritic cells. *Blood* **120,** 1422–1431 (2012).
407. Slauch, J. M. How does the oxidative burst of macrophages kill bacteria? Still an open question. *Molecular Microbiology* **80,** 580–583 (2011).
408. Fang, F. C. Antimicrobial Actions of Reactive Oxygen Species. *Mbio* **2,** –e00141–11 (2011).
409. Babior, B. M. Phagocytes and oxidative stress. *Am. J. Med.* **109,** 33–44 (2000).
410. Splettstoesser, W. D. & Schuff-Werner, P. Oxidative stress in phagocytes - 'The enemy within'. *Microsc. Res. Tech.* **57,** 441–455 (2002).
411. Paull, T. T. Mechanisms of ATM Activation. *Annu. Rev. Biochem.* **84,** 711–738 (2015).
412. Bakkenist, C. J. & Kastan, M. B. DNA damage activates ATM through intermolecular autophosphorylation and dimer dissociation. *Nature* **421,** 499–506 (2003).
413. Gatei, M. *et al.* Ataxia telangiectasia mutated (ATM) kinase and ATM and Rad3 related kinase mediate phosphorylation of Brca1 at distinct and overlapping sites. In vivo assessment using phospho-specific antibodies. *Journal of Biological Chemistry* **276,** 17276–17280 (2001).

414. Shackelford, R. E. *et al.* The Ataxia telangiectasia gene product is required for oxidative stress-induced G1 and G2 checkpoint function in human fibroblasts. *Journal of Biological Chemistry* **276,** 21951–21959 (2001).
415. Kurz, E. U., Douglas, P. & Lees-Miller, S. P. Doxorubicin activates ATM-dependent phosphorylation of multiple downstream targets in part through the generation of reactive oxygen species. *Journal of Biological Chemistry* **279,** 53272–53281 (2004).
416. Bencokova, Z. *et al.* ATM activation and signaling under hypoxic conditions. *Molecular and Cellular Biology* **29,** 526–537 (2009).
417. Kamsler, A. *et al.* Increased oxidative stress in ataxia telangiectasia evidenced by alterations in redox state of brains from Atm-deficient mice. *Cancer Res* **61,** 1849–1854 (2001).
418. Guo, Z., Deshpande, R. & Paull, T. T. ATM activation in the presence of oxidative stress. *Cell Cycle* **9,** 4805–4811 (2010).
419. Kumar, T. R.Muralidhara. Induction of oxidative stress by organic hydroperoxides in testis and epididymal sperm of rats in vivo. *J. Androl.* **28,** 77–85 (2007).
420. Aboua, Y. G., Plessis, du, S. S. & Brooks, N. Impact of organic hydroperoxides on rat testicular tissue and epididymal sperm. *African Journal of Biotechnology* **8,** (2009).
421. Prasad, K. D., Ram, M. S., Sawhney, R. C., Havazhagan, G. & Banerjee, P. K. Mechanism of tert-butylhydroperoxide induced cytotoxicity in U-937 macrophages by alteration of mitochondrial function and generation of ROS. *Toxicol In Vitro* **21,** 846–854 (2007).
422. Zafarullah, M., Li, W. Q., Sylvester, J. & Ahmad, M. Molecular mechanisms of N-acetylcysteine actions. *CMLS, Cell. Mol. Life Sci.* **60,** 6–20 (2003).
423. De Flora, S., Izzotti, A., D'Agostini, F. & Balansky, R. M. Mechanisms of N-acetylcysteine in the prevention of DNA damage and cancer, with special reference to smoking-related end-points. *Carcinogenesis* **22,** 999–1013 (2001).
424. Cavanagh, L. L., Saal, R. J., Grimmett, K. L. & Thomas, R. Proliferation in monocyte-derived dendritic cell cultures is caused by progenitor cells capable of myeloid differentiation. *Blood* **92,** 1598–1607 (1998).
425. Palucka, K. A. & Taquet, N. Dendritic cells as the terminal stage of monocyte differentiation. *The Journal of …* (1998).
426. Fortini, P. & Dogliotti, E. Mechanisms of dealing with DNA damage in terminally differentiated cells. *Mutat. Res.* **685,** 38–44 (2010).
427. Nouspikel, T. & Hanawalt, P. C. Terminally differentiated human neurons repair transcribed genes but display attenuated global DNA repair and modulation of repair gene expression. *Molecular and Cellular Biology* **20,** 1562–1570 (2000).
428. Nouspikel, T. DNA repair in differentiated cells: some new answers to old questions. *Neuroscience* **145,** 1213–1221 (2007).
429. Briegert, M. & Kaina, B. Human monocytes, but not dendritic cells derived from them, are defective in base excision repair and hypersensitive to methylating agents. *Cancer Res* **67,** 26–31 (2007).
430. Bauer, M. *et al.* Human monocytes are severely impaired in base and DNA double-strand break repair that renders them vulnerable to oxidative stress. *Proc. Natl. Acad. Sci. U.S.A.* **108,** 21105–21110 (2011).

431. McManus, K. J. & Hendzel, M. J. ATM-dependent DNA damage-independent mitotic phosphorylation of H2AX in normally growing mammalian cells. *Mol. Biol. Cell* **16,** 5013–5025 (2005).
432. Xu, B., Kim St & Kastan, M. B. Involvement of Brca1 in S-phase and G(2)-phase checkpoints after ionizing irradiation. *Molecular and Cellular Biology* **21,** 3445–3450 (2001).
433. Feng, Z., Kachnic, L., Zhang, J., Powell, S. N. & Xia, F. DNA damage induces p53-dependent BRCA1 nuclear export. *Journal of Biological Chemistry* **279,** 28574–28584 (2004).
434. Hickson, I., Zhao, Y., Richardson, C. J. & Green, S. J. Identification and characterization of a novel and specific inhibitor of the ataxia-telangiectasia mutated kinase ATM. *Cancer Res* (2004).
435. Jobson, A. G. *et al.* Identification of a Bis-guanylhydrazone [4,4'-Diacetyldiphenylurea-bis(guanylhydrazone); NSC 109555] as a novel chemotype for inhibition of Chk2 kinase. *Mol. Pharmacol.* **72,** 876–884 (2007).
436. Fokas, E. *et al.* Targeting ATR in vivo using the novel inhibitor VE-822 results in selective sensitization of pancreatic tumors to radiation. *Cell Death Dis* **3,** e441 (2012).
437. Matsuoka, S. *et al.* Ataxia telangiectasia-mutated phosphorylates Chk2 in vivo and in vitro. *Proceedings of the National Academy of Sciences* **97,** 10389–10394 (2000).
438. Pabla, N., Huang, S., Mi, Q.-S., Daniel, R. & Dong, Z. ATR-Chk2 signaling in p53 activation and DNA damage response during cisplatin-induced apoptosis. *Journal of Biological Chemistry* **283,** 6572–6583 (2008).
439. Wang, X. Q., Redpath, J. L. & Fan, S. T. ATR dependent activation of Chk2. *Journal of cellular …* (2006).
440. Cuenda, A., Rouse, J., Doza, Y. N., Meier, R. & Cohen, P. SB 203580 is a specific inhibitor of a MAP kinase homologue which is stimulated by cellular stresses and interleukin-1. *FEBS Letters* (1995). doi:10.1002/(ISSN)1873-3468/retrieve/pii/001457939500357F
441. Han, J., Lee, J. D., Bibbs, L. & Ulevitch, R. J. A MAP kinase targeted by endotoxin and hyperosmolarity in mammalian cells. *Science* **265,** 808–811 (1994).
442. Lee, J. C. *et al.* A protein kinase involved in the regulation of inflammatory cytokine biosynthesis. *, Published online: 29 December 1994; | doi:10.1038/372739a0* **372,** 739–746 (1994).
443. Yamamoto, A. *et al.* Bafilomycin A1 Prevents Maturation of Autophagic Vacuoles by Inhibiting Fusion between Autophagosomes and Lysosomes in Rat Hepatoma Cell Line, H-4-II-E Cells. *Cell Structure and Function* **23,** 33–42 (1998).
444. Roberts, P. J. & Der, C. J. Targeting the Raf-MEK-ERK mitogen-activated protein kinase cascade for the treatment of cancer. *Oncogene* **26,** 3291–3310 (2007).
445. Seger, R. & Krebs, E. G. The MAPK signaling cascade. *FASEB J* **9,** 726–735 (1995).
446. Fettelschoss, A. *et al.* Inflammasome activation and IL-1β target IL-1α for secretion as opposed to surface expression. *Proc. Natl. Acad. Sci. U.S.A.* **108,** 18055–18060 (2011).
447. Satoh, T., Kambe, N. & Matsue, H. NLRP3 activation induces ASC-dependent programmed necrotic cell death, which leads to neutrophilic inflammation. *Cell*

Death Dis **4,** e644 (2013).
448. Bain, J. *et al.* The selectivity of protein kinase inhibitors: a further update. *Biochem. J.* **408,** 297–315 (2007).
449. Burns, J. C., Friedmann, T., Driever, W., Burrascano, M. & Yee, J. K. Vesicular stomatitis virus G glycoprotein pseudotyped retroviral vectors: concentration to very high titer and efficient gene transfer into mammalian and nonmammalian cells. *Proceedings of the National Academy of Sciences* **90,** 8033–8037 (1993).
450. Lahouassa, H. *et al.* SAMHD1 restricts the replication of human immunodeficiency virus type 1 by depleting the intracellular pool of deoxynucleoside triphosphates. *Nat Immunol* **13,** 223–228 (2012).
451. White, T. E. *et al.* Contribution of SAM and HD domains to retroviral restriction mediated by human SAMHD1. *Virology* **436,** 81–90 (2013).
452. Kim, B., Nguyen, L. A. & Daddacha, W. Tight interplay among SAMHD1 protein level, cellular dNTP levels, and HIV-1 proviral DNA synthesis kinetics in human primary monocyte-derived …. *Journal of Biological …* (2012).
453. Laguette, N. *et al.* SAMHD1 is the dendritic- and myeloid-cell-specific HIV-1 restriction factor counteracted by Vpx. *Nature* **474,** 654–657 (2011).
454. Berger, A. *et al.* SAMHD1-Deficient CD14+ Cells from Individuals with Aicardi-Goutières Syndrome Are Highly Susceptible to HIV-1 Infection. *PLoS Pathog* **7,** e1002425 (2011).
455. Manning, J. S., Hackett, A. J. & Darby, N. B. Effect of polycations on sensitivity of BALD-3T3 cells to murine leukemia and sarcoma virus infectivity. *Applied Microbiology* **22,** 1162–1163 (1971).
456. McCarthy, M. M. *et al.* HSP90 as a marker of progression in melanoma. *Ann. Oncol.* **19,** 590–594 (2008).
457. Marchenko, N. D. *et al.* Stress-mediated nuclear stabilization of p53 is regulated by ubiquitination and importin-alpha3 binding. *Cell Death Differ.* **17,** 255–267 (2010).
458. Müller-Taubenberger, A. *et al.* Calreticulin and calnexin in the endoplasmic reticulum are important for phagocytosis. *The EMBO Journal* **20,** 6772–6782 (2001).
459. Shi, Y. *et al.* Histone demethylation mediated by the nuclear amine oxidase homolog LSD1. *Cell* **119,** 941–953 (2004).
460. Mazia, D., Schatten, G. & Sale, W. Adhesion of cells to surfaces coated with polylysine. Applications to electron microscopy. *J Cell Biol* **66,** 198–200 (1975).
461. Neupert, W. PROTEIN IMPORT INTO MITOCHONDRIA. *http://dx.doi.org/10.1146/annurev.biochem.66.1.863* **66,** 863–917 (2003).
462. Maniccia, A. W. *et al.* Mitochondrial localization, ELK-1 transcriptional regulation and growth inhibitory functions of BRCA1, BRCA1a, and BRCA1b proteins. *J. Cell. Physiol.* **219,** 634–641 (2009).
463. Henderson, B. R. The BRCA1 Breast Cancer Suppressor: Regulation of Transport, Dynamics, and Function at Multiple Subcellular Locations. *Scientifica (Cairo)* **2012,** 796808–15 (2012).
464. Schrag, J. D. *et al.* The Structure of calnexin, an ER chaperone involved in quality control of protein folding. *Molecular Cell* **8,** 633–644 (2001).
465. Linstedt, A. D. & Hauri, H. P. Giantin, a novel conserved Golgi membrane

protein containing a cytoplasmic domain of at least 350 kDa. *Mol. Biol. Cell* **4,** 679–693 (1993).
466. Shaul, Y. D. & Seger, R. The MEK/ERK cascade: from signaling specificity to diverse functions. *Biochim. Biophys. Acta* **1773,** 1213–1226 (2007).
467. Razandi, M., Pedram, A., Rosen, E. M. & Levin, E. R. BRCA1 inhibits membrane estrogen and growth factor receptor signaling to cell proliferation in breast cancer. *Molecular and Cellular Biology* **24,** 5900–5913 (2004).
468. Möser, C. V. *et al.* TANK-binding kinase 1 (TBK1) modulates inflammatory hyperalgesia by regulating MAP kinases and NF-κB dependent genes. *J Neuroinflammation* **12,** 100 (2015).
469. Abe, T. & Barber, G. N. Cytosolic-DNA-Mediated, STING-Dependent Proinflammatory Gene Induction Necessitates Canonical NF-{kappa}B Activation through TBK1. *J. Virol.* **88,** 5328–5341 (2014).
470. Roux, P. P. & Blenis, J. ERK and p38 MAPK-activated protein kinases: a family of protein kinases with diverse biological functions. *Microbiol. Mol. Biol. Rev.* **68,** 320–344 (2004).
471. Pilli, M. *et al.* TBK-1 promotes autophagy-mediated antimicrobial defense by controlling autophagosome maturation. *Immunity* **37,** 223–234 (2012).
472. Holm, C. K. *et al.* Influenza A virus targets a cGAS-independent STING pathway that controls enveloped RNA viruses. *Nature Communications* **7,** 10680 (2016).
473. Baril, M., Racine, M.-E., Penin, F. & Lamarre, D. MAVS dimer is a crucial signaling component of innate immunity and the target of hepatitis C virus NS3/4A protease. *J. Virol.* **83,** 1299–1311 (2009).
474. Horner, S. M., Liu, H. M., Park, H. S., Briley, J. & Gale, M. Mitochondrial-associated endoplasmic reticulum membranes (MAM) form innate immune synapses and are targeted by hepatitis C virus. *Proc. Natl. Acad. Sci. U.S.A.* **108,** 14590–14595 (2011).
475. van Zuylen, W. J. *et al.* Proteomic profiling of the TRAF3 interactome network reveals a new role for the ER-to-Golgi transport compartments in innate immunity. *PLoS Pathog* **8,** e1002747 (2012).
476. Horner, S. M., Wilkins, C., Badil, S., Iskarpatyoti, J. & Gale, M., Jr. Proteomic Analysis of Mitochondrial-Associated ER Membranes (MAM) during RNA Virus Infection Reveals Dynamic Changes in Protein and Organelle Trafficking. *PLoS ONE* **10,** e0117963 (2015).
477. Deng, C.-X. BRCA1: cell cycle checkpoint, genetic instability, DNA damage response and cancer evolution. *Nucleic Acids Res.* **34,** 1416–1426 (2006).
478. Clark, S. L., Rodriguez, A. M., Snyder, R. R., Hankins, G. D. V. & Boehning, D. STRUCTURE-FUNCTION OF THE TUMOR SUPPRESSOR BRCA1. *Computational and Structural Biotechnology Journal* **1,** 1–8 (2012).
479. Wu, L. C. *et al.* Identification of a RING protein that can interact in vivo with the BRCA1 gene product. *Nature Genetics* **14,** 430–440 (1996).
480. Meza, J. E., Brzovic, P. S., King, M. C. & Klevit, R. E. Mapping the functional domains of BRCA1. Interaction of the ring finger domains of BRCA1 and BARD1. *Journal of Biological Chemistry* **274,** 5659–5665 (1999).
481. Joukov, V., Chen, J., Fox, E. A., Green, J. B. & Livingston, D. M. Functional communication between endogenous BRCA1 and its partner, BARD1, during Xenopus laevis development. *Proceedings of the National Academy of Sciences*

98, 12078–12083 (2001).
482. Mallery, D. L., Vandenberg, C. J. & Hiom, K. Activation of the E3 ligase function of the BRCA1/BARD1 complex by polyubiquitin chains. *The EMBO Journal* **21,** 6755–6762 (2002).
483. Christensen, D. E., Brzovic, P. S. & Klevit, R. E. E2-BRCA1 RING interactions dictate synthesis of mono- or specific polyubiquitin chain linkages. *Nature Structural & Molecular Biology* **14,** 941–948 (2007).
484. Muñoz, M. C. *et al.* TANK-binding kinase 1 mediates phosphorylation of insulin receptor at serine residue 994: a potential link between inflammation and insulin resistance. *J. Endocrinol.* **201,** 185–197 (2009).
485. Tough, D. F. Modulation of T-cell function by type I interferon. *Immunology and Cell Biology* **90,** 492–497 (2012).
486. Parker, B. S., Rautela, J. & Hertzog, P. J. Antitumour actions of interferons: implications for cancer therapy. *Nat Rev Cancer* **16,** 131–144 (2016).
487. Zitvogel, L., Galluzzi, L., Kepp, O., Smyth, M. J. & Kroemer, G. Type I interferons in anticancer immunity. *Nature Publishing Group* **15,** 405–414 (2015).
488. Fuertes, M. B., Woo, S.-R., Burnett, B., Fu, Y.-X. & Gajewski, T. F. Type I interferon response and innate immune sensing of cancer. *Trends in Immunology* **34,** 67–73 (2013).
489. Gleason, C. E., Ordureau, A., Gourlay, R., Arthur, J. S. C. & Cohen, P. Polyubiquitin binding to optineurin is required for optimal activation of TANK-binding kinase 1 and production of interferon β. *J. Biol. Chem.* **286,** 35663–35674 (2011).
490. Pomerantz, J. L. & Baltimore, D. NF-kappaB activation by a signaling complex containing TRAF2, TANK and TBK1, a novel IKK-related kinase. *The EMBO Journal* **18,** 6694–6704 (1999).
491. Jeon, G. S. *et al.* Deregulation of BRCA1 Leads to Impaired Spatiotemporal Dynamics of γ-H2AX and DNA Damage Responses in Huntington's Disease. *Mol Neurobiol* **45,** 550–563 (2012).
492. Krum, S. A., Dalugdugan, E. de L. R., Miranda-Carboni, G. A. & Lane, T. F. BRCA1 Forms a Functional Complex with -H2AX as a Late Response to Genotoxic Stress. *Journal of Nucleic Acids* **2010,** 1–9 (2010).
493. Tsuchiya, S. *et al.* Establishment and characterization of a human acute monocytic leukemia cell line (THP-1). *International Journal of Cancer* **26,** 171–176 (1980).
494. Daigneault, M., Preston, J. A., Marriott, H. M., Whyte, M. K. B. & Dockrell, D. H. The identification of markers of macrophage differentiation in PMA-stimulated THP-1 cells and monocyte-derived macrophages. *PLoS ONE* **5,** e8668 (2010).
495. Schwende, H., Fitzke, E., Ambs, P. & Dieter, P. Differences in the state of differentiation of THP-1 cells induced by phorbol ester and 1,25-dihydroxyvitamin D3. *J. Leukoc. Biol.* **59,** 555–561 (1996).
496. Tsuchiya, S. *et al.* Induction of maturation in cultured human monocytic leukemia cells by a phorbol diester. *Cancer Res* **42,** 1530–1536 (1982).
497. Stetson, D. B. & Medzhitov, R. Recognition of cytosolic DNA activates an IRF3-dependent innate immune response. *Immunity* **24,** 93–103 (2006).
498. Sharma, S. & Fitzgerald, K. A. Innate immune sensing of DNA. *PLoS Pathog* **7,** e1001310 (2011).

499. Fensterl, V. & Sen, G. C. Interferon-induced Ifit proteins: their role in viral pathogenesis. *J. Virol.* **89,** 2462–2468 (2015).
500. Haller, O. & Kochs, G. Human MxA protein: an interferon-induced dynamin-like GTPase with broad antiviral activity. *J. Interferon Cytokine Res.* **31,** 79–87 (2011).
501. Gullberg, M. & Andersson, A.-C. Visualization and quantification of protein-protein interactions in cells and tissues. *Nat Meth* **7,** (2010).
502. Koos, B. *et al.* in *High-Dimensional Single Cell Analysis* **377,** 111–126 (Springer Berlin Heidelberg, 2013).
503. Clark, K. *et al.* Novel cross-talk within the IKK family controls innate immunity. *Biochem. J.* **434,** 93–104 (2011).
504. Ardeshna, K. M. *et al.* Monocyte-derived dendritic cells do not proliferate and are not susceptible to retroviral transduction. *Br. J. Haematol.* **108,** 817–824 (2000).
505. Humbert, J.-M. *et al.* Measles virus glycoprotein-pseudotyped lentiviral vectors are highly superior to vesicular stomatitis virus G pseudotypes for genetic modification of monocyte-derived dendritic cells. *J. Virol.* **86,** 5192–5203 (2012).
506. Fitzgerald, K. A. *et al.* IKK|[epsi]| and TBK1 are essential components of the IRF3 signaling pathway. *Nat Immunol* **4,** 491–496 (2003).
507. Ishikawa, H. & Barber, G. N. STING is an endoplasmic reticulum adaptor that facilitates innate immune signalling. *Nature* **455,** 674–678 (2008).
508. Benezra, M. *et al.* BRCA1 Augments Transcription by the NF- B Transcription Factor by Binding to the Rel Domain of the p65/RelA Subunit. *Journal of Biological Chemistry* **278,** 26333–26341 (2003).
509. Sumpter, R. *et al.* Fanconi Anemia Proteins Function in Mitophagy and Immunity. *Cell* **165,** 867–881 (2016).
510. Buckley, N. E. *et al.* BRCA1 regulates IFN-gamma signaling through a mechanism involving the type I IFNs. *Mol Cancer Res* **5,** 261–270 (2007).
511. Buckley, N. E. *et al.* IRF-7 plays a key role in the BRCA1/IFN-γ mediated apoptotic response. *Cancer Res* **65,** 1271–1271 (2005).
512. Andrews, H. N. *et al.* BRCA1 regulates the interferon gamma-mediated apoptotic response. *Journal of Biological Chemistry* **277,** 26225–26232 (2002).
513. Dutta, D. *et al.* BRCA1 Regulates IFI16 Mediated Nuclear Innate Sensing of Herpes Viral DNA and Subsequent Induction of the Innate Inflammasome and Interferon-β Responses. *PLoS Pathog* **11,** e1005030–47 (2015).
514. Aglipay, J. A. *et al.* A member of the Pyrin family, IFI16, is a novel BRCA1-associated protein involved in the p53-mediated apoptosis pathway. *Oncogene* **22,** 8931–8938 (2003).
515. Tomlinson, G. E. *et al.* Characterization of a breast cancer cell line derived from a germ-line BRCA1 mutation carrier. *Cancer Res* **58,** 3237–3242 (1998).
516. Zhu, B. *et al.* K63-linked ubiquitination of FANCG is required for its association with the Rap80-BRCA1 complex to modulate homologous recombination repair of DNA interstand crosslinks. *Oncogene* **34,** 2867–2878 (2015).
517. Nathan, J. A., Kim, H. T., Ting, L., Gygi, S. P. & Goldberg, A. L. Why do cellular proteins linked to K63-polyubiquitin chains not associate with proteasomes? *The EMBO Journal* **32,** 552–565 (2013).

518. Wu-Baer, F., Lagrazon, K., Yuan, W. & Baer, R. The BRCA1/BARD1 heterodimer assembles polyubiquitin chains through an unconventional linkage involving lysine residue K6 of ubiquitin. *Journal of Biological Chemistry* **278,** 34743–34746 (2003).
519. Yu, X., Fu, S., Lai, M., Baer, R. & Chen, J. BRCA1 ubiquitinates its phosphorylation-dependent binding partner CtIP. *Genes Dev.* **20,** 1721–1726 (2006).
520. Tu, D. *et al.* Structure and ubiquitination-dependent activation of TANK-binding kinase 1. *Cell Reports* **3,** 747–758 (2013).
521. Ikeda, F. *et al.* Involvement of the ubiquitin-like domain of TBK1/IKK-i kinases in regulation of IFN-inducible genes. *The EMBO Journal* **26,** 3451–3462 (2007).
522. Wang, L., Li, S. & Dorf, M. E. NEMO Binds Ubiquitinated TANK-Binding Kinase 1 (TBK1) to Regulate Innate Immune Responses to RNA Viruses. *PLoS ONE* **7,** e43756 (2012).
523. Zeng, W., Xu, M., Liu, S., Sun, L. & Chen, Z. J. Key role of Ubc5 and lysine-63 polyubiquitination in viral activation of IRF3. *Molecular Cell* **36,** 315–325 (2009).
524. Gatot, J. P., Gioia, R. & Chau, T. L. Lipopolysaccharide-mediated Interferon Regulatory Factor Activation Involves TBK1-IKK-dependent Lys 63-linked Polyubiquitination and Phosphorylation of …. *The Journal of …* (2007).
525. Chen, Z. J. Ubiquitination in signaling to and activation of IKK. *Immunol. Rev.* **246,** 95–106 (2012).
526. Zeng, W. *et al.* Reconstitution of the RIG-I pathway reveals a signaling role of unanchored polyubiquitin chains in innate immunity. *Cell* **141,** 315–330 (2010).
527. Ye, J. S. *et al.* Lysine 63-linked TANK-binding kinase 1 ubiquitination by mindbomb E3 ubiquitin protein ligase 2 is mediated by the mitochondrial antiviral signaling protein. *J. Virol.* **88,** 12765–12776 (2014).
528. Zheng, Q. *et al.* Siglec1 suppresses antiviral innate immune response by inducing TBK1 degradation via the ubiquitin ligase TRIM27. *Cell Res.* **25,** 1121–1136 (2015).
529. Liu, D. *et al.* SOCS3 Drives Proteasomal Degradation of TBK1 and Negatively Regulates Antiviral Innate Immunity. *Molecular and Cellular Biology* **35,** 2400–2413 (2015).
530. Shen, R. R. & Hahn, W. C. Emerging roles for the non-canonical IKKs in cancer. *Oncogene* **30,** 631–641 (2011).
531. Hutti, J. E. *et al.* Phosphorylation of the tumor suppressor CYLD by the breast cancer oncogene IKKepsilon promotes cell transformation. *Molecular Cell* **34,** 461–472 (2009).
532. Wei, C. *et al.* Elevated expression of TANK-binding kinase 1 enhances tamoxifen resistance in breast cancer. *Proc. Natl. Acad. Sci. U.S.A.* **111,** E601–10 (2014).
533. Xie, X. *et al.* IkappaB kinase epsilon and TANK-binding kinase 1 activate AKT by direct phosphorylation. *Proc. Natl. Acad. Sci. U.S.A.* **108,** 6474–6479 (2011).
534. Barbie, D. A. *et al.* Systematic RNA interference reveals that oncogenic KRAS-driven cancers require TBK1. *Nature* **462,** 108–112 (2009).
535. Barbie, T. U. *et al.* Targeting an IKBKE cytokine network impairs triple-negative breast cancer growth. *J. Clin. Invest.* **124,** 5411–5423 (2014).

536. Jiang, Z., Liu, J. C., Chung, P. E. D., Egan, S. E. & Zacksenhaus, E. Targeting HER2(+) breast cancer: the TBK1/IKKε axis. *Oncoscience* **1,** 180–182 (2014).
537. Deng, T. *et al.* shRNA Kinome Screen Identifies TBK1 as a Therapeutic Target for HER2+ Breast Cancer. *Cancer Res* **74,** 2119–2130 (2014).
538. Guendel, I. *et al.* BRCA1 functions as a novel transcriptional cofactor in HIV-1 infection. *Virology Journal 2015 12:1* **12,** 1 (2015).
539. Luban, J. Innate Immune Sensing of HIV-1 by Dendritic Cells. *Cell Host & Microbe* **12,** 408–418 (2012).
540. Zhang, Y. *et al.* BRCA1 interaction with human papillomavirus oncoproteins. *Journal of Biological Chemistry* **280,** 33165–33177 (2005).
541. Maul, G. G., Jensen, D. E., Ishov, A. M., Herlyn, M. & Rauscher, F. J. Nuclear redistribution of BRCA1 during viral infection. *Cell Growth Differ.* **9,** 743–755 (1998).
542. Evers, B. & Jonkers, J. Mouse models of BRCA1 and BRCA2 deficiency: past lessons, current understanding and future prospects. *Oncogene* **25,** 5885–5897 (2006).
543. Spadaro, F. *et al.* IFN-alpha enhances cross-presentation in human dendritic cells by modulating antigen survival, endocytic routing, and processing. *Blood* **119,** 1407–1417 (2012).
544. Lattanzi, L. *et al.* IFN-alpha boosts epitope cross-presentation by dendritic cells via modulation of proteasome activity. *Immunobiology* **216,** 537–547 (2011).
545. Belz, G. T., Shortman, K., Bevan, M. J. & Heath, W. R. CD8alpha+ dendritic cells selectively present MHC class I-restricted noncytolytic viral and intracellular bacterial antigens in vivo. *The Journal of Immunology* **175,** 196–200 (2005).
546. Belz, G. T. *et al.* Cutting edge: Conventional CD8 alpha(+) dendritic cells are generally involved in priming CTL immunity to viruses. *The Journal of Immunology* **172,** 1996–2000 (2004).
547. Curtsinger, J. M., Valenzuela, J. O., Agarwal, P., Lins, D. & Mescher, M. F. Type I IFNs provide a third signal to CD8 T cells to stimulate clonal expansion and differentiation. *The Journal of Immunology* **174,** 4465–4469 (2005).
548. Le Bon, A. *et al.* Direct stimulation of T cells by type IIFN enhances the CD8(+) T cell response during cross-priming. *The Journal of Immunology* **176,** 4682–4689 (2006).
549. Xu, H. C. *et al.* Type I Interferon Protects Antiviral CD8(+) T Cells from NK Cell Cytotoxicity. *Immunity* **40,** 949–960 (2014).
550. Havenar-Daughton, C., Kolumam, G. A. & Murali-Krishna, K. Cutting Edge: The direct action of type I IFN on CD4 T cells is critical for sustaining clonal expansion in response to a viral but not a bacterial infection. *The Journal of Immunology* **176,** 3315–3319 (2006).
551. Apetoh, L. *et al.* Toll-like receptor 4-dependent contribution of the immune system to anticancer chemotherapy and radiotherapy. *Nature Medicine* **13,** 1050–1059 (2007).
552. Lande, R. *et al.* Plasmacytoid dendritic cells sense self-DNA coupled with antimicrobial peptide. *Nature* **449,** 564–U6 (2007).
553. Freeman, G. J. *et al.* Engagement of the PD-1 immunoinhibitory receptor by a novel B7 family member leads to negative regulation of lymphocyte activation. *Journal of Experimental Medicine* **192,** 1027–1034 (2000).

554. Terawaki, S. *et al.* IFN-alpha Directly Promotes Programmed Cell Death-1 Transcription and Limits the Duration of T Cell-Mediated Immunity. *The Journal of Immunology* **186,** 2772–2779 (2011).
555. Sistigu, A. *et al.* Cancer cell–autonomous contribution of type I interferon signaling to the efficacy of chemotherapy. *Nature Medicine* **20,** 1301–1309 (2014).